

# **IMPLICATIONS OF SOLID AND LIQUID WASTE CO-DISPOSAL ON ORGANIC STABILITY AND BIOCHEMICAL COMPATIBILITY**

Christopher A. Bareither, Emily M. Cook, and Sajjad Karimi

*Dept. of Civil & Environmental Engineering, Colorado State University, Fort Collins, Colorado  
1372 Campus Delivery, Fort Collins, CO 80223  
christopher.bareither@colostate.edu, (970) 491-4660*

Keywords: bioreactor, co-disposal, landfill, liquid waste, municipal solid waste

## **FINAL REPORT**

Prepared for the  
**Environmental Research and Education Foundation**



2020

## EXECUTIVE SUMMARY

This report includes two studies: (i) implications of solid and liquid waste co-disposal on biodegradation and biochemical compatibility; and (ii) influence of moisture enhancement on solid waste biodegradation. The study comprising co-disposal is herein named Research Study 1 and the study pertaining to moisture enhancement is herein named Research Study 2. Thus, this report is separated into the two research studies, which include methods, results, and conclusions for each study.

### Research Study 1

Co-disposal of solid and liquid waste in municipal solid waste (MSW) landfills can enhance waste moisture content to potentially accelerate in situ waste biodegradation. However, current co-disposal practices in full-scale landfills are ad hoc, and implications of co-disposing different types of solid, liquid, and sludge waste on general landfill processes are not well established. The objective of this study was to evaluate waste biodegradation and biochemical compatibility for different co-disposed solid and liquid wastes in MSW. To meet this objective, laboratory-scale reactors were operated for several months to evaluate the potential impacts of co-disposal and ultimately to provide guidance for full-scale MSW landfill operations. Waste collected for this project was identified as MSW, special solid waste (SW), liquid waste (LW), and sludge waste (Sludge), such that reactor experiments were conducted with representative co-disposal combinations of MSW-SW, MSW-LW, and MSW-Sludge. The MSW-SW and MSW-Sludge reactors included landfill leachate as a liquid source to generate effluent; MSW-LW reactors were operated with unique liquid wastes.

Early and aggressive addition of liquid wastes during reactor startup appeared not to promote accelerated anaerobic decomposition of fresh MSW. The majority of the liquid waste reactors were stuck in the acid formation phase and had leachate with pH < 6 and chemical oxygen demand (COD) approaching or exceeding 50,000 mg-O<sub>2</sub>/L. The MSW exhibited the ability to buffer and potentially treat liquid waste when not in an anaerobic degradation phase, which was observed in a COD reduction in the high-strength manufacturing wastewater reactors. Given the bioreactor conditions used in this study, the majority of liquid wastes were not observed to be effective inoculums to establish methane generation in fresh MSW and would not be recommended as the sole moisture source for bioreactor landfills. Although full-scale landfills likely have higher buffering capacity that may mitigate high acid accumulation and potential anaerobic inhibition, a source of anaerobic microorganisms (e.g., mature landfill leachate or anaerobic digestion sludge) should be considered with liquid waste co-disposal to promote biodegradation of organic waste. Treatment of high-strength wastewater is possible in MSW. However, addition of high-strength liquid waste should be implemented following established methane generation, which has been shown to be an effective moisture enhancement technique in full-scale MSW landfills.

The anaerobic digestion sludge and industrial sludge appeared beneficial for accelerating anaerobic biodegradation. Enhanced early methane production was observed in the MSW-Sludge reactors relative to the landfill leachate control reactors and all other waste combinations evaluated in this study. Sludge wastes appear to have been beneficial for anaerobic biodegradation and should be considered as potential sources of moisture and organic loading for waste decomposition. The anaerobic digestion sludge provided active methanogenic microorganisms to accelerate methane

generation and is likely a beneficial seed source in full-scale landfills. There are several operational considerations for sludge waste co-disposal: (i) early gas collection is needed to manage accelerated production of biogas; (ii) the amount of sludge that can be added while maintaining the observed benefits remains undetermined; and (iii) clogging of liquid and gas infrastructure due to sludge may be an issue (e.g., tubing and filters were prone to clogging in MSW-Sludge reactor experiments).

Methane generation was observed in reactors operated with foundry waste or gypsum board co-disposed with MSW. Despite biochemical methane potential (BMP) results that indicated methane generation would be inhibited with these two waste streams, co-disposing with MSW did not completely inhibit anaerobic degradation. The high sulfate content of gypsum board appeared to have led to sulfate reduction, which likely created a reduced environment favorable for methane generation in the reactors, as was observed by low values of oxidation reduction potential (ORP). Materials with an elevated sulfate content may generate H<sub>2</sub>S gas. The more methanogenically active of the two foundry waste reactors demonstrated that a solid waste stream that appeared to be inhibitory for methane generation, based on leachate chemistry (low pH, high OPR, high COD), still promoted biodegradation.

The BMP assays provided methane yield from organic substrate degradation under ideal conditions and did not capture other benefits of co-disposal (e.g., impacts of moisture addition). A potential co-disposal waste source should not be ruled out by BMP results alone. The BMP results for solid wastes did not show good agreement with reactor data; e.g., negative BMP results corresponded to some solid waste reactors that were actively generating methane. The BMP assay would not have been a good selection tool in these cases. Thus, BMP assays that simulate ideal anaerobic conditions do not appear to be an effective screening tool that can be used alone to determine compatibility of co-disposal waste streams.

## **Research Study 2**

Moisture addition to solid waste landfills via leachate recirculation and liquid waste addition / solidification are methods used to promote in situ anaerobic biodegradation. However, operations for moisture addition are generally ad hoc and controlling the amount of liquid added and frequency of dosing is challenging. The objective of this study was to assess the influence of moisture enhancement strategies on biodegradation of MSW in laboratory-scale reactors. Moisture enhancement strategies were varied with respect to dose volume (40, 80, 160, and 320 L/Mg-MSW) and dose frequency (dosing every ½, 1, 2, and 4 weeks). Biodegradation was evaluated based on methane generation to identify moisture enhancement strategies that can (i) reduce the lag-time between the start of liquid dosing and onset of methane generation and (ii) increase the first-order decay rate for methane generation.

In general, the more aggressive liquid dosing strategies (i.e., higher dose volumes and more frequent dosing) yielded leachate chemistry that displayed anticipated hydrolysis, acidogenesis, and methanogenesis phases. These processes were assumed to develop within reactors operated with the lowest dose volume (40 L/Mg-MSW) and low frequencies (e.g., 2 and 4 weeks) prior to leachate generation based initial effluent leachate showing neutral pH and low COD coupled with active methane generation. The first-order decay rate for methane generation increased with an increase in dose volume for all four of the dose frequencies. For example, the peak methane flow rate increased from 0.27 to 1.29 m<sup>3</sup>/Mg-MSW/d from reactors operated with a dose volume of 40 L/Mg-MSW as the dose frequency increased from every 4

weeks to every  $\frac{1}{2}$  week. Although minor differences were observed in methane generation for reactors operated with a dose volume of 160 L/Mg-MSW, there were negligible differences in methane yield and flow rate considering dose frequencies of  $\frac{1}{2}$ , 1, and 2 weeks. In addition, reactors operated with dose frequencies of  $\frac{1}{2}$  and 2 weeks and a dose volume of 320 L/Mg-MSW yielded the highest methane flow rates ( $\approx 2.8$  l/yr) and highest methane yields ( $\approx 125$  m<sup>3</sup>/Mg-MSW) among the reactors operated in this study.

Trends of increased decay rate and reduced lag-time with an increase in dose frequency were observed for reactors operated with dose volumes of 40, 80, and 160 L/Mg-MSW. Thus, more rapid dosing was advantageous to enhancing methane generation in a shorter amount of time after the first inoculum dose was added. A key conclusion from this study was that reactors with more aggressive moisture enhancement (i.e., higher monthly dosing) attained elevated methane generation (higher decay rate) that initiated at shorter elapsed times following the onset of dosing (reduced lag-time). An assessment of liquid dosing / recirculation per month indicated that there was a more pronounced trend of increasing decay rate and decreasing lag-time as moisture enhancement increased from 40 L/Mg-MSW/month to 320 L/Mg-MSW/month as compared to the effects observed for additional increases in moisture above 320 L/Mg-MSW/month.

# TABLE OF CONTENTS

EXECUTIVE SUMMARY .....	i
RESEARCH STUDY 1: Implications of Solid and Liquid Waste Co-Disposal on Biodegradation and Biochemical Compatibility .....	1
CHAPTER 1: INTRODUCTION .....	1
1.1 Problem Statement .....	1
1.2 Research Objectives and Tasks .....	2
CHAPTER 2: BACKGROUND.....	3
2.1 Bioreactor Landfills .....	3
2.1.1 Waste Stabilization.....	3
2.1.2 Anaerobic Digestion Inhibition.....	4
2.1.3 Performance Evaluation of Bioreactor Landfills.....	5
2.2 Co-Disposal in Landfills .....	5
2.2.1 Co-Disposal of MSW with Liquid Waste.....	6
2.2.2 Co-Disposal of MSW with Sludge Waste .....	8
2.2.3 Co-Disposal of MSW with Industrial Solid Waste .....	8
CHAPTER 3: RESULTS AND DISCUSSION .....	12
3.1 Physical Reactor Characteristics .....	12
3.1.1 Recirculation Volumes.....	12
3.1.2 Settlement .....	13
3.2 Leachate Quality .....	13
3.2.1 Leachate Composition – Bulk Parameters .....	13
3.2.2 Leachate Composition – Elemental Analysis .....	14
3.3 Transition to Methanogenesis.....	15
3.3.1 Leachate Indicator Parameter Trends.....	15
3.3.2 Biogas Generation and Anaerobic Biodegradation .....	16
3.3.3 Biogas Composition .....	17
3.4 Liquid Waste Treatment Implications.....	18
3.5 Biochemical Methane Potential Assays.....	19
CHAPTER 4: SUMMARY AND CONCLUSIONS .....	34
CHAPTER 5: METHODOLOGY .....	36
5.1 Experimental Overview.....	36
5.2 Materials .....	36

5.2.1	Municipal Solid Waste .....	36
5.2.2	Industrial Solid Waste.....	36
5.2.3	Liquid Waste .....	37
5.2.4	Sludge Waste .....	37
5.3	Reactor Design .....	38
5.4	Reactor Leachate Recirculation and Sampling .....	39
5.5	Analytical Methods.....	40
5.5.1	Solids Analysis.....	40
5.5.2	Liquid Analysis.....	40
5.5.3	Gas Collection and Analysis .....	40
5.5.4	Biochemical Methane Potential Assay .....	41
RESEARCH STUDY 2: The Influence of Moisture Enhancement on Solid Waste		
	Biodegradation .....	49
	CHAPTER 1: INTRODUCTION .....	49
	CHAPTER 2: RESULTS AND DISCUSSION .....	50
2.1	Reactor Operation and Data Processing .....	50
2.2	Moisture Response .....	51
2.3	Leachate Chemistry .....	51
2.4	Methane Generation .....	52
2.5	First-Order Decay Rate and Lag-Time.....	54
2.6	Practical Implications .....	55
	CHAPTER 3: SUMMARY AND CONCLUSIONS .....	65
	CHAPTER 4: MATERIALS AND METHODS.....	66
4.1	Experiment Overview .....	66
4.2	Reactor Design.....	66
4.3	Municipal Solid Waste .....	66
4.4	Liquid Management.....	67
4.5	Biogas Management and Analysis .....	67
4.5.1	Biogas Measurement and Composition .....	67
4.5.2	Decay Rate and Lag-Time .....	68
	ACKNOWLEDGEMENTS .....	71
	REFERENCES.....	72

APPENDIX A – Compilation of Reactor Data for Research Study 1 .....	77
APPENDIX B – Compilation of Select Heavy Metals and Other Inorganic Elements Evaluated in Leachate Samples from the Laboratory Reactors Operated in Research Study 1 .....	101
APPENDIX C – Photos of Reactors and Biochemical Methane Potential Assays from Research Study 1 .....	104
APPENDIX D – Compilation of Reactor Data for Study 2 .....	111
APPENDIX E – Photographs from Reactor Setup and Operation for Research Study 2.....	142

# RESEARCH STUDY 1: IMPLICATIONS OF SOLID AND LIQUID WASTE CO-DISPOSAL ON BIODEGRADATION AND BIOCHEMICAL COMPATIBILITY

## CHAPTER 1: INTRODUCTION

### 1.1 Problem Statement

There is considerable interest in solid waste management to develop operational strategies that accelerate waste decomposition, enhance methane (CH<sub>4</sub>) production, and provide in-situ leachate treatment in municipal solid waste (MSW) landfills. The most common strategy is to operate a landfill as a bioreactor, which is typically achieved through leachate recirculation and addition of supplemental liquids to increase the in-situ moisture content and stimulate microbial-induced biodegradation (e.g., Bareither et al. 2010; Barlaz et al. 2010; Townsend et al. 2015). The specific strategy of interest for this study was the co-disposal of supplemental liquid waste with solid waste.

Co-disposal of solid and liquid waste is a practical waste management approach for landfills operating with a U.S. EPA Subtitle D Research, Development, and Demonstration permit (RD&D – 40CFR 285.4). An RD&D permit provides landfill owners operational and technological flexibility to enhance waste moisture content as long as there are no detrimental impacts on human health and the environment. The U.S. EPA initiated the RD&D rule in 2004 to promote innovative landfill technologies, which include bulk liquid waste addition. Individual states must apply and receive formal approval from the U.S. EPA prior to issuing permits to landfills. A ten-year review of the rule revealed that 16 states had adopted the rule and that 30 landfills had active RD&D permits (USEPA 2014b).

Although the U.S. EPA RD&D review indicated relatively low participation nationally, landfills located in states where regulations require a reduction in degradable organic material prior to landfill closure have successfully implemented the RD&D rule. Of the active RD&D projects, nearly half (13 of 30) are located in the state of Wisconsin (USEPA 2014b). The Wisconsin Department of Natural Resources initiated an Organic Stability Rule (OSR) (Section NR 514.07(9), Wis. Adm. Code) in 2007 that requires landfills to reduce the amount of biodegradable organic material remaining after closure to reduce the time required for organic stability and post-closure care. Landfill operators in the state of Wisconsin have elected to participate in the RD&D program and use liquid waste addition to promote organic stability (Bareither et al. 2017).

A state-of-practice (SOP) review on organic waste stabilization in MSW landfills in Wisconsin indicated that in-situ anaerobic treatment via liquid waste addition and leachate recirculation was the predominant strategy to enhance waste stabilization (Bareither et al. 2017). Typical supplemental liquids added to MSW landfills included storm water, groundwater, on-site rinse water, gas condensate, commercial and residential liquid wastes, and solidified liquid wastes (e.g., sludge) (Bareither et al. 2017; Nwaokorie et al. 2018). At all landfills practicing liquid waste addition, owners noted that co-disposal of solid and liquid waste was economically and environmentally attractive due to revenue from waste tipping fees and promotion of organic waste decomposition. Additionally, at sites where leachate treatment costs were high and liquid waste

disposal was a revenue source, operators sought out high moisture retaining wastes, such as foundry waste and automobile shredder residue, to co-dispose with the liquid waste. However, compatibility testing to evaluate unintended consequences that may arise from co-disposal of a wide variety of waste types was not implemented at any of the landfills. Thus, one of the limitations identified during the OSR review of Wisconsin landfills operating with RD&D permits was a lack of understanding of the effects of co-disposing diverse solid and liquid wastes on biochemical compatibility and organic waste decomposition (Bareither et al. 2017).

## **1.2 Research Objectives and Tasks**

Currently, there is no guidance on assessing biochemical compatibility of solid and liquid wastes co-disposed in MSW landfills, and there are no requirements to assess compatibility prior to co-disposal to ensure that the environmental benefits attributed to enhanced waste decomposition are realized. Additionally, increasing contributions of special solid wastes in MSW landfills may introduce unknown biochemical compatibility issues that hinder organic waste decomposition. Thus, there is a need to evaluate the effects of solid and liquid waste co-disposal on CH<sub>4</sub> generation and leachate quality (i.e., monitoring parameters of organic waste decomposition) with a future goal of developing decision tools to guide landfill-based solid waste management. There is also a need to establish indicator parameters based on waste composition that can be used to identify potentially compatible and incompatible solid and liquid wastes.

The objective of this project was to evaluate co-disposal of solid and liquid waste in laboratory-scale MSW reactors to develop guidance on biochemical compatibility issues and develop guidance for co-disposal operations. The following research tasks were conducted to complete this study:

- I. Procured and characterized representative non-hazardous solid, liquid, and sludge wastes;
- II. Conducted biochemical methane potential assays to characterize the anaerobic degradability and CH<sub>4</sub> yield of each waste type for use as a potential indicator parameter in selection of compatible wastes for co-disposal;
- III. Designed, constructed, and operated laboratory-scale reactors that facilitated gas collection and leachate recirculation to study the co-disposal of different combinations of solid-solid, solid-liquid, and solid-sludge wastes;
- IV. Quantified and characterized leachate and gas generated in each reactor throughout operation; and
- V. Developed recommendations for landfill operators for the co-disposal of non-hazardous solid, liquid, and sludge waste streams in MSW landfills.

## CHAPTER 2: BACKGROUND

### 2.1 Bioreactor Landfills

A landfill is an engineered solid waste disposal facility that is designed and operated in a manner to protect human health and the environment. Conventional operation of landfills limits the ingress of moisture into the waste mass to minimize leachate generation. Waste containment barrier systems (i.e., liners and covers) are used to isolate the waste mass and prevent environmental contamination. With this conventional or “dry-tomb” approach, waste can remain undegraded for long periods of time, possibly in excess of the design life of the barrier system, which extends the time required for post-closure monitoring and maintenance of a landfill (Reinhart et al. 2002).

Biodegradation of the organic fraction of solid waste can be accelerated through operation of a landfill as a bioreactor. An anaerobic bioreactor landfill is an MSW landfill operated with the intended goal of enhanced anaerobic biodegradation of the organic fraction of the solid waste (Bareither et al. 2010). A schematic of a bioreactor landfill is included in Fig. 1.1 (Waste Management 2004). The benefits realized from operating a landfill as a bioreactor include increased potential for waste-to-energy conversion, storage and on-site treatment of leachate, airspace recovery from more rapid settlement, and reduced time required for long-term monitoring and maintenance of the landfill after closure (Reinhart et al. 2002; Barlaz et al. 2010). To stimulate the rate of biodegradation, favorable environmental conditions including pH, temperature, moisture content, waste particle size, oxidation-reduction potential, nutrient availability, and the absence of toxins can be modified. The most critical control parameter to enhance biodegradation has been found to be the waste moisture content (Reinhart and Al-Yousfi 1996; Reinhart et al. 2002).

The most common strategy to enhance waste moisture content in landfills is leachate recirculation and supplemental liquid addition (Bareither et al. 2010). Leachate recirculation has been found to be the most practical approach for moisture enhancement, such that most bioreactor strategies incorporate this technique (Reinhart et al. 2002). Leachate recirculation is also a proven method for in-situ leachate treatment. Studies have shown that leachate recirculation reduces waste stabilization time, improves final leachate quality, and enhances biogas generation (Reinhart and Al-Yousfi 1996; Sponza and Agdag 2004; Barlaz et al. 2010).

Landfill gas (LFG) is the major end product of biological decomposition in a landfill (Barlaz et al. 2009). The primary components of LFG are 50-60% CH<sub>4</sub> and 40-50% carbon dioxide (CO<sub>2</sub>) during active anaerobic biodegradation (Amini et al. 2012). Methane is an important greenhouse gas and landfills are estimated to be the second largest source of anthropogenic CH<sub>4</sub> emissions in the U.S. (Barlaz et al. 2009). Therefore, LFG management is an important environmental consideration, especially in bioreactor landfills where gas production is accelerated.

Early and aggressive gas management strategies need to be initiated in bioreactor landfills operating to enhance waste degradation. The shortened lag-time between waste placement and gas generation combined with the enhanced rate of biogas generation from a bioreactor are advantageous from a gas collection and energy generation perspective. However, a more rapid onset and enhanced rate of biogas generation can increase fugitive emissions and odors, which are regulatory and operational concerns (Bareither et al. 2017).

#### 2.1.1 Waste Stabilization

The goal of moisture addition in landfills is to stabilize the organic waste fraction in a shorter duration than a conventional landfill to reduce the post-closure care period. Organic stability is viewed as a state of near complete decomposition of organic waste constituents such

that human health, environmental, and financial risks associated with undecomposed waste are reduced (Bareither et al. 2017). Waste stabilization in landfills occurs in five phases: (i) initial adjustment phase, (ii) transition phase, (iii) acid formation phase, (iv) methanogenesis, and (v) maturation phase (Pohland and Gould 1986; Reinhart and Al-Yousfi 1996; Dhesi 2003). Temporal trends of gas generation, gas composition, and leachate chemistry during the five phases of waste stabilization are shown in Fig. 1.2 (Pohland and Gould 1986).

- I. Initial adjustment: This phase is associated with initial solid waste placement and continues until sufficient moisture accumulates to support microbial activity.
- II. Transition: The transformation from an aerobic to anaerobic environment occurs in this phase. Reducing conditions are established, oxygen ( $O_2$ ) is displaced by  $CO_2$ , and increasing concentrations of total volatile acids (TVA) and chemical oxygen demand (COD) are observed in the leachate.
- III. Acid Formation: In the acid phase, hydrolysis of solids followed by microbial conversion of organic compounds to intermediate organic acids occurs. The high acid concentrations result in a pH decrease in the leachate.
- IV. Methanogenesis: In this phase, intermediate organic acids are consumed by methanogenic bacteria and mineralized to  $CH_4$  and  $CO_2$ . Additionally, sulfates are reduced to sulfides, nitrates are reduced to ammonia, pH increases, and leachate strength decreases (e.g., reduction in COD).
- V. Maturation: In the final phase of waste stabilization, nutrients and degradable substrate becomes limiting. As a result, biological activity and gas production dramatically decrease, and leachate quality remains constant at low concentrations.

### **2.1.2 Anaerobic Digestion Inhibition**

Certain operational practices can be inhibitory to anaerobic digestion. Stable anaerobic digestion processes require an established microbial community to completely degrade organic substrate into  $CH_4$ ,  $CO_2$ , and water (Griffin et al 1998). Failure to maintain balance between acid forming and  $CH_4$  forming microorganisms was identified as a primary cause of reactor instability (Griffin et al. 1998; Chen et al. 2008). In a biosolids co-disposal experiment, an aggressive anaerobic digester start-up with high initial substrate loading resulted in organic acid accumulation, which lead to suboptimal digester performance. A more gradual reactor start-up strategy was recommended for anaerobic digesters to maintain sufficient methanogens in the system (Griffin et al. 1998). In general, leachate recirculation is an effective method for waste decomposition if managed properly; however, large recirculation volumes can generate high organic acid concentrations and yield low pH that can be inhibitory to methanogenesis (Sponza and Agdag 2004).

In addition to organic acid accumulation, common inhibitors to anaerobic digestion, including ammonia, sulfide, sodium, and heavy metals, were found to cause reactor upset when accumulation of these compounds occurred. Methanogens are the least tolerant of the anaerobic microorganisms and most likely to cease growth due to ammonia inhibition. Ammonia has been found to be inhibitory to anaerobic digestion at concentrations as low as 1,700 mg  $NH_3$ -N/L. Sulfate reduction to sulfide can suppress  $CH_4$  production through competition for substrates. High sodium concentrations exceeding 3,500 mg/L can affect metabolic activity of methanogens. Heavy metal accumulation can disrupt enzyme function and also be a cause of digester instability. Co-digestion with other wastes can improve anaerobic treatment and counteract inhibition via buffering and dilution of inhibitory compounds (Chen et al. 2008).

### **2.1.3 Performance Evaluation of Bioreactor Landfills**

A review of bioreactor landfill performance in the U.S. was conducted by Bareither et al. (2010) and Barlaz et al. (2010). Five full-scale landfills that recirculated leachate, and in some cases disposed supplemental liquids, were included in their study. Rationale for bioreactor operation at these sites included on-site leachate treatment, airspace recovery, enhanced gas generation, and maximization of waste decomposition to reduce long-term risks and costs of landfill operation. Contaminated runoff and leachate were the primary liquids recirculated in the landfills evaluated. In one landfill, pretreated industrial wastewater and septage from an on-site wastewater treatment plant were recirculated. Liquid dosing via horizontal trenches ranged from 30 to 419 L/Mg of waste, on average. Overall, only landfills with aggressive recirculation achieved moisture contents approaching field capacity, and supplemental liquid addition was identified as a potential option to further increase the moisture content and achieve field capacity (Bareither et al. 2010).

In addition to the physical aspects of bioreactor landfills, the study in Bareither et al. (2010) and Barlaz et al. (2010) addressed biological and chemical aspects. Data supported accelerated CH<sub>4</sub> generation and increased gas collection. Trends in leachate chemistry were consistent with bioreactor behavior. The pH recovered to a value above neutral, consistent with conversion of organic acids to CH<sub>4</sub>, the ratio of biological oxygen demand to chemical oxygen demand (BOD:COD) showed a decreasing trend consistent with degradation of organics, and ammonia concentrations increased, but not to inhibitory levels. Heavy metals and organic chemicals were not significantly different from leachate generated in conventional landfills (Barlaz et al. 2010).

Additional performance reviews were conducted on bioreactor landfills practicing moisture enhancement under the OSR in the state of Wisconsin (Bareither et al. 2017; Nwaokorie et al. 2018). Wisconsin regulations now require that within 40 years of closure, new landfills are to have a monthly average gas production rate of  $\leq 5\%$  of the peak value and a cumulative gas yield of  $\geq 75\%$  of the projected total production (Bareither et al. 2017). This review included 10 landfills and found that leachate recirculation and liquid waste addition were the predominant operational strategies implemented. Eight of the ten landfills were practicing liquid addition under an RD&D permit. Common liquid waste sources included manufacturing cleaning water, automobile wash water, and industrial sludge. Liquids were added in volumes ranging from 0 to nearly 12,000 m<sup>3</sup>/yr. Incompatibility during solid-liquid co-disposal was not observed, but the potential for biochemical incompatibility exists as more liquid wastes are disposed. Implementation of the OSR resulted in accelerated decomposition with no apparent negative environmental impacts, and all 10 landfills were on track to achieve the OSR requirements (Bareither et al. 2017).

Nwaokorie et al. (2018) conducted a site-specific study to determine first-order decay rates for a bioreactor landfill with different moisture enhancement strategies that included leachate recirculation and liquid addition. Liquid waste was added in different phases of the landfill, with cumulative application up to 76 L/Mg of waste. Increased gas generation in all phases of the landfill demonstrated that the implemented moisture enhancement strategies promoted waste degradation. The greatest CH<sub>4</sub> flow rates per MSW mass and the largest cumulative CH<sub>4</sub> generation per MSW mass were measured in the operational phase that implemented early and aggressive recirculation as well as continuous liquid waste addition.

## **2.2 Co-Disposal in Landfills**

Co-disposal in landfills has been described as the disposal of industrial wastewaters and sludges in landfills containing domestic and other non-industrial wastes (Watson-Craik and Sinclair 1995). Properly managed co-disposal of compatible solid and liquid waste streams in

landfills can be an effective method to manage multiple waste streams in one process through concurrent wastewater treatment and accelerated solid waste stabilization. The benefits of co-disposing wastes with complementary characteristics include dilution of potentially inhibitory compounds, improved availability of essential nutrients, synergistic effect of microorganisms, increased biodegradable organic loading, enhanced CH<sub>4</sub> yield, and increased anaerobic digestion rates (Agdag and Sponza 2005; Agdag and Sponza 2007; Sosnowski et al. 2003).

To achieve safe and effective co-disposal of liquid waste in landfills with no reduction in leachate quality, a thorough understanding of biochemical removal mechanisms of each waste and the effect on microbial communities is required (Watson-Craik and Senior 1989). The pH of the liquid waste is a major factor to consider before disposing liquid in a landfill, and the impact on microbial communities or the need to buffer should be assessed. Elevated concentrations of inhibitory compounds such as salts and heavy metals should also be evaluated. Municipal solid waste has some capacity to attenuate toxins and buffer against extreme pH values, but chemical composition of a liquid waste should be carefully evaluated prior to disposal (Townsend et al. 2015)

Biochemical methane potential assays are a convenient method to assess substrate degradation and ultimate CH<sub>4</sub> yield and can also serve as an indicator parameter for initial waste selection or screening for co-disposal applications (Townsend et al. 2015). Several different waste streams that represent a range of potential solid, liquid, or sludge wastes for co-disposal can be analyzed using a BMP assay. Wastes that show high methane potential indicate that co-disposal could enhance the degradation and methane yield relative to degradation of MSW alone. However, BMP assays create optimal conditions for anaerobic degradation and methane production, often masking toxicity issues. Therefore, BMP results and their use as a selection tool for co-disposal applications should be validated with lab-scale experiments (Moody et al. 2011).

### **2.2.1 Co-Disposal of MSW with Liquid Waste**

Liquid waste co-disposal in landfills can be advantageous as this practice may generate revenue for landfills, relieve industrial wastewater loading at wastewater treatment plants, provide a disposal alternative to industrial liquid generators, and aid in in-situ waste degradation (Bareither et al. 2017). Additionally, percolation through the waste body can provide treatment to the liquid waste due to the ability of the waste mass to serve as an anaerobic biofilter for the degradation of industrial wastewaters (Rahim and Watson-Craik 1997; Diamantis et al. 2013). The disposal of commercial liquid wastes can be a sustainable practice to achieve enhanced degradation compared to supplementing recirculation with groundwater or freshwater sources (Dhesi 2003). A potential limitation of liquid waste co-disposal in landfills is the development of more concentrated leachate that may require pre-treatment and treatment either off- or on-site.

In addition to bioreactor projects that have used liquid waste co-disposal in the U.S. (Bareither et al. 2010; Barlaz et al. 2010; USEPA 2014b; Bareither et al. 2017; Nwaokorie et al. 2018), industrial liquid waste co-disposal with MSW has been documented in landfills in the United Kingdom (Knox 1983), Kuwait (Al Yaqout 2003), and Korea (Behera et al. 2011). Knox reported no adverse impacts on leachate quality from the disposal of liquid wastes directly into landfills over a 20-yr period. However, Al Yaqout (2003) reported that liquid and sludge waste comprised approximately 37% of the total waste disposed by mass, and these large unregulated quantities disposed in unlined landfills posed a major risk to the surrounding environment. Behera et al. (2011) demonstrated that food waste leachate injection directly into landfills could be a sustainable waste management solution that provides treatment to the leachate and enhances CH<sub>4</sub> production.

Limited laboratory-scale research has been conducted on the co-disposal of liquid wastes with MSW. Laboratory studies using lysimeters, refuse columns, and biochemical

methane potential (BMP) assays have evaluated the following: olive vegetation wastewater (Cossu et al. 1993); phenolic wastewater (Watson-Craik and Senior 1989; Percival and Senior 1998); supplemental water for leachate recirculation (Sanphoti et al. 2006); food waste leachate (Lee et al. 2009); livestock wastewater (Zhang et al. 2012); dairy wastewater (Ko et al. 2012); brewery wastewater (Rahim and Watson-Craik 1997; Ko et al. 2012); and fishery wastewater (Ko et al. 2012). General trends and recommendations reported by these studies are summarized below.

- Co-disposal of liquid waste did not reduce leachate quality, but in fact, improved leachate quality with recirculation of the dissolved organic matter (Cossu et al. 1993, Rahim and Watson-Craik 1997). This is consistent with the common finding that leachate recirculation is more beneficial for waste decomposition than single elution experiments, because degradable substrates are reapplied to the waste containing microbial communities rather than flushed out with the leachate (Watson-Craik and Senior 1989; Percival and Senior 1998; Sponza and Agdag 2004; Sanphoti et al. 2006).
- Methane generation was enhanced by co-disposal with liquid waste (Watson-Craik and Senior 1989; Rahim and Watson-Craik 1997; Sanphoti et al. 2006).
- Wastewater loading and strength should be controlled, as high-strength wastewaters can adversely affect CH<sub>4</sub> production (Rahim and Watson-Craik 1997) or cause MSW to release rather than attenuate contaminants (Percival and Senior 1998).
- Fresh waste, compared to aged methanogenically active waste, requires buffering against acidic conditions (Watson-Craik and Senior 1989; Cossu et al. 1993; Percival and Senior 1998) and buffering was found to accelerate MSW stabilization (Sanphoti et al. 2006). Several studies recommended that wastewater should be applied during methanogenesis, rather than the acid formation phase, to achieve greater CH<sub>4</sub> generation and improved leachate quality. Wastewater application during the acid formation phase could inhibit or delay methanogenesis (Cossu et al. 1993; Percival and Senior 1998; Ko et al. 2012). However, reactor experiments conducted by Sanphoti et al. (2006) suggested that supplemental water addition in the early acid formation phase accelerated CH<sub>4</sub> production and resulted in higher CH<sub>4</sub> generation, indicating early addition of water to the waste can be an effective strategy for the acceleration of the CH<sub>4</sub> generation phase.
- Ko et al. (2012) identified that the phase when CH<sub>4</sub> generation begins to accelerate is the most environmentally sensitive period for methanogenesis and that liquid addition could have either a positive or a negative effect depending on the liquid chemistry. However, the largest demand for moisture in a bioreactor is also when CH<sub>4</sub> generation begins to accelerate, therefore evaluation of moisture addition during this phase should be further evaluated.

Co-disposal can be an effective means for both wastewater treatment and solid waste stabilization if operational parameters are carefully researched and controlled (Rahim and Watson-Craik 1997; Percival and Senior 1998). However, basic information regarding liquid waste disposal in landfills is not currently available and the research available may have limited relevance due to varying environmental factors and diverse waste types (Sanphoti et al. 2006).

In addition to laboratory- and field-scale research on liquid addition in landfills, comprehensive literature reviews were conducted to better understand the impacts of liquid waste co-disposal. Dhesi (2003) evaluated potential industrial wastewaters for co-disposal and conducted feasibility studies as well as economic, hydraulic, and gas modeling. Several wastewater types were considered potential co-disposal sources, and four wastewater types were evaluated (municipal, food processing, brewery, and bakery). Dhesi (2003) reported that industrial wastewater co-disposal in landfills is feasible through theoretical simulations and calculations, but recommended more laboratory- and large-scale studies of industrial

wastewater disposal in landfills to validate the models. Diamantis et al. (2013) investigated the feasibility of treating olive oil mill wastewater via disposal into closed landfills. They suggested that comprehensive guidelines to wastewater co-disposal are currently lacking and called for more field studies to establish reliable design data for wastewater disposal in landfills.

### **2.2.2 Co-Disposal of MSW with Sludge Waste**

Co-disposal of sludge waste with MSW is another method of interest to enhance waste degradation. Sludge wastes provide a source of supplemental moisture as well as potential revenue to a landfill owner via disposal fees. Research regarding the co-disposal of MSW with industrial sludge is limited. Studies have been conducted in laboratory-scale reactors to investigate co-disposal of MSW with heavy metal sludge (Pohland and Gould 1986), dye industry sludge (Agdag and Sponza 2005), and mixed sludge from textile, metal plating, electronic, chemical, and plastic industries (Agdag and Sponza 2007). Pohland and Gould (1986) found that higher loading rates of heavy metal sludge inhibited landfill microbial processes, but landfills were able to acclimate at low sludge loading levels. Agdag and Sponza (2005) reported that high concentrations of dye industry sludge containing metals showed toxic effects, but low concentrations of trace metals provided nutrients that positively influenced methanogenic growth. Overall leachate quality was improved with sludge co-disposal but CH<sub>4</sub> generation decreased (Agdag and Sponza 2005). In a follow-up study investigating a mixed source of industrial sludge, Agdag and Sponza (2007) reported that industrial sludge co-disposal improved leachate quality and had a stimulatory effect on CH<sub>4</sub> generation, which suggested co-disposal of MSW with mixed industrial sludge was a viable management technique.

The co-disposal of sewage sludge with MSW has been researched to a greater extent and is the most commonly proposed sludge for co-disposal applications. There is some reluctance from landfill operators to co-dispose sewage solids due to operational difficulties (mixing and compacting), odors, and health risks associated with pathogenic organisms (Townsend et al. 2015). However, when co-disposed with MSW, sewage sludge provides moisture, CH<sub>4</sub> potential, nutrients and a source of anaerobic microorganisms (Watson-Craik and Sinclair 1995; Bae et al. 1998; Townsend et al. 2015). A laboratory-scale study investigating co-disposal of anaerobically digested sludge with MSW indicated that the continuous addition of active methanogens was significantly more effective in waste stabilization than leachate recirculation. In that study, the reactor receiving anaerobic sludge produced 78 times more CH<sub>4</sub> than the reactor recirculating landfill leachate (Bae et al. 1998).

### **2.2.3 Co-Disposal of MSW with Industrial Solid Waste**

Industrial solid waste streams disposed in MSW landfills can also influence biochemistry of the landfill and impact CH<sub>4</sub> generation and leachate quality. Construction and demolition (C&D) waste is one of the larger fractions of solid waste (Townsend et al. 1999; USEPA 2014a), and has been reported to be approximately 20% of total solids (MSW plus C&D) discarded in landfills (Staley and Barlaz 2009). The primary components include concrete, asphalt, wood, metal, gypsum board, cardboard, plastic, soil, and vegetation. Gypsum (CaSO<sub>4</sub>) is the most biologically relevant component of C&D waste and is a major source of corrosion and hydrogen sulfide (H<sub>2</sub>S) production (Fairweather and Barlaz 1998). Hydrogen sulfide gas is toxic and poses a health threat in confined spaces. High H<sub>2</sub>S concentrations can cause rapid corrosion of gas handling equipment, and flared H<sub>2</sub>S converts to SO<sub>2</sub> in the atmosphere (Xu et al. 2011). Sulfate reduction and methanogenesis can occur concurrently, and in fact, sulfate reduction can create reduced environments more suitable for methanogenesis, whereby the onset of CH<sub>4</sub> production is accelerated (Rahim and Watson-Craik 1997; Fairweather and Barlaz 1998).

Foundry waste and automobile shredder residue were identified as absorbent waste materials for moisture retention during liquid waste co-disposal (Bareither et al. 2017). Foundries use high-quality, size-specific silica sands for use in their molding and casting processes. Waste foundry sand typically consists of silica sand and a binder to form molds for ferrous and nonferrous metal castings. The chemical composition of the waste foundry sand depends on the type of metal and binder, but leachate generated from waste foundry sand generally consists of various organic compounds, polyaromatic compounds, phenols, formaldehyde, metals (Pb, Ni, Cu, Zn, and Hg), and mineral oils (Siddique et al. 2010).

Automobile shredder residue is waste that remains from vehicles after recovery of metals and dismantled parts. The shredder residue typically consists of plastics, metals, rubber, textile, foam, glass, and wood. The composition of automobile shredder residue can vary between sites and landfill personnel have reported varying effectiveness as an absorbent material (e.g., less foam and textiles decrease the ability to absorb liquid). Metals contained in shredder residue (Fe, Al, Zn, and Cu) can influence gas production. Studies conducted by Aghdam et al. (2016) found that iron and copper in shredder residue inhibited CH<sub>4</sub> generation, but aluminum and zinc contributed to higher CH<sub>4</sub> percentages and lower CO<sub>2</sub> percentages than typically observed in landfills. Hydrogen production from bio-corrosion of aluminum and zinc can be utilized by methanogens to convert CO<sub>2</sub> to CH<sub>4</sub> (Aghdam et al. 2016).

# Anaerobic Bioreactor

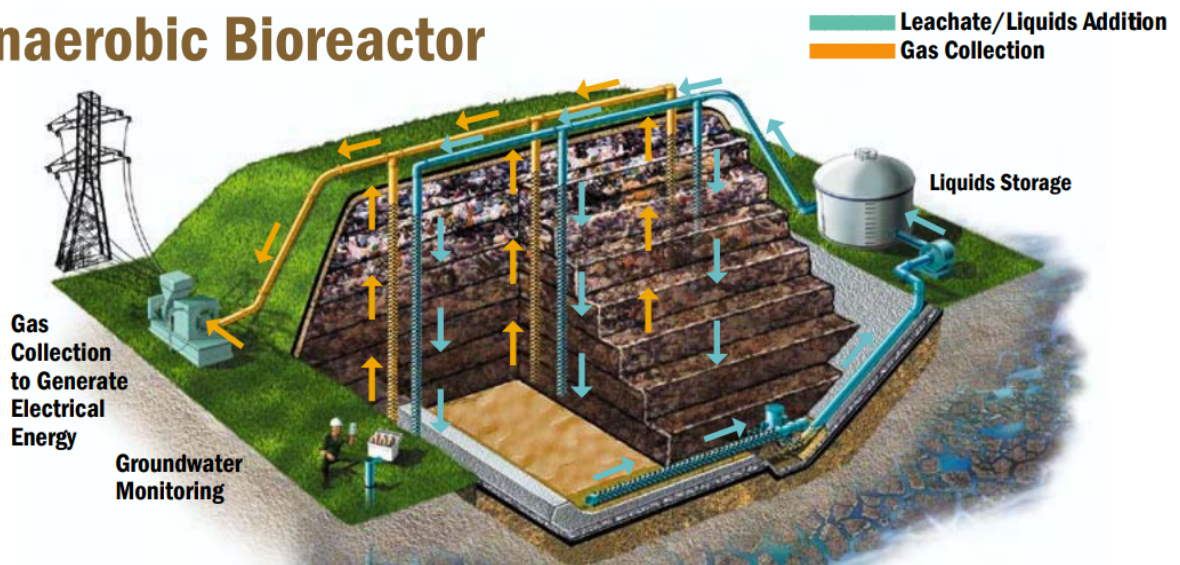


Fig. 1.1. Schematic of an anaerobic bioreactor (Waste Management 2004).

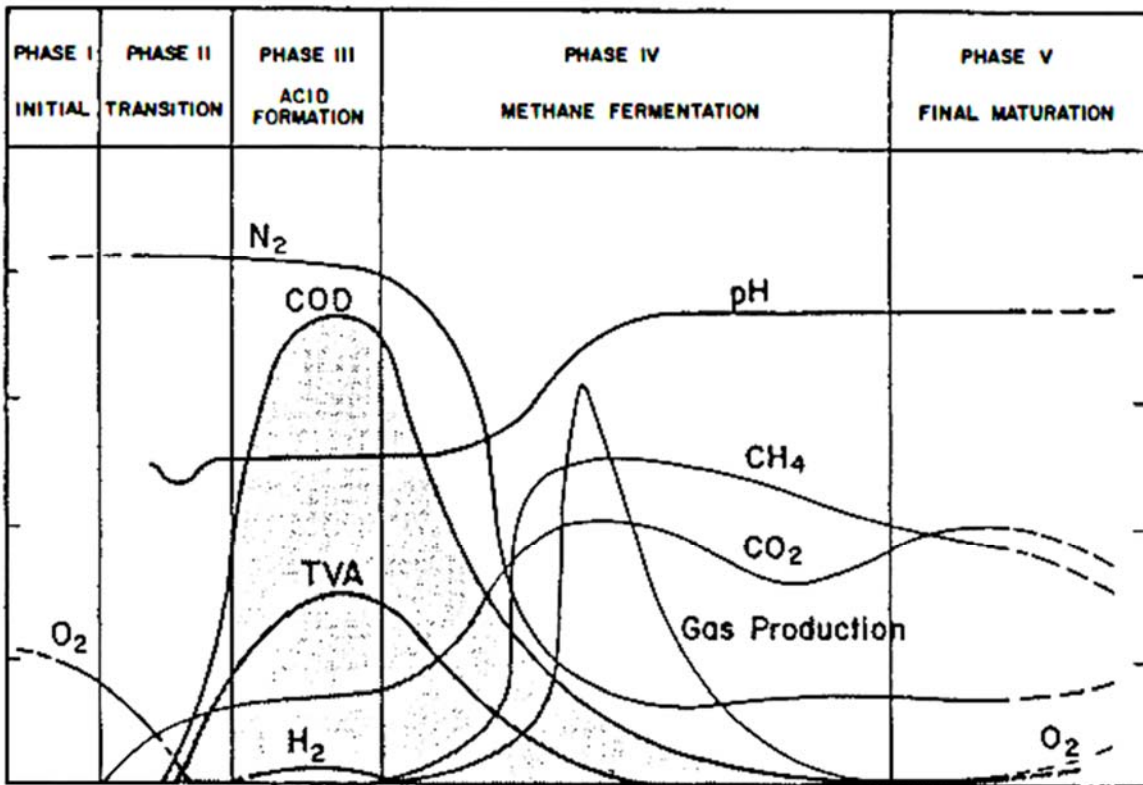


Fig. 1.2. Changes in selected indicator parameters during the phases of landfill stabilization (Pohland and Gould 1986).

## CHAPTER 3: RESULTS AND DISCUSSION

A summary of the co-disposal reactors is in Table 1.1 and includes the following: experiment duration, cumulative liquid recirculated per mass of waste, average weekly dose rate, percent settlement, pH, peak COD, COD reduction, total CH<sub>4</sub> generation, peak percent contribution of CH<sub>4</sub>, and peak CH<sub>4</sub> flow rate. Reactor effluent was recirculated and sampled weekly, whereas gas was analyzed as needed (e.g., higher sampling rates were adopted for reactors that generated more gas). Parameters monitored in the reactors and included in this analysis were effluent recirculation volumes, leachate chemistry [pH, electrical conductivity (EC), oxidation-reduction potential (ORP), COD, ammonia], select heavy metals and inorganic elements in leachate, and CH<sub>4</sub> generation. Complete data sets for the 24 reactor experiments are included in Appendix A (plots and summary data).

Results from the reactors were grouped by reactor type: controls [de-ionized water (DIW) and landfill leachate (LL) reactors], MSW + liquid waste (MSW-LW) [brewery wastewater (BW), cheese production water (CW), automobile wash water (AWW), high-strength manufacturing wastewater (MW-H), and low-strength manufacturing wastewater (MW-L)], MSW + solid waste (MSW-SW) [gypsum board (GB), automobile shredder residue (ASR), and foundry waste (FW)], and MSW + sludge waste (MSW-Sludge) [anaerobic digestion sludge (AD) and industrial sludge (IS)]. In general, the majority of the control and liquid waste reactors remained in the acid formation phase throughout the duration of reactor operation, with exception of LL-1 and MW-L1. The four sludge reactors all reached methanogenesis and there were varied results for the solid waste reactors.

Duplicate reactors showed repeatable results prior to the onset of CH<sub>4</sub> generation. Once CH<sub>4</sub> generation began in one of the duplicates, differences observed in leachate and gas data were likely attributed to the biological activity. Control and liquid waste reactors did not produce considerable CH<sub>4</sub>, and therefore data between duplicates was repeatable. In cases where the duplicates yielded comparable data, the data were averaged for clarity when preparing summary graphs. Several of the solid waste reactors and all of the sludge waste reactors produced CH<sub>4</sub> and exhibited variations in temporal monitoring data due to differences in the onset and extent of biological activity; these reactors are discussed individually.

### 3.1 Physical Reactor Characteristics

#### 3.1.1 *Recirculation Volumes*

Cumulative recirculation volumes, excluding the initial dosing, and average weekly dose rates for the reactors are in Table 1.1. Liquid was added to each reactor with a series of initial doses intended to exceed the moisture holding capacity of the waste and generate effluent for subsequent sampling and recirculation. The initial dose volumes ranged from 450 to 1800 mL (188 to 750 L/Mg-waste), with a target volume of 1500 mL to represent typical liquid dosing rates in liters of liquid added per mass of total waste (L/Mg-waste) in full-scale landfills (Bareither et al. 2010; Nwaokorie et al. 2017). Dry-weight water contents after dosing ranged from 60% to 150%; the highest water contents were in the MSW-Sludge reactors and lowest were in the MSW-SW reactors, which reflected differences in moisture holding capacity as a function of waste composition. The dry-weight water after initial dosing in all MSW-LW reactors and the MSW reactor with DIW were similar, and ranged between 97% and 108%, indicating that moisture retention of the MSW was similar for the six different liquid wastes and DIW.

Weekly recirculation rates after initial dosing ranged between 39 and 85 L/Mg-waste. These rates were comparable to recirculation rates used in similar laboratory-scale bioreactor experiments (Bareither et al. 2012a; Bareither et al. 2013) and were representative of recirculation operations implemented in full-scale bioreactor landfills (Benson et al. 2007;

Bareither et al. 2010; Barlaz et al. 2010). Cumulative liquid recirculated into the reactors ranged from 1224 to 3584 L/Mg-waste. These amounts are above the upper-end of the range of cumulative leachate recirculation and liquid addition reported in literature for full-scale bioreactor landfills (e.g., Bareither et al. 2010).

Reactors received supplemental dosing of fresh liquid (e.g., liquid waste) when sampling depleted the quantity of effluent available to an amount that prohibited further sampling. The DIW control, brewery wastewater, high-strength manufacturing wastewater, and automobile shredder residue (recirculated with landfill leachate) reactors received an additional 200 mL of liquid during reactor operation.

### **3.1.2 Settlement**

The initial specimen thicknesses ranged from 121 mm to 208 mm, resulting in total densities ranging between 0.35 and 0.61 g/cm<sup>3</sup> ( $\approx$  590 and 1030 lb/yd<sup>3</sup>). These densities agree with MSW landfill densities for low-effort compaction and minimal soil in the waste composition based on the compilation of MSW density reported in Zekkos et al. (2006). Waste settlement was aided in each reactor via a gravel layer placed above the waste specimens, exerting a 2 kPa vertical stress. Waste settlement strain ranged from 1.7% to 15.9% (Table 1.1). The average settlement observed in the reactors (6.6%) was at the low range relative to settlement observed in bioreactor landfills (3-25%) (Benson et al. 2007). The low magnitudes of settlement observed in the reactors were attributed to compaction of the waste specimens, the small surface stress applied by the gravel layer (Bareither et al. 2012b), and incomplete waste decomposition. Analyses were not conducted to assess contributions of settlement that developed due to loading, creep, or biocompression.

## **3.2 Leachate Quality**

Leachate from full-scale MSW landfills contains four types of pollutants: dissolved organic matter, inorganic macrocomponents, heavy metals, and xenobiotic organic compounds (Kjeldsen et al. 2002). In this study, reactor leachate chemistry was analyzed to investigate the first three types of pollutants. Leachate composition and presence of select contaminants are dependent on the waste decomposition phase. Indicator parameters (pH, COD, ORP) were used to determine the decomposition phase in each reactor. Leachate strength was assessed via COD, ammonia, and EC, which were used to assess effectiveness of the waste to provide leachate treatment. Heavy metals and inorganic macrocomponents were quantified to assess ability of the waste to mobilize or release potential pollutants. The heavy metals and inorganic macrocomponents evaluated for each of the reactors are compiled in Appendix B.

### **3.2.1 Leachate Composition – Bulk Parameters**

Temporal trends of reactor leachate pH, ORP, COD, and ammonia are shown in Figs. 1.3, 4, and 5 for MSW-LS, MSW-SW, and MSW-Sludge reactors, respectively. Electrical conductivity trends were similar to COD and were not included (EC data are in Appendix A). Leachate chemistry at the end of the experiments generally agreed with ranges of pH, COD, EC, and ammonia for full-scale MSW landfills (e.g., Kjeldsen et al. 2002; Barlaz et al. 2010).

The pH of the reactor leachate was monitored to determine if acidic conditions were present in the waste. Landfill leachate typically has pH ranging between 4.5 and 9.0 (Kjeldsen et al. 2002). The final pH ranged from 5.7 to 6.1 in the LL and DIW reactors, from 5.8 to 7.9 in the MSW-LW reactors, from 6.0 to 7.5 in the MSW-SW reactors, and from 7.8 to 8.2 in the MSW-Sludge reactors (Table 1.1). The MW-L1, GB, FW, AD, and IS reactors achieved a neutral pH during the experiment.

Oxidation-reduction potential was monitored to determine if a reducing environment suitable for CH<sub>4</sub> generation was achieved (i.e., ORP < -200 mV). Oxidation-reduction potential less than -200 mV was measured in the MW-L1, GB, FW, AD, and IS reactors. These reactors also generated CH<sub>4</sub> (described subsequently), which supports the leachate chemistry trends in pH and ORP.

Reactor leachate COD was monitored to determine leachate strength and when organic acids were generated (increasing COD) and either buffered or mineralized to biogas (decreasing COD). Landfill leachate COD can encompass a broad range in full-scale landfills, from 140 to 152,000 mg O<sub>2</sub>/L (Kjeldsen et al. 2002). The COD measured in the reactor experiments was within the range reported for full-scale landfills, with the highest COD achieved in the brewery wastewater reactors (peak COD = 65,720 mg-O<sub>2</sub>/L in BW-1, Table 1.1). The DIW, LL, and all MSW-LW reactors exhibit increasing or constant COD trends during reactor operation. The one exception was MW-L1, which was the only liquid waste reactor to achieve methanogenesis and displayed a decreasing COD concentration starting on Day 200 of operation (Fig. A-7 in Appendix A). The MSW-Sludge reactors as well as the GB and FW reactors exhibited increasing COD concurrent with hydrolytic degradation that was followed by decreasing COD trends during active methanogenesis. In the reactors where COD appeared to continue to increase, acid generating microorganisms were likely the dominant microbial community.

Ammonia was measured in all reactors to evaluate if elevated ammonia concentrations were established and whether these could be linked to potential reactor inhibition. Ammonia inhibition of methanogenesis has been reported at concentrations as low as 1,700 mg NH<sub>3</sub>-N/L (Chen et al. 2008), but concentrations up to 2,200 mg NH<sub>3</sub>-N/L are typical in landfill leachate (Kjeldsen et al. 2002). The brewery wastewater (BW in Fig. 1.3d) and the industrial sludge reactors (IS-1 and IS-2 in Fig. 1.5d) generated ammonia concentrations that exceeded the low-end inhibition threshold of 1,700 mg NH<sub>3</sub>-N/L. The brewery wastewater did not exceed the typical landfill leachate range for ammonia, and inhibition in the BW reactors, as well as all of the other liquid waste reactors, was most likely due to acidic conditions rather than ammonia concentrations. Although both industrial sludge reactors exceeded ammonia concentrations of 2,500 mg NH<sub>3</sub>-N/L, ammonia did not inhibit CH<sub>4</sub> generation, as CH<sub>4</sub> generation was observed in both of the IS reactors.

The electrical conductivity of the reactor leachate is presented with the complete reactor data sets in Appendix A. Typical leachate EC reported for landfills ranges from 2.5 to 35 mS/cm (Kjeldsen et al 2002). Approximately half of the reactors (DIW-1 & 2, LL-1 & 2, BW-1 & 2, AWW-1 & 2, MW-H1, MW-L1 & 2, FW-2, and IS-2) exceeded the 35 mS/cm threshold at some point during the experiment, but all values were within the range reported by Kjeldsen et al. (2002) at the final day of leachate sampling. Temporal trends in EC were similar to COD trends, whereby EC increased with COD generation and decreased with COD removal.

### **3.2.2 Leachate Composition – Elemental Analysis**

Liquid wastes and reactor leachate samples were analyzed for heavy metals and other common elements found in landfill leachate. Results from the ICP analysis for the liquid wastes sources, the initial recirculated volume of leachate generated, and the final volume of leachate generated are discussed briefly here. The complete data set is reported in Appendix B. Results were compared to typical landfill leachate concentrations as well as federal drinking water maximum contaminant levels (MCL – 40CFR 141.11) and non-enforceable secondary MCL concentrations (40CFR 143.3). Heavy metals and other elements generally did not exceed typical concentrations reported for landfills (Kjeldsen et al. 2002), but several MCL and secondary MCL concentrations were exceeded.

With few exceptions, heavy metal and inorganic component concentrations increased with one recirculation through the waste mass relative to concentrations measured in the initial wastewater source. Final concentrations in the recirculated reactor leachate did not exceed typical landfill leachate concentrations in literature (Kjeldsen et al. 2002). Phosphorus was the exception, whereby the concentration in most reactors exceeded 23 mg/L at the initial measurement and after the duration of the experiment. In the majority of reactors, Ca, Fe, K, Mn, Na, Ni, Pb, and Zn concentrations increased with recirculation. In all of the reactors, the concentration of Al, Cd, Cu, and P decreased with recirculation.

Maximum contaminant levels for Cd, Cr, and Pb were exceeded in several reactors at the end of the experiment. Secondary MCL concentrations were exceeded for Mn in all reactors, Fe in all but one reactor, and Al and Zn in several reactors at the end of the experiment. However, none of these concentrations exceeded limits typical of landfill leachate.

Increases in Na concentrations were observed in most of the reactors. The increase in Na concentration was attributed to the use of NaOH to buffer the reactor leachate and increase pH prior to recirculation. Sodium can be inhibitory at concentrations as low as 3,500 mg/L (Chen et al. 2008), but concentrations in the reactor leachate did not exceed this threshold.

### **3.3 Transition to Methanogenesis**

#### **3.3.1 Leachate Indicator Parameter Trends**

In the reactor experiments, pH, ORP, and COD were used as leachate indicator parameters to determine if a reactor was transitioning from the acid formation phase to methanogenesis. Concurrent increasing pH and decreasing COD trends are indicative of the conversion of organic acids to biogas. A decrease in ORP to negative values indicates development of a reduced environment suitable for CH<sub>4</sub> generation.

Leachate chemistry data for the liquid waste co-disposal reactors, previously presented in Fig. 1.3, suggest that the DIW reactors and nearly all liquid waste reactors were potentially stuck in the acid formation phase. The pH appeared to decrease in all control and liquid waste reactors until approximately 60 d, and then appeared to increase. The potential increase in pH from Day 60 onwards was likely attributed to leachate buffering with NaOH, which was used to help prevent stagnant acidic conditions. Oxidation-reduction potential for the control and liquid waste reactors converged to approximately -100 mV (Fig. 1.3b), which typically is not low enough for a favorable methanogenic environment. In the majority of the liquid waste reactors, COD showed an increasing trend, indicating generation and subsequent accumulation of organic acids. The two greatest strength liquid wastes (BW and MW-H) showed high but fairly constant COD throughout the experiments.

Noteworthy methane generation only was observed in the two landfill leachate reactors (LL-1 and LL-2) and one of the low-strength manufacturing wastewater reactors (MW-L1). The onset of CH<sub>4</sub> generation from the landfill leachate reactors was anticipated; however, both reactors were slow to transition and leachate chemistry at the end of the experiment on Day 253 for both LL reactors still showed low pH and high COD concentration. The MW-L1 reactor was the only MSW-Liquid co-disposal reactor that successfully achieved methanogenesis (Fig. A-7). Although the reasons for this transition to methanogenesis were unknown relative to the other liquid waste reactors, the successful transition to methanogenesis suggests that liquid waste can be used as the sole source of liquid to achieve anaerobic biodegradation in MSW.

Leachate chemistry trends in the MSW-SW (Fig. 1.4) and MSW-Sludge (Fig. 1.5) reactors exhibited variability that was more pronounced during operation as compared to the liquid waste reactors. The main factor influencing temporal variability in leachate chemistry in the solid waste and sludge reactors was the development of methanogenesis in select reactors. For example, leachate chemistry trends in the industrial sludge reactors (IS-1 and IS-2) and

anaerobic digestion sludge reactors (AD-1 and AD-2) exhibited increasing pH, ORP < -200 mV, and decreasing COD, which are all coincident with active methanogenesis (e.g., Pohland and Gould 1986; Reinhart and Al-Yousfi 1996). The solid waste reactors with gypsum board (GB-1 and GB-2) also exhibited similar temporal trends of leachate chemistry that coincided with methanogenesis. The FW reactors showed trends in leachate chemistry consistent with the acid generation phase, and FW-1 successfully achieved and appeared to complete methanogenesis. The ASR reactors were the only set of MSW-SW reactors that did not achieve a neutral pH, low ORP, or decreasing COD concentration and did not produce measurable CH<sub>4</sub> flow rates (biogas discussed subsequently).

### **3.3.2 Biogas Generation and Anaerobic Biodegradation**

Total CH<sub>4</sub> generation, peak percent CH<sub>4</sub> composition, and peak CH<sub>4</sub> generation rate are tabulated for each reactor in Table 1.1. Although methane gas was detected in all reactors, half of the reactors did not generate more than 1 L of methane during operation. The DIW control reactors did not achieve methanogenesis, whereas both LL reactors did; LL-1 yielded approximately 50 L of CH<sub>4</sub> and LL-2 was transitioning to active methanogenesis when terminated. The only MSW-Liquid waste reactor that generated considerable CH<sub>4</sub> was MW-L1, whereas all other MSW-Liquid waste reactors generated less than approximately 1 L of CH<sub>4</sub>. Regarding the MSW-Solid waste reactors, the GB and FW reactors reached methanogenesis, whereas the ASR reactors did not. Finally, all four MSW-Sludge reactors (AD and IS) were very methanogenically active.

Temporal trends of methane generation in the LL and MW-L reactors are shown in Fig. 1.6. Similarity in methane generation yield was observed for LL-1 and MW-L1, whereas LL-2 was starting to generate methane at the time of reactor termination and MW-L2 yielded only 0.2 L of methane. Temporal trends of leachate pH and COD accompanied with methane generation for the LL and MW-L reactors are shown in Fig. 1.7. The two reactors that did not yield considerable methane (LL-2 and MW-L2) were characterized by high COD concentrations ( $\geq 40,000$  mg-O<sub>2</sub>/L) and pH < 6 throughout the duration of reactor operation. These leachate chemistry trends are consistent with pronounced hydrolysis and acidogenesis, and an absence of methanogenesis (i.e., acid stuck conditions). In contrast, MW-L2 exhibited a decrease in COD and increase in pH with the onset and subsequent generation of methane. Although LL-1 also reached methanogenesis and generated a similar amount of methane to MW-L1 (Fig. 1.6), leachate chemistry trends did not express a decrease in COD or increase in pH during methane generation. The reason for the lack of change in the leachate chemistry signature of LL-1 was unknown, particularly considering all other reactors in this study that yielded considerable methane expressed the anticipated trends of decreasing COD and increasing pH.

Adding landfill leachate to MSW and subsequently recirculating leachate has been shown effective for establishing anaerobic biodegradation. Although LL-2 only began to generate methane at the time of reactor termination (Fig. 1.7b), continuing that reactor experiment would have led to additional methane generation. Active biodegradation is anticipated with landfill leachate dosing and recirculation as leachate commonly contains an active source of anaerobic microorganisms that promote biodegradation. Establishment of methanogenesis via the addition low-strength manufacturing wastewater and subsequent recirculation of leachate generated from this liquid waste addition was a notable outcome from the MSW-Liquid waste reactors. The relevant anaerobic microorganisms necessary for biodegradation of organic waste could have been present in the low-strength manufacturing wastewater or within the MSW. Considering that only MW-L1 reached methanogenesis and MW-L2 remained acid stuck, additional research is needed to investigate potential sources of anaerobic microorganisms with the MSW and MW-L. Considering that only MW-L1 reached active methanogenesis among all MSW-Liquid waste reactors operated in this study, co-

disposal of MSW and industrial liquid wastes does not appear to be an effective method for establishing anaerobic biodegradation in MSW.

Temporal trends of cumulative CH<sub>4</sub> generation in the MSW-Sludge reactors are shown in Fig. 1.8. The anaerobic digester sludge reactors, AD-1 and AD-2, produced 86 L and 68 L, respectively, and the industrial sludge reactors, IS-1 and IS-2, produced 67 L and 74 L, respectively. The AD reactors achieved the highest CH<sub>4</sub> generation rates, with AD-1 producing 1.9 L/d and AD-2 producing 1.5 L/d. An active anaerobic microbial community that was present in the AD sludge most likely aided the development of active methane generation in reactors.

Temporal trends of leachate chemistry (pH and COD) and cumulative CH<sub>4</sub> generation that highlight the transition to methanogenesis for the anaerobic digestion sludge reactors (AD-1 and AD-2) and the industrial sludge reactors (IS-1 and IS-2) are shown in Fig. 1.8. As noted previously, methanogenesis developed in all sludge reactors, which coincided with an increase in pH, decrease in COD, and increase in CH<sub>4</sub> generation that occurred simultaneously. The acceleration of methane production phase in all four sludge reactors coincided with a decrease in COD that occurs when a proliferating population of methanogenic microorganisms consumes readily-available soluble organic constituents in the liquid phase. These trends were identical to those trends of anaerobic biodegradation observed for MW-L2 (Fig. 1.7c). The sludge wastes used for the co-disposal experiments in this study appeared beneficial for anaerobic biodegradation. Furthermore, in comparison to the landfill leachate control reactors (Fig. 1.8), the industrial sludge and anaerobic digestion sludge accelerated the onset of methanogenesis.

Temporal trends of cumulative CH<sub>4</sub> generation in the MSW-SW reactors are shown in Fig. 1.10. The solid wastes that generated considerable amounts of methane (i.e., GB-1 and FW-1) produced 5.2 L and 42.8 L, respectively. Their counterpart reactors, GB-2 and FW-2, only generated 1.3 L and 3.7 L, respectively. The range of methane generation observed and the delay in the onset of methanogenesis between duplicates could be a result of the heterogeneous nature of solid waste.

Temporal trends of leachate chemistry (pH and COD) and cumulative CH<sub>4</sub> generation for the GB and FW reactors are shown in Fig. 1.11. The FW-1 reactor (Fig. 1.11c) exhibited the anticipated trends in leachate chemistry with the onset and subsequent establishment of methanogenesis (i.e., decreasing COD and increasing pH). Leachate chemistry data for FW-2 exhibited a transition to decreasing COD and increasing pH at the time of experiment termination. Thus, FW-2 may have been initiating a transition from the acid stuck conditions of the first 200 days of operation to active methanogenesis at the time the experiment was terminated.

The temporal trends of leachate COD and pH in the GB reactors were unique and different from all other reactor data. Leachate pH neutralized to approximately 7 as the concentration of COD began a slow decreasing trend that appeared to continue throughout the entire duration of the experiment. Furthermore, the COD concentrations measured in the GB reactors were lower (peak COD < 30,000 mg-O<sub>2</sub>/L) relative to the other reactors that generated methane. Low COD concentrations were observed in similar MSW-gypsum board reactor experiments conducted by Fairweather and Barlaz (1998). Although methane was generated in both reactors, generation peaked early with the neutralization of pH (see Appendix A, Fig. A-8c) and then continued at a flow rate less than 0.02 L/d. These observations suggest that the addition of gypsum board to MSW was inhibitory to methane generation.

### **3.3.3 Biogas Composition**

Temporal trends in methane composition for the low-strength manufacturing wastewater, MSW-SW, and MSW-Sludge reactors are shown in Fig. 1.12. The trends of methane composition measured in the LL reactors are reproduced in each plot in Fig. 1.12 for comparison. Typical CH<sub>4</sub> composition in landfills undergoing active anaerobic decomposition

ranges from 50-60% (Amini et al. 2012). The peak CH<sub>4</sub> composition in the LL-1, MW-L1, and both AD and IS reactors reached peak CH<sub>4</sub> concentrations ranging between 64 and 70%. The CH<sub>4</sub> composition observed in these reactors was consistent with typical landfills and indicative of established methanogenesis. Reactor FW-1 achieved a CH<sub>4</sub> composition of 58% and Reactor FW-2 achieved a CH<sub>4</sub> composition of 58%, which also agree with the typical range for landfills.

The GB-1 reactor exhibited decreasing CH<sub>4</sub> composition with time compared to the other reactors generating CH<sub>4</sub>, and only achieved a peak CH<sub>4</sub> composition of 34%. GB-2 also exhibited low CH<sub>4</sub> content, and only achieved a peak composition of 15%. Gypsum board has high sulfate content, and potential sulfate reduction was noted in the GB reactors by the black coloration that developed (photograph included in Appendix C) and the observed odors of H<sub>2</sub>S gas (Rahim and Watson-Craik 1996). Hydrogen sulfide gas was only identified via odor; gas samples were not analyzed for the presence of H<sub>2</sub>S. Although sulfate reduction can create favorable conditions for CH<sub>4</sub> generation (i.e., negative ORP), the low and decreasing trend of CH<sub>4</sub> content in GB-1 was likely attributed to competition between sulfate reducing bacteria and methanogens. This trend is consistent with similar MSW-gypsum board reactor experiments that observed decreased CH<sub>4</sub> content, which was attributed to organic carbon being diverted to sulfate reducers (Fairweather and Barlaz 1998).

Methane was detected in the reactor headspace for some of the reactors that did not generate sufficient biogas for volumetric measurement (Table 1.1). For example, headspace samples from the AWW, MW-H, and ASR reactors all indicated peak CH<sub>4</sub> compositions ranging between 15% and 25%. Thus, there appeared to be minor development of anaerobic biodegradation in these reactors; however, establishment of methanogenesis and abundant CH<sub>4</sub> generation never occurred.

### **3.4 Liquid Waste Treatment Implications**

In addition to development of active methanogenesis, waste treatment was also evaluated via reductions in leachate COD. Reactors that reached the CH<sub>4</sub> generation phase showed consumption of organic acids and a reduction in COD (Table 1.1). For example, COD removals ranging from 26,100 to 52,490 mg-O<sub>2</sub>/L (81 to 91% removal of the peak COD) were computed for the MSW-Sludge reactors, which achieved pronounced CH<sub>4</sub> generation. These reactors showed improved leachate quality relative to the initial recirculation of leachate and demonstrated leachate treatment that exists in landfills with active CH<sub>4</sub> generation. The majority of the reactors that remained in the acid formation phase exhibited increasing COD during operation as the generation and accumulation of organic acids continued. The COD concentration of the leachate in the acid stuck reactors was greater than the initial liquid added to the reactors based on the higher COD concentrations. Although a reduction in COD was computed for all reactors (Table 1.1), the lower COD reductions, especially in the MSW-LW and control reactors, were likely attributed to variations in the temporal trend of COD as compared to actual leachate treatment and reduction in COD.

High-strength wastewater treatment by the MSW was observed in the MW-H reactors. High-strength manufacturing wastewater had an initial COD concentration of approximately 370,000 mg O<sub>2</sub>/L (Table 1.4). After initial dosing of the reactor with high-strength manufacturing wastewater, COD of the reactor leachate reduced to less than 50,000 mg O<sub>2</sub>/L in both MW-H reactors with the first recirculation through the waste body (Fig. 1.4c). This immediate reduction in liquid waste COD was likely attributed to adsorption of metals and manufacturing chemicals to MSW components. The high-strength manufacturing wastewater was cloudy white in color and had a relatively high initial solids content (TS = 8.6%, Table 1.4), which was not observed in the translucent brown leachate after percolation through the waste (photographs included in Appendix C). Adsorption of phenolic compounds was observed during recirculation in reactor experiments studying phenolic wastewater co-disposal (Percival and Senior 1998).

Ammonia reduction was observed in the MSW-Sludge reactors (Fig. 1.6d), which demonstrated a potential ability of the industrial and anaerobic digestion sludge to treat ammonia. The concentration of ammonia appeared to initially increase, and then appeared to decrease in all four sludge reactors upon transition from acidic to methanogenic conditions (i.e., between Days 50 to 70 in Fig. 1.6d). The potential reduction in ammonia is an interesting observation considering there is no known mechanism for ammonia degradation under methanogenic conditions. Kjeldsen et al. (2002) stated that the only reported removal mechanism of ammonia in solid waste landfills was through leaching, which suggests an alternative mechanism may have occurred in the sludge reactors to decrease ammonia. Additional research is needed to evaluate potential ammonia treatment in solid waste reactors mixed with industrial sludge or anaerobic digestion sludge.

### 3.5 Biochemical Methane Potential Assays

Biochemical methane potential assays were conducted for 60 d to obtain ultimate CH<sub>4</sub> yields for all of the solid, liquid, and sludge wastes. These relative CH<sub>4</sub> yields (previously reported in Tables 2 and 3) were used to assess the applicability of the BMP test as a co-disposal selection tool for solid and liquid wastes. Plots for CH<sub>4</sub> generation and CH<sub>4</sub> composition are shown in Fig. 1.12 for solid wastes and Fig. 1.13 for liquid wastes. Methane yield was normalized to amount of waste disposed, on a total mass basis, to compare to default values reported for MSW in literature. Methane yield was also normalized on a g-VS basis for solid wastes (Fig. 1.12b) and on a g-COD basis for liquid wastes and the glucose control (Fig 13b).

A glucose positive control was used to ensure that an active inoculum was present and that there were no limiting nutrients. At the end of 60 days the glucose BMP assays generated 187.8 mL-CH<sub>4</sub>/g-COD, which was relatively low compared to the theoretical value of 395 mL CH<sub>4</sub> generated/g COD reduced (Moody et al. 2011). The glucose assay was still increasing in gas generation at 60 d and likely would have achieved a CH<sub>4</sub> yield closer to the theoretical value had the test continued longer than 60 d. The BMP assays on MSW also provided a check on the MSW blend prepared for this study with respect to potential CH<sub>4</sub> yield. At the end of the 60-d BMP test, the CH<sub>4</sub> yield for MSW was 95.3 mL-CH<sub>4</sub>/g-MSW. This CH<sub>4</sub> yield was close to values reported in literature. The USEPA AP-42 (1998) default value for methane generation potential is 100 m<sup>3</sup>-CH<sub>4</sub>/Mg-MSW (100 mL-CH<sub>4</sub>/g-MSW) and more recent BMP experiments yielded an average value of 80 m<sup>3</sup>-CH<sub>4</sub>/Mg-MSW (90 mL-CH<sub>4</sub>/g-MSW) (Chickering et al. 2018).

Liquid waste BMP assays ranged from 0.0 to 22.6 mL-CH<sub>4</sub>/mL-liquid waste. The liquid wastes that were used undiluted for the BMP assays (LL, CW, and AWW) had COD concentrations less than 5 g-COD/L. These low strength liquid wastes did not yield much CH<sub>4</sub> (LL = 0.3, CW = 0.6, and AWW = 0.0 mL-CH<sub>4</sub>/mL-liquid waste). The high variability observed in the AWW data in Fig 13b was potentially attributed to the low COD (0.2 g O<sub>2</sub>/L) and its influence after the data was normalized to g-COD. The high strength liquid wastes (BW = 57.7 and MW-H = 367.1 g COD/L) that were diluted down to 5 g-COD/L produced much higher CH<sub>4</sub> yields (BW = 18.7 and MW-H = 22.6 mL-CH<sub>4</sub>/mL-liquid waste). These higher CH<sub>4</sub> yields suggest that high strength liquid wastes can potentially increase CH<sub>4</sub> yields in co-disposal applications. However, the liquid waste reactors remained in the acid formation phase of decomposition for the extent of the experiment duration; thus, no performance comparisons can yet be made between liquid waste co-disposal and BMP assay results.

The solid and sludge waste BMP assays showed greater variation than the BMP assays on liquid waste, with CH<sub>4</sub> yields ranging from -3.0 to 95.3 mL-CH<sub>4</sub>/g-solid waste. The GB and FW hindered CH<sub>4</sub> generation relative to the blank control assays, as indicated by negative CH<sub>4</sub> yields (GB = -3.0 and FW = -0.2 mL CH<sub>4</sub>/g solid waste). The finding that GB and FW waste potentially inhibited CH<sub>4</sub> generation in the BMP assays contradicts results from the reactor experiments. Reactors GB-1 and FW-1 exhibited relatively high CH<sub>4</sub> generation relative to the

other MSW-SW reactors, and their counterpart reactors, GB-2 and FW-2, did generate small amounts of methane.

The BMP assays on ASR and IS indicate that these two wastes have potential benefit in co-disposal applications based on a  $\text{CH}_4$  yields of 20.0 and 9.2 mL- $\text{CH}_4$ /g-solid waste, respectively. Industrial sludge results from the BMP assays were corroborated with  $\text{CH}_4$  generated in the reactor experiments; however, the potential for IS as a seed source is uncertain based on the addition of MSW landfill leachate to generate effluent in the reactor for subsequent recirculation. The ASR reactors were still in the acid formation phase and cannot be compared to the BMP results. Anaerobic digestion sludge was not tested for  $\text{CH}_4$  yield because the sludge was used as the inoculum source in the BMP assays. The use of AD sludge as a concentrated methanogenic community in the BMP assays, combined with the observation of healthy methanogenic conditions in the reactor experiments (Fig. 1.8), suggests that addition of AD sludge to a landfill can aid solid waste decomposition and  $\text{CH}_4$  generation.

Biogas composition for the BMP assays is reported in Figures 11c and 12c. Regardless of the volume of  $\text{CH}_4$  generated, most of the solid and liquid waste BMP assays converged to a methane content between approximately 60 and 70%, which was similar to the reactor experiments when active methanogenesis was established and was comparable to typical  $\text{CH}_4$  composition of 50-60% reported for landfills (Amini et al. 2012). The gypsum board BMP assays showed decreased  $\text{CH}_4$  content, which only reached 41%. This decreased  $\text{CH}_4$  content was also observed in the gypsum board reactors. The gypsum board had high sulfate content, such that the decreased  $\text{CH}_4$  was likely due to competition with sulfate reducers. Hydrogen sulfide generation was noted in the BMP assays on gypsum board by olfactory observation.

Table 1.1. Summary of reactor experiment duration, cumulative and weekly recirculation volumes, settlement, chemical oxygen demand (COD) peak strength and removal, methane (CH<sub>4</sub>) generation and rate, and CH<sub>4</sub> composition.

Reactor Type	Reactor Name	Experiment Duration [d]	Cumulative Recirculation <sup>a</sup> [L/Mg-Waste]	Average Weekly Dose <sup>a</sup> [L/Mg-Waste]	Settle-ment [%]	pH	Peak COD [mg O <sub>2</sub> /L]	COD Reduction [mg O <sub>2</sub> /L]	Total CH <sub>4</sub> Generation [L]	Peak CH <sub>4</sub> [%]	Peak CH <sub>4</sub> Rate [L/d]
Control	DIW-1	267	1528	42	4.6	6.1	45,780	4680	0.03	5	0.02
	DIW-2	267	2066	57	3.1	6.1	46,150	4230	0.07	4	0.02
MSW-LW	LL-1	253	1838	54	3.1	5.7	52,810	6620	49.5	68	0.99
	LL-2	253	2160	64	4.8	5.8	58,000	1470	6.2	47	0.30
	BW-1	253	1511	44	4.6	5.9	65,720	16,450	0.02	2	0.01
	BW-2	253	2190	64	4.6	6.1	61,540	11,670	0.03	1	0.02
	CW-1	253	1995	59	3.2	6.2	44,680	2850	0.05	7	0.02
	CW-2	253	1485	44	7.1	6.2	43,810	4040	0.003	1	0
	AWW-1	253	2604	77	4.8	5.8	51,760	2760	1.2	23	0.01
	AWW-2	253	2005	59	6.9	6.2	44,400	4090	0.3	16	0.01
	MW-H1	253	2061	61	6.3	5.9	46,380	0	0.4	21	0.02
	MW-H2	253	1390	41	6.2	6.0	50,970	7900	0.08	15	0
	MW-L1	253	1670	49	5.5	7.9	42,660	33,810	68.6	70	1.20
MW-L2	253	2225	65	3.0	5.9	46,240	3540	0.2	16	0.02	
MSW-SW	GB-1	233	2626	85	3.5	6.9	24,140	20,720	5.2	34	0.25
	GB-2	233	1372	44	3.2	7.2	29,980	26,670	1.3	15	0.03
	ASR-1	233	1859	60	1.7	6.6	28,190	3950	0.2	17	0
	ASR-2	233	1224	39	1.7	6.0	29,660	1380	0.5	25	0
	FW-1	233	1353	44	4.2	7.5	45,140	40,080	42.8	58	0.94
	FW-2	233	1318	43	5.0	7.2	50,880	23,060	3.7	59	0.05
MSW-Sludge	AD-1	232	3584	81	15.9	7.8	32,320	26,100	86.4	66	1.90
	AD-2	232	2561	70	12.5	7.9	41,370	34,830	68.4	64	1.46
	IS-1	233	2268	58	9.1	8.2	56,190	50,740	66.7	68	1.12
	IS-2	233	1556	50	5.0	8.1	57,750	52,490	73.7	68	1.86
Average		245	1936	56	5.4	6.6	45,690	16,000	19.8	32	0.43
Min		232	1224	39	1.7	5.7	24,140	0	0.003	1	0
Max		267	3584	85	15.9	8.2	65,720	52,490	86.4	70	1.90

Notes: DIW = de-ionized water; LL = landfill leachate; BW = brewery wastewater; CW = cheese production wastewater; AWW = automobile wash water; MW-H = high-strength manufacturing wastewater; MW-L = low-strength manufacturing wastewater; GB = gypsum board; ASR = automobile shredder residue; FW = foundry waste; AD = anaerobic digestion sludge; and IS = industrial sludge.

<sup>a</sup> Cumulative recirculation and average weekly dose do not include initial dosing; rates based on initial waste mass.

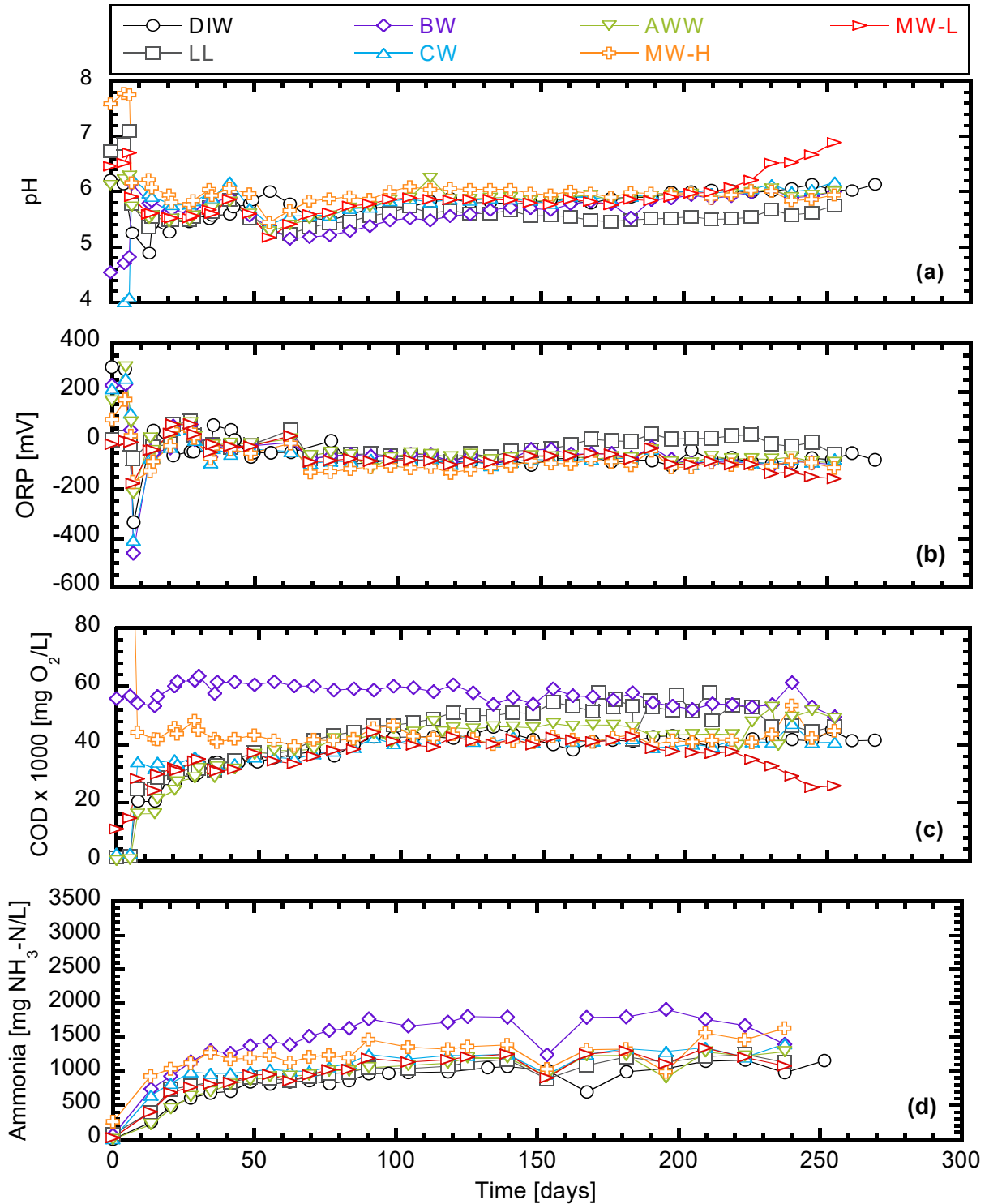


Fig. 1.3. Temporal trends of leachate chemistry in liquid waste reactors: (a) pH, (b) oxidation reduction potential (ORP), (c) chemical oxygen demand (COD), and (d) ammonia. Notes: DIW = de-ionized water, LL = landfill leachate; BW = brewery wastewater, CW = cheese processing wastewater, AWW = automobile wash water, MW-H = high-strength manufacturing wastewater), and MW-L = low-strength manufacturing wastewater.

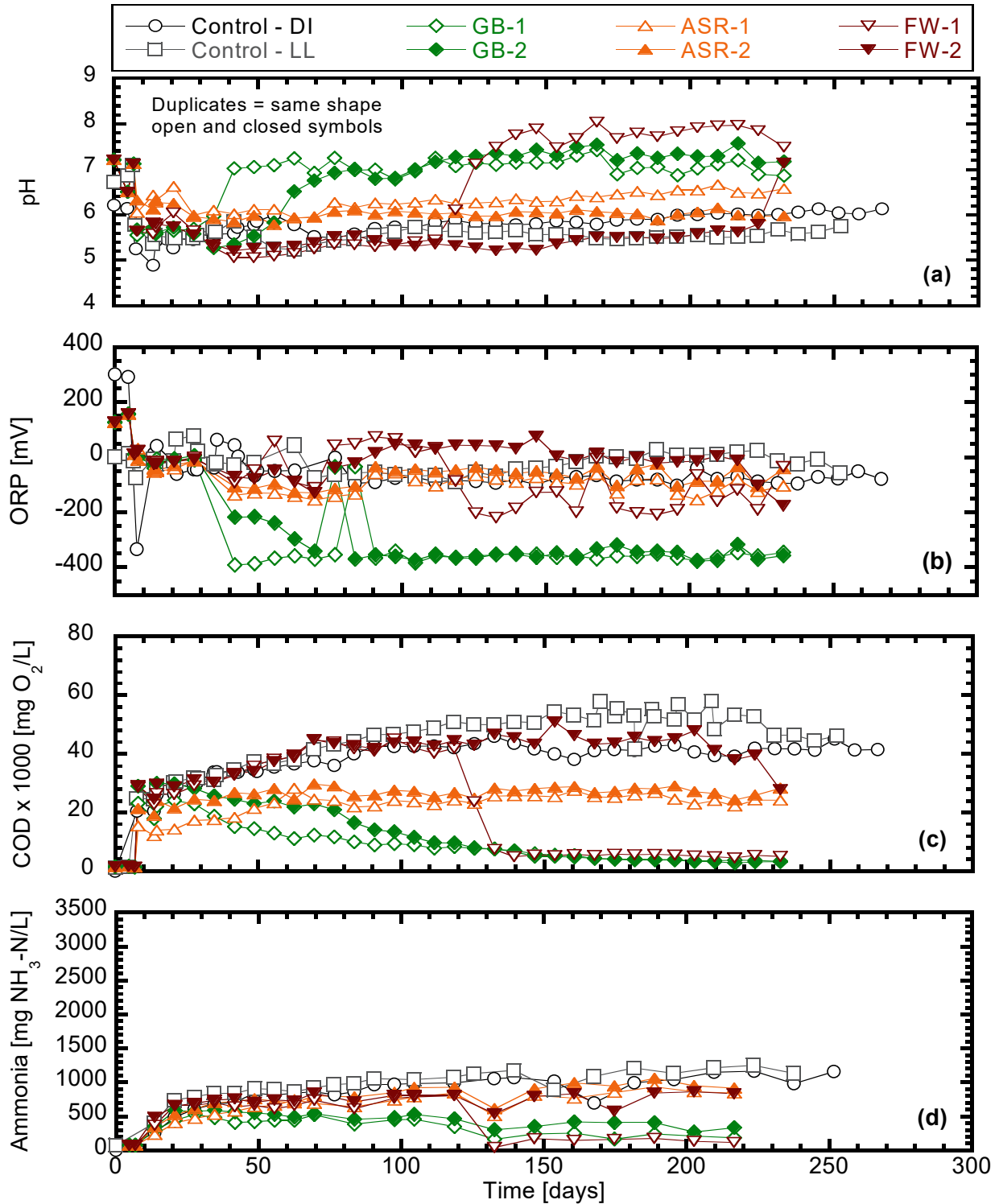


Fig. 1.4. Temporal trends in (a) pH, (b) oxidation reduction potential (ORP), (c) chemical oxygen demand (COD), and (d) ammonia in the solid waste reactors. Notes: DIW = de-ionized water, LL = landfill leachate, GB = gypsum board, ASR = automobile shredder residue, and FW = foundry waste.

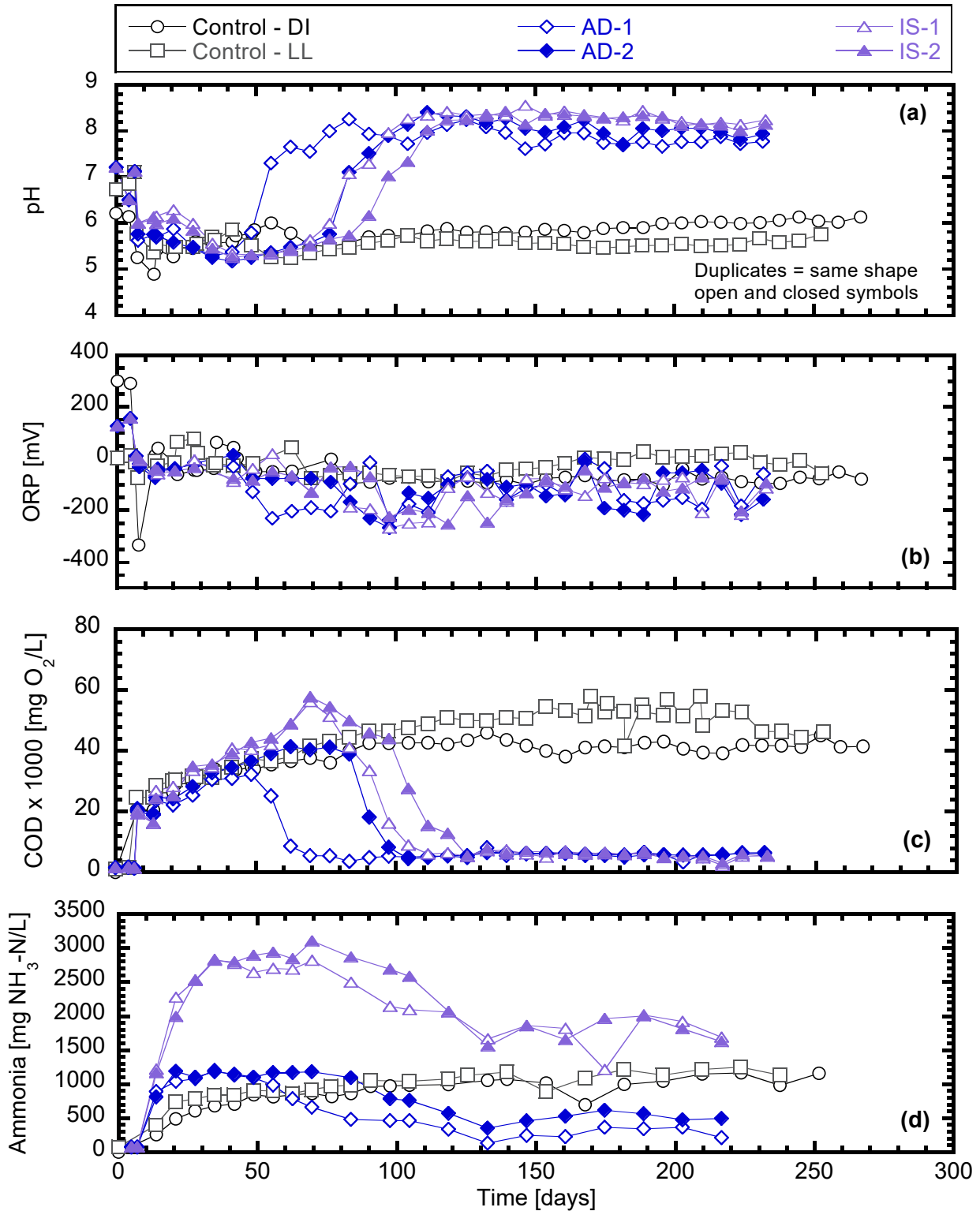


Fig. 1.5. Temporal trends in leachate (a) pH, (b) oxidation reduction potential (ORP), (c) chemical oxygen demand (COD), and (d) ammonia in the sludge waste reactors. Notes: DIW = de-ionized water, LL = landfill leachate, AD = anaerobic digestion sludge, and IS = industrial sludge.

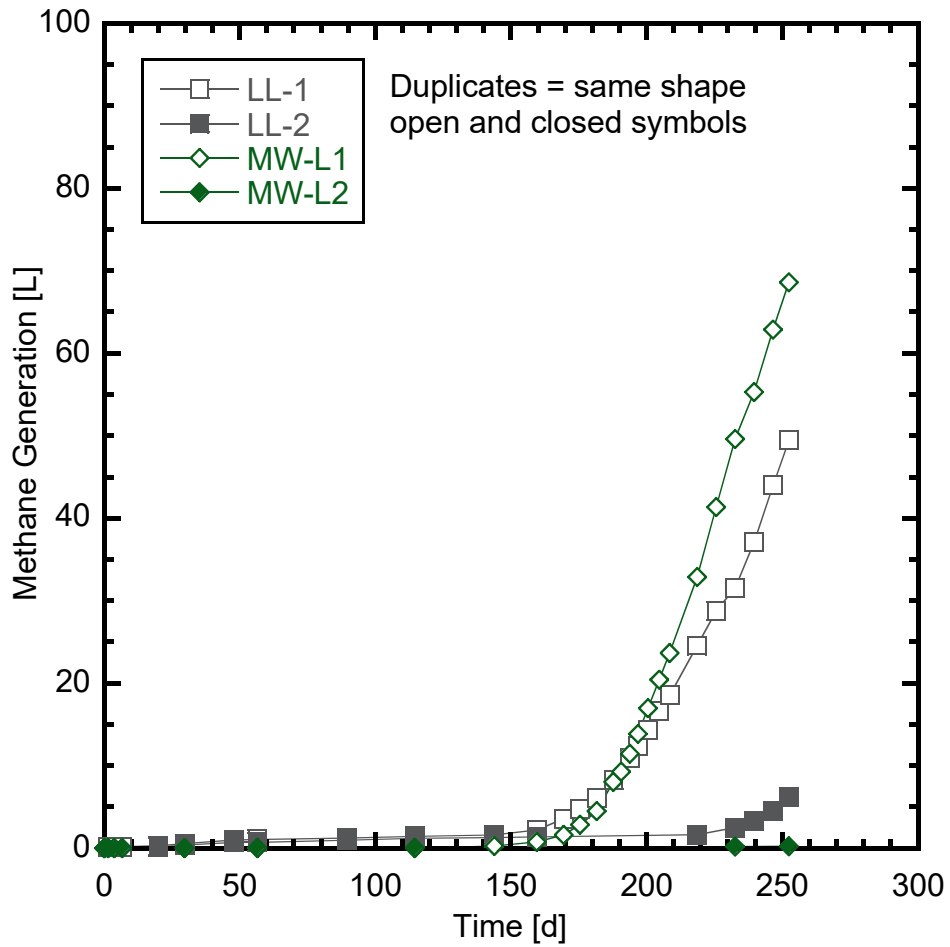


Fig. 1.6. Temporal trends in methane generation in the landfill leachate (LL) and low-strength manufacturing wastewater (MW-L) reactors.

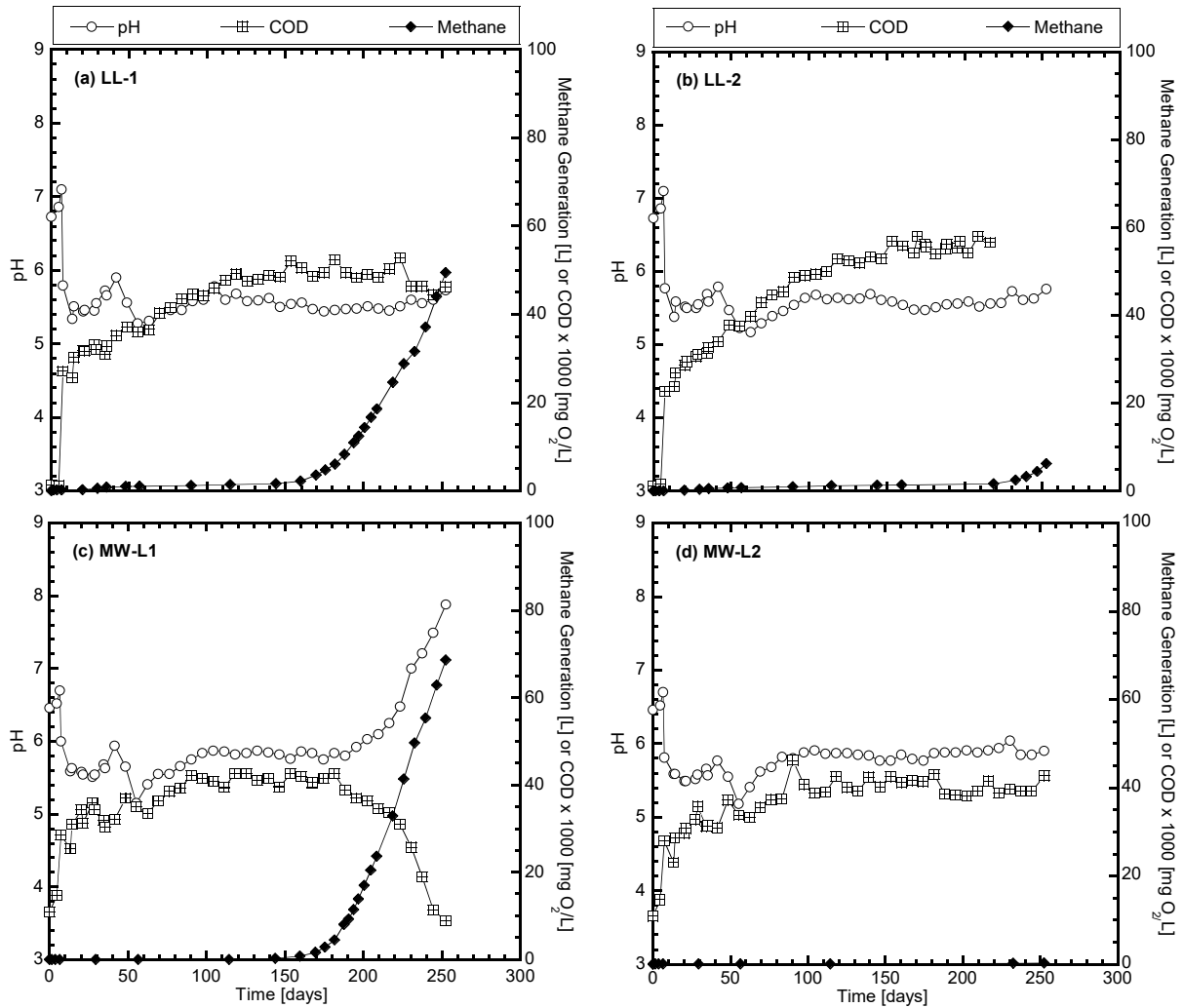


Fig. 1.7. Temporal trends of pH and chemical oxygen demand (COD) in reactor leachate and methane generation for (a) landfill leachate reactor 1 (LL-1), (b) landfill leachate reactor 2 (LL-2), (c) low-strength manufacturing wastewater reactor 1 (MW-L1), and (d) low-strength manufacturing wastewater reactor 2 (MW-L2).

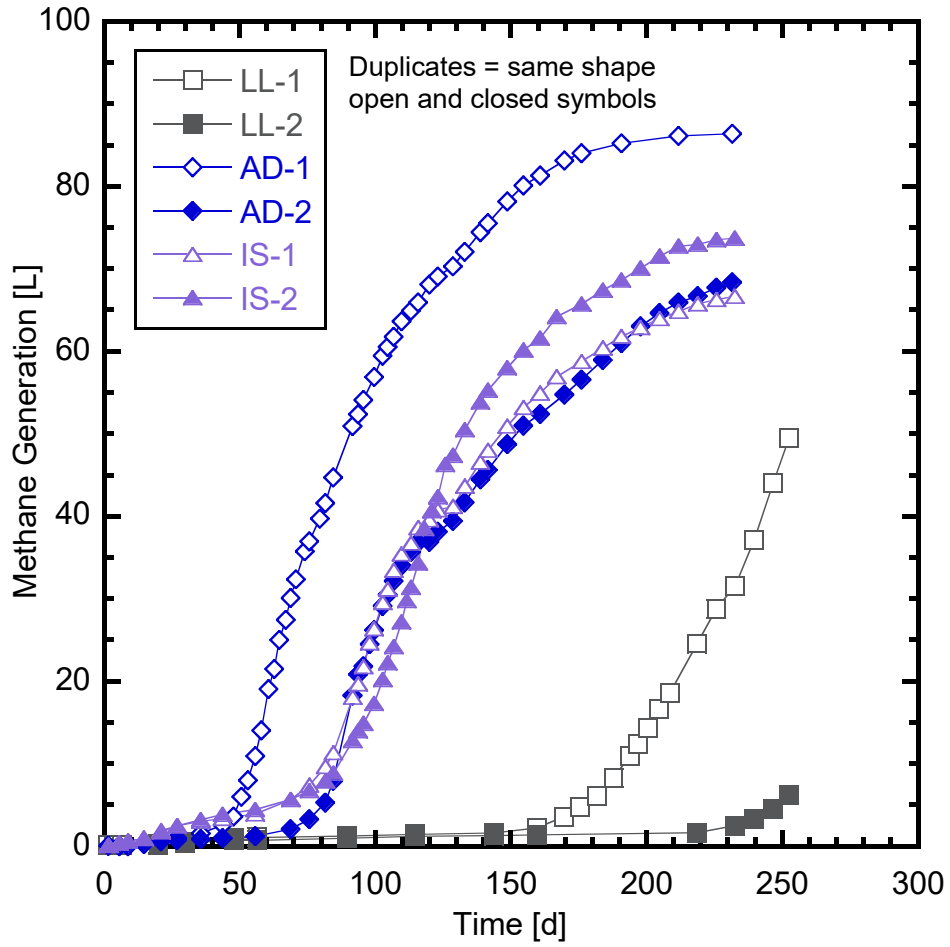


Fig. 1.8. Temporal trends in methane generation in sludge waste reactors. Notes: LL = landfill leachate, AD = anaerobic digestion sludge, and IS = industrial sludge.

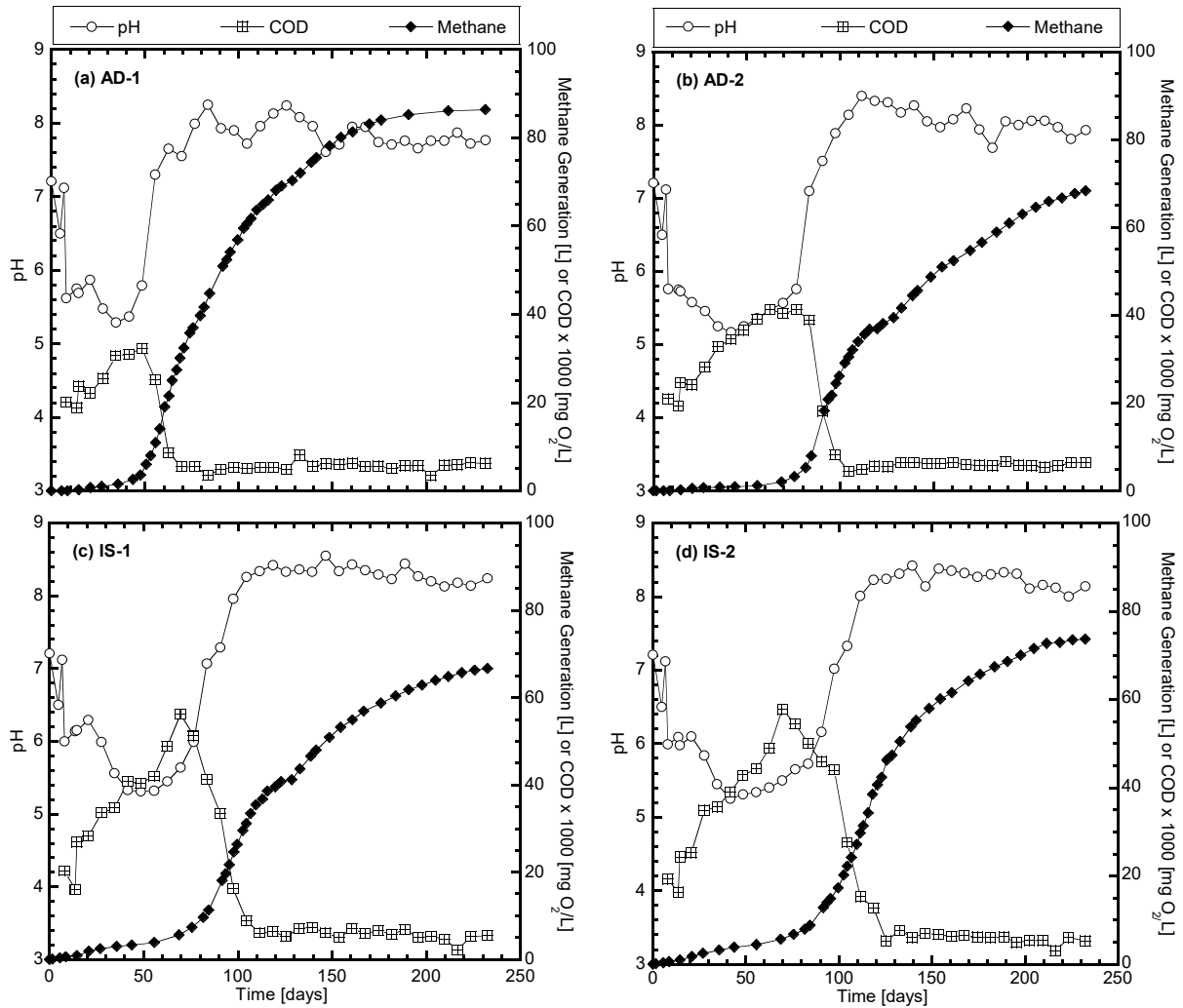


Fig. 1.9. Temporal trends of pH and chemical oxygen demand (COD) in reactor leachate and methane generation of the sludge reactors actively generating biogas: (a) anaerobic digestion sludge reactor 1 (AD-1), (b) anaerobic digestion sludge reactor 2 (AD-2), (c) industrial sludge reactor 1 (IS-1), and (d) industrial sludge reactor 2 (IS-2).

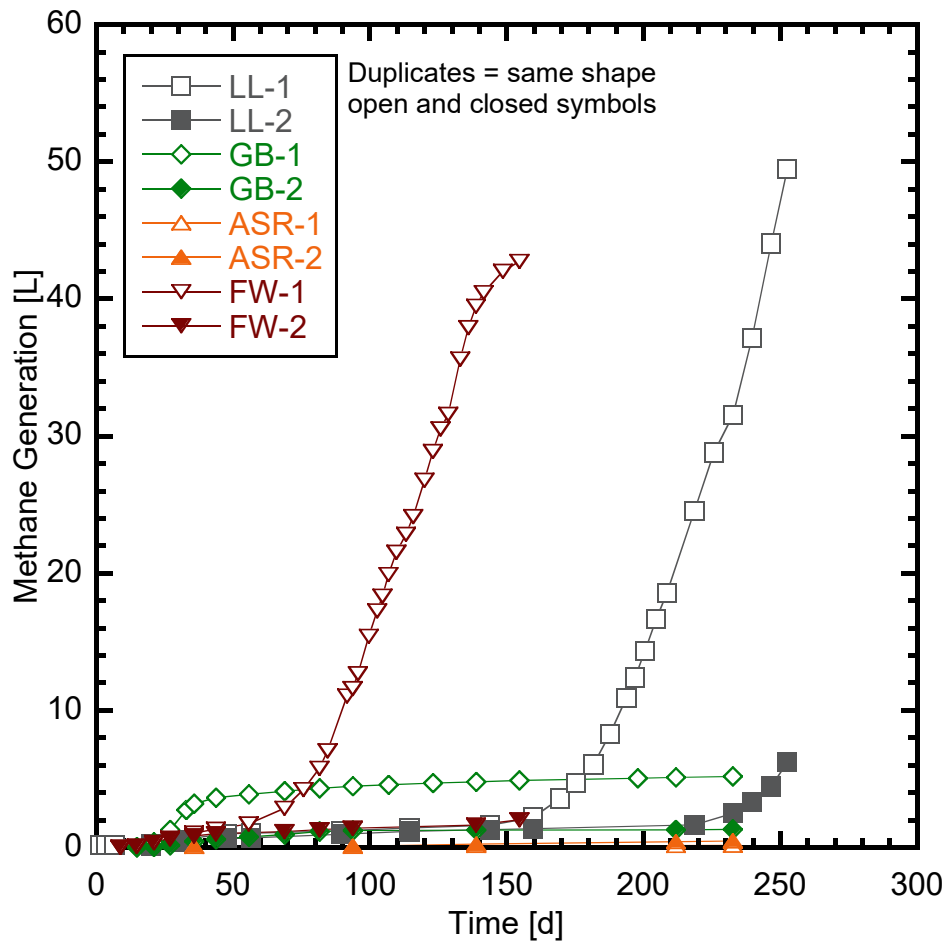


Fig. 1.10. Temporal trends in methane generation in solid waste reactors. Notes: LL = landfill leachate, GB = gypsum board, ASR = automobile shredder residue, and FW = foundry waste.

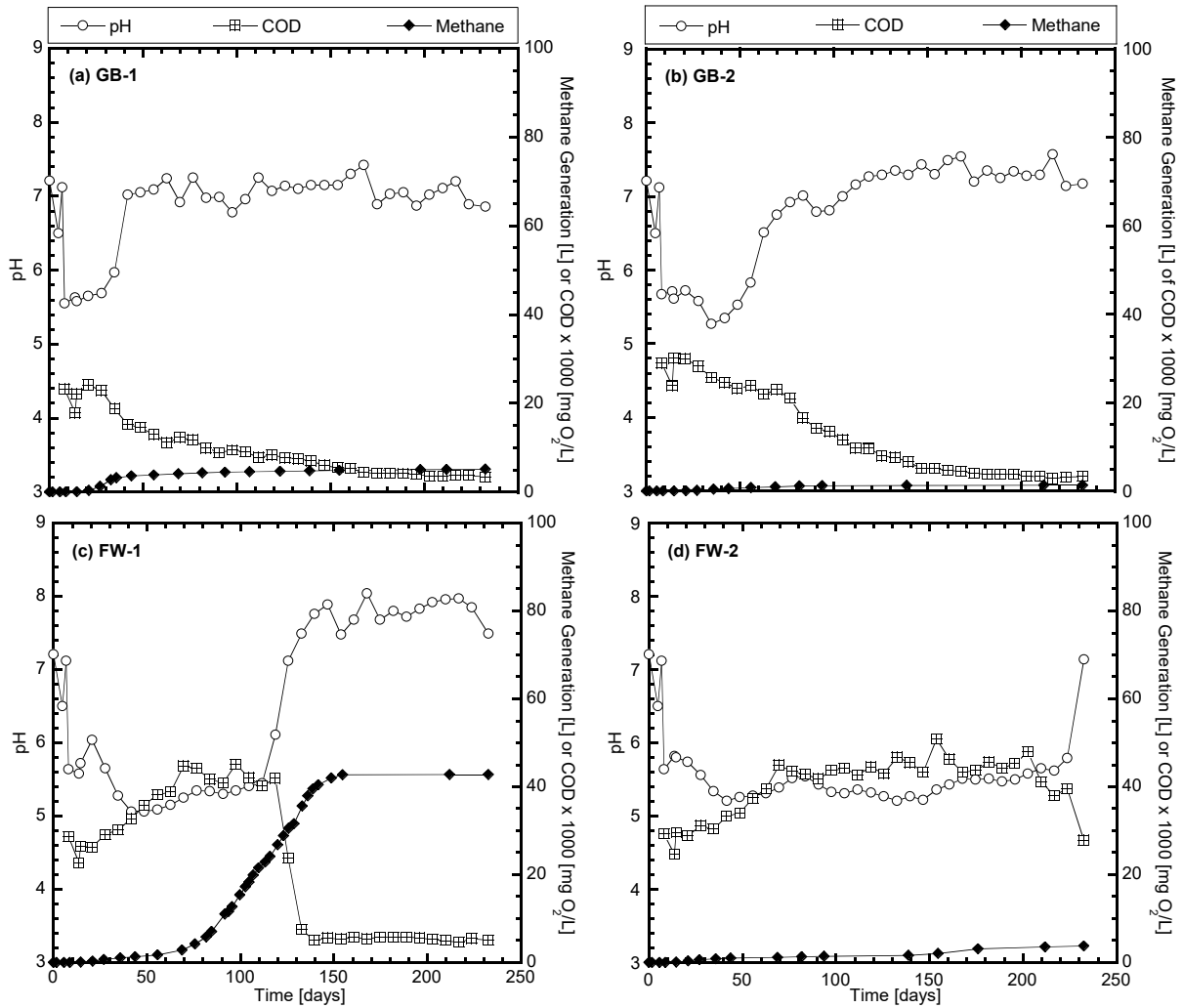


Fig. 1.11. Temporal trends of pH and chemical oxygen demand (COD) in reactor leachate and methane generation of the solid waste reactors actively generating biogas: (a) gypsum board reactor 1 (GB-1), (b) gypsum board reactor 2 (GB-2), (c) foundry waste reactor 1 (FW-1), and (d) foundry waste reactor 2 (FW-2).

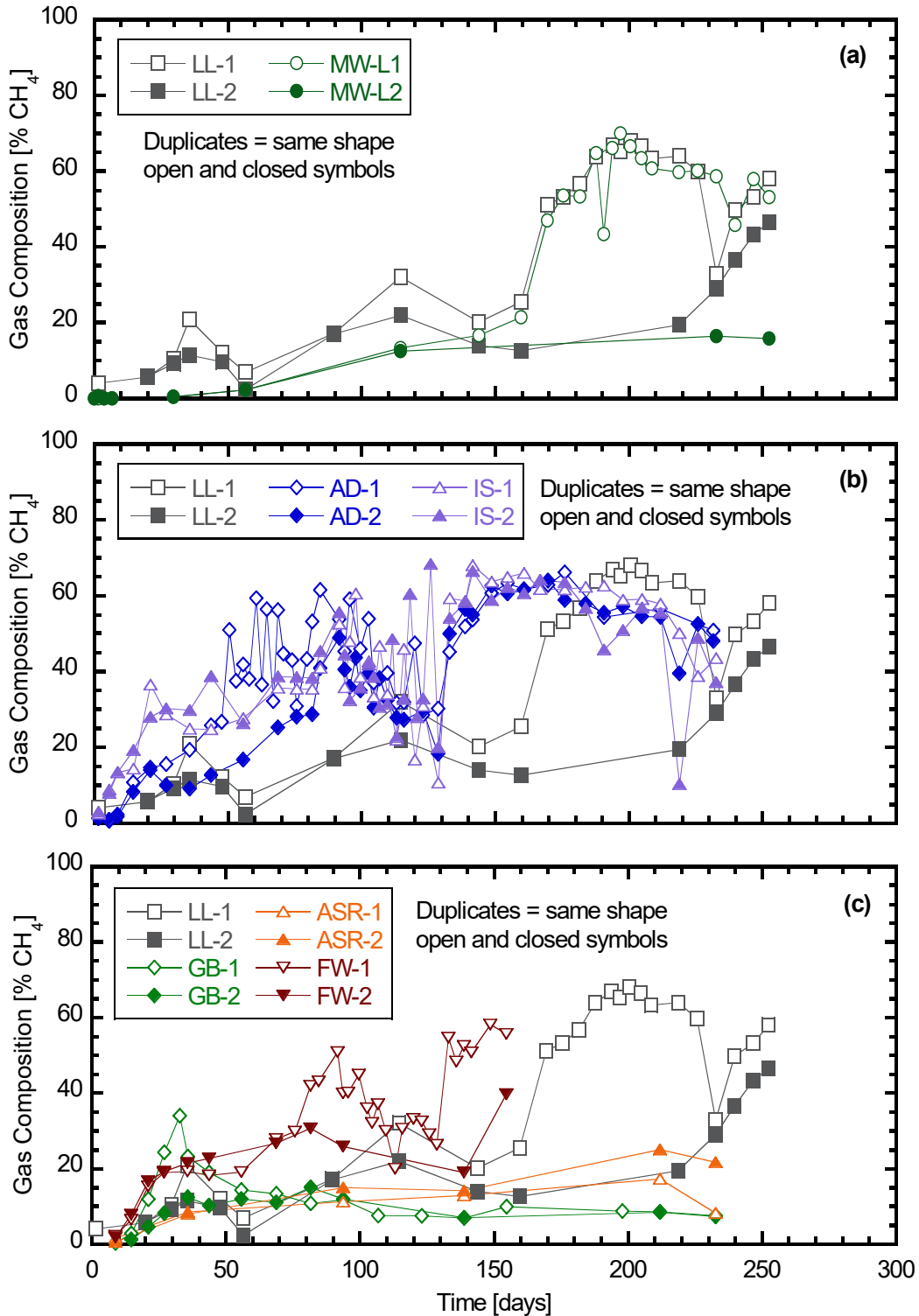


Fig. 1.12. Temporal trends of percent methane composition for (a) low-strength manufacturing wastewater, (b) sludge waste reactors, and (c) solid waste reactors. Data from landfill leachate (LL) reactors are reproduced in each plot for comparison. Notes: AD = anaerobic digestion sludge, IS = industrial sludge, GB = gypsum board, ASR = automobile shredder residue, and FW = foundry waste.

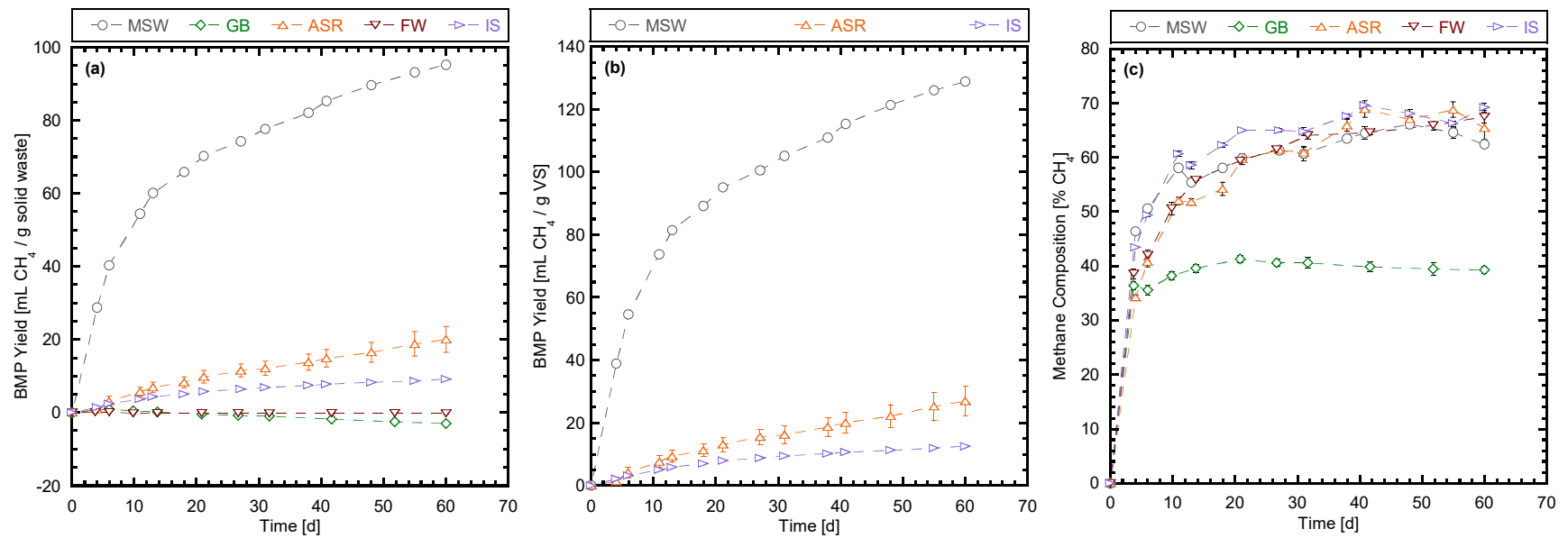


Fig. 1.13. Solid waste biochemical methane potential (BMP) results for (a) methane (CH<sub>4</sub>) yield normalized to mass of waste, (b) CH<sub>4</sub> yield normalized to volatile solids (VS) and, (c) CH<sub>4</sub> composition. Note: MSW = municipal solid waste, ASR = automobile shredder residue, FW = foundry waste, GB = gypsum board, and IS = industrial sludge.

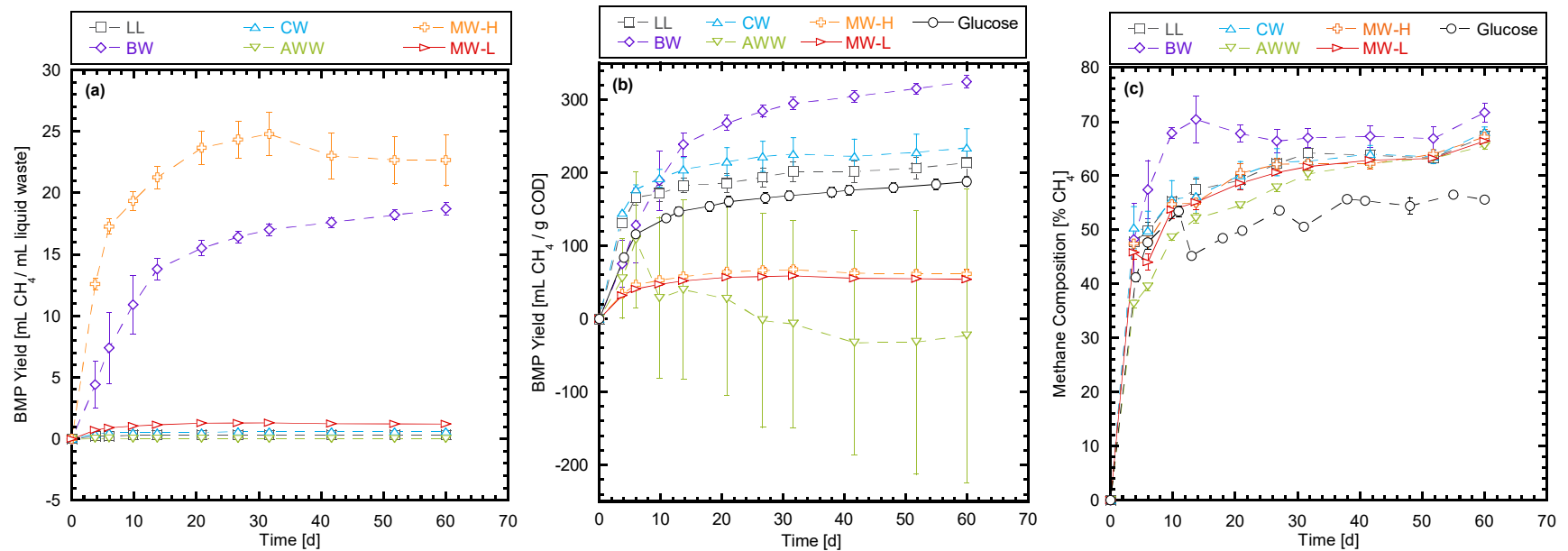


Fig. 1.14. Liquid waste and glucose biochemical methane potential (BMP) results for (a) methane (CH<sub>4</sub>) yield normalized to volume of waste, (b) CH<sub>4</sub> yield normalized to chemical oxygen demand (COD) and, (c) CH<sub>4</sub> composition. Note: LL = landfill leachate, BW = brewery wastewater, CW = cheese processing wastewater, AWW = automobile wash water, MW-L = high strength manufacturing wastewater, MW-H = high strength manufacturing wastewater.

## CHAPTER 4: SUMMARY AND CONCLUSIONS

The objective of this research was to evaluate the impacts of co-disposal of diverse solid, liquid, and/or sludge wastes in MSW on biodegradation and biochemical compatibility. Several key observations and conclusions regarding co-disposal were made from the laboratory study. These observations and conclusions were also used to develop suggested guidance for the practice of co-disposal in solid waste landfills.

- Early and aggressive addition of commercial liquid wastes during reactor startup appeared not to promote accelerated anaerobic decomposition of fresh MSW. The majority of the liquid waste reactors were stuck in the acid formation phase and had leachate with pH values < 6 and COD values approaching or exceeding 50,000 mg O<sub>2</sub>/L.
- The MSW exhibited the ability to buffer and potentially treat liquid waste when not in an anaerobic degradation phase. Pronounced reduction of COD was measured in the high-strength manufacturing wastewater reactors following a single recirculation dose. In addition, the BMP assays indicated that high-strength manufacturing wastewater had relatively high methane yield, which suggests high-strength liquid wastes are treatable and have potential benefit in co-disposal applications.
- The anaerobic digestion sludge and industrial sludge appeared beneficial for accelerating anaerobic biodegradation. Enhanced early methane production was observed in the MSW-Sludge reactors relative to the landfill leachate control reactors and all other waste combinations evaluated in the reactors.
- Anaerobic biodegradation and methane generation were observed in reactors operated with foundry waste or gypsum board co-disposed with MSW. Despite BMP results that indicated methane generation would be inhibited with these two waste streams, co-disposing with MSW did not completely inhibit anaerobic degradation, and appeared to have promoted generation in one of the two duplicates for foundry waste.
- The high sulfate content of gypsum board appeared to have led to sulfate reduction, which likely created a reduced environment favorable for methane generation in the reactors, as was observed by low ORP values. Materials with an elevated sulfate content may generate H<sub>2</sub>S gas.
- The more methanogenically active of the two foundry waste reactors demonstrated that a solid waste stream that appeared to be inhibitory for methane generation, based on leachate chemistry (low pH, high ORP, high COD), still promoted biodegradation. Components specific to the foundry waste may have been beneficial to methane generation, but were not identified as part of the study.
- The BMP assays only provided methane yield from organic substrate degradation under ideal conditions and did not capture other benefits of co-disposal (e.g., impacts of moisture addition). A potential co-disposal waste source should not be ruled out by BMP results alone.
- The BMP results for solid wastes did not show good agreement with reactor data; e.g., negative BMP results corresponded to some of the best-performing solid waste reactors. The BMP assay would not have been a good selection tool in these cases.

The following guidance for co-disposal of solid, liquid, and sludge wastes in full-scale landfills was developed from the reactor experiments and BMP assays conducted in this study.

- Given the bioreactor conditions used in this study, the majority of liquid wastes were not observed to be effective inoculums to establish methane generation in fresh MSW and would not be recommended as the sole moisture source for bioreactor landfills. Although full-scale landfills likely have higher buffering capacity that may mitigate high acid accumulation and potential anaerobic inhibition, a source of anaerobic microorganisms (e.g., mature landfill leachate or anaerobic digestion sludge) should be considered with liquid waste co-disposal to promote biodegradation of organic waste.
- Treatment of high-strength wastewater is possible in MSW. However, addition of high-strength liquid waste should be implemented following established methane generation, which has been shown to be an effective moisture enhancement technique in full-scale MSW landfills.
- Sludge wastes appear to have been beneficial to anaerobic biodegradation and should be considered as potential sources of moisture and organic loading for waste decomposition. The anaerobic digestion sludge provided active methanogenic microorganisms to accelerate methane generation and is likely a beneficial seed source in full-scale landfills. There are several operational considerations for sludge waste co-disposal: (i) early gas collection is needed to manage accelerated production of biogas; (ii) the amount of sludge that can be added while maintaining the observed benefits remains undetermined; and (iii) clogging of liquid and gas infrastructure due to sludge may be an issue (e.g., tubing and filters were prone to clogging in MSW-Sludge reactor experiments).
- Recirculation coupled with certain waste types (e.g., brewery wastewater and industrial sludge) showed increases in ammonia that exceeded concentrations known to be inhibitory. Ammonia accumulation can negatively influence anaerobic degradation and wastes that lead to ammonia accumulation should be used cautiously.
- Biochemical methane potential assays on the individual solid, liquid, and sludge wastes did not yield consistent data that were useful for inferring anticipated behavior in the co-disposal reactors. Thus, BMP assays that simulate ideal anaerobic conditions do not appear to be an effective screening tool that can be used alone to determine compatibility of co-disposal waste streams.

## CHAPTER 5: METHODOLOGY

### 5.1 Experimental Overview

Laboratory-scale column reactors were designed and constructed to study the co-disposal of solid and liquid waste that could occur in MSW landfills. Reactors were designed to facilitate gas collection and leachate recirculation during experimental operation. Wastes used in this study included MSW, three types of industrial solid waste, two types of sludge waste, and six types of liquid waste. The specific wastes were selected to represent common wastes co-disposed in landfills based on a study of ten solid waste landfills (Bareither et al. 2017). A compilation of reactor photographs is included in Appendix D.

### 5.2 Materials

#### 5.2.1 *Municipal Solid Waste*

A summary of the percent composition of the target MSW as well as the MSW composition used for experiments conducted in this study is in Table 1.2. The target MSW was based on summaries of the U.S. national average reported in literature (Staley and Barlaz 2009; USEPA 2014a). The actual MSW composition for this study was adjusted to simplify two waste categories (paper and plastics) and omit the “other” waste category reported in literature. The USEPA (2014) did not distinguish between paper and cardboard or rigid plastic and film plastic, so these percentages were further refined based on Staley and Barlaz (2009).

The MSW was collected from a local landfill, separated into individual components, air dried, shredded using a motorized shredder (Model 1-SHRED-H-0800 Sludge Grinder, JWC Environmental, Santa Ana, CA), and passed through a 19-mm sieve. The processed waste was stored in sealed containers at room temperature, with the exception of food waste. Pre-consumer, pulped produce was collected fresh from Colorado State University dining facilities and stored at 4 °C prior to creating an MSW mixture for experimentation. Individual waste components were recombined proportionately to achieve the initial waste composition reported in Table 1.2. All waste fractions were added based on air-dried mass, except food waste, which was added based on total (wet) mass to add moisture to the initial MSW mixture.

Characterization of the solid wastes included dry-weight water content ( $w_d$ ), volatile solids (VS), and biochemical methane potential (BMP) (analytical procedures for solid waste characterization described subsequently). The initial  $w_d$ , VS, and BMP of the MSW used for all reactor experiments is in Table 1.3. The  $w_d$  after food waste addition was approximately 33% (wet-weight water content,  $w_w$  = 25%), which is typical for fresh MSW disposed in landfills (Hanson et al. 2010; Bareither et al. 2012a; Bareither et al. 2013). The BMP for MSW was 95.3 mL-CH<sub>4</sub>/g MSW (95.3 m<sup>3</sup>-CH<sub>4</sub>/Mg-MSW), on a dry mass basis. This methane yield is similar to ranges reported in literature for MSW (Chickering et al. 2018).

#### 5.2.2 *Industrial Solid Waste*

Representative industrial solid wastes selected for this study included construction and demolition (C&D) waste, automobile shredder residue (ASR), and foundry waste. The C&D waste was represented using gypsum board (GB), which is the most biologically important component in C&D waste. The ASR consisted of shredded

non-metallic, non-recyclable components of vehicles and was collected from a local vehicle salvage facility. The foundry waste (FW) was collected from a local bronze casting facility and consisted primarily of non-reusable casting shell. The casting shell was made from a mixture of silica flour and water. The industrial solid wastes were shredded, sieved, and stored in sealed containers at room temperature until used.

The initial  $w_d$ , VS, and BMP of the three industrial solid wastes are in Table 1.3. The high VS content (76%) and high BMP (20 mL-CH<sub>4</sub>/g-waste) of the ASR indicate that the material may be beneficial for co-disposal. Low VS content for FW (0.0%) and GB (3.5%), and the negative BMP values (FW = -0.2 and GB = -3.0 mL-CH<sub>4</sub>/g-waste), suggest that FW and GB waste streams could perform poorly or even inhibit anaerobic biodegradation if co-disposed with MSW. The negative BMP indicates that the BMP assays for the FW and GB yielded less CH<sub>4</sub> relative to the inoculum alone. The  $w_d$  of the industrial solids was low ( $w_d < 21\%$ ) due to the air-drying step during waste processing.

### **5.2.3 Liquid Waste**

Representative liquid wastes selected for this study included landfill leachate (LL), brewery wastewater (BW), cheese production wastewater (CW), automobile wash water (AWW), high-strength manufacturing plant wastewater (MW-H), and low-strength manufacturing plant wastewater (MW-L). High-strength manufacturing plant wastewater consisted of degreasers, coolants, and other industrial chemicals. The low-strength manufacturing plant wastewater was high-strength wastewater that had been filtered and treated for oils and grease and then mixed with plant cleaning water. Landfill leachate was collected from a local MSW landfill and the other liquid wastes were collected directly from the local wastewater generators. Liquids were stored in collapsible containers with minimal headspace at 4 °C until used. Deionized water (DIW) was used as a control liquid.

The initial characteristics of the liquid wastes are in Table 1.4. Characterization of the liquid wastes included total solids, VS, COD, ammonia, pH, electrical conductivity (EC), oxidation-reduction potential (ORP), and BMP (analytical procedures for liquid characterization described subsequently). Most of the liquid wastes, except MW-H, had a pH less than neutral. The MW-H and BW wastewaters had the greatest COD (367,140 and 57,750 mg O<sub>2</sub>/L, respectively), and the greatest BMP yields (23 and 19 mL-CH<sub>4</sub>/mL-liquid waste, respectively). These relatively high COD and BMP levels indicate high organic loading and suggest that these high strength wastewaters could potentially enhance CH<sub>4</sub> generation in co-disposal applications relative to MSW alone. The liquid wastes with lower COD (< 2,500 mg O<sub>2</sub>/L) corresponded to low BMP (< 0.6 mL-CH<sub>4</sub>/mL-liquid waste). The liquid wastes generally had low EC and ammonia levels, suggesting that increased ammonia or salinity inhibition from their addition to MSW should not occur.

### **5.2.4 Sludge Waste**

The sludge wastes selected for this study include anaerobic digester (AD) sludge from the anaerobic digester of a local wastewater treatment plant and industrial sludge (IS) from the fracking industry. The AD sludge had low solids content and was characterized similar to the liquid wastes (Table 1.4), whereas the industrial sludge had higher solids content and was characterized similar to the solid wastes (Table 1.3). The industrial sludge was fracking sludge waste provided by a manufacturer. Although this material had a very high water content ( $w_d = 760\%$ ), the industrial sludge would classify as “solidified waste” based on passing the paint filter test (EPA Method 9095B). In

contrast, the AD sludge was more liquid-like than the industrial sludge, but trial experiments resulted in clogging of the filter (photograph included in Appendix D) and tubing and indicated that the AD sludge could not be treated similar to the other liquid wastes. Thus, the AD sludge was viewed similar to the industrial sludge to provide further distinction between the wastes used in this study (i.e., solid, liquid, and sludge).

Both IS and AD sludge were expected to perform well in co-disposal experiments. The industrial and anaerobic sludge wastes both had high VS contents (VS > 73%) and high  $w_d$  to serve as a moisture source. The IS sludge showed relatively high BMP compared to the other solid wastes (Table 1.3). The AD sludge was not evaluated for BMP because the sludge was used as inoculum in the assays. The anaerobic sludge was a good source of methanogenic organisms and the sludge yielded the lowest ORP (-56.5 mV) of all of the liquid wastes.

The AD sludge was collected from the digesters of a local wastewater treatment plant in collapsible storage containers and stored at 4 °C with minimal headspace in the container. The fracking sludge was received in sealed 5-gallon buckets and stored at 4 °C until use. The buckets of fracking sludge were >  $\frac{3}{4}$  full when received; thus, there was some headspace present in the sealed buckets when received.

### 5.3 Reactor Design

A summary of the 24 reactors operated for this study is in Table 1.5. The 24 reactors included 12 unique combinations of wastes, and each waste combination was evaluated in duplicate. The waste combinations represented MSW plus solid waste co-disposal (MSW-SW), MSW plus sludge waste co-disposal (MSW-Sludge), and MSW plus liquid waste co-disposal (MSW-LW). All 12 waste combinations include MSW that was mixed with a unique solid, sludge, or liquid waste. The MSW-SW reactors included mixtures prepared with gypsum board, auto shredder residue, or foundry waste. The MSW-Sludge reactors included MSW mixed with industrial sludge or anaerobic digestion sludge. The MSW-LW reactors included MSW mixed with auto wash water, brewery wastewater, cheese production wastewater, the high- and low-strength manufacturing plant wastewaters, and landfill leachate. A set of control reactors was operated only with MSW and DIW.

Effluent from each reactor was recirculated during reactor operation. In the MSW-LW reactors, effluent was generated from the liquid waste addition and these reactors were constrained to only MSW and a single liquid waste. In the MSW-SW and MSW-Sludge reactors, leachate collected from an MSW landfill (LL in Table 1.4) was used to help generate effluent, which subsequently was recirculated in a given reactor (Table 1.5). The MSW-LW reactor that received landfill leachate also served as a control for these solid and sludge co-disposal combinations.

A schematic for a laboratory reactor is shown in Fig. 1.15. Each reactor included a 457-mm-tall by 203-mm-diameter polycarbonate cylinder. The cylinder was fitted with an effluent port installed in the base cap for leachate collection and an influent port installed in the top cap for liquid addition and leachate recirculation. Each port was fitted with a two-way valve to maintain a gas tight system and allow effluent collection or recirculation as needed. The top cap of the cylinder was also fitted with a gas line connected to a 10-L flexfoil gas collection bag (SKC Inc., Eight Four, PA). The gas line was fitted with a four-way valve (with a “closed” position) to facilitate gas sampling and detachment of the collection bag during volume measurement. The reactor base was epoxied to the cylinder and the reactor lid was secured to the cylinder using silicon sealant to create a gas-tight system. After each reactor was filled with waste, they were

flushed with nitrogen gas to promote anaerobic conditions. All reactors were operated in a temperature-controlled room maintained at 37°C to create mesophilic conditions.

The waste specimens in each reactor were sandwiched between layers of nonwoven geotextiles and gravel (Fig. 1.15). A 50-mm-thick layer of washed gravel was placed at the base of the reactor to allow for drainage and effluent storage between recirculation intervals. A gravel layer was placed on top of the waste specimen to distribute evenly recirculated liquid to the surface of a waste specimen. The surface gravel provided a 2-kPa surface stress on the waste specimens that represented interim landfill cover (Bareither et al. 2013). Settlement of each waste specimen was measured via a measuring tape adhered to the outside of the clear cylinder. Nonwoven geotextiles were placed between the gravel layers and the waste to provide separation between the materials and prevent clogging of the drainage layer and effluent port.

Initial waste specimen thickness and density in each reactor are tabulated in Table 1.5. Each specimen was prepared with a 2.4-kg solid waste mixture. A total mass of 2.4 kg was selected because this mass of MSW approximated the target specimen thickness of 203 mm when compacted via hand tamping in four equal layers. All MSW-LW reactors included similarly prepared MSW specimens (Table 1.5) that included an initial total MSW mass of 2.4 kg. In contrast, the MSW-SW and MSW-Sludge specimens were mixed with MSW at a ratio of 60:40 MSW to solid waste or MSW to sludge waste, by total mass; this ratio was selected based on data from a study of 10 solid waste landfills (Bareither et al. 2017).

The individual MSW components combined to create the MSW for each reactor were thoroughly mixed to ensure each reactor include a similar MSW composition. Special solid and sludge wastes were also thoroughly mixed with MSW to achieve as homogenous of a waste mixture as possible in these select reactors. Food waste, and sludge when applicable, was added to the mixture 24 h prior to starting an experiment to hydrate the waste specimen. The initial specimen thicknesses in all reactors ranged from 121 mm to 208 mm, resulting in a total density range between 0.35 and 0.61 g/cm<sup>3</sup> ( $\approx$  590 and 1030 lb/yd<sup>3</sup>) (Table 1.5).

#### 5.4 Reactor Leachate Recirculation and Sampling

A summary of the initial liquid dose volume, initial recirculation volume, and  $w_d$  after dosing is in Table 1.5. The initial liquid dose volume was added in increments during the first week of reactor operation via injection into the top influent port of the reactor (Fig. 1.15). Dosing began on Day 1 of each experiment, and liquid was added incrementally to promote liquid retention within a given waste specimen. The initial dose volumes ranged from 450 to 1800 mL (188 to 750 L/Mg-waste), with a target volume of 1500 mL to represent typical liquid dosing rates of liters of liquid added per mass of total waste (L/Mg-waste) in full-scale landfills (Bareither et al. 2010; Nwaokorie et al. 2017). Smaller dose volumes were added to the MSW-Sludge specimens since the as-prepared waste mixtures with sludge had high initial  $w_d$ . Initial dose volumes in the MSW-SW were adjusted based on observed effluent generation. The overarching goal of liquid addition in all reactors was to exceed moisture-holding capacity of the waste and generate sufficient effluent liquid for recirculation.

Dry-weight water contents after dosing ranged from 60% to 150% (Table 1.5) and initial recirculated volumes ranged from 130 to 330 mL (53 to 139 L/Mg-waste). The greatest  $w_d$  after initial dosing were in the MSW-Sludge reactors due to the high initial water contents of the sludge. In contrast, the lowest  $w_d$  after dosing were in the MSW-SW reactors, which varied between 59% and 94% based on initial dose volume and moisture retention capacity of the solid waste. The  $w_d$  after initial dosing in all MSW-LW

reactors and the MSW reactor with DIW were similar, and ranged between 97% and 108%, indicating that moisture retention of the MSW was similar for the six different liquid wastes and DIW.

Effluent was extracted from the drainage layer via syringe once per week and recirculated (Fig. 1.15). Recirculated liquid was buffered using a 2M sodium hydroxide solution to raise the pH above 7 to mitigate against acidic conditions in the waste that can inhibit methanogenesis. The entire volume of liquid collected from the drainage layer, minus a small amount extracted to assess liquid chemistry, was recirculated each week. Recirculated liquid was injected into the top influent port via a syringe.

Effluent samples were collected weekly and analyzed immediately for pH, EC, ORP, and ammonia. The effluent samples were then preserved via acidification to pH  $\leq$  2 using sulfuric acid (approximately 4 drops per 5 mL sample) and stored at 4 °C for COD analysis. Select effluent samples were filtered using a 0.45- $\mu$ m syringe filter and preserved with nitric acid (approximately 1 drop per 5 mL sample) for elemental analysis. Since the weekly effluent volumes extracted for liquid chemistry were not replaced, additional fresh liquid was added, as needed, to generate effluent. Additional dose volumes of 200 mL were added when effluent generation was needed, and similar dose volumes were always added to the duplicate reactors to maintain consistency between duplicates.

## **5.5 Analytical Methods**

### **5.5.1 Solids Analysis**

Solid waste was analyzed for  $w_d$  and VS. Water contents were determined by oven drying samples for a minimum of 24 h at 105 °C, or until the change in mass was negligible with continued oven drying. Volatile solids were measured as the mass loss on ignition at 550 °C. The VS specimens were ignited for a minimum of 2 h, or until the change in mass loss was negligible.

### **5.5.2 Liquid Analysis**

The as-collected liquid wastes were analyzed for total solids, VS, pH, EC, ORP, COD, ammonia, metals, and other elements. The total solids content was determined by evaporating samples in a steam bath and then oven drying the remaining solids at 105 °C until the change in mass was negligible. Volatile solids were determined as previously described for solid wastes. The pH, EC, and ORP were measured using a portable multi-parameter meter (Hach Sension+ MM150) with a multi-sensor probe (Sension+ 5048). Chemical oxygen demand was measured using a Hach 0-1500 mg/L test kit. The COD samples were digested using a Hach DRB200 heating block and results were read using a Hach DR2500 spectrophotometer. Five-point calibration curves covering the entire concentration range of the test kit for COD were generated with a potassium hydrogen phthalate solution. Ammonia was measured using a Hach 0.4-50 mg NH<sub>3</sub>-N/L test kit. Measurements were conducted on the Hach DR2500 spectrophotometer and five-point calibration curves were generated with an ammonium sulfate solution. Metals and elemental analysis were conducted using an inductively coupled plasma-optical emission spectrometer (Optima 7300, PerkinElmer, Waltham, MA).

### **5.5.3 Gas Collection and Analysis**

Biogas generated during reactor operation was collected in 10-L flexfoil bags. Gas volume was measured via water displacement. Gas was evacuated from a collection bag into the measuring device using a vacuum pump. The measuring device was an inverted 1-L graduated cylinder submerged in water acidified to pH  $\approx$  3 with hydrochloric acid. Gas volume measurements were recorded after the displaced cylinder equilibrated with atmospheric conditions.

Biogas was sampled for composition analysis each time a gasbag was evacuated for volume measurement. Gas was extracted from the gas line sampling port using a syringe and was injected into gas-tight evacuated glass vials. Gas samples were then extracted from the glass vials using a 100- $\mu$ L gas tight syringe (Hamilton GASTIGHT #1730, Reno, NV) and were injected into a gas chromatograph (GC). Samples were analyzed for CO<sub>2</sub> and CH<sub>4</sub> using an HP6890 GC (Hewlett-Packard, Palo Alto, CA) equipped with a thermal conductivity detector (TCD) and RT-Q-Bond column (Restek Corporation, Bellefonte, PA). OpenLAB chromatography software (Agilent Technologies, Santa Clara, CA) was used as the data interface for the GC. A program was created within OpenLAB to achieve separation between nitrogen, CH<sub>4</sub>, and CO<sub>2</sub>. Deviations from the software defaults include 30 °C inlet and oven temperature, 200 °C TCD temperature, 50 cm/s linear velocity in the column, 40:1 split flow, and hydrogen was used as the carrier gas. Percentages of CO<sub>2</sub> and CH<sub>4</sub> were determined relative to calibration curves generated from chemically pure CO<sub>2</sub> and CH<sub>4</sub> gas (Airgas, Radnor, PA).

#### **5.5.4 Biochemical Methane Potential Assay**

The BMP assays were conducted to determine the maximum amount of CH<sub>4</sub> generated per mass of VS or COD of a given substrate under ideal anaerobic degradation conditions. A compilation of BMP photographs is included in Appendix D. Biochemical methane potential assays were conducted using a modified procedure based on protocols described in the literature (Owen et al. 1979; Wang et al. 1994; Moody et al. 2011; Wilson et al. 2013). Solid wastes for BMP tests were ground using a Wiley mill (Standard Model No. 3, Arthur H. Thomas Co., Philadelphia, PA) and passed through a 2-mm screen. Solid waste masses were selected to achieve a target value of 5 g-VS/L in the assay bottle. An arbitrary mass of 5 g was selected for the drywall and foundry waste assays because these wastes contained negligible VS. Liquid samples for BMP tests were prepared to target a concentration of 5 g-COD/L. The MSW leachate, automobile wash water, and cheese processing wastewaters all had initial COD concentrations < 5 g COD/L; therefore, these liquids were tested as-received.

Active anaerobic bacteria and sufficient nutrients were supplied to each BMP assay to ensure ideal conditions for anaerobic biodegradation. Nutrient media was created following the protocol described in Owen et al. (1978). Concentrated stock solutions were mixed and stored at 4 °C. Nutrient media was mixed fresh the day a BMP test was initiated. In assays containing liquid samples, the liquid waste was used as the diluent water to make the media solution in lieu of DIW to conserve specimen volume in the assay bottles. Anaerobically digested sludge from the local wastewater treatment plant was collected fresh and was used as the inoculum. Media and inoculum were supplied to test bottles at a 1:1 ratio (Wilson et al. 2013). Assays were prepared in 165-mL serum bottles with 50 mL of media and 50 mL of inoculum. Negative controls containing inoculum and media with no substrate were created to measure background CH<sub>4</sub> production from the inoculum and to adjust measured gas volumes of the other assays. For quality assurance purposes, positive controls were also created using

readily degradable glucose to ensure inoculum and media were not limiting CH<sub>4</sub> production. All BMP tests were run in triplicate for a given waste.

The BMP tests were carried out at 37 °C and bottles were continuously mixed using a shaker table operating at 150 rpm. Serum bottles were sealed with a rubber septum and aluminum crimp caps. The headspace in the assay bottles was flushed with nitrogen gas for several minutes after sealing the caps and then the bottles were vented to atmospheric conditions using a wetted 10-mL glass syringe. Gas volume was measured periodically using a wetted 10-mL glass syringe. Samples were analyzed for CH<sub>4</sub> composition each time gas volume was measured. Samples for gas analysis were extracted directly from the serum bottle using a 100- $\mu$ L gas tight syringe and immediately injected into the GC for composition analysis (as previously described).

Table 1.2. Target municipal solid waste (MSW) composition based on literature and the adjusted MSW composition used in this study.

Individual MSW Component	Target Composition (%)	Adjusted Composition used in This Study (%) <sup>a</sup>
Paper and cardboard	14.3	
Paper <sup>b</sup>	10.9	11.4
Cardboard <sup>b</sup>	3.4	3.5
Yard trimmings	7.9	8.2
Metals	9.4	9.8
Glass	5.2	5.4
Plastics	18.5	
Rigid <sup>b</sup>	14.9	15.5
Film <sup>b</sup>	3.6	3.8
Wood	8.1	8.5
Food <sup>c</sup>	21.6	22.5
Rubber/leather/textiles	10.8	11.3
Other	4.2	

<sup>a</sup> Percentages adjusted to exclude “other” category reported by the U.S. EPA.

<sup>b</sup> USEPA (2014a) does not distinguish between paper and cardboard, or between rigid and film plastic; target compositions for these categories were established using data reported in Staley and Barlaz (2009).

<sup>c</sup> Food waste added on wet basis to achieve a total mixture water content of approximately 33%.

Table 1.3. Initial dry weight water content ( $w_d$ ), volatile solids (VS), and 60 day biochemical methane potential (BMP) for the solid wastes and industrial sludge.

Solid Waste	$w_d$ [%]	VS [%]	BMP [mL-CH <sub>4</sub> /g-solid waste]	BMP [mL-CH <sub>4</sub> /g-VS]
MSW	32.6	74.0	95.3	128.8
GB	21.1	3.5	-3.0	- <sup>a</sup>
ASR	2.5	76.2	20.0	26.9
FW	0.3	0.0	-0.2	- <sup>a</sup>
IS	759.3	73.2	9.2	12.5

Notes: MSW = municipal solid waste; GM = gypsum board; ASR = automobile shredder residue; FW = foundry waste; IS = industrial sludge. Anaerobic digestion sludge was used as the inoculum for all BMP tests and is not included in the table.

<sup>a</sup> GB and FW volatile solids were too low for BMP on a VS-basis to be conducted

Table 1.4. Initial characteristics of the liquid wastes and anaerobic digester sludge, including total solids content (TS), volatile solids (VS), chemical oxygen demand (COD), ammonia, pH, electrical conductivity (EC), oxidation-reduction potential (ORP), and 60-day biochemical methane potential (BMP).

Liquid Waste	TS [%]	VS [%]	COD [mg O <sub>2</sub> /L]	Ammonia [mg/L NH <sub>3</sub> -N]	pH	EC [mS/cm]	ORP [mV]	BMP [mL-CH <sub>4</sub> /mL-liquid waste]	BMP [mL-CH <sub>4</sub> /g-COD]
LL	2.5	9.3	1,460	86.4	6.8	3.2	7.5	0.3	213.6
BW	2.3	96.8	57,750	58.0	4.6	1.6	228.5	18.7	324.6
CW	0.2	55.4	2,530	9.0	3.9	2.0	234.5	0.6	234.3
AWW	0.1	38.4	230	0.6	6.2	0.2	232.6	0.0	-22.9
MW-H	8.6	96.4	367,140	275.8	7.7	2.2	127.3	22.6	61.6
MW-L	0.4	83.4	22,110	24.8	6.5	0.7	-7.3	1.2	54.3
AD	1.8	77.0	20,990	1129.9	7.2	7.5	-56.5	- <sup>a</sup>	- <sup>a</sup>

Notes: LL = landfill leachate; BW = brewery wastewater; CW = cheese production wastewater; AWW = automobile wash water; MW-H = manufacturing plant high-strength wastewater; MW-L = manufacturing plant low-strength wastewater; AD = anaerobically digested sludge.

<sup>a</sup> Anaerobic sludge served as the inoculum in BMP assays and was therefore not analyzed for a BMP yield.

Table 1.5. Summary of the laboratory reactors, including waste components of each reactor, initial specimen thickness and density, initial liquid dose volume, initial liquid recirculation volume, and dry-weight water content ( $w_d$ ) after initial dosing.

Reactor	Solid Waste	Liquid Source	Thickness [cm]	Density [g/cm <sup>3</sup> & lb/yd <sup>3</sup> ]	Initial Dose [L/Mg-waste]	Initial Recirculated Volume [L/Mg-waste]	$w_d$ after Dosing [%]
DIW-1	MSW	DIW	20.6	0.36 (607)	625	95	103
DIW-2	MSW	DIW	20.8	0.36 (607)	625	124	99
LL-1	MSW	LL	20.6	0.36 (607)	625	109	101
LL-2	MSW	LL	20.0	0.37 (624)	625	113	100
BW-1	MSW	BW	20.6	0.36 (607)	625	55	108
BW-2	MSW	BW	20.6	0.36 (607)	625	76	105
CW-1	MSW	CW	20.0	0.37 (624)	625	120	100
CW-2	MSW	CW	20.2	0.37 (624)	625	91	103
AWW-1	MSW	AWW	20.0	0.37 (624)	625	123	99
AWW-2	MSW	AWW	20.8	0.36 (607)	625	139	97
MW-H1	MSW	MW-H	20.3	0.36 (607)	625	87	104
MW-H2	MSW	MW-H	20.6	0.36 (607)	625	60	108
MW-L1	MSW	MW-L	20.3	0.36 (607)	625	104	102
MW-L2	MSW	MW-L	21.1	0.35 (590)	625	109	101
GB-1	MSW + GB	LL	18.4	0.40 (674)	750	114	92
GB-2	MSW + GB	LL	20.0	0.37 (624)	750	95	94
ASR-1	MSW + ASR	LL	18.7	0.40 (674)	458	102	59
ASR-2	MSW + ARR	LL	18.4	0.40 (674)	458	53	65
FW-1	MSW + FW	LL	15.2	0.49 (826)	458	70	63
FW-2	MSW + FW	LL	16.0	0.46 (775)	458	59	64
AD-1	MSW + AD	LL	14.0	0.53 (893)	188	109	135
AD-2	MSW + AD	LL	12.7	0.58 (978)	188	110	135
IS-1	MSW + IS	LL	12.7	0.58 (978)	333	93	149
IS-2	MSW + IS	LL	12.1	0.61 (1030)	333	75	152
Average			18.5	0.41 (691)	547	95	102
Minimum			12.1	0.35 (590)	188	53	59
Maximum			21.1	0.61 (1030)	750	139	152

Notes: DIW = deionized water; MSW = municipal solid waste; GM = gypsum board; ASR = automobile shredder residue; FW = foundry waste; IS = industrial sludge; LL = landfill leachate; BW = brewery wastewater; CW = cheese production wastewater; AWW = automobile wash water; MW-H = manufacturing plant high-strength wastewater; MW-L = manufacturing plant low-strength wastewater; AD = anaerobically digested sludge.

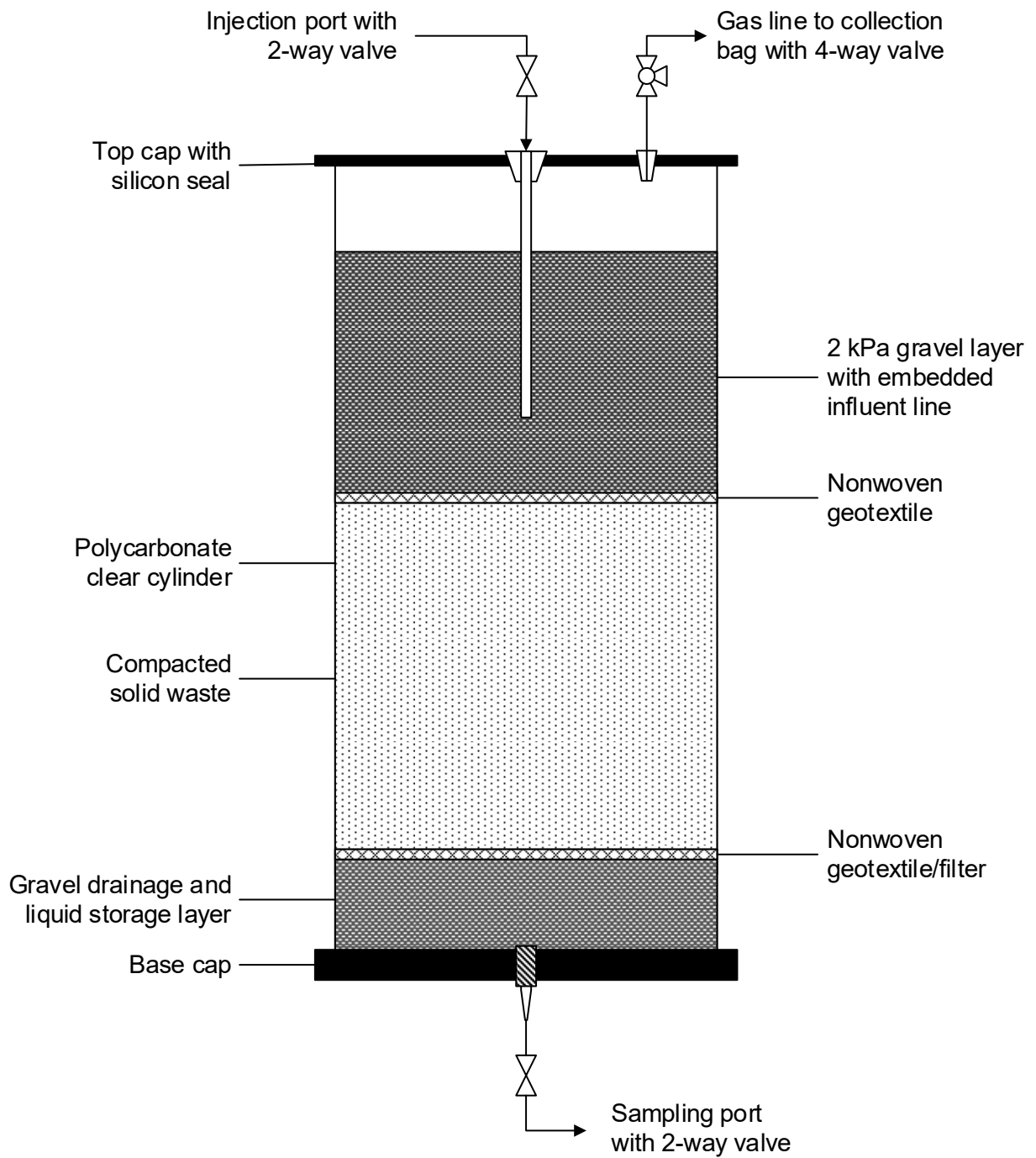


Fig. 1.15. Schematic of a laboratory reactor.



# RESEARCH STUDY 2: THE INFLUENCE OF MOISTURE ENHANCEMENT ON SOLID WASTE BIODEGRADATION

## CHAPTER 1: INTRODUCTION

Solid waste landfills are an integral part of solid waste management in the U.S., with more than 50% of municipal solid waste (MSW) generated in 2015 disposed in landfills (US EPA 2015). Although landfilling has evolved during the past decades and environmental regulations have reduced negative impacts associated with landfills, there remain challenges associated with leachate leakage into groundwater, air pollution, odors, settlement, greenhouse gases emissions, and long-term post-closure care (Morris et al. 2012; Loureiro et al. 2013; Bareither and Kwak 2015; Pantini et al. 2015; Townsend et al. 2015). Bioreactor landfills address some of the aforementioned challenges related with solid waste landfills. The primary objective of a bioreactor landfill is to promote in situ waste decomposition, which most commonly is achieved via enhancing anaerobic conditions that are beneficial to increasing the rate of organic waste decomposition (Benson et al. 2007; Bareither et al. 2010; Barlaz et al. 2010; Bareither et al. 2017).

The most common strategy to enhance in situ anaerobic biodegradation in bioreactor landfills is moisture enhancement, which can include leachate addition and recirculation as well as liquid waste addition and solidification (Bareither et al. 2017). Methods to add liquids (i.e., liquid waste and leachate) to landfills include direct disposal at the working face, vertical wells, horizontal trenches, and permeable blankets (Townsend et al. 2015). Bareither et al. (2010) evaluated leachate recirculation operations for five full-scale bioreactor landfills and reported that operations included broad ranges of dose volumes and frequencies. Bareither et al. (2017) reported that landfills operating with a U.S. EPA Research Development and Demonstration (RD&D) Permit indicated that direct disposal of liquid waste in solid waste landfills was attractive due to revenue from waste tipping fees and progression towards organic stability. Nwaokorie et al. (2018) assessed moisture enhancement strategies at a full-scale landfill and reported that early, aggressive leachate recirculation combined with continuous leachate recirculation and liquid waste addition resulted in enhanced biogas generation.

Although the objective of moisture enhancement is to increase the rate and extent of in situ anaerobic biodegradation, there is limited guidance on dose rates and frequencies of liquid addition / leachate recirculation that are most beneficial to gas generation and organic waste stabilization. Field-scale operations for moisture addition are generally ad hoc and controlling the amount of liquid added and frequency of dosing is challenging as operations depend on multiple factors, such as moisture availability (e.g., leachate to recirculate, liquid waste, etc.), landfill infrastructure, and landfill personnel. However, controlling the frequency and amount of moisture addition to MSW can be achieved at laboratory scale to provide an assessment of moisture enhancement techniques that can be relevant for full-scale bioreactor landfills.

The overall objective of this research was to assess the influence of moisture enhancement strategies on biodegradation of MSW in laboratory-scale reactors. Moisture enhancement strategies were varied with respect to dose volume and dose frequency. Biodegradation was evaluated based on methane generation to identify relevant and practical moisture enhancement strategies that can (i) reduce the lag-time between waste disposal and onset of methane generation and (ii) increase the first-order decay rate for methane generation.

## CHAPTER 2: RESULTS AND DISCUSSION

### 2.1 Reactor Operation and Data Processing

A summary of the 17 laboratory reactors (R1 – R17) conducted for this study is in Table 2. The summary in Table 2 includes dose volume, dose frequency, total liquid added per MSW mass, total CH<sub>4</sub> yield, peak CH<sub>4</sub> flow rate, ratio of CH<sub>4</sub> yield per MSW mass to CH<sub>4</sub> potential, lag-time between onset of liquid dosing and CH<sub>4</sub> generation, and the modeled decay rate based on Eq. 3. Reactors were operated for 220 d, and inoculum dosing in all reactors started on Day 22. The average initial dry weight water was 34% (wet weight water content ≈ 25%), which represented the as-prepared MSW specimens at the time inoculum dosing initiated.

Temporal trends of data collected during reactor operation are shown for R14 in Fig. 2.1. This reactor was operated with a dose volume of 320 L/Mg-MSW and a dose frequency of 1 week, which meant that 320 L/Mg-MSW (768 mL based on initial mass of the MSW specimen) of leachate and additional fresh inoculum (as needed) was added to the reactor each week. The ratio of effluent leachate volume to influent dose volume rapidly approached unity (Fig. 2.1a) due to the large dose volume and high frequency, and the wet weight water content increased and remained at approximately 67% for the duration of the experiment (Fig. 2.1b). Leachate chemistry of pH, EC, ORP, and COD shown in Fig. 2.1 depict anticipated trends for anaerobic biodegradation. pH initially decreased to approximately 5 on Day 50 and concurrently COD reached a maximum of nearly 35,000 mg-O<sub>2</sub>/L, which reflected hydrolysis and acidogenesis. During the subsequent 4-5 weeks, ORP reduced to less than -200 mV reflecting the onset of methanogenic conditions, pH increased and stabilized above neutral, and COD decreased to less than 10,000 mg-O<sub>2</sub>/L. These leachate chemistry trends support the onset of CH<sub>4</sub> generation observed in R14 during this same time period (Fig. 2.1).

Biogas generation in R14 initiated quickly after initial inoculum dosing on Day 22. The ratio of CH<sub>4</sub>:CO<sub>2</sub> increased from Day 22 until reaching a maximum between 1.2 and 1.3 on Day 80. This increase in the CH<sub>4</sub>:CO<sub>2</sub> ratio also coincided with the increase and peak CH<sub>4</sub> flow rate. At the end of the experiment, R14 generated 351 L of biogas, of which 173 L were CH<sub>4</sub>.

Reactor operation data for R14 are representative of data collected for all reactors in which leachate recirculation was implemented (i.e., R1 through R16). Data compilation for R1 through R16 is included in Appendix 2, which includes initial and final conditions as well as temporal relationships of dosing, water content, biogas, and leachate chemistry. Reactors that were operated with higher dose volumes and, in particular higher dose frequencies, yielded a greater potential to collect and analyze leachate chemistry. However, limited leachate chemistry data were obtained for R3 and R8, and no leachate chemistry data were obtained for R4. These reactors had low dose volumes and dose frequencies of either 2 or 4 weeks, which limited potential leachate generation. Although leachate never was generated from R4 and only limited leachate was generated from R3 and R8, all reactors produced biogas and achieved methanogenesis (Table 2, Appendix 2).

Methane generation data for each reactor were evaluated to determine two key parameters: (i) lag-time between the onset of inoculum dosing and CH<sub>4</sub> generation (i.e., lag-time); and (ii) first-order decay coefficient (i.e., decay rate or  $k$ ) (Table 2). Cumulative CH<sub>4</sub> generation data from R14 are linearized in Fig. 2.2 and fitted with Eq. 3 to provide an example of the method used to determine the lag-time and decay rate. The x-axis in Fig. 2.2 is elapsed time from onset of liquid dosing and the y-axis is linearized CH<sub>4</sub> production. Eq. 3 was fit to the data using an  $L_0 = 128 \text{ m}^3\text{-CH}_4/\text{Mg-MSW}$  and decay rate

was taken as the slope of linear regression. This  $L_0$  was adopted based on the maximum  $\text{CH}_4$  produced among the 16 reactors (i.e., R13), and was used in the evaluation of all reactors. The variables  $M$  and  $V$  in Eq. 3 were reactor specific, which were the total mass of solid waste (Mg) and cumulative methane generated ( $\text{m}^3$ ), respectively. Lag-time was identified as the intercept of the linear regression (Fig. 2.2), which represented the number of days after the onset of inoculum addition that  $\text{CH}_4$  production began.

## 2.2 Moisture Response

Temporal trends of the ratio of leachate effluent to dose influent volume and wet-weight water content for reactors grouped by dose volume are shown in Fig. 2.3. Each plot in Fig. 2.3 includes the four reactors operated with the same dose volume, but with dose frequencies of  $\frac{1}{2}$ , 1, 2, and 4 weeks. Reactors with a dose volume of 40 L/Mg-MSW (Fig. 2.3a,b) exhibited the broadest range of effluent / influent ratios and water contents during reactor operation. This broad range in moisture response was attributed to the low dose volume. For example, R4 had the least amount of liquid added (40 L/Mg-MSW added every 4 weeks), which resulted in zero leachate generation during the experiment. Each of the reactors operated with a dose volume of 40 L/Mg-MSW achieved a different water content at the end of operation, whereby the water content increased with more frequent dosing.

Liquid dosing at volumes of 80, 160, and 320 L/Mg-MSW exhibited similar trends in the moisture response. The ratio of effluent / influent and moisture contents for dosing conducted at a frequency of  $\frac{1}{2}$  week (i.e., R5, R9, and R13) increased rapidly and leveled off at what represented hydraulic equilibrium. The majority of the reactors generated leachate after reaching wet-weight water contents of 50-52% (dry-weight water contents = 98-107%), and subsequently the ratio of leachate effluent to influent volume increased and leveled off at approximately 90-100%. A decrease in the frequency of dosing for each of the dose volumes (i.e., from  $\frac{1}{2}$  week to 1, 2, and 4 weeks) corresponded with a delay in leachate generation observed as the effluent / influent ratio required more time to reach 90-100% and stabilize. However, as dose volume increased from 80 L/Mg-MSW to 160 L/Mg-MSW and ultimately to 320 L/Mg-MSW, the elapsed time required to generate leachate and achieve hydraulic equilibrium decreased.

The least amount of variability in the equilibrated and final moisture contents of the reactors was observed in those operated with a dose volume of 320 L/Mg-MSW (Fig. 2.3h), which was the largest dose volume used in this study. Wet weight water contents for all reactors that generated leachate ultimately stabilized between 50% and 70% (Fig. 2.3). This range of wet weight water contents is at the upper end of the range observed in full-scale landfills (e.g., Bareither et al. 2010, 2017). The higher range of wet weight water contents observed in the laboratory reactors was attributed to the aggressive moisture enhancement strategies and small volumes of MSW used in the laboratory.

## 2.3 Leachate Chemistry

Temporal trends of leachate pH and COD for reactors grouped by dose volume are shown in Fig. 2.4. Electrical conductivity of the leachate closely replicated the COD response and ORP trends predominantly documented a decrease to below -200 mV for active methanogenic conditions with subsequent increase as COD reduced. Thus, pH and COD were selected as representative parameters to assess leachate chemistry for comparison among the moisture enhancement scenarios while also decreasing the amount of data plotted in Fig. 2.4.

The leachate pH and COD trends observed in the reactors were dependent on the dose volume and dose frequency. The only reactor operated with a dose volume of 40 L/Mg-MSW that exhibited the dynamic nature of increasing pH and decreasing COD was R1, which was operated with a dose frequency of ½ week. The higher rate of dosing for R1 generated sufficient leachate to capture the dynamic changes in leachate chemistry, whereas R2 and R3 with dose frequencies of 1 and 2 weeks, respectively, exhibited pH > 7 and low COD concentration when leachate was first generated (Figs. 2.4a,b). Thus, these low dose frequencies at a dose volume of 40 L/Mg-MSW appear to have allowed hydrolysis, acidogenesis, and methanogenesis to develop within the reactor prior to sufficient inoculum added to generate leachate. Leachate was not generated from R4 and no leachate chemistry data were measured for that reactor.

An increase in dose volume from 40 L/Mg-MSW to 80 L/Mg-MSW did not considerably change the leachate chemistry trends observed as a function of dose frequency. The most pronounced dynamic behavior observed in leachate pH and COD were for R5, which was operated with a dose frequency of ½ week. However, modest increasing pH and decreasing COD trends were also observed in R6 that was operated with a dose frequency of 1 week. Thus, the increase in dose volume from 40 to 80 L/Mg-MSW allowed for more rapid leachate generation at a dose frequency of 1 week (Fig. 2.3a,c) such that the dynamic changes in leachate chemistry were captured. The main difference observed in reactors with a dose volume of 80L/Mg-MSW was pH < 6 measured for R8 upon initial leachate generation on Day 170. Although leachate pH for R8 was considerably acidic upon initial generation, the reactor was generating methane (described subsequently). The third and final leachate chemistry measurement for R8 indicated that pH increased above neutral. The low initial pH measured for R8 may have been due to accumulation of organic acids near the bottom of the waste mass due to gravity-induced seepage of fluid within the waste mass prior to leachate generation. Staley et al. (2011) observed active methanogenesis in laboratory MSW reactors with leachate chemistry representative of below neutral pH. Thus, there could have been an active community of low-pH tolerant methanogens in R8 as postulated by Staley et al. (2011) or the presence of pH-neutral pockets within the reactor that promoted methane generation.

Leachate chemistry data for reactors operated with dose volumes of 160 and 320 L/Mg-MSW exhibited the most dynamic responses as a function of time due to the larger total volumes of liquid added and recirculated. Reactors R9, R13, and R14 all exhibited a complete, characteristic leachate chemistry signature for MSW experiencing hydrolysis, acidogenesis, and methanogenesis. Leachate chemistry from these reactors exhibited a decrease in pH that occurred concurrently with a peak in COD as hydrolysis and acidogenesis were the dominant microbiological process. Subsequently, pH increased above neutral while COD decreased, which reflected consumption of readily-available soluble organic compounds in the leachate (e.g., acetate) as methanogenesis was established and began to flourish (e.g., Barlaz et al. 1989; Pohland and Kim 1999; Bareither et al. 2013). Interestingly, R16 that was operated with a dose volume of 320 L/Mg-MSW and a dose frequency of 4 weeks also showed these characteristic trends in leachate chemistry; however, the elapsed time at which the trends developed was delayed relative to reactors operated with dosing conducted at higher frequencies (i.e., R13 and R14).

## **2.4 Methane Generation**

Temporal trends of cumulative CH<sub>4</sub> yield and CH<sub>4</sub> flow rate for reactors grouped based on dose volume are shown in Fig. 2.5. A consistent increase in CH<sub>4</sub> yield and

flow rate was observed with an increase in dose frequency from 4 weeks to  $\frac{1}{2}$  week for reactors operated with a dose volume of 40 L/Mg-MSW (Fig. 2.5a,b). The peak CH<sub>4</sub> flow rate increased from 0.27 to 1.29 m<sup>3</sup>/Mg-MSW/d from R4 to R1 as the dose frequency increased from every 4 weeks to every  $\frac{1}{2}$  week (Table 2). In addition, only R1 exhibited a sharp peak in CH<sub>4</sub> flow rate, the other three reactors with a dose volume of 40 L/Mg-MSW yielded low CH<sub>4</sub> flow rates that did not exhibit pronounced dynamic changes (Fig. 2.5b). Cumulative CH<sub>4</sub> yields from these four reactors were compared to the highest CH<sub>4</sub> yield measured for the entire set of reactors (i.e., R13, Table 2) to compute a percent CH<sub>4</sub> yield. The increase in dose frequency from R4 to R1 corresponded to an increase in percent CH<sub>4</sub> yield from 19% to 76% (Table 2). Thus, the increase in dose frequency at the lowest dose volume of 40 L/Mg-MSW considerably increased CH<sub>4</sub> yield and flow rate. This enhanced CH<sub>4</sub> generation was attributed to an increase in moisture availability within the reactors.

A similar increase in CH<sub>4</sub> yield and CH<sub>4</sub> flow rate was observed with increasing dose frequency from 4 weeks (R8) to  $\frac{1}{2}$  week (R5) for reactors operated with a dose volume of 80 L/Mg-MSW. Peak CH<sub>4</sub> flow rate increased from 0.56 to 2.02 m<sup>3</sup>/Mg-MSW/d (Table 2). However, the cumulative CH<sub>4</sub> yield for reactors R5 and R6 that were operated with dose frequencies of  $\frac{1}{2}$  week and 1 week, respectively, were essentially the same (Fig. 2.5c). The prolonged acidic conditions of R8 (Fig. 2.4c), discussed previously, likely reduced the cumulative CH<sub>4</sub> yield and CH<sub>4</sub> flow rate for this reactor. However, CH<sub>4</sub> generation was ongoing concurrently while leachate pH was less than 6 (i.e., between 170-190 d). The small peak in CH<sub>4</sub> flow rate for R8 towards the end of the experiment coincided with an increase in leachate pH to above neutral conditions.

The temporal trends of cumulative CH<sub>4</sub> yield and CH<sub>4</sub> flow rate were nearly identical for reactors R9, R10, and R11 (Figs. 2.5e,f), which were operated with a dose volume of 160 L/Mg-MSW and dose frequencies of  $\frac{1}{2}$ , 1, and 2 weeks, respectively. A decrease in dose frequency to 2 weeks resulted in a short lag-time for the pronounced increase in CH<sub>4</sub> flow rate compared to the reactors with dose frequencies of  $\frac{1}{2}$  and 1 week. Regardless, the cumulative CH<sub>4</sub> yield for reactors R9, R10, and R11 ranged between 103 and 107 m<sup>3</sup>/Mg-MSW and peak CH<sub>4</sub> flow rate ranged between 1.95 and 2.04 m<sup>3</sup>/Mg-MSW/d (Table 2). The reduced dose frequency to 4 weeks for R12 did yield a lower CH<sub>4</sub> yield (90 m<sup>3</sup>/Mg-MSW) and substantially lower peak CH<sub>4</sub> flow rate (1.13 m<sup>3</sup>/Mg-MSW/d). Thus, regardless of the difference in CH<sub>4</sub> generation for R12, there were negligible differences in CH<sub>4</sub> yield and flow rate considering dose frequencies of  $\frac{1}{2}$ , 1, and 2 weeks for reactors operated with a dose volume of 160 L/Mg-MSW.

An increase in dose volume from 160 to 320 L/Mg-MSW had limited effect on the trends in CH<sub>4</sub> generation for the four dose frequencies evaluated. The two reactors operated with dose frequencies of  $\frac{1}{2}$  and 2 weeks and a dose volume of 320 L/Mg-MSW (R13 and R15) yielded very comparable CH<sub>4</sub> yield and flow rate (Figs. 2.5g,h and Table 2). The peak CH<sub>4</sub> flow rate and general trend in CH<sub>4</sub> flow rate as a function of time for R14, which was operated with a dose frequency of 1 week, were also similar to R13 and R15. A lower cumulative CH<sub>4</sub> yield for R14 (100 m<sup>3</sup>/Mg-MSW) was measured relative to R13 and R15 (123-128 m<sup>3</sup>/Mg-MSW); however, this difference was likely attributed more to variability in the MSW source material than actual reactor operation. Reactor R16, which was operated with a dose frequency of 4 weeks and dose volume of 320 L/Mg-MSW, yielded the same amount of total CH<sub>4</sub> as R14. The main differences with R16 were that peak CH<sub>4</sub> flow rate prolonged in development (i.e., occurred on Day 140 compared to Day 80 for R14) and was slightly lower. The prolonged development of the peak CH<sub>4</sub> flow rate in R16 corresponded to the prolonged establishment of neutral pH and reduced COD observed in the leachate chemistry (Figs. 2.5g,h). Regardless of the

minor variability observed among the four reactors operated with a dose volume of 320 L/Mg-MSW, the cumulative CH<sub>4</sub> yields were comparable at the end of the experiment.

## 2.5 First-Order Decay Rate and Lag-Time

The relationship between decay rate and dose volume is shown in Fig. 2.6, which includes all reactor data grouped with respect to similar dose frequency. In general, the decay rate increased with an increase in dose volume for all four dose frequencies evaluated. The only reactor that did not fit the general trend was R14, which was operated with dose volume of 320 L/Mg-MSW and frequency of 1 week. The most pronounced difference in decay rate as a function of dose frequency was observed for a dose volume of 40 L/Mg-MSW. An increase in dose frequency from 4 weeks to ½ week increased the decay rate from 0.4 1/yr to 1.91 1/yr (Table 2), which was more than a four-fold increase the rate of CH<sub>4</sub> generation. In addition, for reactors operated with a dose frequency of ½ week, the decay rate increased 50% from 1.91 to 2.78 1/yr with an increase dose volume from 40 L/Mg-MSW to 320 L/Mg-MSW. The highest decay rates determined for the reactors operated in this study were 2.78 and 2.80 1/yr, which were for R13 and R15 (Table 2). These two reactors were operated with a dose volume of 320 L/Mg-MSW and dose frequencies of ½ and 2 weeks, respectively. These reactors also generated the largest CH<sub>4</sub> yields among the 16 reactors (Table 2).

The relationship between decay rate and lag-time between liquid dosing and the onset of CH<sub>4</sub> generation is shown in Fig. 2.7. Data for all reactors are included in Fig. 2.7 and grouped with respect to dose volume. The range of dose frequencies is included in each dose volume group, whereby an increase in symbol size in Fig. 2.7 corresponds to an increase in dose frequency (i.e., symbol size increases from 4 weeks to ½ week). Reactors that were operated with dose volumes of 40, 80, and 160 L/Mg-MSW all individually support the trend of increased decay rate and reduced lag-time with an increase in dose frequency. However, reactors that were operated with a dose volume of 320 L/Mg-MSW all yielded a lag time of 7 d. The absence of any trend in lag-time for reactors operated with the largest dose volume was attributed to sufficient moisture addition with the initial inoculum addition to start CH<sub>4</sub> generation. In contrast, trends between decay rate and lag-time for the lower three dose volumes suggest that more rapid dosing (i.e., increasing the dose frequency from every 4 weeks to every ½ week) was advantageous to initiating CH<sub>4</sub> generation sooner after the first inoculum dose was added.

A final composite analysis of the reactor data was conducted via evaluating the decay rate and lag-time based on the amount of liquid added to each reactor per month. The month time equivalent was used as a method to normalize the data set considering that a month (i.e., 4 weeks) was the longest duration between any two subsequent doses. The relationship between decay rate and lag-time is shown in Fig. 2.8 with individual plots created for cumulative liquid addition ranging from 40 L/Mg-MSW/month (i.e., R4 = 40 L/Mg-MSW added every 4 weeks) to 2560 L/Mg-MSW/Month (i.e., R13 = 320 L/Mg-MSW added every ½ week). The general trend in the composite data set is a shift to higher decay rates and lower lag-times with an increase in monthly dose volume. Thus, reactors with more aggressive moisture enhancement strategies (i.e., higher monthly dosing) attained elevated CH<sub>4</sub> generation (higher decay rate) that initiated in a shorter amount of time following the onset of dosing (reduced lag-time).

The reactors operated with the lowest dose volumes (40 and 80 L/Mg-MSW) that were only added once every 4 weeks potentially lacked sufficient moisture availability, which prolonged the onset of CH<sub>4</sub> generation and reduced CH<sub>4</sub> yield relative to the other

reactors. Reactors that were operated such that they received a cumulative monthly liquid addition  $\geq 320$  L/Mg-MSW achieved decay rates approximately  $\geq 2.0$  1/yr and lag-times  $\leq 22$  d. The two highest decay rates of approximately 2.8 1/yr were determined for reactors operated with a dose volume of 320 L/Mg-MSW added on a  $\frac{1}{2}$ -week and 2-week frequency. If these two reactors are not considered in the composite data set, there was limited change in the decay rate and lag-time as the monthly dose volume increased above 320 L/Mg-MSW. In other words, the influence of additional moisture added to a reactor beyond 320 L/Mg-MSW/month, as a means to increase the decay rate and/or decrease the lag-time was not pronounced. There was more value of increasing the moisture enhancement strategy from 40 L/Mg-MSW/month to 320 L/Mg-MSW/month as a means to increase the decay rate and decrease the lag-time for CH<sub>4</sub> generation.

## 2.6 Practical Implications

In general, laboratory reactors operated with higher dose frequencies or dose volume had shorter lag-times and started methane generation earlier than other reactors. This was attributed to the reactors having sufficient moisture for a suitable microbial environment to accelerate the hydrolysis, fermentation, and acetogenesis phases. The use of centrifuged and diluted anaerobic digester sludge provided the necessary microorganisms for these initial stages of biodegradation, while also providing the necessary methanogenic microorganisms to help transition the reactors to states of active methanogenesis. Considering that operation of laboratory reactors with liquid waste and landfill leachate in the companion study (see Study 1) did not consistently lead to methanogenic conditions in the laboratory reactors, using anaerobic digester sludge, even in a diluted form, is advantageous to anaerobic biodegradation of MSW to generate methane.

Liquid addition and leachate recirculation operations at full-scale landfills have revealed that low amounts of liquid added to MSW do not contribute beneficially to increase CH<sub>4</sub> generation (Nwaokorie et al. 2018). However, landfill operators and engineers have reported issues with watering out of gas wells, leachate seeps, and excessive leachate generation for aggressive moisture enhancement strategies that may include liquid waste addition and leachate recirculation (Bareither et al. 2017). These observations, combined with the data compiled from the reactors operated in this study, suggest that there likely is an optimal range of liquid addition / leachate recirculation that leads to enhanced CH<sub>4</sub> generation without leading to issues when excessive liquid is present within the waste mass.

The subsequent steps to this research effort are to compile data from (i) full-scale bioreactor landfills that have reported magnitudes of liquid addition / leachate recirculation and CH<sub>4</sub> generation, and (ii) full-scale landfills where moisture enhancement has not been conducted that report in-coming and in situ water contents. General trends in full-scale landfill data should be compared with the general trends observed in the reactors operated herein to develop guidance for moisture enhancement strategies. These strategies should be practical for field operations (i.e., implementable based on personnel and infrastructure), while providing enhanced CH<sub>4</sub> generation and reducing anticipated challenges related to excessive moisture within the waste mass.

Table 2.1. Summary of reactor experiments, including dose volume, dose frequency, total liquid added per MSW mass, cumulative methane yield, peak methane flow rate, ratio of methane yield to methane potential, lag-time between onset of liquid dosing and methane generation, and first-order decay rate.

Reactor	Dose Volume (L/Mg-MSW) <sup>a</sup>	Dose Frequency (week)	Total Liquid Added/ Total MSW Mass (m <sup>3</sup> /Mg-MSW)	Cumulative CH <sub>4</sub> (m <sup>3</sup> /Mg-MSW) <sup>b</sup>	Peak CH <sub>4</sub> Flow Rate(m <sup>3</sup> /Mg-MSW/d) <sup>b</sup>	Cumulative CH <sub>4</sub> / L <sub>0</sub> <sup>d</sup>	Lag-Time (d) <sup>e</sup>	Decay Rate (1/yr)
R1	40 (96)	0.5	2.16	97	1.29	0.76	14	1.91
R2		1	1.12	74	0.59	0.58	20	1.23
R3		2	0.56	43	0.56	0.34	32	0.73
R4		4	0.28	25	0.27	0.19	48	0.40
R5	80 (192)	0.5	4.32	101	2.02	0.79	14	2.12
R6		1	2.24	100	1.81	0.78	19	1.97
R7		2	1.12	88	1.05	0.69	22	1.68
R8		4	0.56	48	0.56	0.37	35	0.81
R9	160 (384)	0.5	8.69	107	1.96	0.84	11	2.26
R10		1	4.50	103	1.95	0.81	13	2.10
R11		2	2.25	103	2.04	0.80	22	2.17
R12		4	1.13	90	1.13	0.70	27	1.76
R13	320 (768)	0.5	17.28	123	1.89	0.96	7	2.78
R14		1	8.96	100	1.96	0.78	7	1.91
R15		2	4.48	128	1.97	1	7	2.80
R16		4	2.24	106	1.48	0.83	7	1.93
R17	—	—	—	—	—	—	—	—

<sup>a</sup> Volume of actual dose in mL provided in parentheses.

<sup>b</sup> Cumulative CH<sub>4</sub> and peak CH<sub>4</sub> flow rate were calculated based on dry mass of MSW.

<sup>c</sup> Methane potential was based on wet mass of MSW.

<sup>d</sup> L<sub>0</sub> assumed (128) m<sup>3</sup>/Mg-MSW (wet weight).

<sup>e</sup> Lag-time is time between the initiation of liquid addition and onset of methane generation.

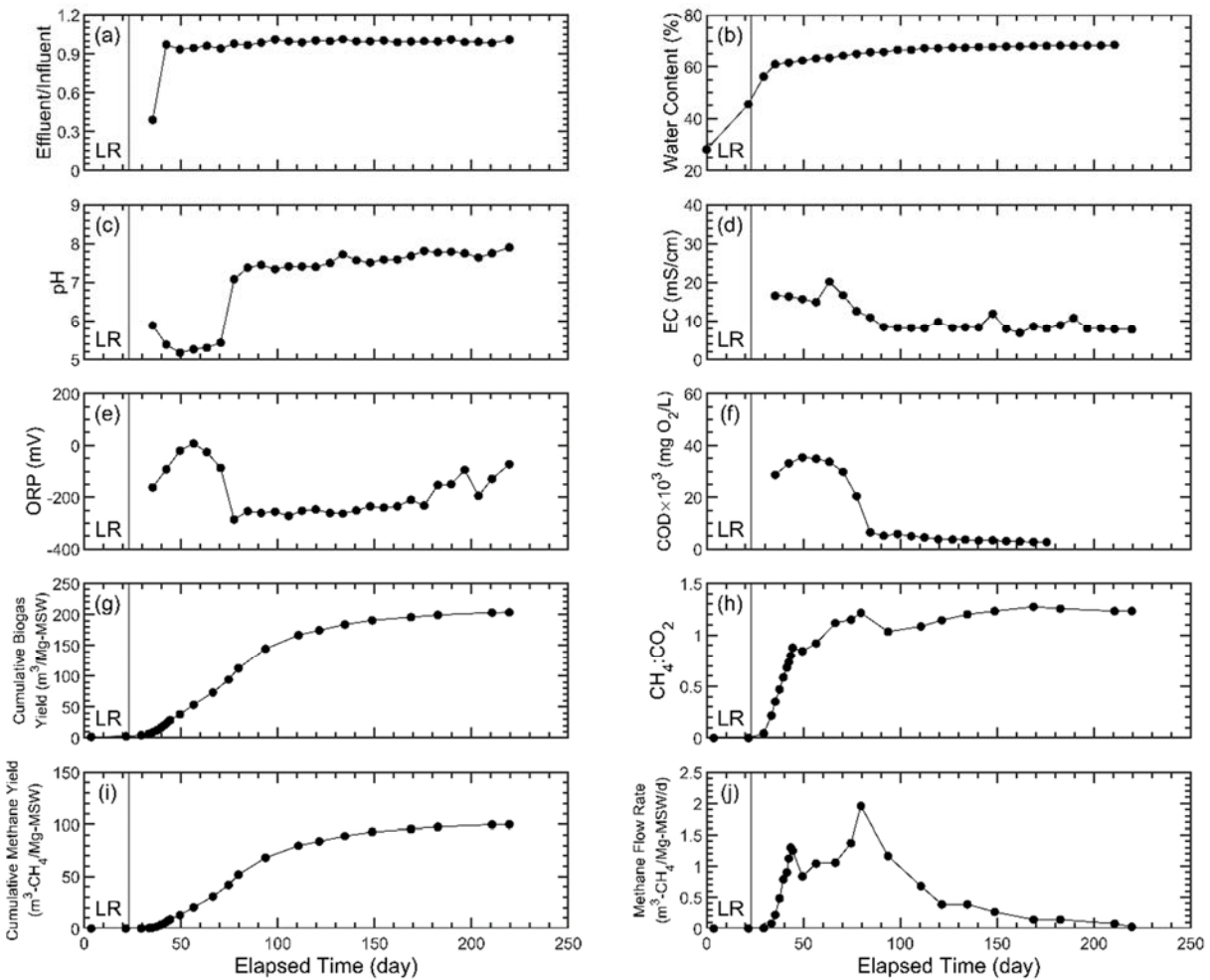


Fig. 2.1. Temporal trends of operational data collected for Reactor 14: (a) ratio of influent to effluent volumes; (b) wet weight water content; (c) leachate pH; (d) leachate electrical conductivity; (e) leachate oxidation reduction potential; (f) leachate chemical oxygen demand; (g) cumulative biogas yield; (h) ratio of methane to carbon dioxide; (i) cumulative methane yield; and (j) methane generation rate.

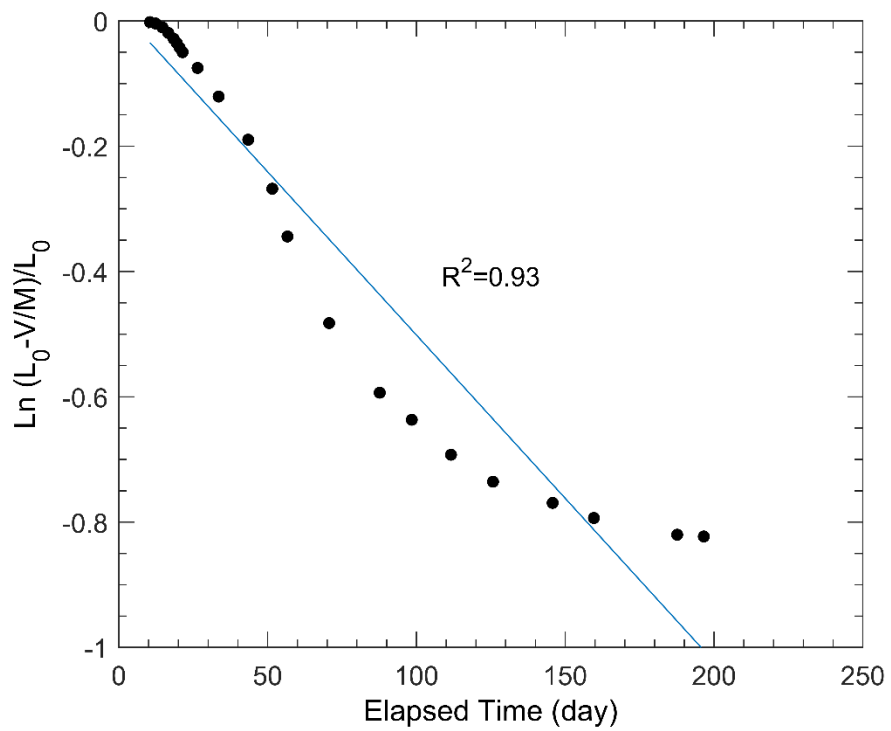


Fig. 2.2. Temporal relationship of linearized, cumulative methane generation for Reactor 14 that was fitted with the first-order decomposition equation in Eq. 3.

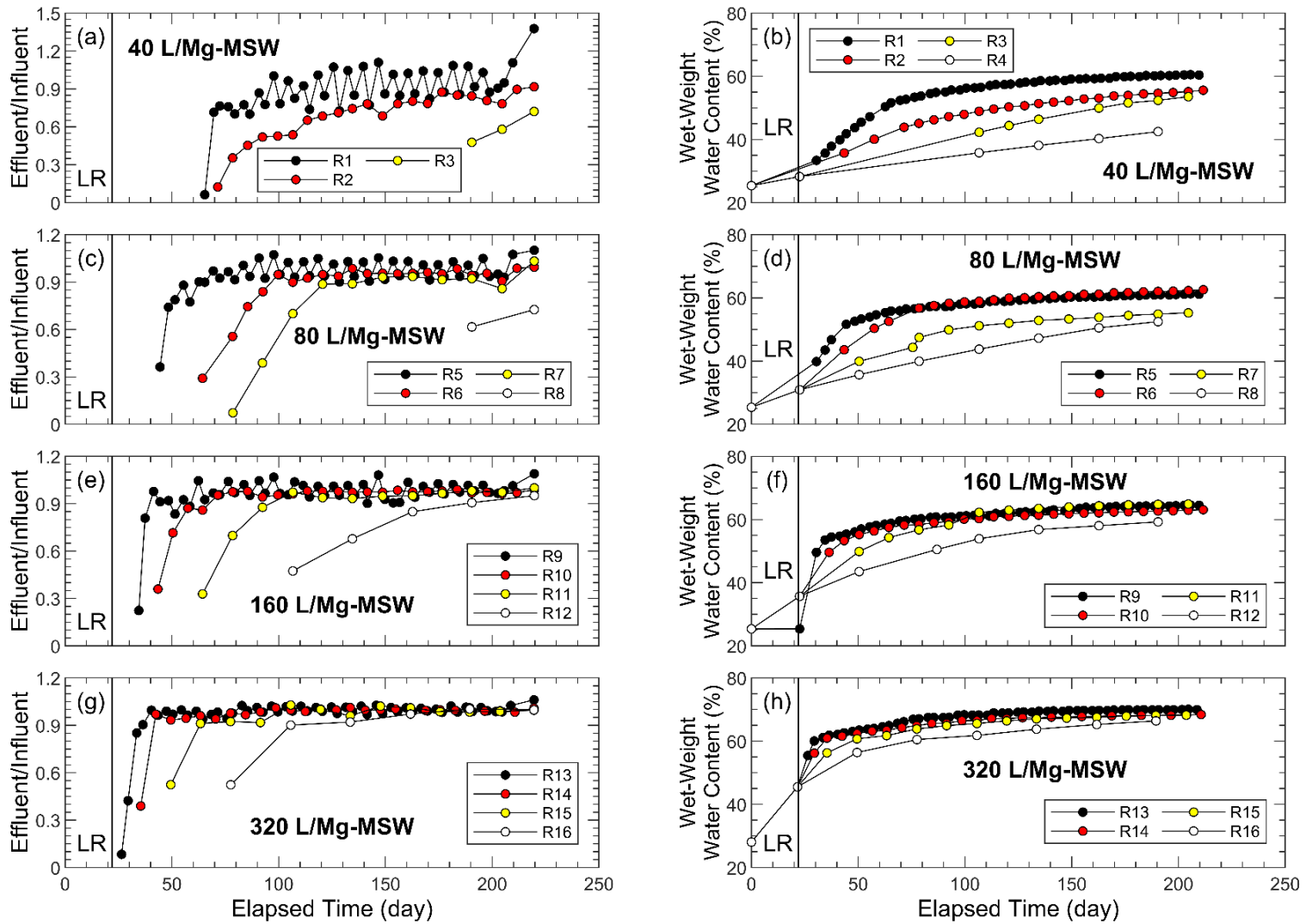


Fig. 2.3. Temporal trends of the ratio of effluent to influent volume and wet-weight water content for reactors grouped based on different dose volumes: (a and b) 40 L/Mg-MSW; (c and d) 80 L/Mg-MSW; (e and f) 160 L/Mg-MSW; and (g and h) 320 L/Mg-MSW. The duration between doses for given dose volume increases with reactor number (e.g., for 40 L/Mg-MSW, R1 = ½ week, R2 = 1 week, R3 = 2 weeks, and R4 = 4 weeks).

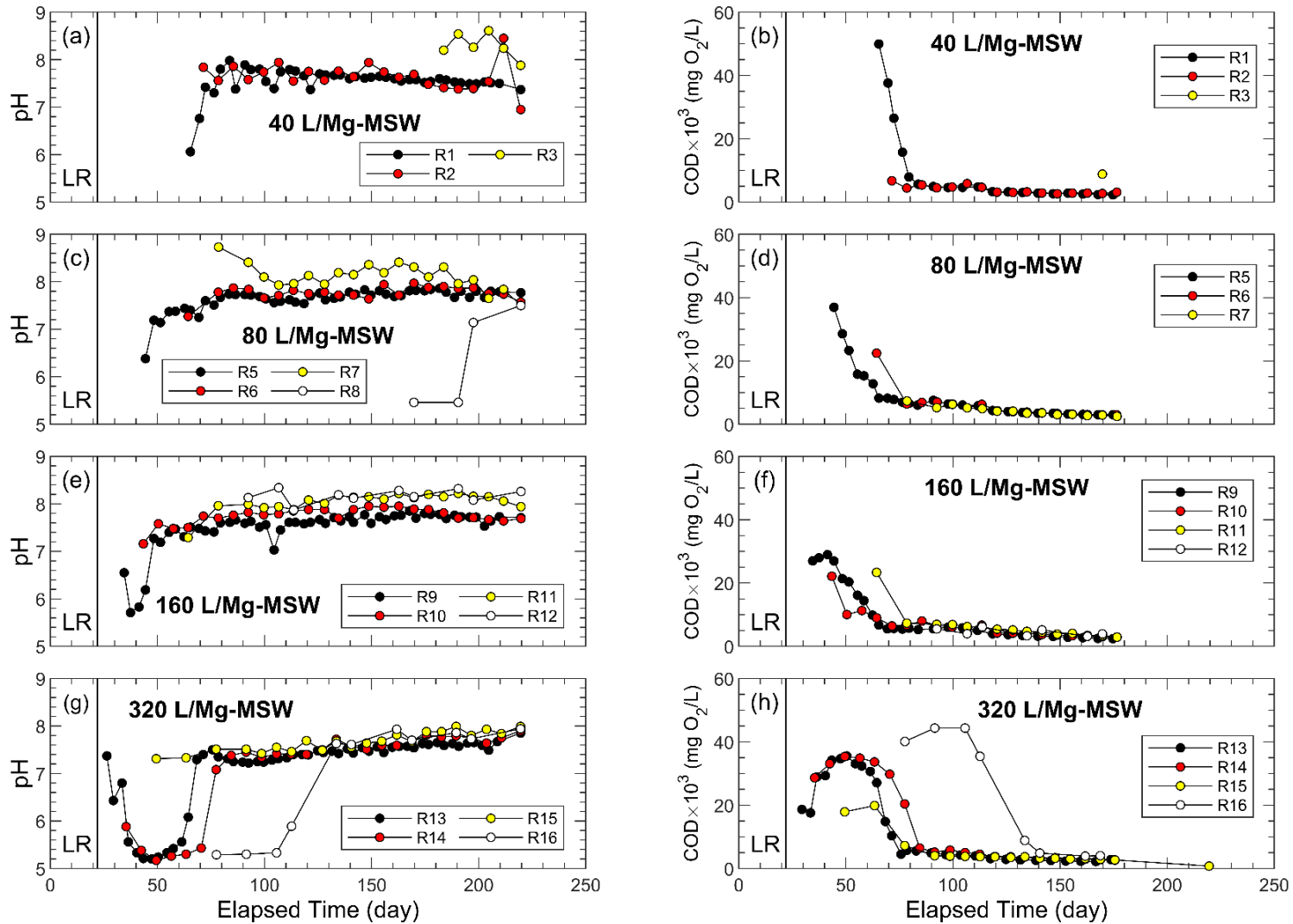


Fig. 2.4. Temporal trends of leachate pH and chemical oxygen demand (COD) for reactors groups based on dose volume: (a and b) 40 L/Mg-MSW; (c and d) 80 L/Mg-MSW; (e and f) 160 L/Mg-MSW; and (g and h) 320 L/Mg-MSW. The duration between doses for given dose volume increases with reactor number (e.g., for 40 L/Mg-MSW, R1 = ½ week, R2 = 1 week, R3 = 2 weeks, and R4 = 4 weeks).

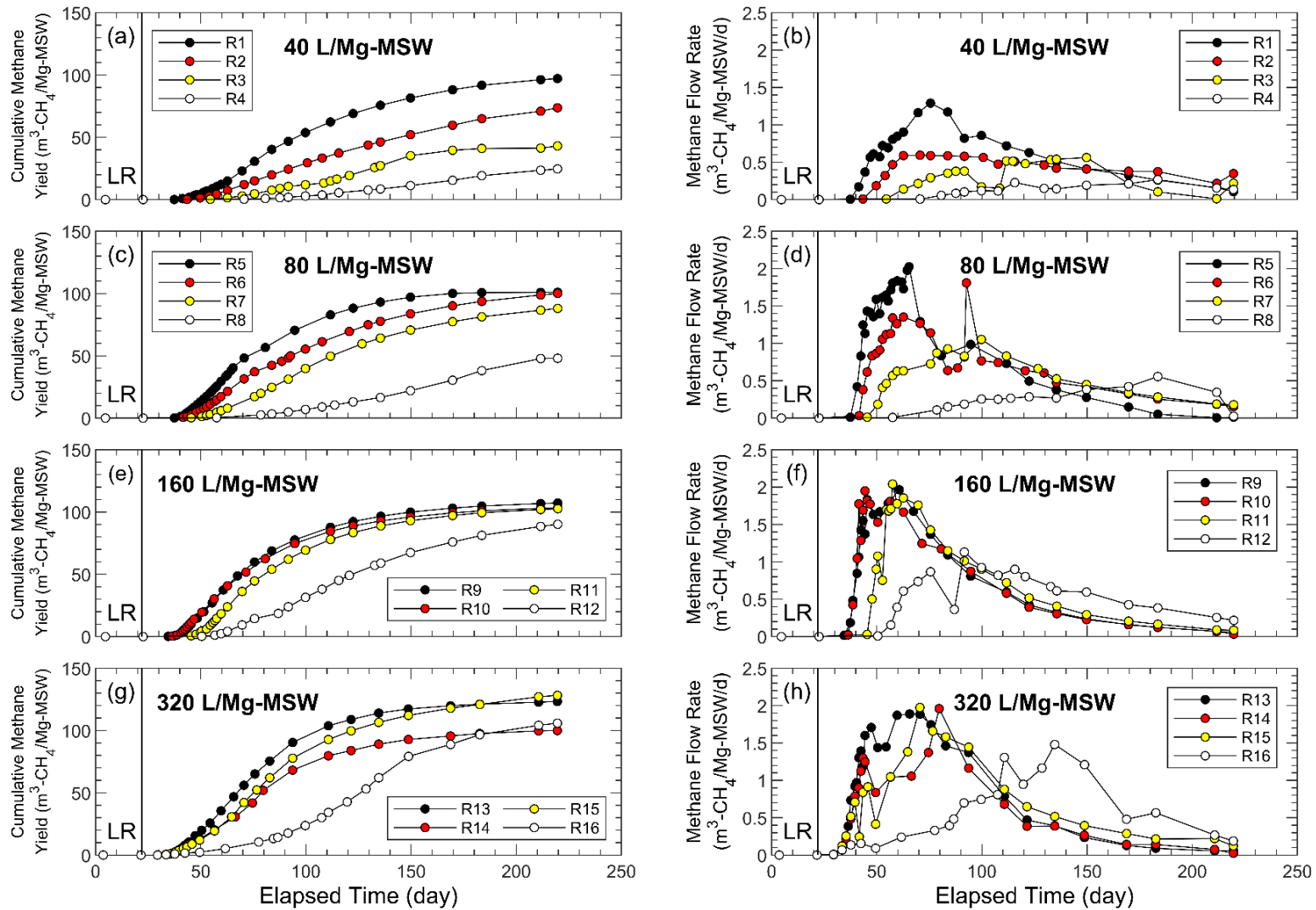


Fig. 2.5. Temporal trends of cumulative methane yield and methane flow rate normalized to MSW mass for reactor groups based on dose volume: (a and b) 40 L/Mg-MSW; (c and d) 80 L/Mg-MSW; (e and f) 160 L/Mg-MSW; and (g and h) 320 L/Mg-MSW. The duration between doses for given dose volume increases with reactor number (e.g., for 40 L/Mg-MSW, R1 = ½ week, R2 = 1 week, R3 = 2 weeks, and R4 = 4 weeks).

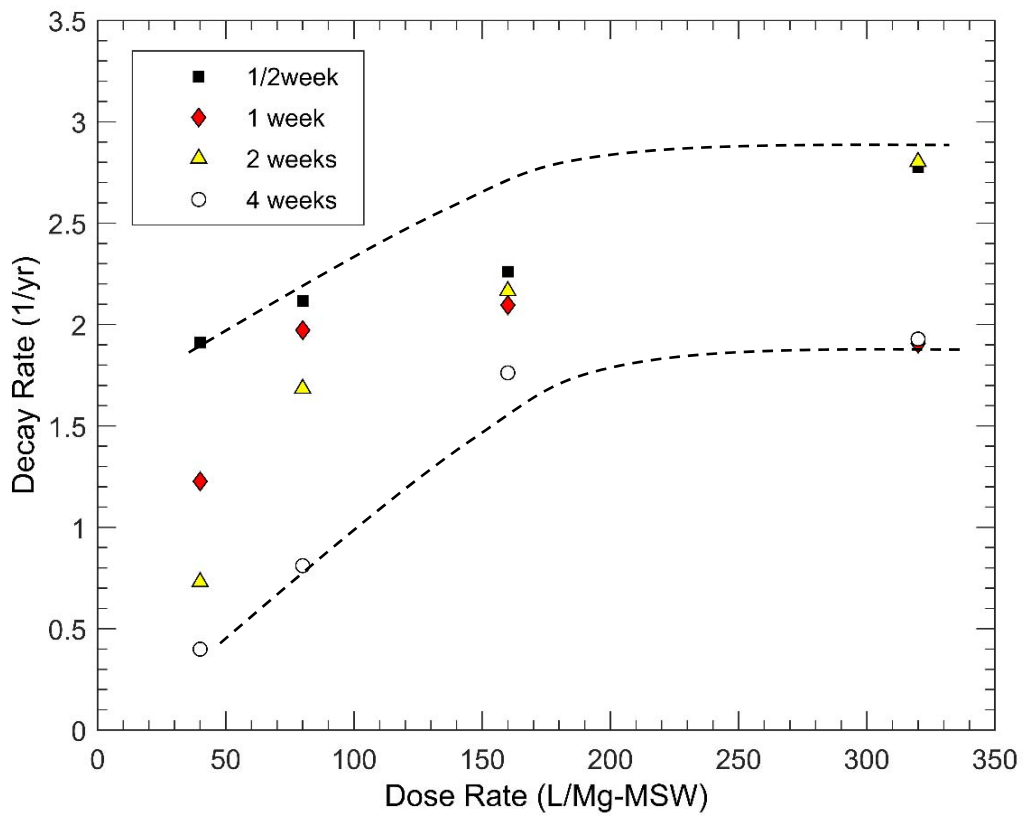


Fig. 2.6. First-order decay rate versus dose volume for reactors grouped into the four different dose frequencies: 1/2 week, 1 week, 2 weeks, and 4 weeks.

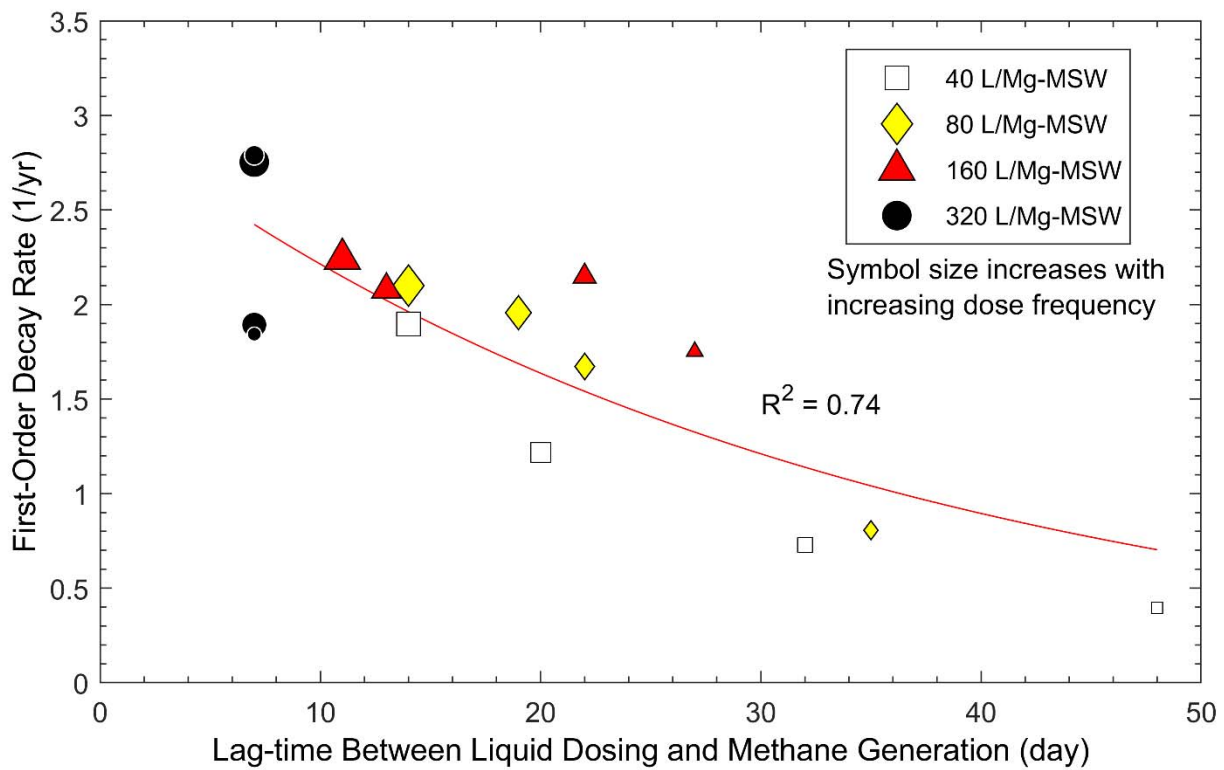


Fig. 2.7. First-order decay rate for methane generation versus lag-time between the start of liquid dosing and onset of biogas generation for the reactors operated with dose volumes of 40, 80, 160, and 320 L/Mg-MSW. Data symbols increase in size with increasing frequency of dosing (i.e., smallest symbol = 4 weeks and largest symbol = ½ week).

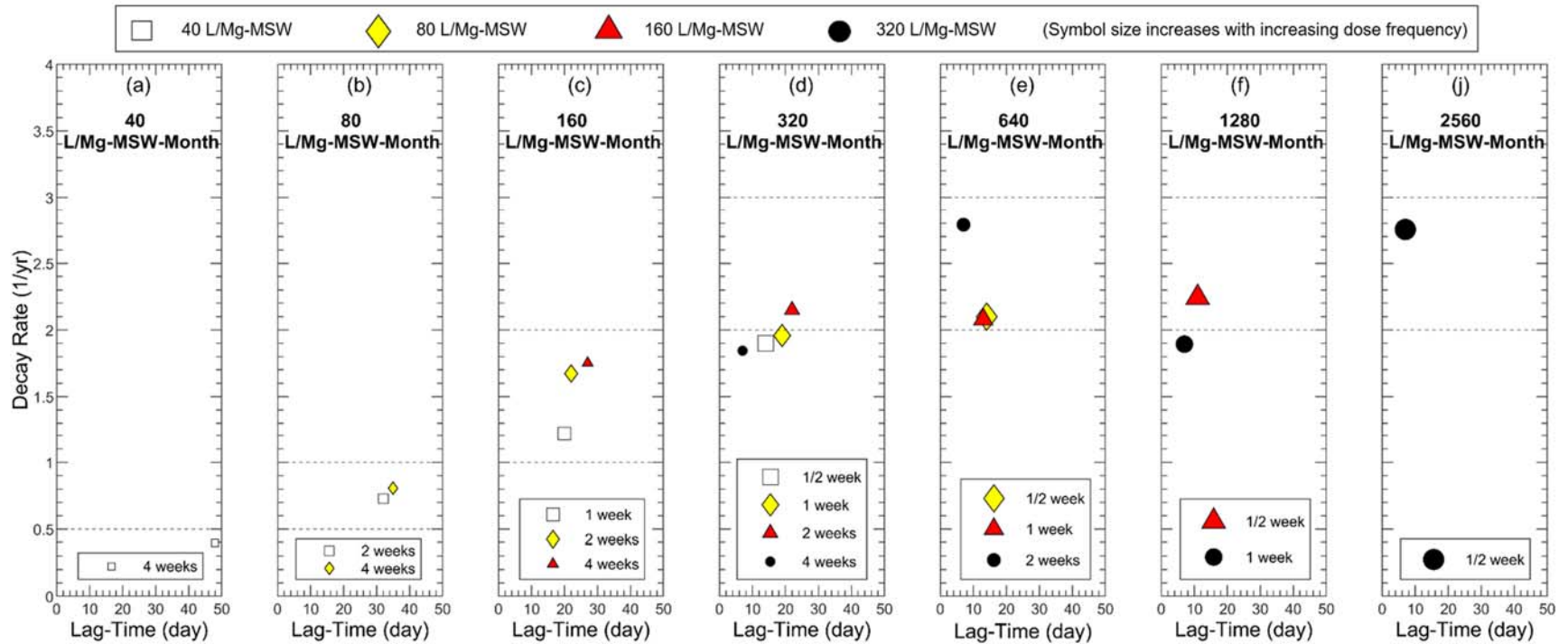


Fig. 2.8. First-order decay rate for methane generation versus lag-time between the start of liquid dosing and onset of biogas generation for the following monthly dose considerations: (a) 40 L/Mg-MSW/month; (b) 80 L/Mg-MSW/month; (c) 160 L/Mg-MSW/month; (d) 320 L/Mg-MSW/month; (e) 640 L/Mg-MSW/month; (f) 1280 L/Mg-MSW/month; (g) 2560 L/Mg-MSW/month.

## CHAPTER 3: SUMMARY AND CONCLUSIONS

A laboratory reactor study was conducted to evaluate the influence of moisture enhancement strategies on the biodegradation of MSW. Moisture enhancement strategies implemented in the reactors included four dose volumes (40, 80, 160, and 320 L/Mg-MSW) that were applied in four dose frequencies ( $\frac{1}{2}$ , 1, 2, and 4 weeks). Data were collected during laboratory operation to assess the moisture response (influent / effluent ratio and moisture content), leachate chemistry (pH, EC, ORP, and COD), and methane generation ( $\text{CH}_4$  yield and  $\text{CH}_4$  flow rate). The methane generation data were evaluated to determine the first-order decay rate and lag-time between the start of liquid dosing and onset of methane generation. The reactor experiment was created and operated under the premise that moisture enhancement strategies (i) reduce the lag-time between liquid addition and onset of methane generation and (ii) increase the rate of methane generation. The following observations and conclusions were based on results from the study.

- The majority of reactors generated leachate after reaching wet weight water contents of 50-52%, which was followed by effluent / influent ratios of approximately 90-100%. The end-of-operation water contents for reactors with dose volumes of 40 L/Mg-MSW increased with more frequent dosing. Wet weight water contents for reactors that generated leachate stabilized between 50% and 70%.
- Biodegradation processes of hydrolysis, acidogenesis, and methanogenesis were assumed to develop within reactors operated with a dose volume of 40 L/Mg-MSW and low frequencies (e.g., 2 and 4 weeks) prior to leachate generation based initial effluent leachate showing neutral pH and low COD coupled with active methane generation.
- In general, the more aggressive liquid dosing strategies (i.e., higher dose volumes and more frequency dosing) all yielded leachate chemistry signatures that displayed hydrolysis, acidogenesis, and methanogenesis phases.
- The first-order decay rate for  $\text{CH}_4$  generation increased with an increase in dose volume for all four dose frequencies. For example, peak  $\text{CH}_4$  flow rate increased from 0.27 to 1.29  $\text{m}^3/\text{Mg-MSW/d}$  from reactors operated with a dose volume of 40 L/Mg-MSW as the dose frequency increased from every 4 weeks to every  $\frac{1}{2}$  week. In addition, cumulative methane yield increased from 19% to 76% (relative to the highest methane yield measured among all reactors) with an increase in dose frequency.
- Regardless of minor differences in  $\text{CH}_4$  generation for reactors operated with a dose volume of 160 L/Mg-MSW, there were negligible differences in  $\text{CH}_4$  yield and flow rate considering dose frequencies of  $\frac{1}{2}$ , 1, and 2 weeks. In addition, reactors operated with dose frequencies of  $\frac{1}{2}$  and 2 weeks and a dose volume of 320 L/Mg-MSW (R13 and R15) yielded the highest  $\text{CH}_4$  flow rates ( $\approx 2.8$  1/yr) and  $\text{CH}_4$  yield ( $\approx 125$   $\text{m}^3/\text{Mg-MSW}$ ).
- Trends of increased decay rate and reduced lag-time with an increase in dose frequency were observed for reactors operated with dose volumes of 40, 80, and 160 L/Mg-MSW. Thus, more rapid dosing was advantageous to initiating  $\text{CH}_4$  generation sooner after the first inoculum dose was added.
- Reactors with more aggressive moisture enhancement (i.e., higher monthly dosing) attained elevated  $\text{CH}_4$  generation (higher decay rate) that initiated at shorter elapsed times following the onset of dosing (reduced lag-time). An assessment of liquid dosing / recirculation per month indicated that there was a more pronounced trend of increasing decay rate and decreasing lag-time as moisture enhancement increased from 40 L/Mg-MSW/month to 320 L/Mg-MSW/month as compared to effects observed for additional increases in moisture above 320 L/Mg-MSW/month.

## CHAPTER 4: MATERIALS AND METHODS

### 4.1 Experiment Overview

Laboratory reactors were operated in a temperature-controlled room at 37 °C, which is near the optimal temperature for mesophilic waste decomposition (e.g., Barlaz et al. 1989). A collection of photographs documenting the setup and operation of the laboratory reactors is included in Appendix 1. The main variable of the experiment was moisture addition, which included leachate dose / recirculation rates of 40, 80, 160, and 320 L/Mg-MSW (wet weight) that were applied at frequencies of every ½ week, 1 week, 2 weeks, and 4 weeks. The possible dose rate and frequency combinations yielded 16 reactors with varying moisture addition strategies; an additional control reactor was operated without any liquid added. The dose rates and frequencies used in this study were selected to represent relevant moisture enhancement strategies observed in full-scale landfills (Bareither et al. 2010; Bareither et al. 2017; Nwaokorie et al. 2018).

### 4.2 Reactor Design

A photograph of a laboratory-scale reactor is shown in Fig. 2.9. Each reactor was filled with 2.4 kg of shredded MSW representative of the U.S. average composition (Staley and Barlaz 2009; US EPA 2015). Reactors were equipped with capabilities of leachate and gas management. Leachate was distributed to the surface of the MSW via a perforated pipe placed within a gravel layer, and was collected in inert plastic bags below the reactors. Biogas generated during organic waste decomposition was collected in gasbags.

The reactors consisted of polycarbonate cylinders with a height of 457 mm and an inside diameter of 203 mm. The MSW specimens were compacted between two layers of nonwoven geotextile and washed gravel. The bottom gravel layer was for leachate collection and the top gravel layer was for liquid/leachate distribution as well as to apply a 2-kPa vertical stress that represented interim landfill cover. Liquid/leachate distribution was conducted via a funnel external to the reactor cell that connected to a perforated PVC pipe network inside the upper gravel layer via a flexible tube (Fig. 2.9). The system included a ball valve below the funnel to limit ingress of atmospheric air into the reactor. Leachate was collected in an IV bag connected to the effluent port in the bottom of reactor.

Biogas generated during MSW biodegradation was collected in 10-L, 25-L, or 40-L Flexfoil gas bags (SKC Inc., Eight Four, PA) depending on the flow rate. A four-way valve was included within the flexible tube that connected the headspace of the reactor to the gasbag. These valves facilitated gas sampling and disconnecting of the gasbag during gas volume measurement.

### 4.3 Municipal Solid Waste

Municipal solid waste was collected during disposal at the working face of Larimer County Landfill in Fort Collins, Colorado, USA. Waste was hand-sorted into relevant categories (e.g., paper, plastic, metal, etc.), air-dried, and stored in sealed barrels. All waste materials used in the laboratory reactors were shredded with a slow-speed, high-torque shredder (Model 1-SHRED-H-0800, JWC Environmental, Santa Ana, CA) to a maximum particle size of approximately 20 mm (i.e., approximately one-tenth the reactor diameter). Food waste for this study was collected as pulped, pre-consumer food waste from Housing & Dining Services at Colorado State University.

A summary of the MSW composition used in the laboratory reactors is in Table 2.2, which was reflective of the U.S. national average (Staley and Barlaz 2009; US EPA 2015). Each

reactor was filled with 2.4 kg of shredded MSW that was moisture equilibrated via addition of food waste and left over night in sealed buckets prior to specimen preparation. Waste specimens were compacted via hand tamping in four layers of equal thickness to an average total unit weight of 3.58 kN/m<sup>3</sup> ( $\approx$  615 lb/yd<sup>3</sup>). Select sub-samples of the MSW reactor specimens were dried in oven at 105 °C for 24 h to determine water content and subsequently combusted at 550 °C for 2 h to determine volatile solids. The average initial dry weight water of the MSW specimens was 34% (wet weight water content  $\approx$  25%) and average initial volatile solids was 72%.

#### **4.4 Liquid Management**

Liquid dosing initiated in all reactors with centrifuged and diluted anaerobic digester sludge (ADS) (i.e., inoculum). The ADS was obtained from the Water Reclamation Facility in Fort Collins, Colorado to provide a source of anaerobic microorganisms to the MSW during initial dosing. The ADS was centrifuged to remove solid particles and then diluted with de-ionized water (DIW) to approximate a chemical oxygen demand (COD) concentration representative of landfill leachate ( $\approx$  2000 mg-O<sub>2</sub>/L) (Kjeldsen et al. 2002). Fresh inoculum was added to all reactors until leachate was generated, whereupon leachate was recirculated with additional fresh inoculum added (as needed) to achieve the target dose volumes. Excess effluent that exceeded the target dose volumes was stored in plastic containers with minimal headspace at 4 °C until required for subsequent recirculation.

Leachate samples were collected from the IV bags on a weekly basis and evaluated for pH, electrical conductivity (EC), oxidation-reduction potential (ORP), and COD. Samples were collected from all reactors prior to recirculating the leachate. An additional leachate sample for the reactors with a 4-week dose frequency was collected one week after recirculation to generate additional leachate chemistry data for analysis. pH, EC, and ORP were measured on 10-mL samples using a portable multi-parameter hand-held meter (Hach Sension+MM150). The 10-mL samples were subsequently acidified with H<sub>2</sub>SO<sub>4</sub> and stored at 4 °C for COD analysis. Chemical oxygen demand was measured with VWR 0-1500 mg/L test kits. A Hach DRB200 heating block and Hach DR3900 spectrometer were used in the COD analysis.

#### **4.5 Biogas Management and Analysis**

##### ***4.5.1 Biogas Measurement and Composition***

The volume of biogas collected in the gasbags was measured via water displacement. Gasbags were removed from the temperature-controlled reactor room and allowed to equilibrate to ambient laboratory temperature ( $\approx$  20 °C) prior to measuring the volume. Biogas was evacuated from the gas bags using a vacuum pump into an inverted 10-L graduated cylinder that was submerged in water acidified with hydrochloric acid (pH  $\approx$  3). Gas volume measurements were made after the displaced cylinder equilibrated with atmospheric pressure.

Biogas samples for composition analysis were collected from each reactor and injected into evacuated 80-mL glass bottles with Butyl Rubber Stoppers. Composition of the biogas was measured with a HP6990 Gas Chromatograph (GC) (Hewlett-Packard, Palo Alto, CA) to determine the relative composition of carbon dioxide (CO<sub>2</sub>) and methane (CH<sub>4</sub>). The GC was equipped with a thermal conductivity detector and RT-Q-Bond column (Restek Corporation, Bellefonte, PA). A small sample of biogas was extracted from the glass bottles and injected into the GC using a 50- $\mu$ L gas tight syringe. OpenLAB chromatography software (Agilent Technologies, Santa Clara, CA) was used as the data interface for the GC. Deviations from the software defaults included a 30 °C inlet and oven temperature, 200 °C thermal conductivity detector temperature, 50 cm/s linear velocity in the column, 40:1 split flow, and hydrogen used

as the carrier gas. Percentages of CO<sub>2</sub> and CH<sub>4</sub> were determined relative to calibration curves generated from chemically pure CO<sub>2</sub> and CH<sub>4</sub> gas (Airgas, Radnor, PA).

#### 4.5.2 Decay Rate and Lag-Time

Methane generation data from the reactors was modeled using the U.S. EPA LandGEM to determine the first-order decay rate (US EPA 2005). The U.S. LandGEM model is

$$Q_n = kL_0 \sum_{i=0}^n \sum_{j=0.0}^{0.9} \frac{M_i}{10} e^{-kt_{ij}} \quad (1)$$

where  $Q_n$  is methane flow rate (m<sup>3</sup>-CH<sub>4</sub>/year) in year  $n$ ,  $M_i$  is the mass of waste accepted (Mg) in year  $i$ ,  $L_0$  is the ultimate methane yield (m<sup>3</sup>-CH<sub>4</sub>/Mg),  $k$  is the first-order decay rate (1/yr),  $j$  is the deci-year time increment, and  $t$  is elapsed time since waste placement (year). LandGEM applied to the reactor data obtained in this study was an integrated and simplified form of Eq. 1 that represented cumulative methane generation:

$$V = L_0 M (1 - e^{-kt}) \quad (2)$$

where  $V$  is cumulative CH<sub>4</sub> collected during the experiment (m<sup>3</sup>) and  $M$  is the initial mass of solid waste (Mg). Eq. (2) can be arranged as shown in Eq. (3), where the numerator on the right side is the remaining methane potential at time  $t$ .

$$-kt = \ln \frac{L_0 - V}{L_0} \quad (3)$$

The decay rate in Eq. 3 was determined via linear regression of the cumulative methane volume versus time relationship with an assumed  $L_0$  and measured  $V$ . The  $L_0$  was assumed equal to 128 L-CH<sub>4</sub>/Mg-MSW (dry mass) based on the maximum CH<sub>4</sub> yield among the reactors operated in this study.

The amount of potential CH<sub>4</sub> generation from the inoculum added to the reactors was evaluated for the reactor with the largest amount of inoculum added. Potential CH<sub>4</sub> generated from the inoculum was calculated via the measured CH<sub>4</sub> potential of the inoculum (1.34 mL-CH<sub>4</sub>/mL) multiplied by the total volume of fresh inoculum added. The total potential CH<sub>4</sub> generated due to fresh inoculum was negligible (i.e., < 1.8% of total CH<sub>4</sub> collected from the reactor); thus, corrections were not applied to CH<sub>4</sub> generation data from the reactors.

Table 2.2. Summary of waste composition

Composition	Percentage (%) <sup>a</sup>
Paper	11.4 (274)
Cardboard	3.5 (84)
Yard trimmings	8.2 (198)
Metals	9.8 (235)
Glass	5.4 (130)
Rigid plastic	15.5 (373)
Film plastic	3.8 (91)
Wood	8.5 (203)
Food	22.5 (541)
Rubber/leather/textiles	11.3 (271)
Total	100 (2400)

<sup>a</sup> Mass of each waste fraction in grams provided in parentheses

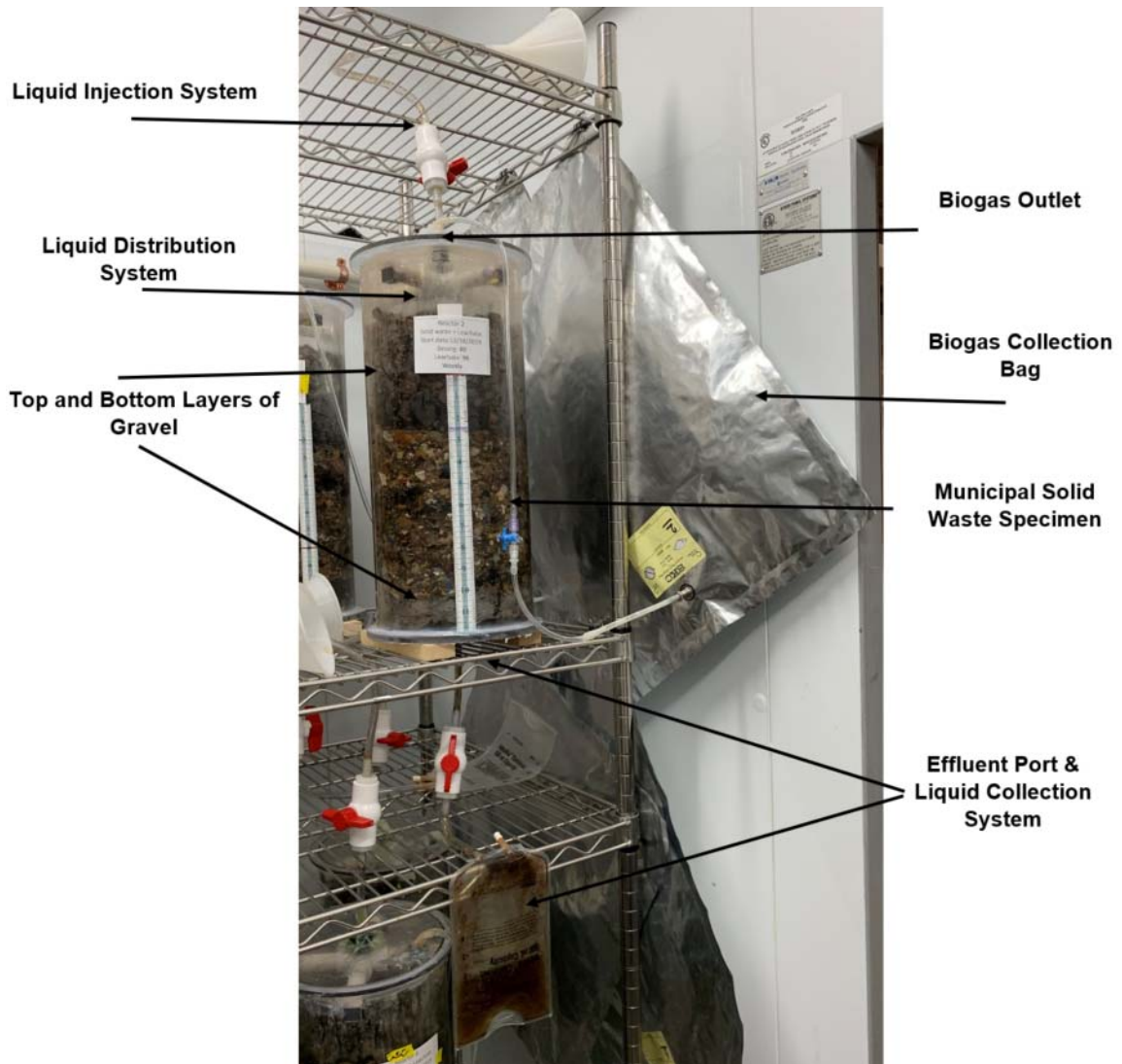


Fig. 2.9. Photograph of a laboratory-scale reactor.

## **ACKNOWLEDGEMENTS**

Financial support for this study was provided by the Environmental Research and Education Foundation (EREF) through a contract with Colorado State University (CSU). The support is gratefully acknowledged. The opinions expressed in this paper are solely those of the authors and do not reflect the policies or opinions of EREF or CSU.

## REFERENCES

- Agdag, O., and Sponza, T. (2005). Co-digestion of industrial sludge with municipal solid wastes in anaerobic simulated landfilling bioreactors. *Process Biochemistry*, 40, 1871-1879.
- Agdag, O., and Sponza, T. (2007). Co-digestion of mixed industrial sludge with municipal solid wastes in anaerobic simulated landfilling bioreactors. *Journal of Hazardous Materials*, 140, 75-85.
- Aghdam, E., Scheutz, C., and Kjeldsen, P. (2017). Assessment of methane production from shredder waste in landfills: The influence of temperature, moisture, and metals. *Waste Management*, 63, 226-237.
- Al Yaqout, A. (2003). Assessment and analysis of industrial liquid waste and sludge disposal at unlined landfill sites in arid climate. *Waste Management*, 23, 817-824.
- Amini, H., Reinhart, D., and Mackie, K. (2012). Determination of first-order landfill gas modeling parameters and uncertainties. *Waste Management*, 32, 305-316.
- Bae, J., Cho, K., Lee, S., Bum, B., and Yoon, B. (1998). Effects of leachate recycle and anaerobic digester sludge recycle on the methane production from solid wastes. *Water Science Technology*, 38(2) 159-168.
- Bareither, C., Benson, C., Barlaz, M., Edil, T., and Tolaymat, T. (2010). Performance of North American bioreactor landfills. I: Leachate hydrology and waste settlement. *Journal of Environmental Engineering*, 136(8), 824-838.
- Bareither, C., Benson, C., and Edil, T. (2012a). Effects of waste composition and decomposition on the shear strength of municipal solid waste. *Journal of Geotechnical and Geoenvironmental Engineering*, 138(10), 1161-1174.
- Bareither, C., Benson, C., and Edil, T. (2012b). Comparison of waste settlement parameters for bioreactor landfills derived from physical, chemical, and biological processes, *Proc. Global Waste Management Symposium*, Penton Media, 1-5.
- Bareither, C., Benson, C., and Edil, T. (2013). Compression of municipal solid waste in bioreactor landfills: Mechanical creep and biocompression. *Journal of Geotechnical and Geoenvironmental Engineering*, 139(7), 1007-1021.
- Bareither, C.A. and Kwak, S. (2015). Assessment of municipal solid waste settlement models based on field-scale data analysis. *Waste Management*, 42, 101-117.
- Bareither, C., Barlaz, M., Doran, M., and Benson, C. (2017). Retrospective analysis of Wisconsin's landfill organic stability rule. *Journal of Environmental Engineering*, 143(5).
- Barlaz, M.A., Schaefer, D.M., and Ham, R.K. (1989). Bacterial population development and chemical characteristics of refuse decomposition in a simulated sanitary landfill. *Applied and Environmental Microbiology*, 55(1), 55-65.

- Barlaz, M., Chanton, J., and Green, R. (2009). Controls on landfill gas collection efficiency: Instantaneous and lifetime performance. *Journal of the Air & Waste Management Association*, 59, 1399-1404.
- Barlaz, M., Bareither, C., Hossain, A., Saquing, J., Mezzari, I., Benson, C., Tolaymat, T., and Yazdani, R. (2010). Performance of North American bioreactor landfills. II: Chemical and biological characteristics. *Journal of Environmental Engineering*, 136(8), 839-853.
- Behera, S., Kim, D., Shin, H., Cho, S., Yoon, S., and Park, H. (2011). Enhanced methane recovery by food waste leachate injection into a landfill in Korea. *Waste Management*, 31, 2126-2132.
- Benson, C., Barlaz, M., Lane, D., and Rawe, J. (2007). Practice review of five bioreactor/recirculation landfills. *Waste Management*, 27, 13-29.
- Chen, Y., Cheng, J., and Creamer, K. (2008). Inhibition of anaerobic digestion process: A review. *Bioresource Technology*, 99, 4044-4064.
- Chickering, G. Krause, M., and Townsend, T. (2018). Determination of as-discarded methane potential in residential and commercial municipal solid waste. *Waste Management*.
- Cossu, R., Blakey, N., and Cannas, P. (1993). Influence of codisposal of municipal solid waste and olive vegetation water on the anaerobic digestion of a sanitary landfill. *Water Science Technology*, 27(2), 261-271.
- Dhesi, P. (2003). *Study of addition of non-hazardous industrial and municipal wastewater to bioreactor landfills*, MS Thesis, University of Central Florida, Orlando, FL, USA.
- Diamantis, V., Erguder, T., Aivasidis, A., Verstraete, W., and Voudrias, E. (2013). Wastewater disposal to landfill-sites: A synergistic solution for centralized management of olive mill wastewater and enhanced production of landfill gas. *Journal of Environmental Management*, 128, 427-434.
- Fairweather, R., and Barlaz, M. (1998). Hydrogen sulfide production during decomposition of landfill inputs. *Journal of Environmental Engineering*, 124(4), 353-361.
- Griffin, M., McMahon, K., Mackie, R., and Raskin, L. (1998). Methanogenic population dynamics during start-up of anaerobic digesters treating municipals solid waste and biosolids. *Biotechnology and bioengineering*, 57(3), 342-355.
- Hanson, J., Yesiller, N., Von Stockhausen, S., and Wong, W. (2010). Compaction characteristics of municipal solid waste. *Journal of Geotechnical and Geoenvironmental Engineering*, 136(8), 1095-1102.
- Kjeldsen, P., Barlaz, M., Rooker, A., Baun, A., Ledin, A., and Christensen, T. (2002). Present and long-term composition of MSW landfill leachate: A review. *Environmental Science and Technology*, 32(4), 297-336.
- Knox, K. (1983). Treatability studies on leachate from a co-disposal landfill. *Environmental Pollution*, 5 (Series B), 157-174.

- Ko, J., and Townsend, T. (2012). Evaluation of the potential methane yield of industrial wastewaters used in bioreactor landfills. *Journal of Material Cycles Waste Management*, 14, 162-168.
- Lee, D., Behera, S., Kim, J., and Park, H. (2009). Methane production potential of leachate generated from Korean food waste recycling facilities: A lab-scale study. *Waste Management*, 29, 876-882.
- Loureiro, S.M., Rovere, E.L.L., and Mahler, C.F. (2013). Analysis of potential for reducing emissions of greenhouse gases in municipal solid waste in Brazil, in the state and city of Rio de Janeiro. *Waste Management*, 33(5), 1302–1312.
- Moody, L., Burns, R., Bishop, G., Sell, S., and Spajic, R. (2011). Using biochemical methane potential assays to aid in co-substrate selection for co-digestion. *Applied Engineering in Agriculture*, 27(3), 433-439.
- Morris, J. W. F., Crest, M., Barlaz, M. A., Spokas, K. A., Åkerman, A., & Yuan, L. (2012). Improved methodology to assess modification and completion of landfill gas management in the aftercare period. *Waste Management*, 32(12), 2364–2373.
- Nwaokorie, K. (2017). *Phase-based analysis to determine first-order decay rates for a bioreactor landfill*. MS Thesis, Colorado State University, Fort Collins, CO, USA.
- Owen, W., Stuckey, D., Healy, J., Young, L., and McCarty, P. (1979). Bioassay for monitoring biochemical methane potential and anaerobic toxicity. *Water Research*, 13(6), 473-560.
- Pantini, S., Verginelli, I., & Lombardi, F. (2015). Analysis and modeling of metals release from MBT wastes through batch and up-flow column tests. *Waste Management*, 38(1), 22–32.
- Percival, L., and Senior, E. (1998). An assessment of the effects of the dual co-disposal of phenol and waste activated sewage sludge with refuse on the refuse anaerobic fermentation and leachate quality. *Water SA*, 24(1), 57-70.
- Pohland, F., and Gould, J. (1986). Co-disposal of municipal refuse and industrial waste sludge in landfills. *Water Science Technology*, 18(12). 177-192.
- Pohland, F.G. and Kim, J.C., (1999). In situ anaerobic treatment of leachate in landfill bioreactors. *Water Science & Technology*, 40 (8), 203–210.
- Rahim, R., and Watson-Craik, I. (1997). The co-disposal of a model brewery wastewater with domestic refuse. *Letters in Applied Microbiology*, 24, 281-285.
- Reinhart, D., and Al-Yousfi, A. (1996). The impact of leachate recirculation on municipal solid waste landfill operating characteristics. *Waste Management and Research*, 14, 337-346.
- Reinhart, D., McCreanor, P., and Townsend, T. (2002). The bioreactor landfill: Its status and future. *Waste Management & Research*, 20, 172-186.
- Sanphoti, N., Towprayoon, S., Chaiprasert, P., and Nopharatana, A. (2006). The effects of leachate recirculation with supplemental water addition on methane production and waste

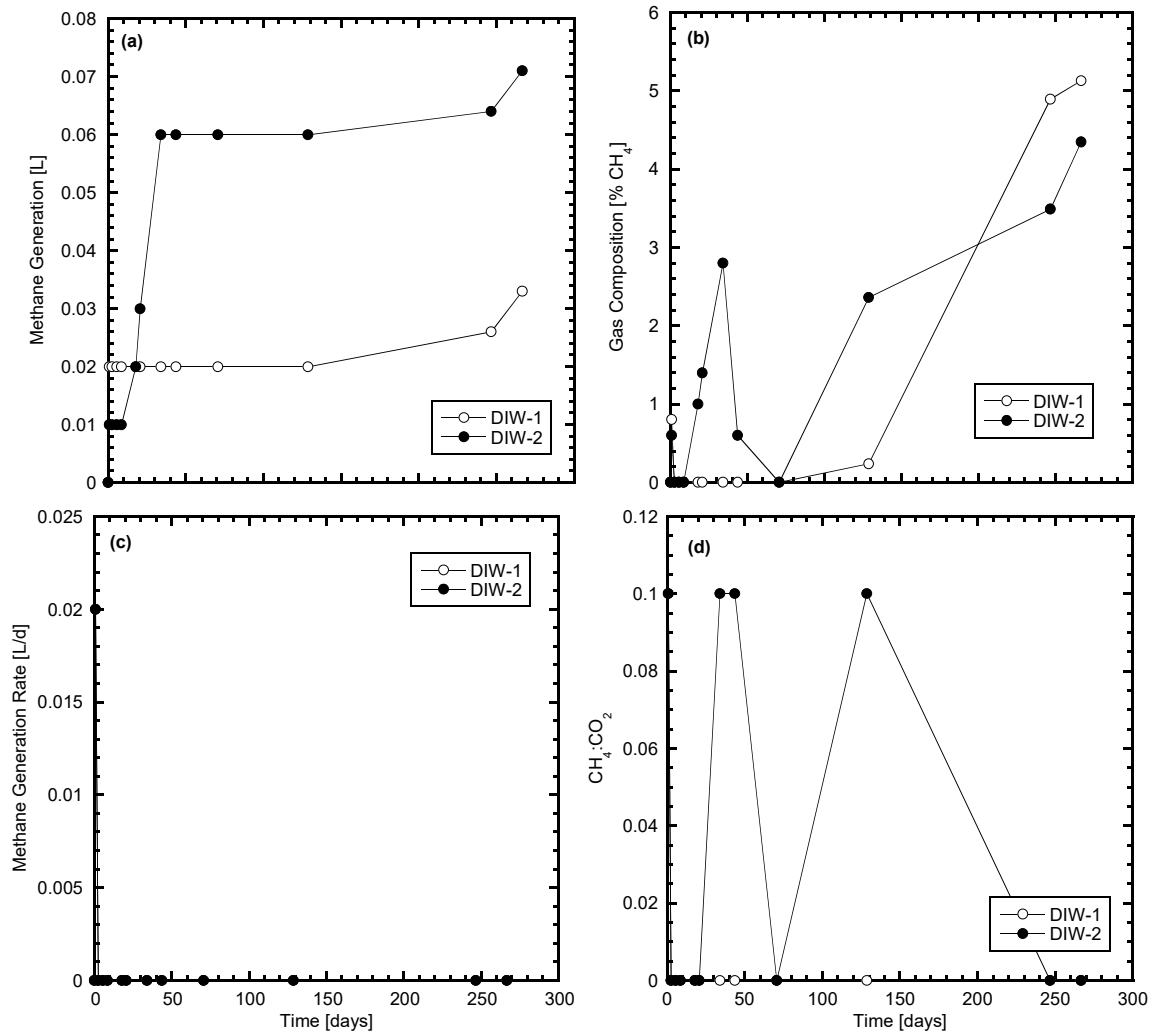
- decomposition in a simulated tropical landfill. *Journal of Environmental Management*, 81, 27-35.
- Siddique, R., Kaur, G., and Rajor, A. (2010). Waste foundry sand and its leachate characteristics. *Resources, Conservation and Recycling*, 54, 1027-1036.
- Sosnowski, P., Wieczorek, A., and Ledakowicz, S. (2003). Anaerobic co-digestion of sewage sludge and organic fraction of municipal solid wastes. *Advances in Environmental Research*, 7, 609-616.
- Sponza, T., and Agdag, O. (2004). Impact of leachate recirculation and recirculation volume on stabilization of municipal solid wastes in simulated anaerobic bioreactors. *Process Biochemistry*, 39, 2157-2165.
- Staley, B., and Barlaz, M. (2009). Composition of municipal solid waste in the united states and implications for carbon sequestration and methane yield. *Journal of Environmental Engineering*, 135(10), 901-909.
- Staley, B., de los Reyes III, S., and Barlaz, M. (2011). Effect of special differences in microbial activity, pH, and substrate levels on methanogenesis initiation in refuse. *Applied and Environmental Microbiology*, 77(7), 2381-2391.
- Townsend, T., Jang, Y., and Thurn, L. (1999). Simulation of construction and demolition waste leachate. *Journal of Environmental Engineering*, 125(11), 1071-1081.
- Townsend T.G., Powell J., Jain P., Xu Q., Tolaymat T., and Reinhart D. (2015) *Moisture Supply and Conveyance. In: Sustainable Practices for Landfill Design and Operation. Waste Management Principles and Practice*. Springer, New York, NY
- US EPA (2005). Landfill gas emissions model (LandGEM) version 3.02 user's guide. EPA/600/R-05/047, United States Environmental Protection Agency, Research Triangle Park, NC 2005.
- USEPA (2014a). Advancing sustainable materials management: 2014 fact sheet. United States Environmental Protection Agency, Washington, DC.
- USEPA (2014b). Permitting of landfill bioreactor operations: Ten years after the RD&D rule. United States Environmental Protection Agency, Washington, DC.
- US EPA (2015) Advancing Sustainable Materials Management: 2015 Fact Sheet. Assessing Trends in Material Generation, Recycling, Composting, Combustion with Energy Recovery and Landfilling in the United States July 2018.
- Wang, Y., Byrd, C., and Barlaz, M. (1994). Anaerobic biodegradability of cellulose and hemicellulose in excavated refuse samples using a biochemical methane potential assay. *Journal of Industrial Microbiology*, 13(3), 147-153.
- Waste Management (2004). The bioreactor landfill: Next generation landfill technology. *Bioreactor Program*. Waste Management, Cincinnati, OH, USA.

- Watson-Craik, I., and Senior, E. (1989). Treatment of phenolic wastewaters by co-disposal with refuse. *Water Resources*, 23(10), 1293-1303.
- Watson-Craik, I., and Sinclair, K. (1995). Co-disposal of industrial wastewaters and sludge. *Microbiology of Landfill Sites*, 91-130.
- Wilson, P., Loetscher, L., Sharvelle, S., and De Long, S. (2013). Microbial community acclimation enhances waste hydrolysis rates under elevated ammonia and salinity conditions. *Bioresource Technology*, 146, 15-22.
- Xu, Q., Townsend, T., and Bitton, G. (2011). Inhibition of hydrogen sulfide generation from disposed gypsum drywall using chemical inhibitors. *Journal of Hazardous Materials*, 191, 204-211.
- Zekkos, D., Bray, J., Kavazanjian, E., Matasovic, N., Rathje, E., Riemer, M., and Stokoe, K. (2006). Unit weight of municipal solid waste. *Journal of Geotechnical and Geoenvironmental Engineering*, 132(10), 1250–1261.
- Zhang, Y., Zhang, H., Jia, B., Wang, W., Zhu, W., Huang, T., and Kong, X. (2012). Landfill CH<sub>4</sub> oxidation by mineralized refuse: Effects of NH<sub>4</sub><sup>+</sup>-N incubation, water content and temperature. *Science of the Total Environment*, 426, 406-413.

## APPENDIX A – Compilation of Reactor Data for Research Study 1

Table A-1. Reactor information, initial conditions, and final conditions for the de-ionized water (DIW) reactor duplicates.

REACTOR INFORMATION		INITIAL CONDITIONS	DIW-1	DIW-2
Reactors:	DIW-1 & DIW-2	Specimen thickness [cm]:	20.6	20.8
Startup date:	1/10/2018	Specimen density [g/cm <sup>3</sup> ]:	0.36	0.36
Experiment duration [days]:	267	Initial recirculated volume [L/Mg-waste]:	95	124
Solid waste fraction:	Municipal Solid Waste	Initial $w_d$ after dosing [%]:	103	99
MSW [g]:	2400	<b>FINAL CONDITIONS</b>		
Liquid waste fraction:	De-ionized Water	Cumulative recirculated liquid [L/Mg-waste]:	1528	2066
Initial liquid dose [L/Mg-waste]:	625	Average weekly recirculated liquid [L/Mg-waste]:	42	57
		Settlement Strain [%]:	4.6	3.1



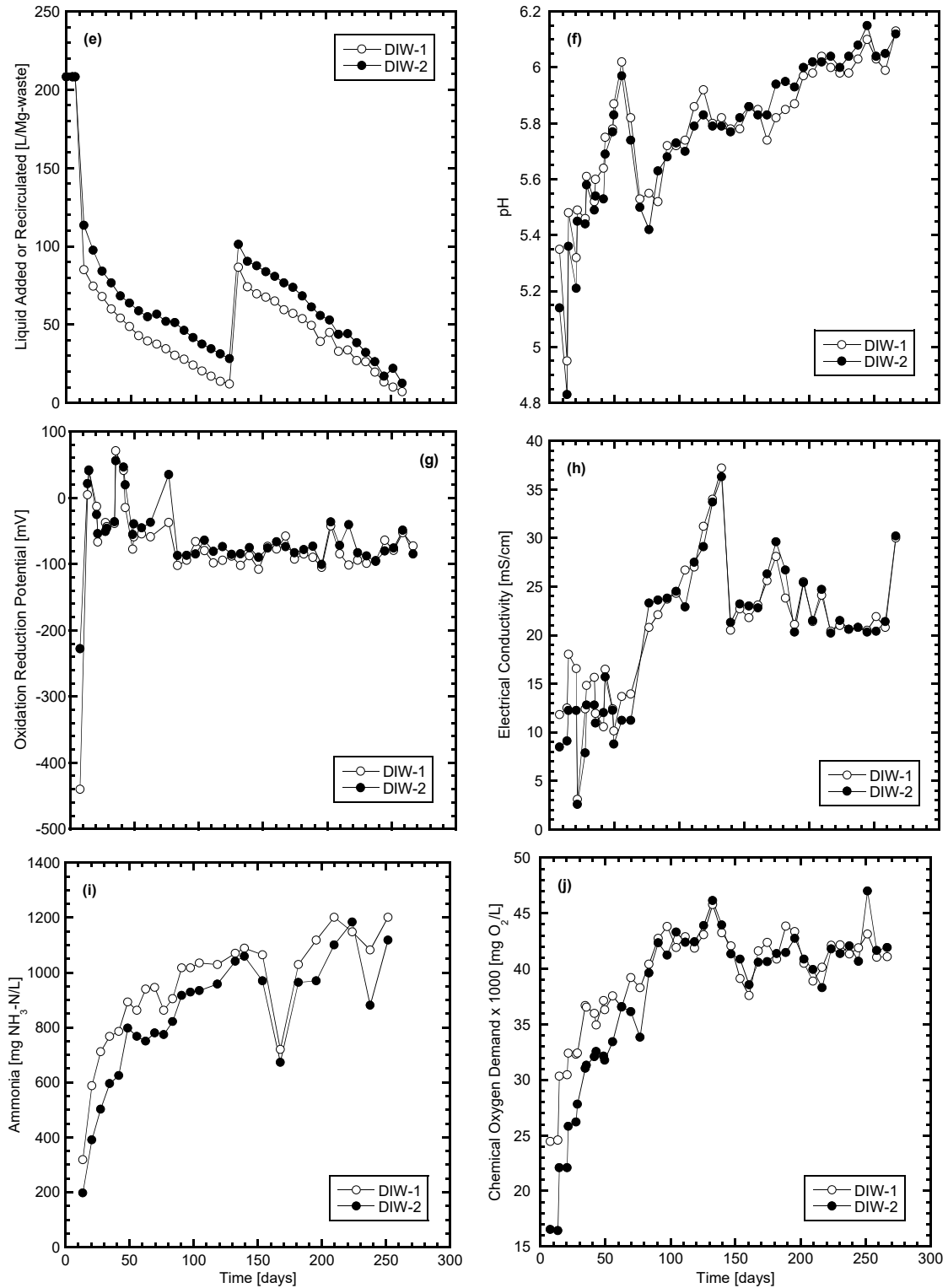
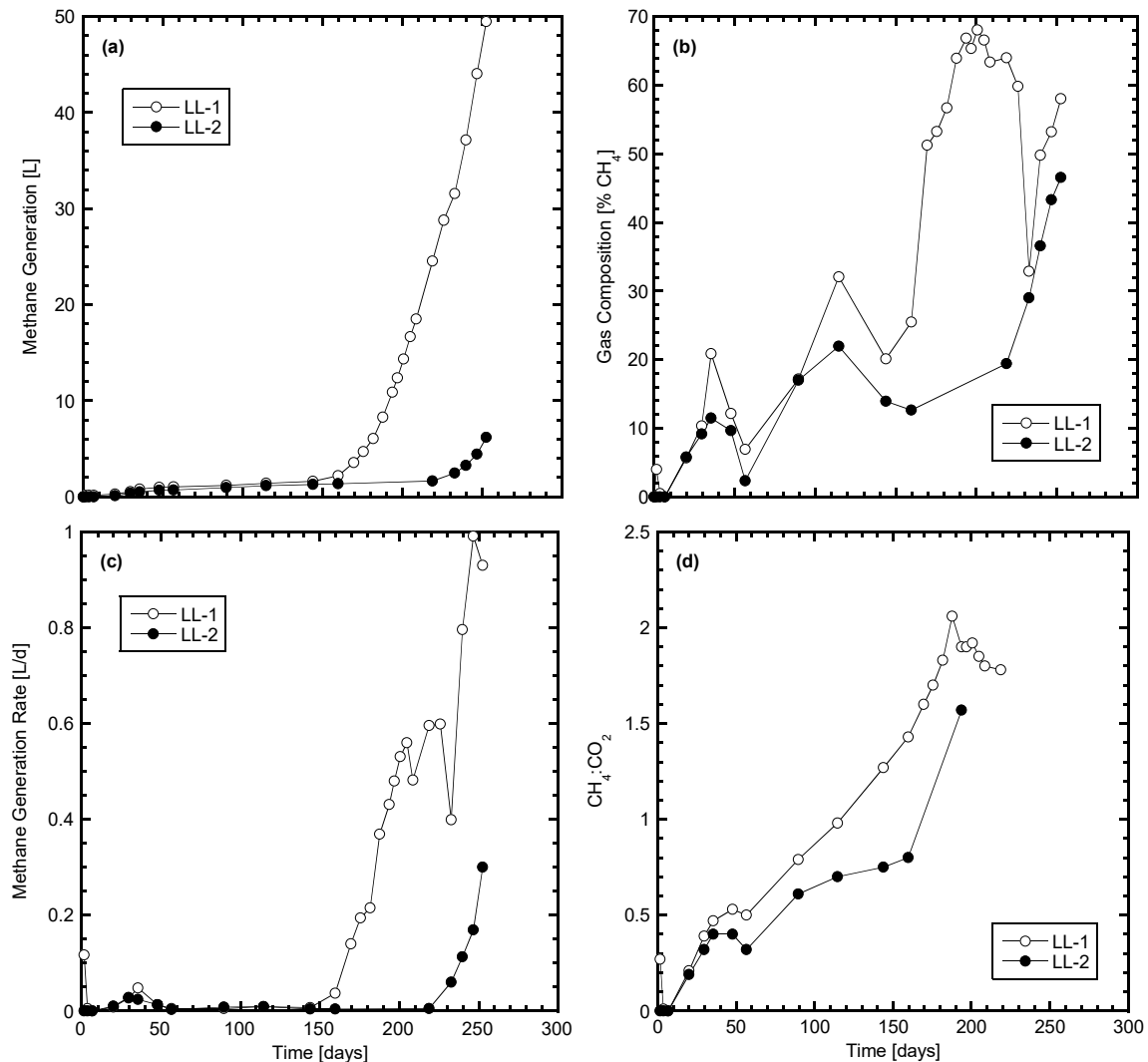


Figure A-1. Summary data, including (a) methane generation, (b) gas composition, (c) methane generation rate, (d) methane to carbon dioxide ratio, (e) liquid addition or recirculation, (f) pH, (g) oxidation reduction potential, (h) electrical conductivity, (i) ammonia, and (j) chemical oxygen demand for the de-ionized water (DIW) reactor duplicates.

Table A-2. Reactor information, initial conditions, and final conditions for the landfill leachate (LL) reactor duplicates.

REACTOR INFORMATION		INITIAL CONDITIONS	LL-1	LL-2
Reactors:	LL-1 & LL-2	Specimen thickness [cm]:	20.6	20.0
Startup date:	1/24/2018	Specimen density [g/cm <sup>3</sup> ]:	0.36	0.37
Experiment duration [days]:	253	Initial recirculated volume [L/Mg-waste]:	109	113
Solid waste fraction: MSW [g]:	Municipal Solid Waste 2400	Initial $w_d$ after dosing [%]:	101	100
Liquid waste fraction: Initial liquid dose [L/Mg-waste]:	Landfill Leachate 625	FINAL CONDITIONS		
		Cumulative recirculated liquid [L/Mg-waste]:	1838	2160
		Average weekly recirculated liquid [L/Mg-waste]:	54	64
		Settlement Strain [%]:	3.1	4.8



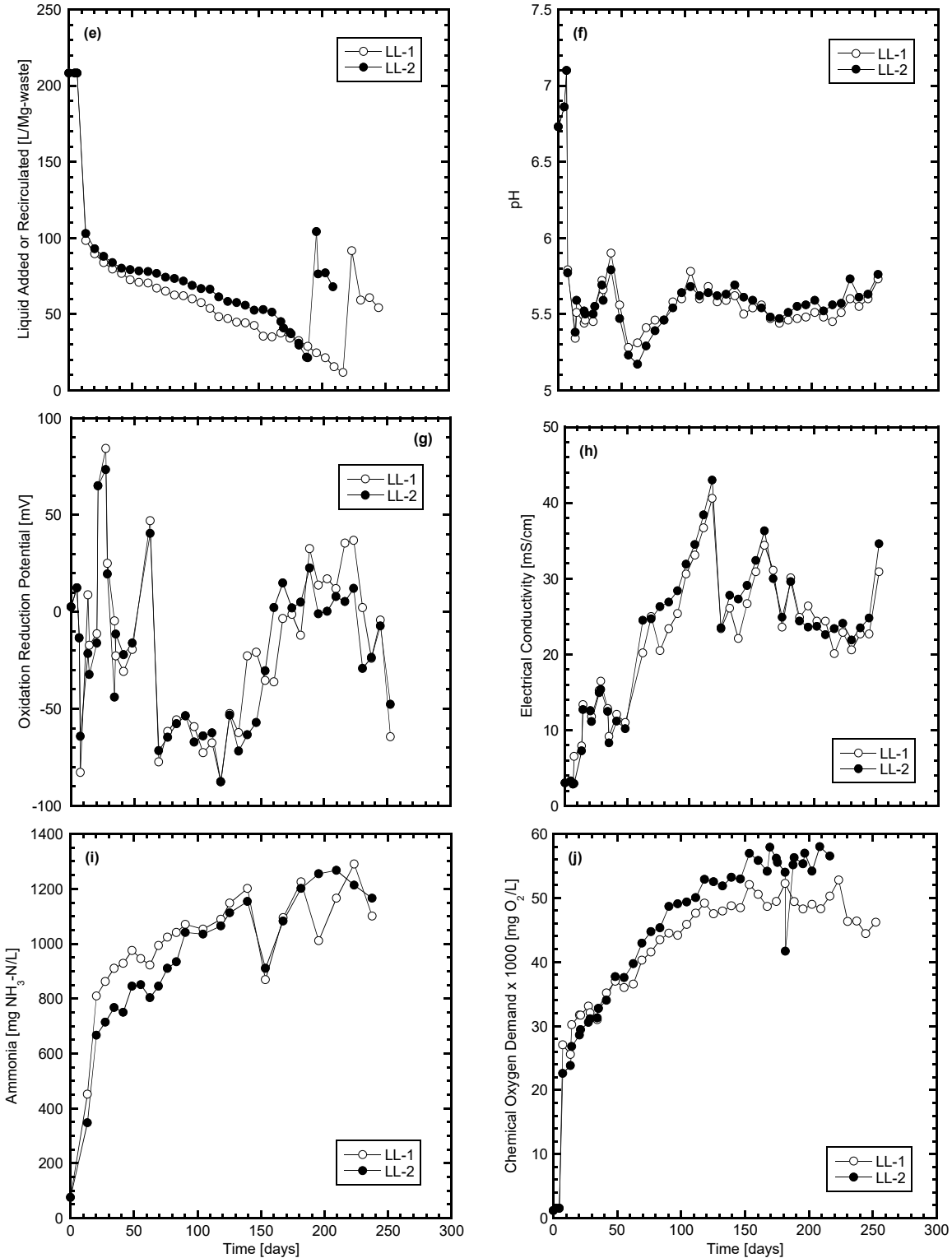
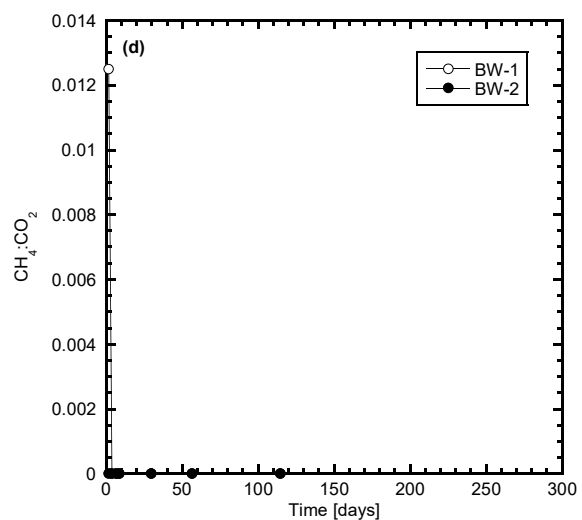
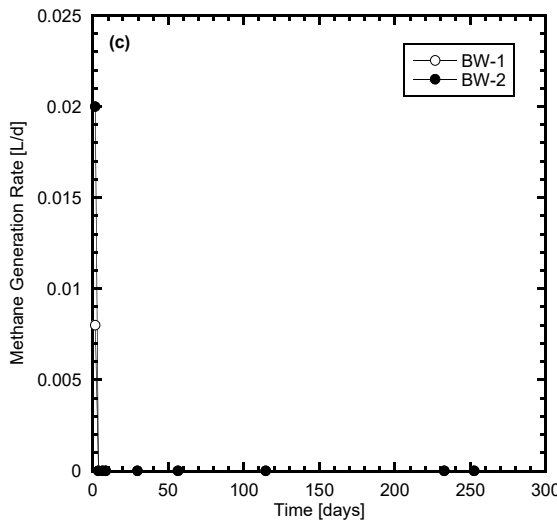
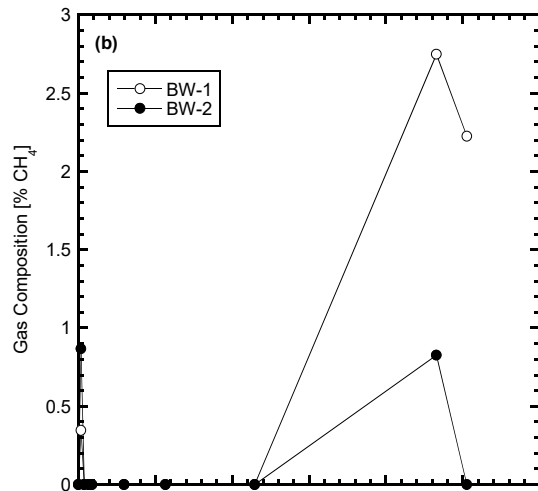
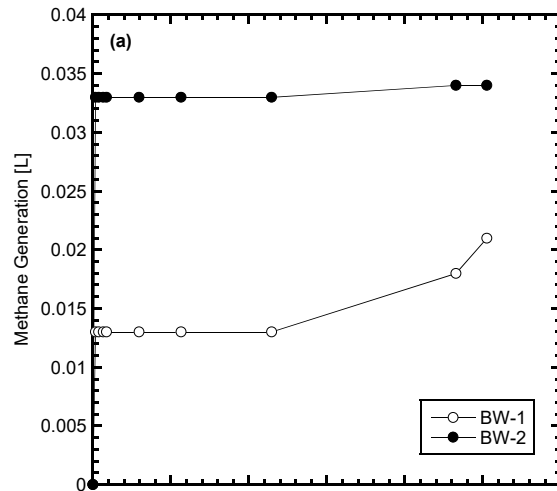


Figure A-2. Summary data for the landfill leachate (LL) reactor duplicates: (a) methane generation, (b) gas composition, (c) methane generation rate, (d) methane to carbon dioxide ratio, (e) liquid addition or recirculation, (f) pH, (g) oxidation reduction potential, (h) electrical conductivity, (i) ammonia, and (j) chemical oxygen demand.

Table A-3. Reactor information, initial conditions, and final conditions for the brewery wastewater (BW) reactor duplicates.

REACTOR INFORMATION		INITIAL CONDITIONS	BW-1	BW-2
Reactors:	BW-1 & BW-2	Specimen thickness [cm]:	20.6	20.6
Startup date:	1/24/2018	Specimen density [g/cm <sup>3</sup> ]:	0.36	0.36
Experiment duration [days]:	253	Initial recirculated volume [L/Mg-waste]:	55	76
Solid waste fraction:	Municipal Solid Waste	Initial $w_d$ after dosing [%]:	108	105
MSW [g]:	2400			
Liquid waste fraction:	Brewery Wastewater	FINAL CONDITIONS		
Initial liquid dose [L/Mg-waste]:	625	Cumulative recirculated liquid [L/Mg-waste]:	1511	2190
		Average weekly recirculated liquid [L/Mg-waste]:	44	64
		Settlement Strain [%]:	4.6	4.6



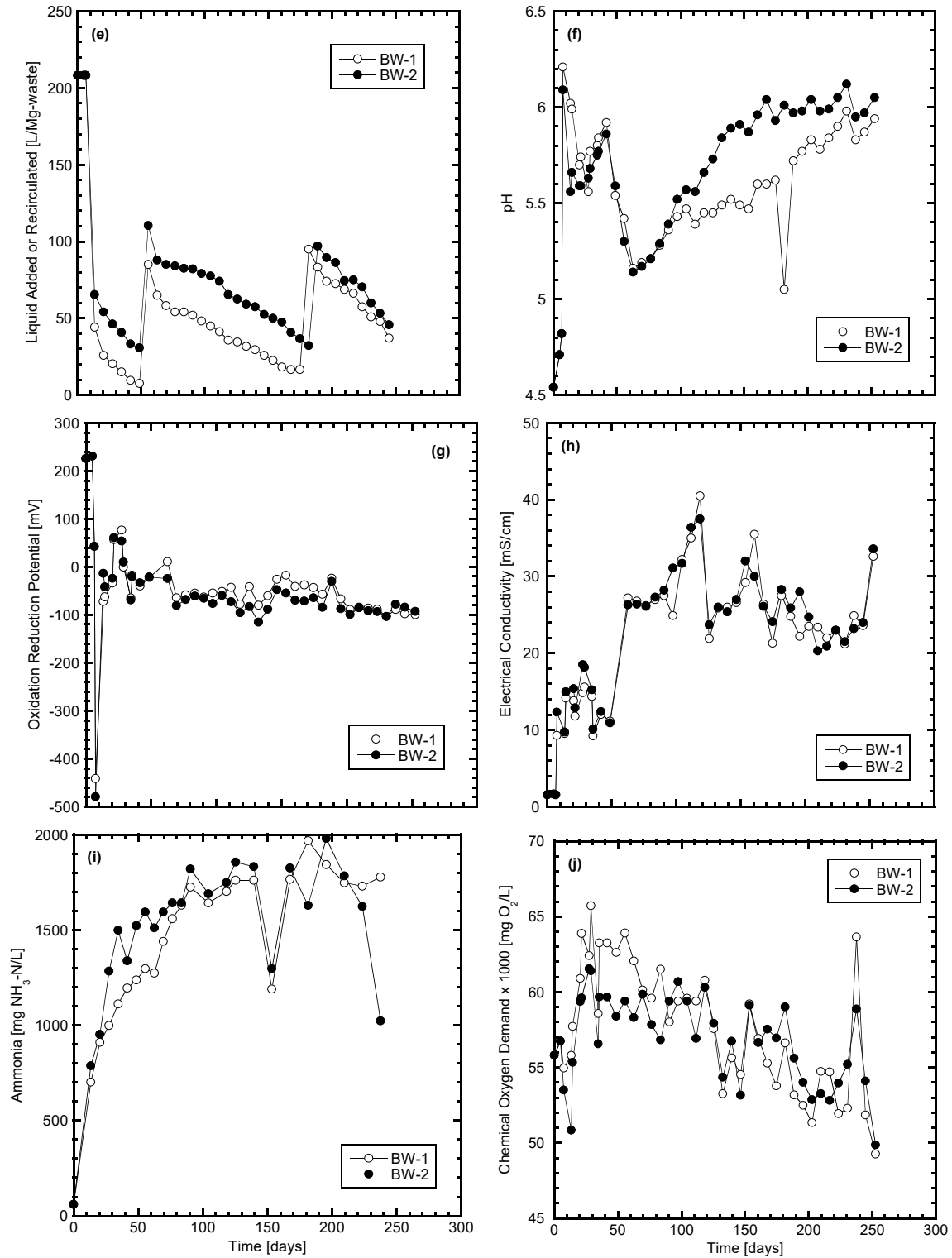
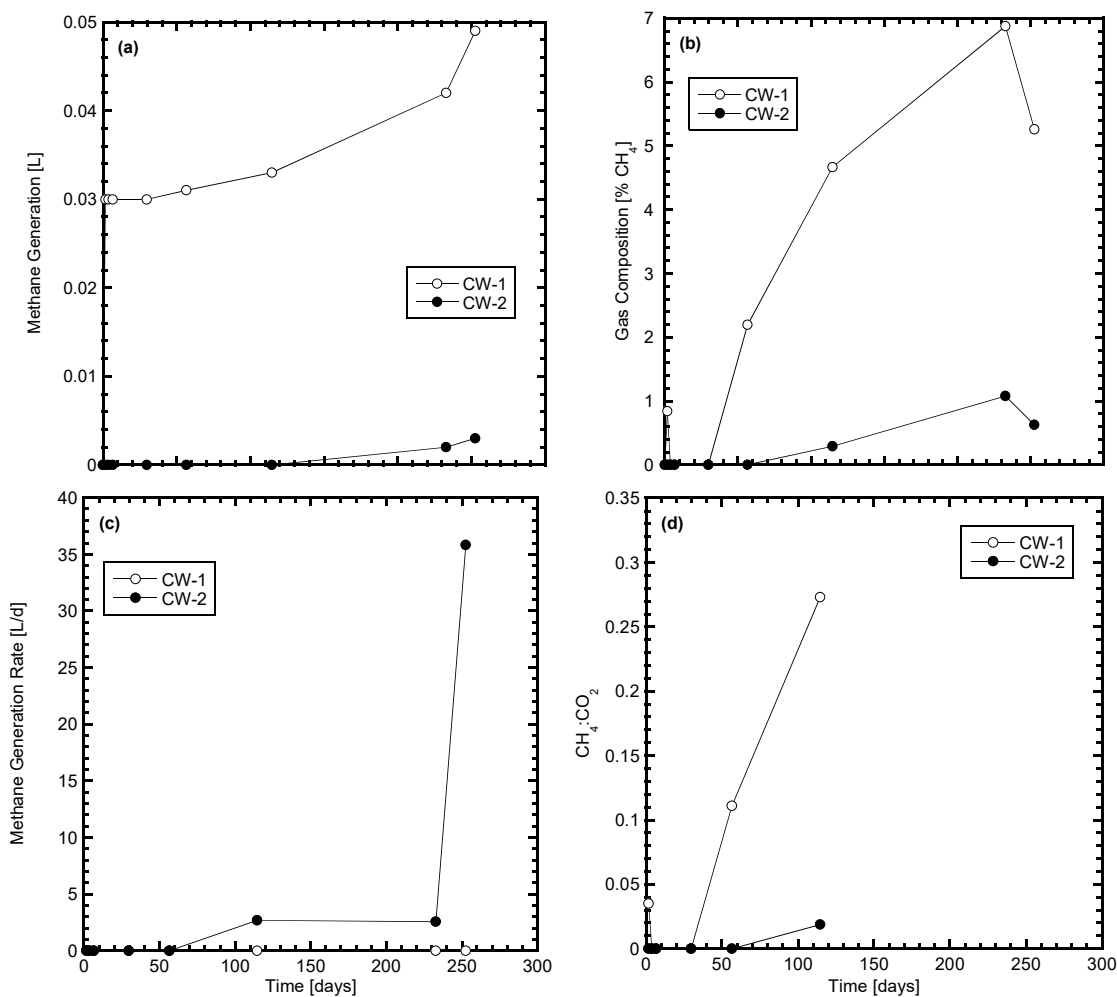


Figure A-3. Summary data for the brewery wastewater (BW) reactor duplicates: (a) methane generation, (b) gas composition, (c) methane generation rate, (d) methane to carbon dioxide ratio, (e) liquid addition or recirculation, (f) pH, (g) oxidation reduction potential, (h) electrical conductivity, (i) ammonia, and (j) chemical oxygen demand.

Table A-4. Reactor information, initial conditions, and final conditions for the cheese processing wastewater (CW) reactor duplicates.

REACTOR INFORMATION		INITIAL CONDITIONS	CW-1	CW-2
Reactors:	CW-1 & CW-2	Specimen thickness [cm]:	20.0	20.2
Startup date:	1/24/2018	Specimen density [g/cm <sup>3</sup> ]:	0.37	0.37
Experiment duration [days]:	253	Initial recirculated volume [L/Mg-waste]:	120	91
Solid waste fraction:	Municipal Solid Waste	Initial $w_d$ after dosing [%]:	100	103
MSW [g]:	2400			
		FINAL CONDITIONS		
Liquid waste fraction:	Cheese Processing Wastewater	Cumulative recirculated liquid [L/Mg-waste]:	1995	1485
Initial liquid dose [L/Mg-waste]:	625	Average weekly recirculated liquid [L/Mg-waste]:	59	44
		Settlement Strain [%]:	3.2	7.1



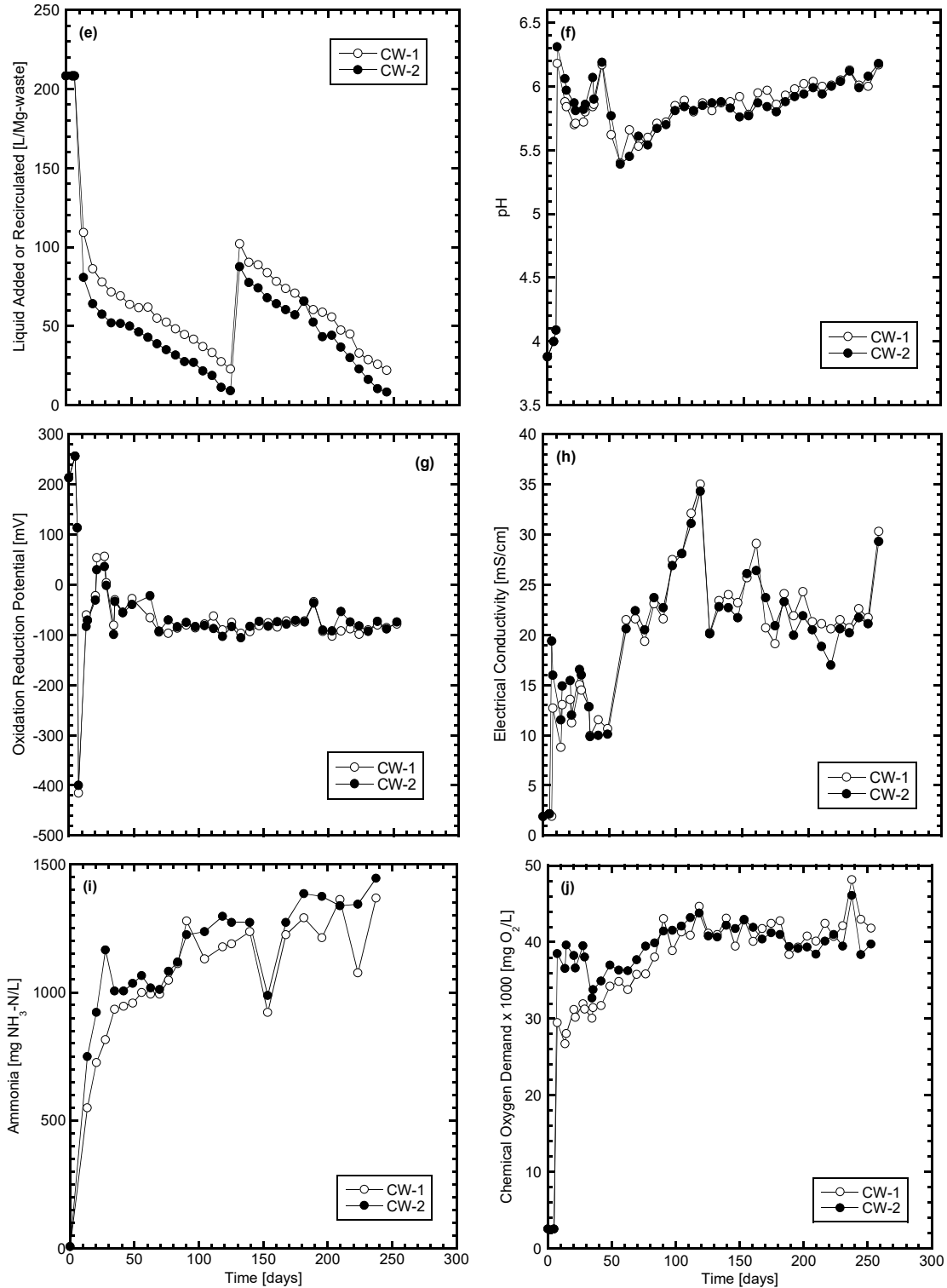
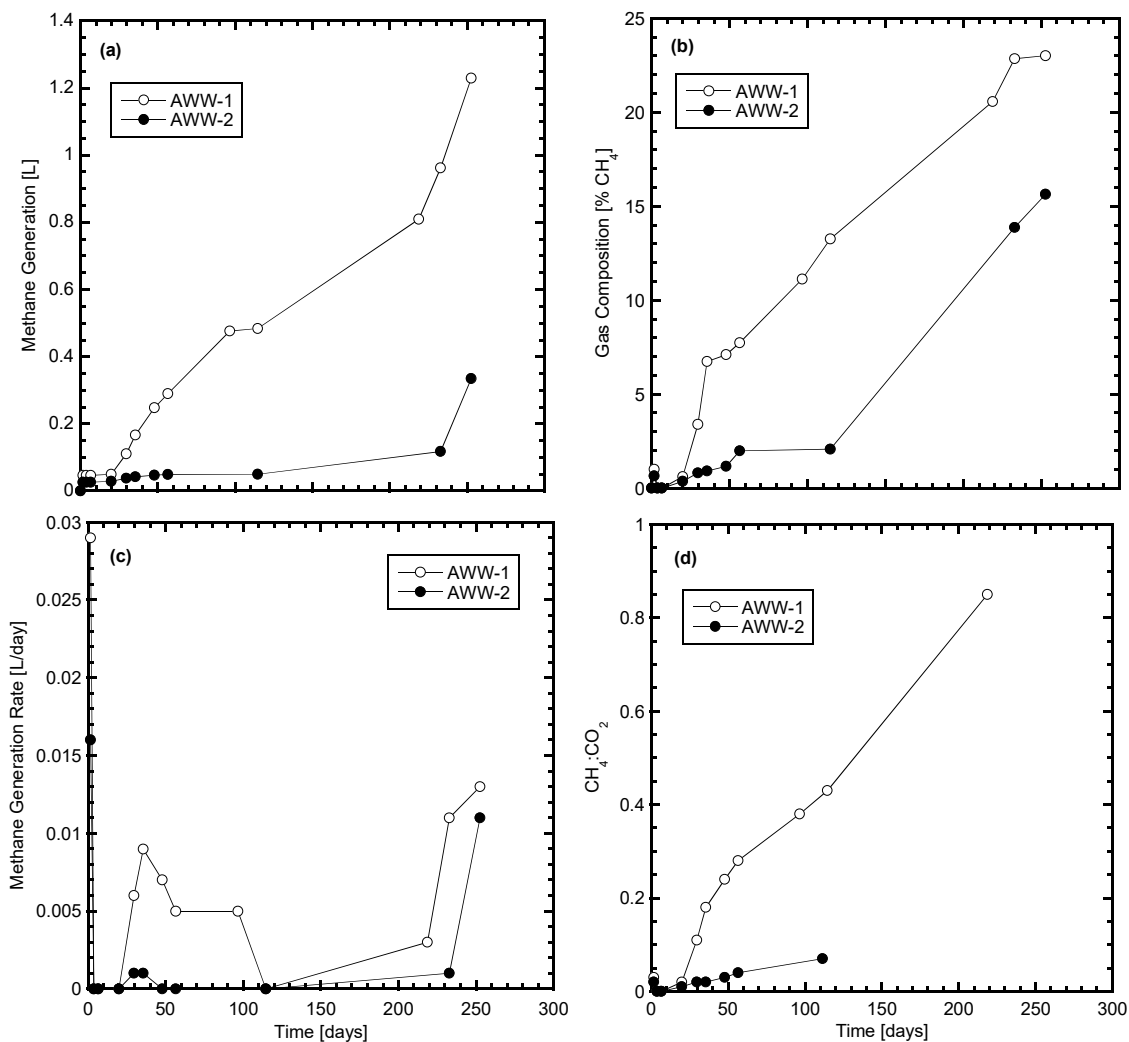


Figure A-4. Summary data for the cheese processing wastewater (CW) reactor duplicates: (a) methane generation, (b) gas composition, (c) methane generation rate, (d) methane to carbon dioxide ratio, (e) liquid addition or recirculation, (f) pH, (g) oxidation reduction potential, (h) electrical conductivity, (i) ammonia, and (j) chemical oxygen demand.

Table A-5. Reactor information, initial conditions, and final conditions for the automobile wash water (AWW) reactor duplicates.

REACTOR INFORMATION		INITIAL CONDITIONS	AWW-1	AWW-2
Reactors:	AWW-1 & AWW-2	Specimen thickness [cm]:	20.0	20.8
Startup date:	1/24/2018	Specimen density [g/cm <sup>3</sup> ]:	0.37	0.36
Experiment duration [days]:	253	Initial recirculated volume [L/Mg-waste]:	123	139
Solid waste fraction: MSW [g]:	Municipal Solid Waste 2400	Initial $w_d$ after dosing [%]:	99	97
Liquid waste fraction:	Automobile Wash Water	FINAL CONDITIONS		
Initial liquid dose [L/Mg-waste]:	625	Cumulative recirculated liquid [L/Mg-waste]:	2604	2005
		Average weekly recirculated liquid [L/Mg-waste]:	77	59
		Settlement Strain [%]:	4.8	6.9



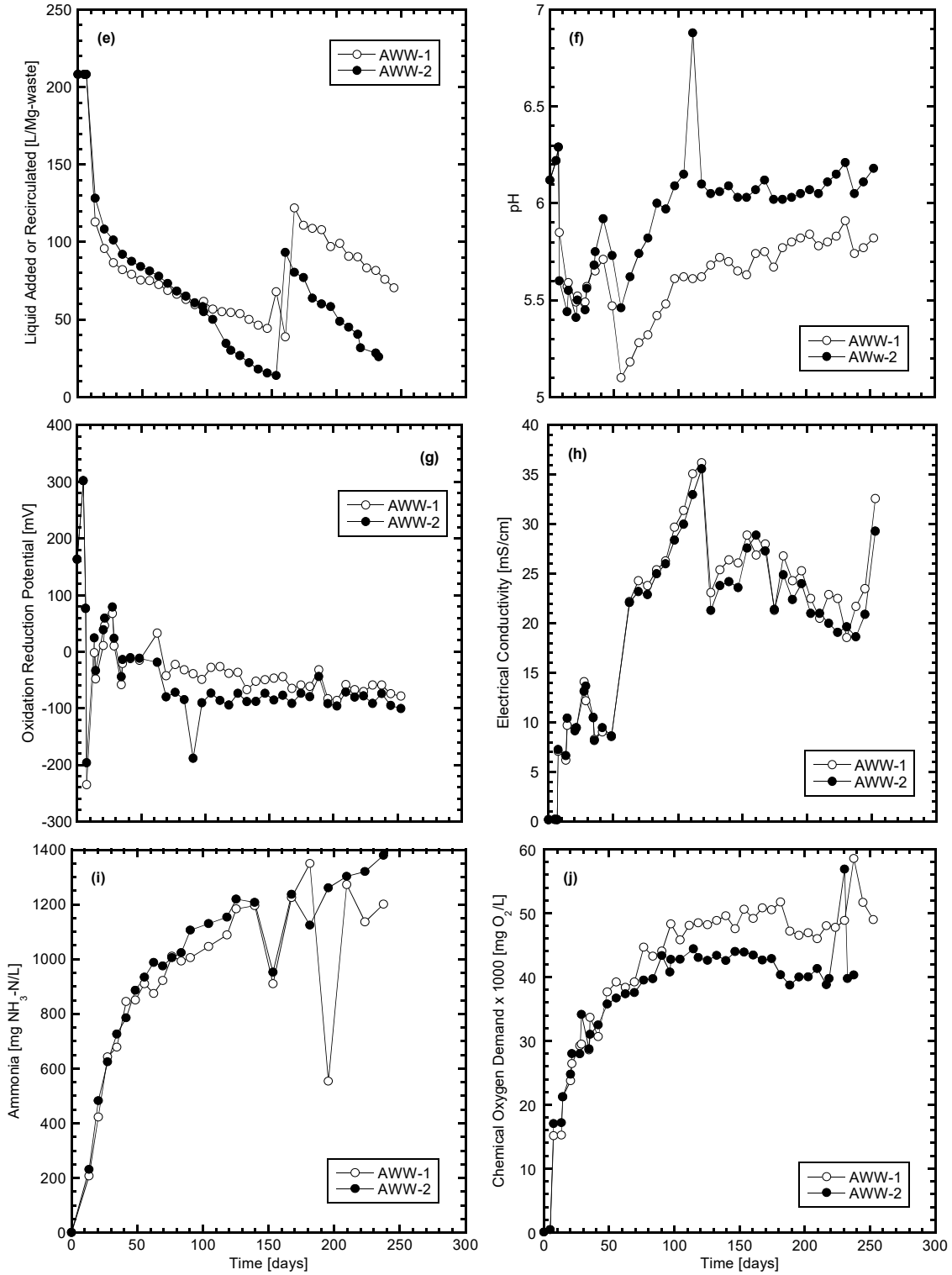
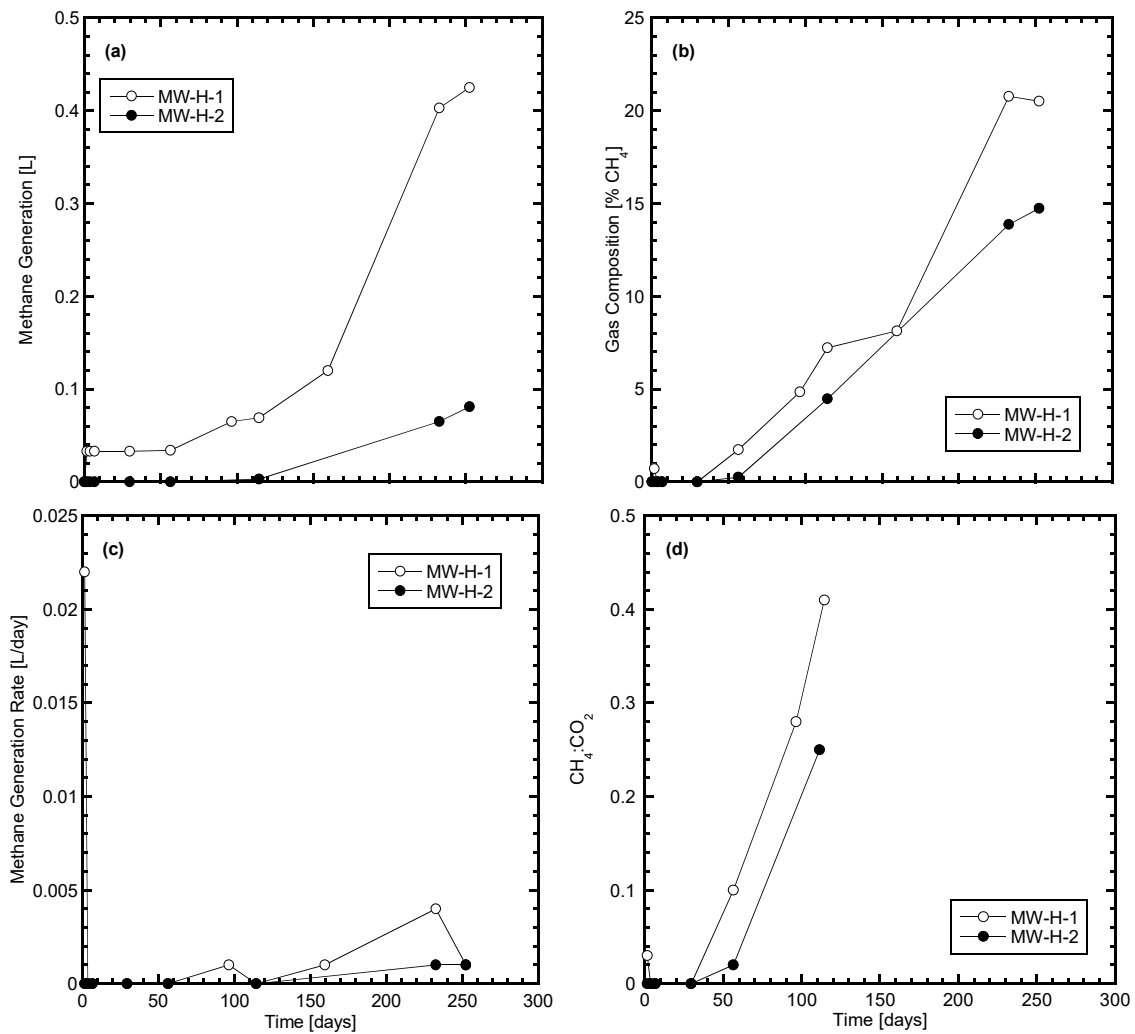


Figure A-5. Summary data for the automobile wash water (AWW) reactor duplicates: (a) methane generation, (b) gas composition, (c) methane generation rate, (d) methane to carbon dioxide ratio, (e) liquid addition or recirculation, (f) pH, (g) oxidation reduction potential, (h) electrical conductivity, (i) ammonia, and (j) chemical oxygen demand.

Table A-6. Reactor information, initial conditions, and final conditions for the high strength manufacturing wastewater (MW-H) reactor duplicates.

REACTOR INFORMATION		INITIAL CONDITIONS	MW-H1	MW-H2
Reactors:	MW-H1 & MW-H2	Specimen thickness [cm]:	20.3	20.6
Startup date:	1/24/2018	Specimen density [g/cm <sup>3</sup> ]:	0.36	0.36
Experiment duration [days]:	253	Initial recirculated volume [L/Mg-waste]:	87	60
Solid waste fraction:	Municipal Solid Waste	Initial $w_d$ after dosing [%]:	104	108
MSW [g]:	2400	<b>FINAL CONDITIONS</b>		
Liquid waste fraction:	High Strength Manufacturing Wastewater	Cumulative recirculated liquid [L/Mg-waste]:	2061	1390
Initial liquid dose [L/Mg-waste]:	625	Average weekly recirculated liquid [L/Mg-waste]:	61	41
		Settlement Strain [%]:	6.3	6.2



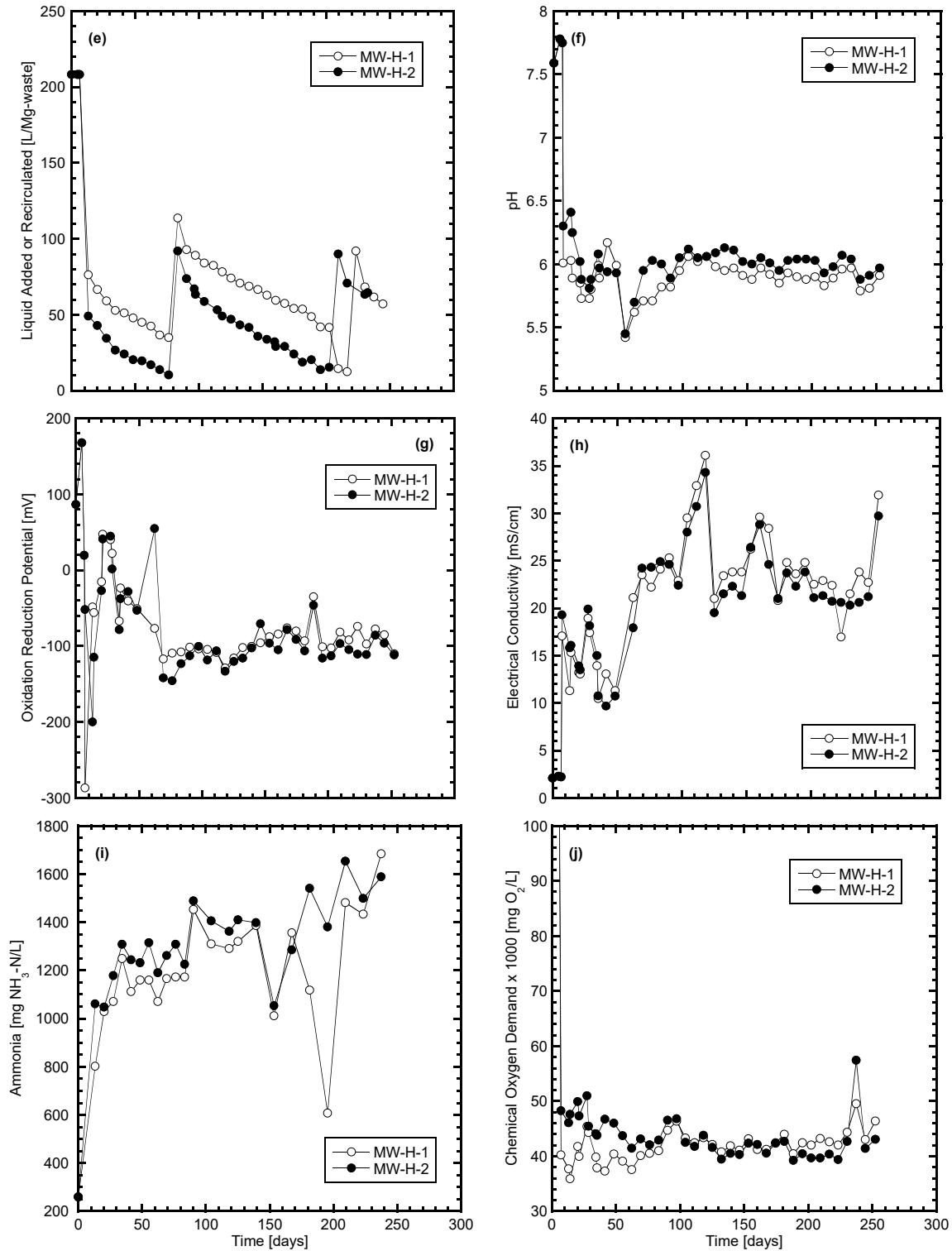
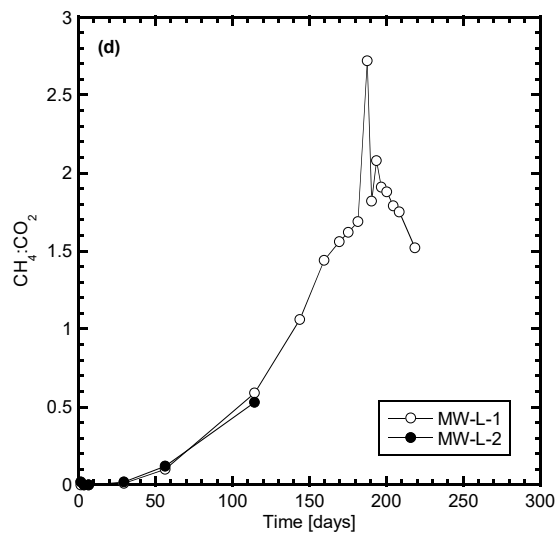
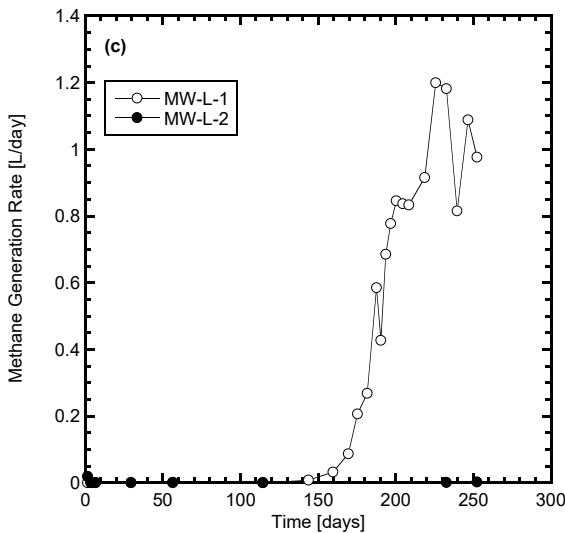
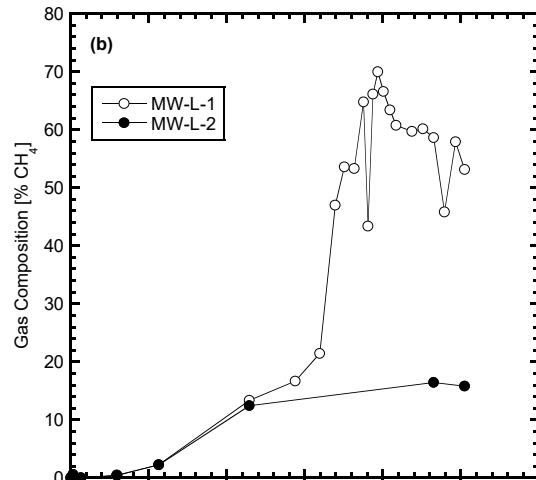
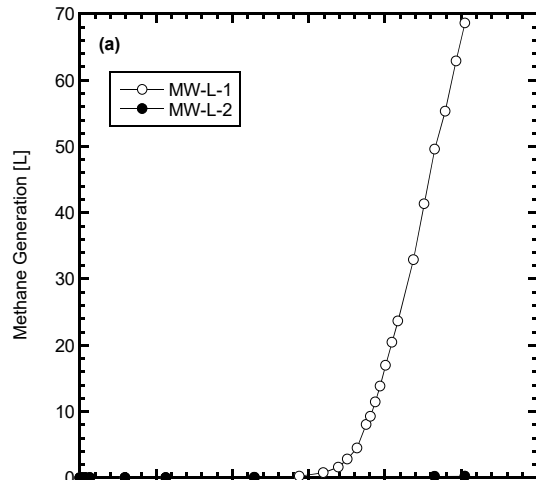


Figure A-6. Summary data for the high-strength manufacturing wastewater (MW-H) reactor duplicates: (a) methane generation, (b) gas composition, (c) methane generation rate, (d) methane to carbon dioxide ratio, (e) liquid addition or recirculation, (f) pH, (g) oxidation reduction potential, (h) electrical conductivity, (i) ammonia, and (j) chemical oxygen demand.

Table A-7. Reactor information, initial conditions, and final conditions for the low strength manufacturing wastewater (MW-L) reactor duplicates.

REACTOR INFORMATION		INITIAL CONDITIONS	MW-L-1	MW-L-2
Reactors:	MW-L1 & MW-L2	Specimen thickness [cm]:	20.3	21.1
Startup date:	1/24/2018	Specimen density [g/cm <sup>3</sup> ]:	0.36	0.35
Experiment duration [days]:	253	Initial recirculated volume [L/Mg-waste]:	104	109
Solid waste fraction:	Municipal Solid Waste	Initial $w_d$ after dosing [%]:	102	101
MSW [g]:	2400			
Liquid waste fraction:	Low Strength Manufacturing Wastewater	FINAL CONDITIONS		
Initial liquid dose [L/Mg-waste]:	625	Cumulative recirculated liquid [L/Mg-waste]:	1670	2225
		Average weekly recirculated liquid [L/Mg-waste]:	49	65
		Settlement Strain [%]:	5.5	3.0



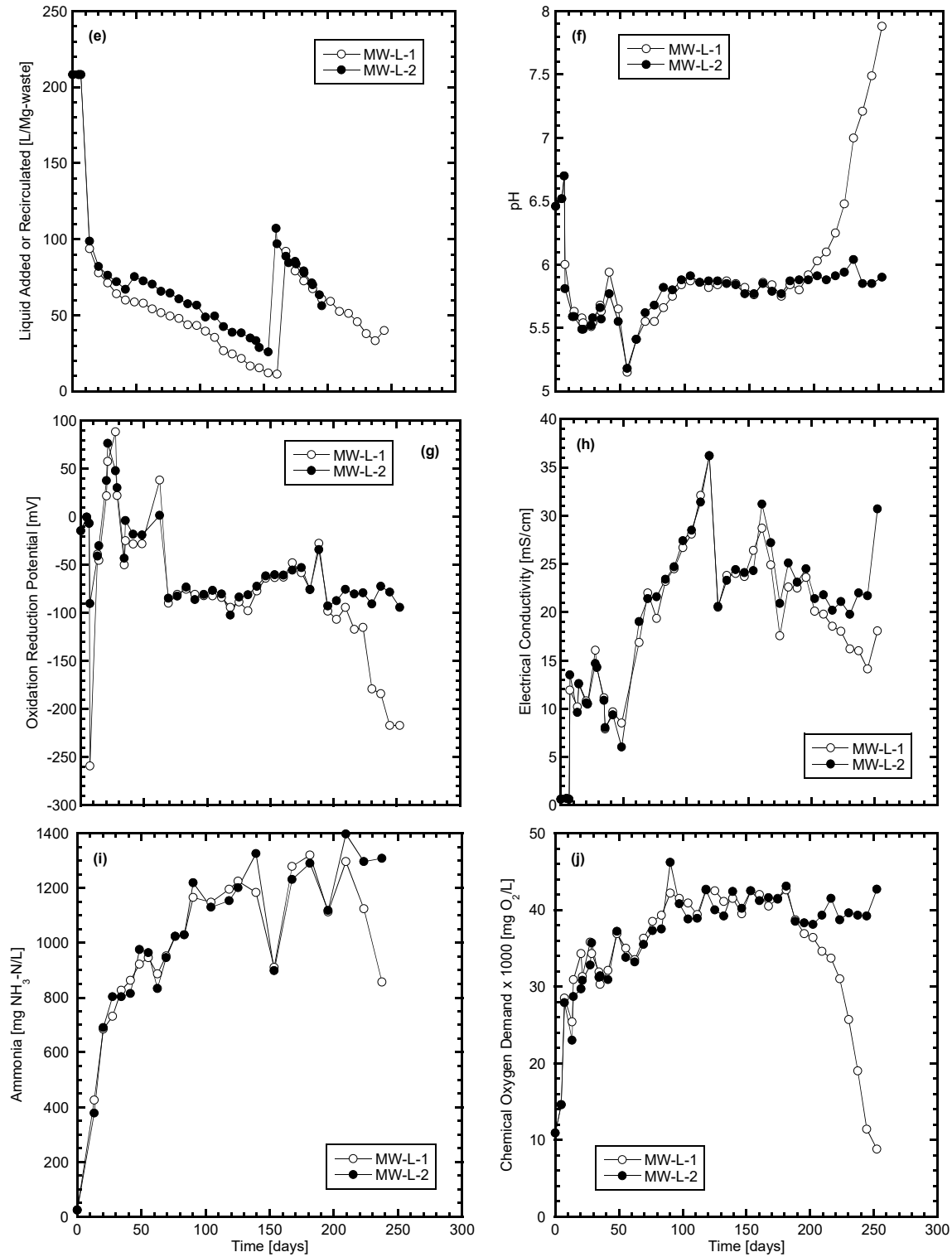
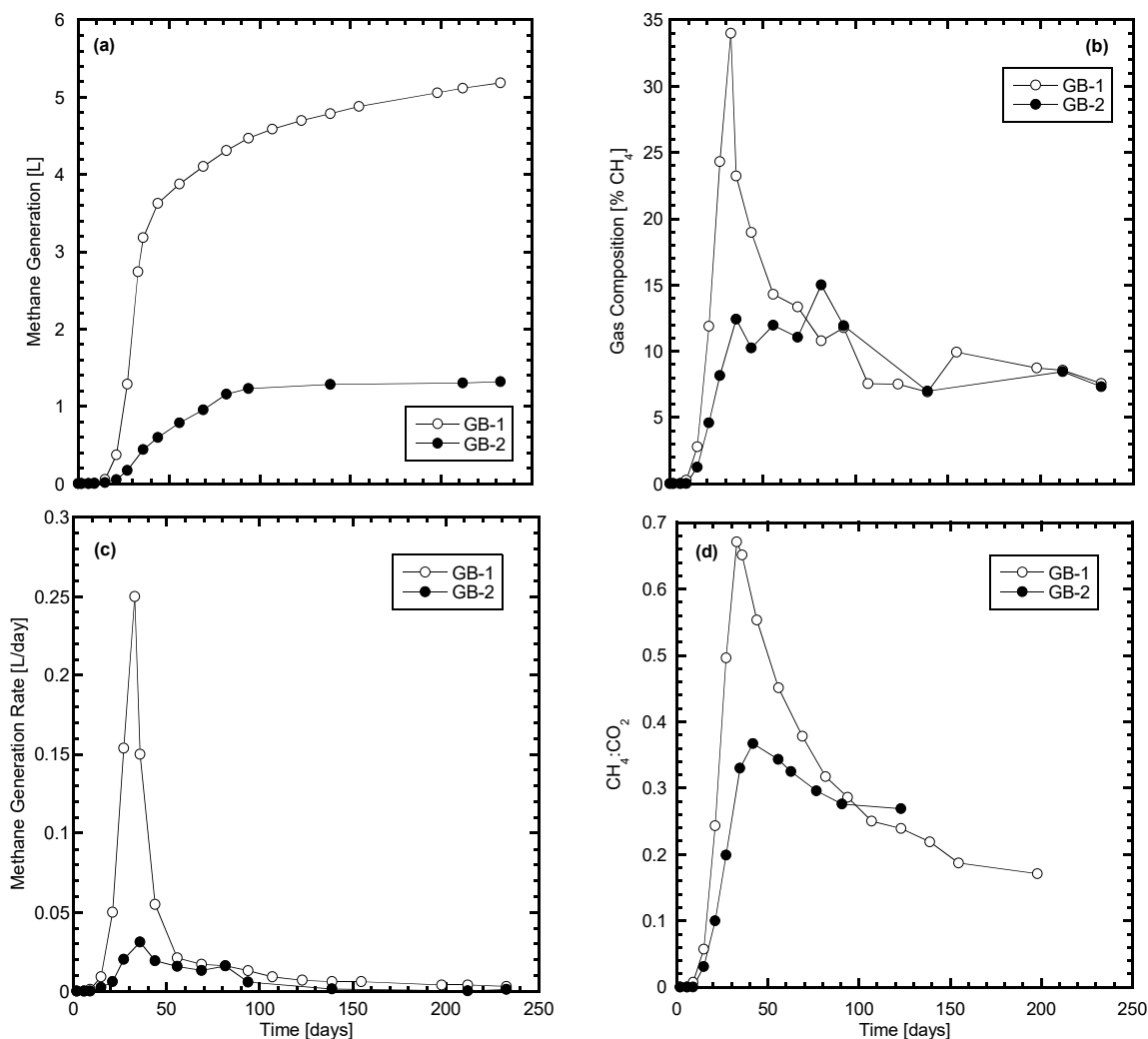


Figure A-7. Summary data for the low-strength manufacturing wastewater (MW-L) reactor duplicates: (a) methane generation, (b) gas composition, (c) methane generation rate, (d) methane to carbon dioxide ratio, (e) liquid addition or recirculation, (f) pH, (g) oxidation reduction potential, (h) electrical conductivity, (i) ammonia, and (j) chemical oxygen demand.

Table A-8. Reactor information, initial conditions, and final conditions for the gypsum board (GB) reactor duplicates.

REACTOR INFORMATION		INITIAL CONDITIONS	GB-1	GB-2
Reactors:	GB-1 & GB-2	Specimen thickness [cm]:	18.4	20.0
Startup date:	2/14/2018	Specimen density [g/cm <sup>3</sup> ]:	0.40	0.37
Experiment duration [days]:	233	Initial recirculated volume [L/Mg-waste]:	114	95
Solid waste fraction:	Municipal Solid Waste and Gypsum Board	Initial $w_a$ after dosing [%]:	92	94
MSW [g]:	1440	FINAL CONDITIONS		
Gypsum Board [g]:	960	Cumulative recirculated liquid [L/Mg-waste]:	2626	1372
Liquid waste fraction:	Landfill Leachate	Average weekly recirculated liquid [L/Mg-waste]:	85	44
Initial liquid dose [L/Mg-waste]:	750	Settlement Strain [%]:	3.5	3.2



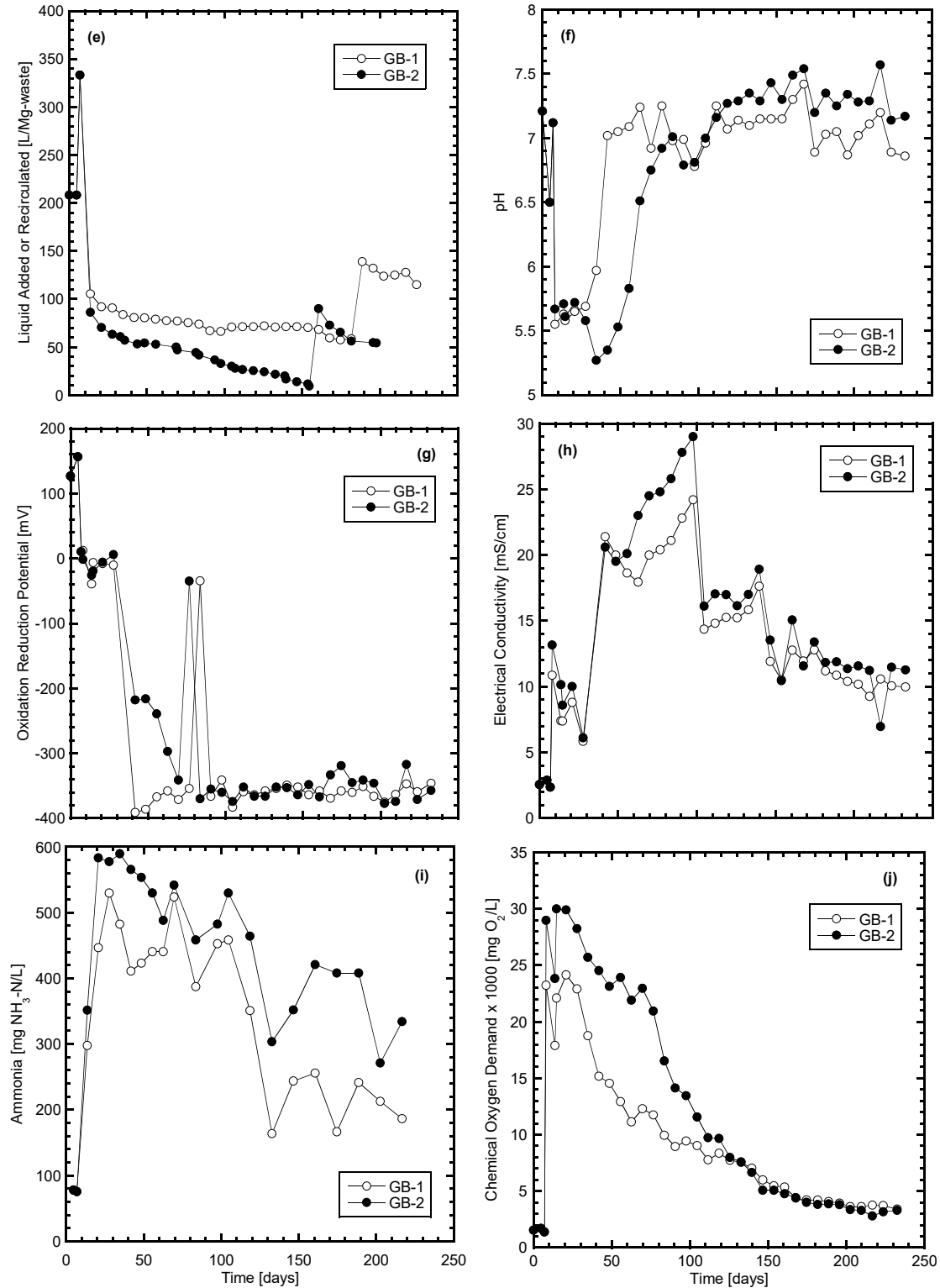
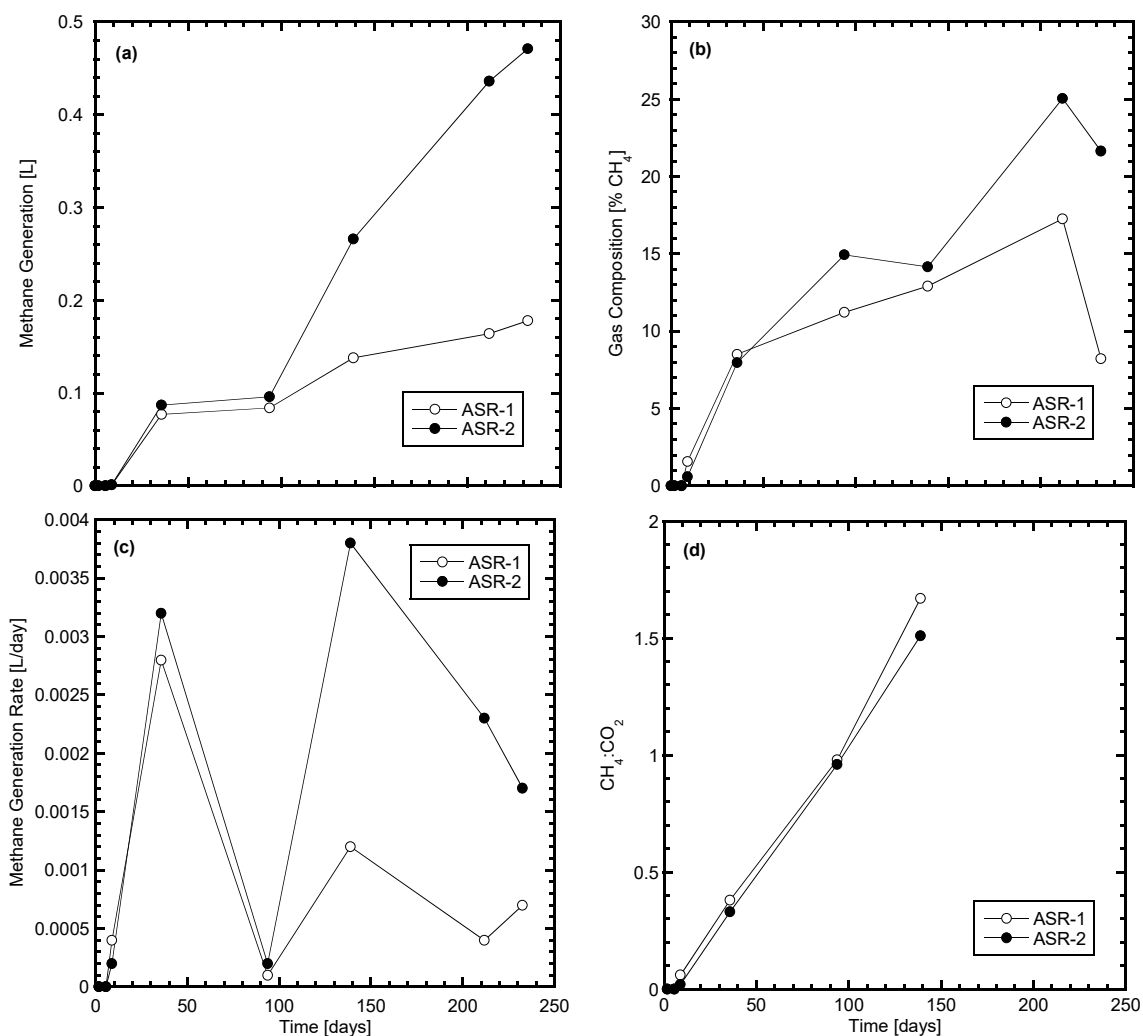


Figure A-8. Summary data for the gypsum board (GB) reactor duplicates: (a) methane generation, (b) gas composition, (c) methane generation rate, (d) methane to carbon dioxide ratio, (e) liquid addition or recirculation, (f) pH, (g) oxidation reduction potential, (h) electrical conductivity, (i) ammonia, and (j) chemical oxygen demand.

Table A-9. Reactor information, initial conditions, and final conditions for the automobile shredder residue (ASR) reactor duplicates.

REACTOR INFORMATION		INITIAL CONDITIONS	ASR-1	ASR-2
Reactors:	ASR-1 & ASR-2	Specimen thickness [cm]:	18.7	18.4
Startup date:	2/14/2018	Specimen density [g/cm <sup>3</sup> ]:	0.40	0.40
Experiment duration [days]:	233	Initial recirculated volume [L/Mg-waste]:	102	53
Solid waste fraction:	Municipal Solid Waste and Auto Shredder Residue	Initial $w_d$ after dosing [%]:	59	65
MSW [g]:	1440	FINAL CONDITIONS		
Auto Shredder Residue [g]:	960	Cumulative recirculated liquid [L/Mg-waste]:	1859	1224
Liquid waste fraction:	Landfill Leachate	Average weekly recirculated liquid [L/Mg-waste]:	60	39
Initial liquid dose [L/Mg-waste]:	458	Settlement Strain [%]:	1.7	1.7



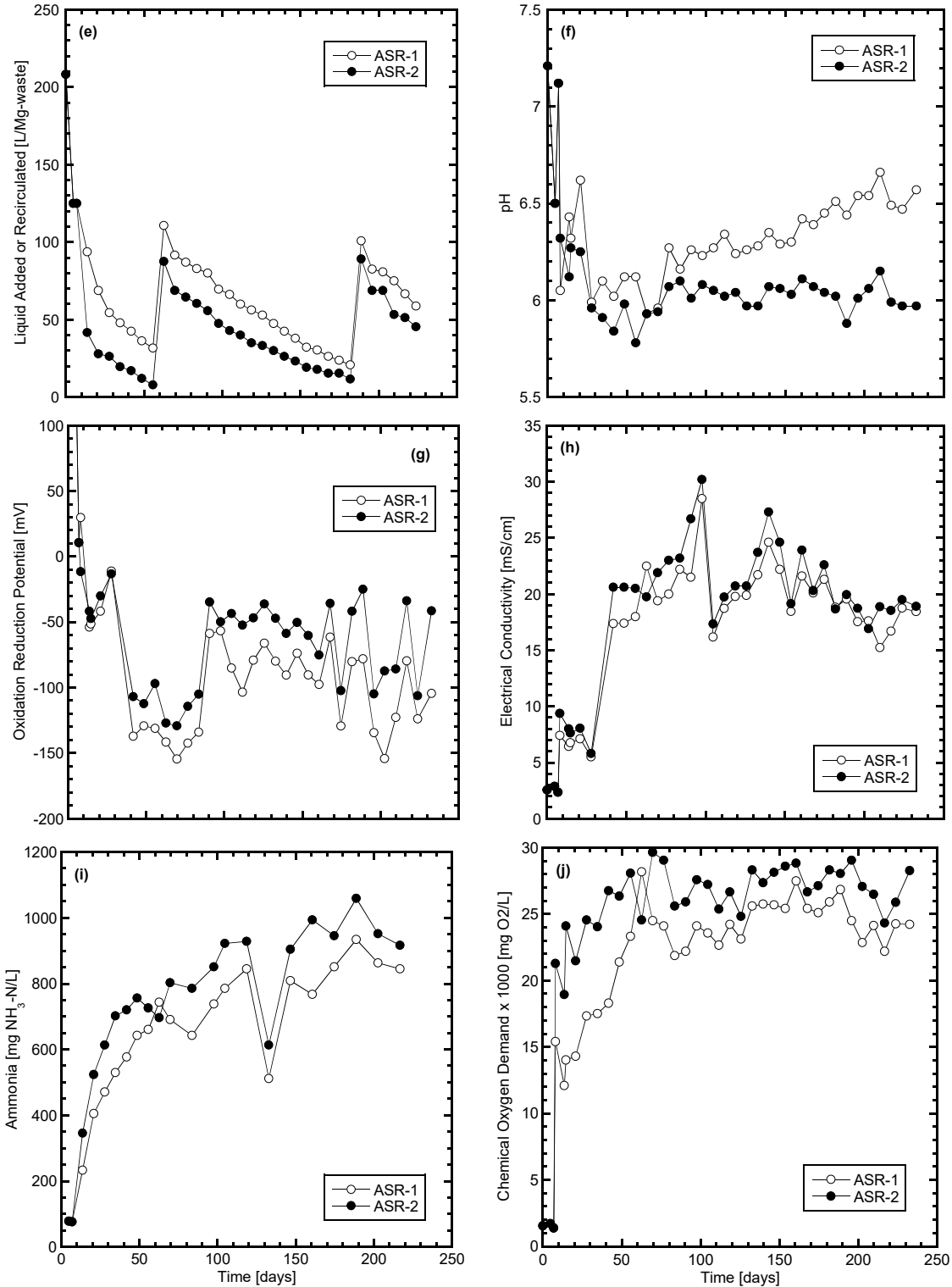
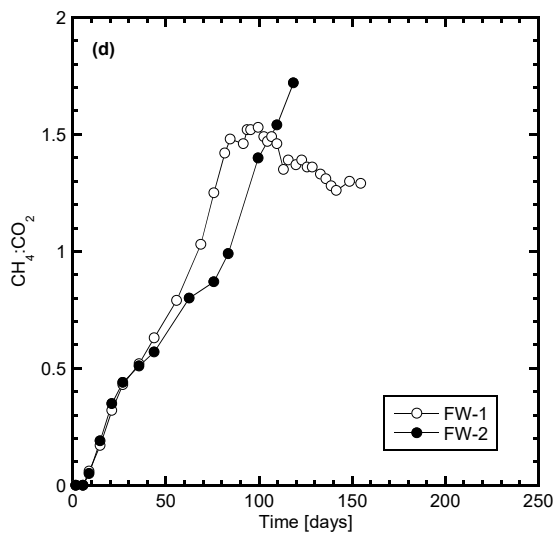
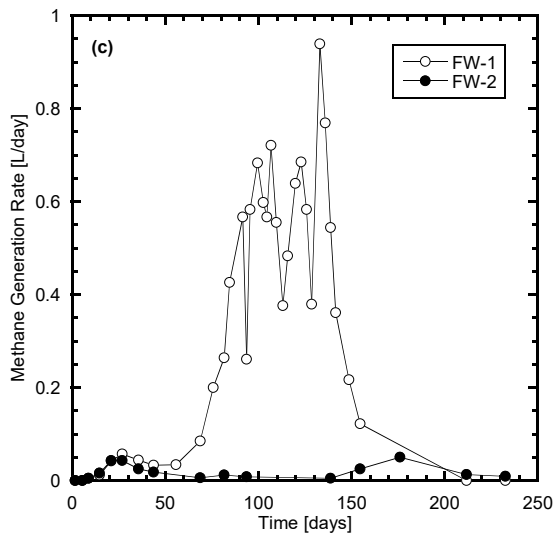
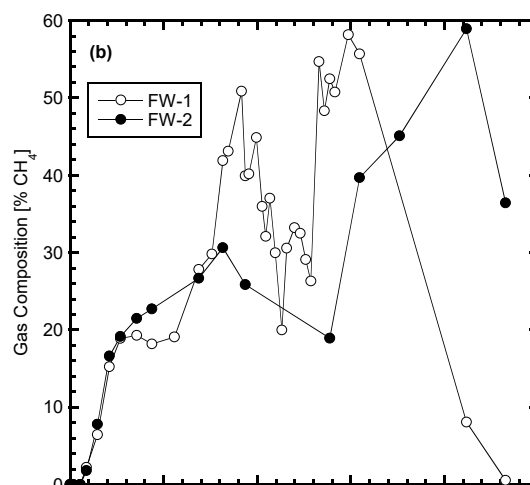
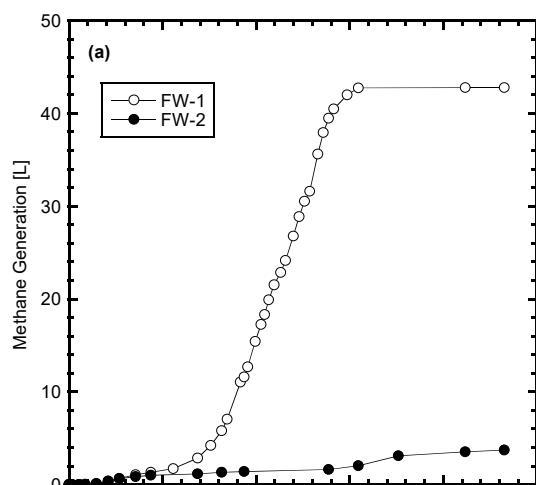


Figure A-9. Summary data for the automobile shredder residue (ASR) reactor duplicates: (a) methane generation, (b) gas composition, (c) methane generation rate, (d) methane to carbon dioxide ratio, (e) liquid addition or recirculation, (f) pH, (g) oxidation reduction potential, (h) electrical conductivity, (i) ammonia, and (j) chemical oxygen demand.

Table A-10. Reactor information, initial conditions, and final conditions for the foundry waste (FW) reactor duplicates.

REACTOR INFORMATION		INITIAL CONDITIONS	FW-1	FW-2
Reactors:	FW-1 & FW-2	Specimen thickness [cm]:	15.2	16.0
Startup date:	2/14/2018	Specimen density [g/cm <sup>3</sup> ]:	0.49	0.46
Experiment duration [days]:	233	Initial recirculated volume [L/Mg-waste]:	70	59
Solid waste fraction:	Municipal Solid Waste and Foundry Waste	Initial $w_d$ after dosing [%]:	63	64
MSW [g]:	1440	FINAL CONDITIONS		
Foundry Waste [g]:	960	Cumulative recirculated liquid [L/Mg-waste]:	1353	1318
Liquid waste fraction:	Landfill Leachate	Average weekly recirculated liquid [L/Mg-waste]:	44	43
Initial liquid dose [L/Mg-waste]:	458	Settlement Strain [%]:	4.2	5.0



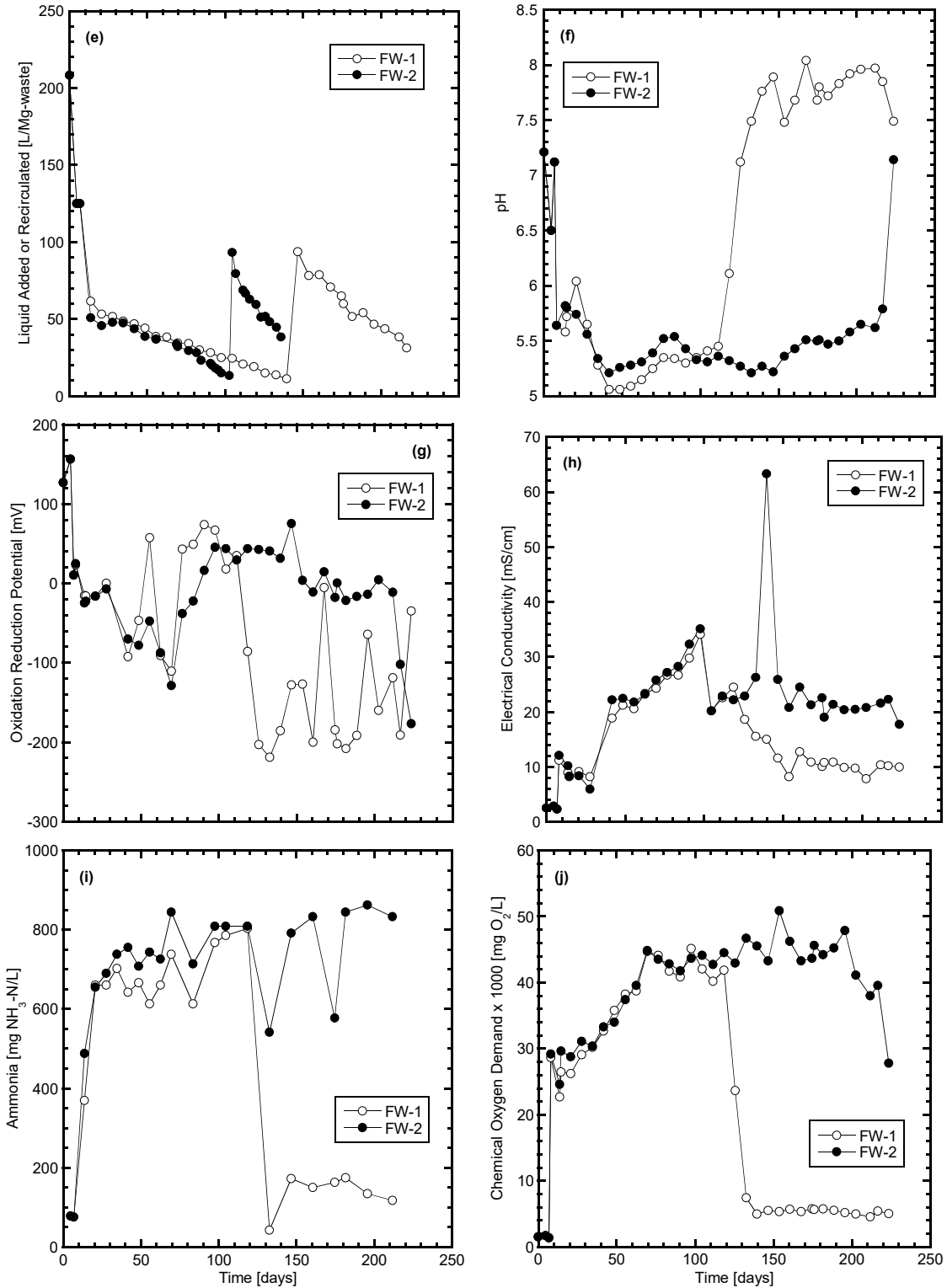
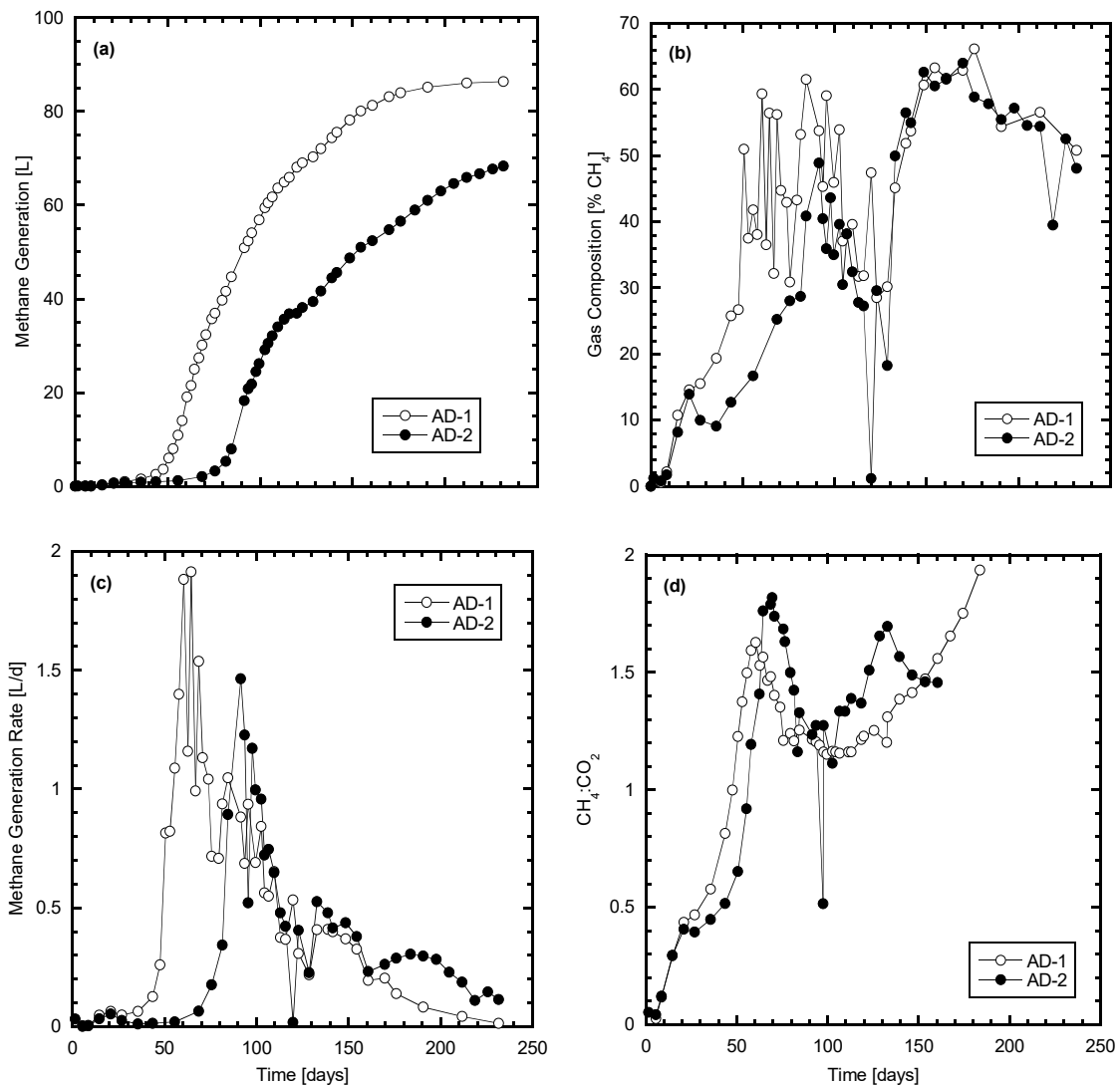


Figure A-10. Summary data for the foundry waste (FW) reactor duplicates: (a) methane generation, (b) gas composition, (c) methane generation rate, (d) methane to carbon dioxide ratio, (e) liquid addition or recirculation, (f) pH, (g) oxidation reduction potential, (h) electrical conductivity, (i) ammonia, and (j) chemical oxygen demand.

Table A-11. Reactor information, initial conditions, and final conditions for the anaerobic digestion sludge (AD) reactor duplicates.

REACTOR INFORMATION		INITIAL CONDITIONS	AD-1	AD-2
Reactors:	AD-1 & AD-2	Specimen thickness [cm]:	14.0	12.7
Startup date:	2/14/2018	Specimen density [g/cm <sup>3</sup> ]:	0.53	0.58
Experiment duration [days]:	232	Initial recirculated volume [L/Mg-waste]:	109	110
Solid waste fraction:	Municipal Solid Waste and Anaerobic Sludge	Initial w <sub>a</sub> after dosing [%]:	135	135
MSW [g]:	1440	FINAL CONDITIONS		
Anaerobic Sludge [g]:	960	Cumulative recirculated liquid [L/Mg-waste]:	3584	2561
Liquid waste fraction:	Landfill Leachate	Average weekly recirculated liquid [L/Mg-waste]:	81	70
Initial liquid dose [L/Mg-waste]:	188	Settlement Strain [%]:	15.9	12.5



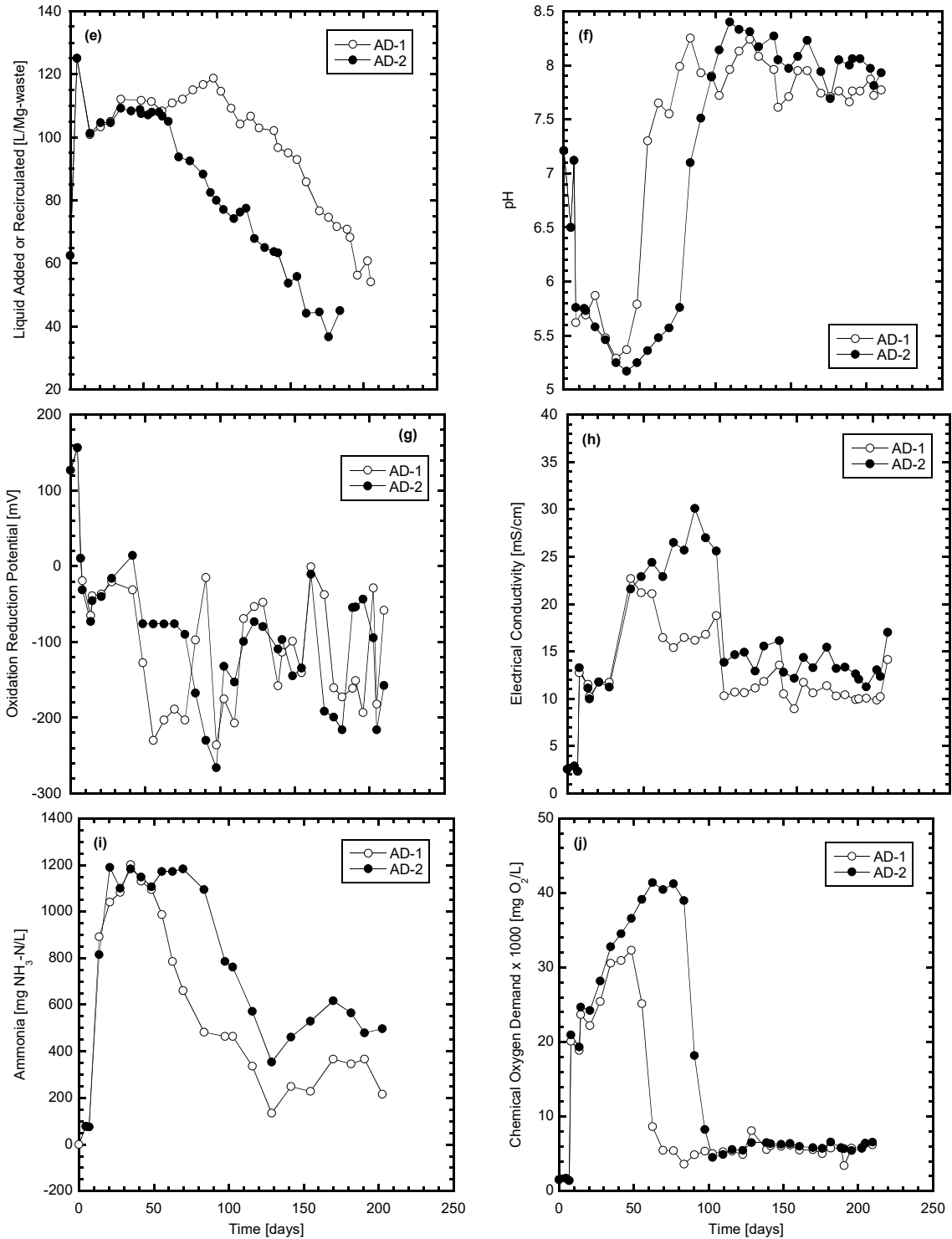
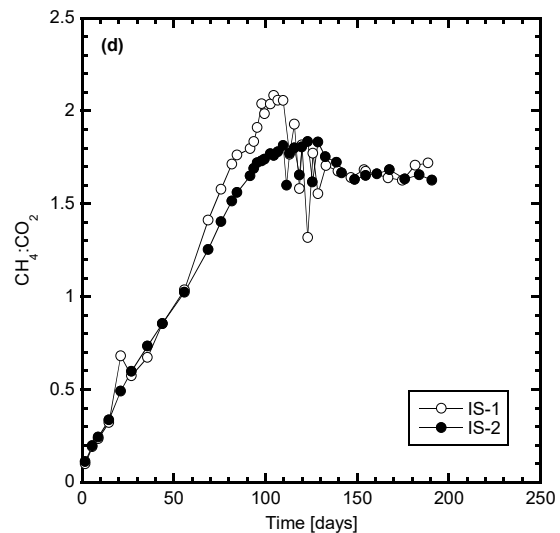
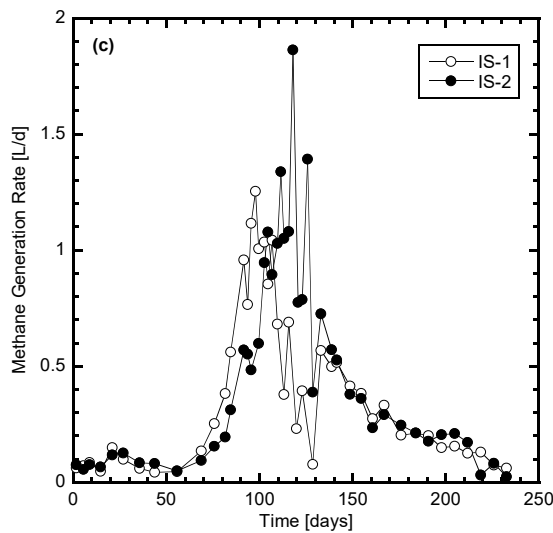
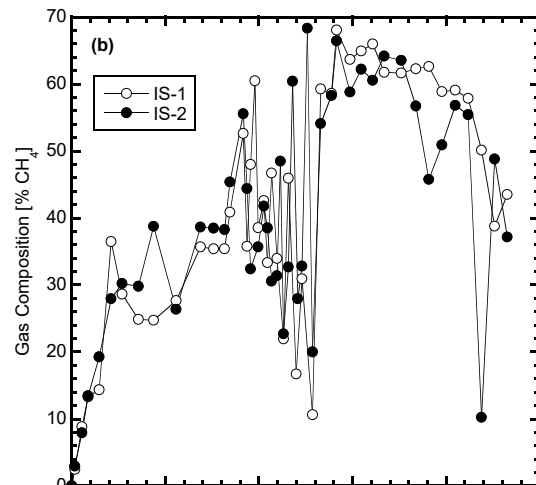
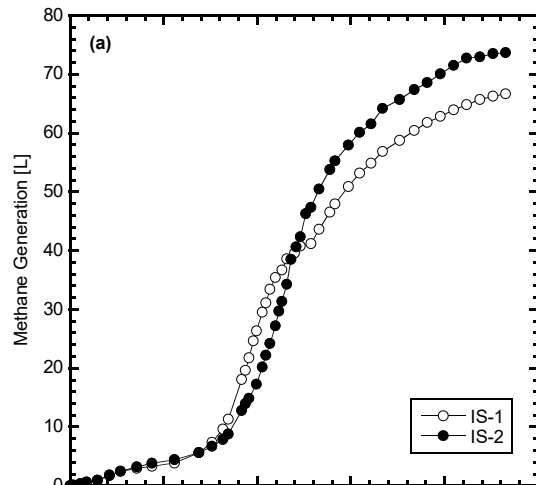


Figure A-11. Summary data for the anaerobic digestion sludge (AD) reactor duplicates: (a) methane generation, (b) gas composition, (c) methane generation rate, (d) methane to carbon dioxide ratio, (e) liquid addition or recirculation, (f) pH, (g) oxidation reduction potential, (h) electrical conductivity, (i) ammonia, and (j) chemical oxygen demand.

Table A-12. Reactor information, initial conditions, and final conditions for the industrial sludge (IS) reactor duplicates.

REACTOR INFORMATION		INITIAL CONDITIONS	IS-1	IS-2
Reactors:	IS-1 & IS-2	Specimen thickness [cm]:	12.7	12.1
Startup date:	2/14/2018	Specimen density [g/cm <sup>3</sup> ]:	0.58	0.61
Experiment duration [days]:	233	Initial recirculated volume [L/Mg-waste]:	93	75
Solid waste fraction:	Municipal Solid Waste and Industrial Sludge	Initial $w_d$ after dosing [%]:	149	152
MSW [g]:	1440	FINAL CONDITIONS		
Industrial Sludge [g]:	960	Cumulative recirculated liquid [L/Mg-waste]:	2268	1556
Liquid waste fraction:	Landfill Leachate	Average weekly recirculated liquid [L/Mg-waste]:	58	50
Initial liquid dose [L/Mg-waste]:	333	Settlement Strain [%]:	9.1	5.0



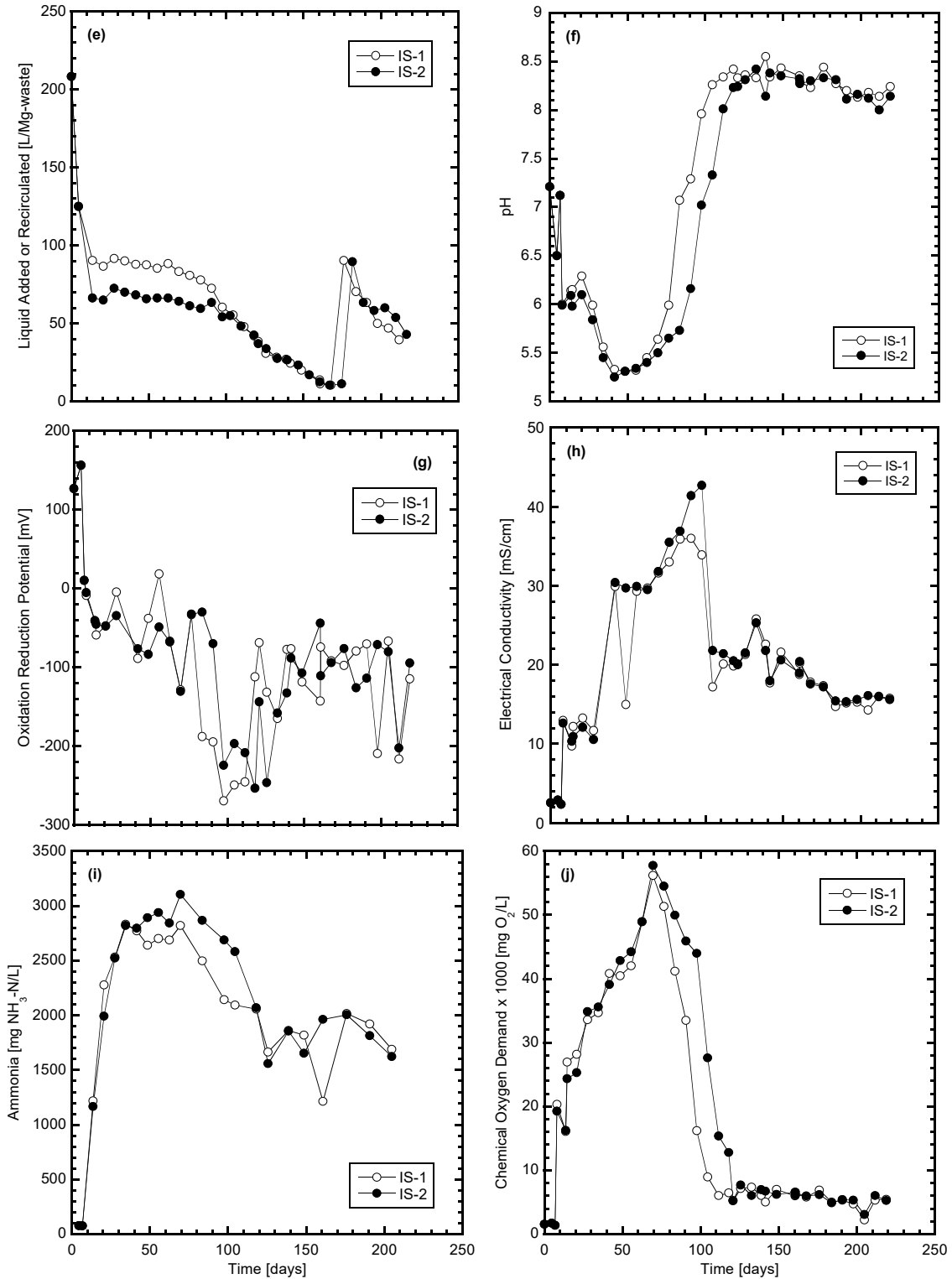


Figure A-12. Summary data for the industrial sludge (IS) reactor duplicates: (a) methane generation, (b) gas composition, (c) methane generation rate, (d) methane to carbon dioxide ratio, (e) liquid addition or recirculation, (f) pH, (g) oxidation reduction potential, (h) electrical conductivity, (i) ammonia, and (j) chemical oxygen demand.

**APPENDIX B – Compilation of Select Heavy Metals and Other Inorganic Elements Evaluated in Leachate Samples from the Laboratory Reactors Operated in Research Study 1**

Table B-1. Heavy metals and other inorganic elements data for liquid waste sources.

Liquid Waste	Liquid Waste Concentrations [mg/L]													
	Al	Ca	Cd	Cr	Cu	Fe	K	Mg	Mn	Na	Ni	P	Pb	Zn
Control Landfill Leachate	0.00	218	0.013	0.00	0.00	24.0	60	78	0.7	423	0.1	1.1	0.000	0.2
Brewery Wastewater	0.00	14	0.041	0.00	0.02	0.4	216	57	0.1	18	0.1	263.8	0.000	0.0
Cheese Processing Wastewater	0.00	245	0.000	0.00	0.00	0.5	236	22	0.0	138	0.1	139.9	0.005	0.2
Automobile Wash Water	0.00	69	0.013	0.00	0.06	0.7	6	3	0.0	8	0.1	1.3	0.000	0.4
Manufacturing High Strength	6.15	377	0.043	0.00	0.30	35.9	55	35	1.3	422	0.2	148.7	0.238	3.0
Manufacturing Low Strength	0.41	102	0.000	0.00	0.02	8.2	13	3	0.3	58	0.2	50.9	0.007	0.4
Landfill Leachate for MSW-SW and MSW-Sludge Reactors	0.15	240	0.009	0.00	0.00	41.0	57	82	0.8	402	0.1	1.6	0.000	0.0

Table B-2. Heavy metals and other inorganic elements data for initial recirculation samples.

Reactor	Initial Recirculation Concentrations [mg/L]													
	Al	Ca	Cd	Cr	Cu	Fe	K	Mg	Mn	Na	Ni	P	Pb	Zn
Control-1	1.62	922	0.032	0.18	0.43	47.5	1650	221	8.8	469	0.4	85.7	0.000	3.5
Control-2	1.09	851	0.014	0.00	0.10	84.1	1040	167	8.8	314	0.2	73.4	0.087	2.0
LL-1	2.67	720	0.033	1.09	0.13	37.3	1691	227	8.5	711	0.3	83.4	0.000	3.0
LL-2	1.56	841	0.025	0.08	0.07	36.5	1299	212	8.7	650	0.3	69.4	0.000	1.0
BW-1	3.43	745	0.065	0.22	0.11	26.0	1869	256	6.9	589	0.3	91.1	0.000	3.0
BW-2	2.48	617	0.057	0.06	0.08	27.4	2041	256	6.9	573	0.2	120.4	0.000	2.6
CW-1	1.80	725	0.043	0.61	0.04	23.4	1847	231	8.4	583	0.2	95.5	0.000	1.7
CW-2	4.21	953	0.018	1.24	0.08	31.1	2656	293	9.7	733	0.3	75.7	0.000	2.3
AWW-1	1.02	850	0.011	0.68	0.01	32.5	796	152	8.4	316	0.3	49.3	0.063	0.3
AWW-2	0.95	867	0.032	0.00	0.01	58.2	865	164	9.4	331	0.3	64.9	0.030	1.0
MW-H-1	6.11	683	0.047	0.37	0.12	39.3	2623	266	8.0	884	0.4	112.3	0.000	5.9
MW-H-2	9.53	859	0.042	0.59	0.11	41.1	3186	305	9.6	893	0.3	105.2	0.000	7.5
MW-L-1	2.22	811	0.050	0.13	0.06	28.5	1536	216	7.7	502	0.3	87.3	0.000	2.3
MW-L-2	2.84	826	0.051	0.42	0.11	28.2	1414	215	8.7	478	0.3	104.4	0.000	3.2
GB-1	2.09	993	0.037	0.18	0.02	51.7	1159	235	10.5	758	0.3	48.6	0.000	0.7
GB-2	3.06	907	0.056	0.49	0.01	32.9	1655	279	9.9	963	0.4	66.9	0.000	0.2
ASR-1	1.10	692	0.008	0.00	0.14	64.6	628	156	12.3	641	0.9	8.8	0.000	14.3
ASR-2	1.39	807	0.027	0.36	0.14	104.5	1277	214	15.5	785	1.3	13.8	0.011	28.9
FW-1	1.65	886	0.037	0.00	0.04	74.6	1557	229	11.8	856	0.3	67.5	0.000	0.7
FW-2	1.87	809	0.028	0.03	0.05	42.2	1641	233	9.4	850	0.3	75.4	0.000	0.6
AD-1	1.37	854	0.033	0.87	0.05	77.2	1296	220	9.5	481	0.3	222.7	0.000	0.5
AD-2	1.75	866	0.022	3.27	0.08	52.0	1354	220	7.3	477	0.3	248.5	0.000	0.6
IS-1	0.82	951	0.012	0.00	0.05	34.3	774	191	10.0	429	0.5	245.1	0.000	0.2
IS-2	0.80	1076	0.007	0.00	0.04	31.0	770	201	9.3	444	0.5	224.3	0.115	0.0
MCL			0.005	0.1	1.3								0.015	
Secondary MCL	0.05				1	0.3			0.05					5
Typical Leachate (Kjeldsen et al. 2002)		7200	0.4	1.5	10	5500	3700	15000	1400	7700	13	23	5	1000

Table B-3. Heavy metals and other inorganic elements data for final recirculation samples.

Reactor	Final Recirculation Concentrations [mg/L]													
	Al	Ca	Cd	Cr	Cu	Fe	K	Mg	Mn	Na	Ni	P	Pb	Zn
Control-1	0.00	2002	0.009	0.06	0.00	378.8	2716	190	22.6	1429	0.4	27.1	0.128	5.7
Control-2	0.00	1931	0.000	0.05	0.00	385.5	2748	188	20.6	1733	0.3	25.2	0.102	6.1
LL-1	0.11	1947	0.000	0.48	0.00	416.9	2775	189	23.6	2186	0.3	28.9	0.190	21.6
LL-2	0.11	2000	0.000	0.22	0.00	415.4	2653	183	22.9	2450	0.2	27.4	0.162	4.1
BW-1	0.06	1908	0.006	0.12	0.00	386.1	2740	171	21.7	1016	0.3	53.0	0.050	4.6
BW-2	0.00	1673	0.015	0.05	0.00	324.9	2859	175	19.1	1604	0.3	63.6	0.051	7.7
CW-1	0.00	1624	0.003	0.13	0.00	294.4	2684	183	17.5	1399	0.3	29.1	0.056	6.3
CW-2	0.00	1641	0.000	0.12	0.00	310.9	2556	184	18.9	1077	0.3	31.5	0.090	3.0
AWW-1	0.09	1923	0.000	0.12	0.00	336.4	2428	180	21.2	1691	0.3	25.7	0.065	1.4
AWW-2	0.00	1720	0.006	0.10	0.00	261.8	2502	183	16.3	1594	0.3	23.5	0.034	2.7
MW-H-1	0.17	1280	0.006	0.07	0.00	264.5	2411	183	13.9	1538	0.5	29.1	0.105	1.0
MW-H-2	0.14	1279	0.003	0.07	0.00	231.0	2294	180	12.4	1129	0.5	32.3	0.043	0.5
MW-L-1	0.00	1654	0.004	0.17	0.00	295.6	2300	181	15.7	1323	0.3	29.4	0.104	1.5
MW-L-2	0.12	1620	0.003	0.25	0.00	269.0	2366	184	16.0	1532	0.4	30.0	0.055	1.4
GB-1	0.00	1244	0.012	0.21	0.00	1.9	961	146	1.9	926	0.0	7.0	0.013	0.0
GB-2	0.00	1785	0.020	0.09	0.00	0.2	941	151	2.7	924	0.0	6.2	0.000	0.0
ASR-1	0.00	1236	0.000	0.03	0.00	259.5	1371	187	30.6	1177	1.3	4.1	0.055	34.7
ASR-2	0.05	1287	0.000	0.16	0.00	354.0	1668	190	32.5	1080	1.7	5.0	0.153	47.9
FW-1	0.04	1984	0.009	0.01	0.00	285.9	2202	186	26.2	1587	0.2	26.2	0.065	11.4
FW-2	0.03	1983	0.000	0.09	0.00	323.7	2095	184	24.2	1478	0.2	21.9	0.118	2.1
AD-1	0.19	83	0.000	0.14	0.00	10.9	951	107	0.4	995	0.2	22.4	0.011	0.1
AD-2	0.00	97	0.000	0.13	0.00	13.0	1116	138	0.2	1506	0.1	16.6	0.011	0.1
IS-1	0.00	94	0.000	0.00	0.00	24.1	1151	147	0.1	1074	0.1	16.6	0.013	0.0
IS-2	0.00	1097	0.006	0.00	0.00	230.3	1457	173	4.4	1150	0.1	11.5	0.048	0.1
MCL			0.005	0.1	1.3								0.015	
Secondary MCL	0.05				1	0.3			0.05					5
Typical Leachate (Kjeldsen et al. 2002)		7200	0.4	1.5	10	5500	3700	15000	1400	7700	13	23	5	1000

**APPENDIX C – Photos of Reactors and Biochemical Methane Potential Assays  
from Research Study 1**

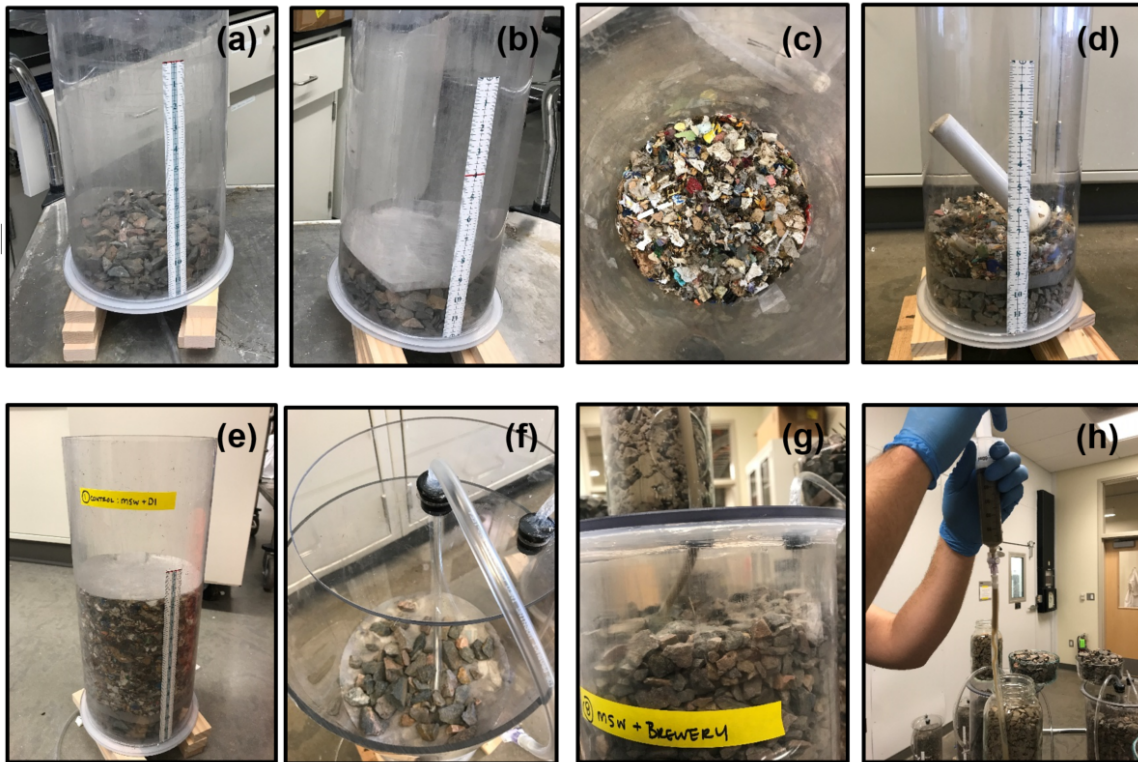


Figure C-1. Reactor construction of (a) drainage layer, (b) geotextile filter, (c) waste lift, (d) hand-tamped waste lift, (e) upper geotextile, (f) influent line buried in upper gravel layer, (g) gravel load and lid secured with silicon, and (h) injecting initial liquid dose.

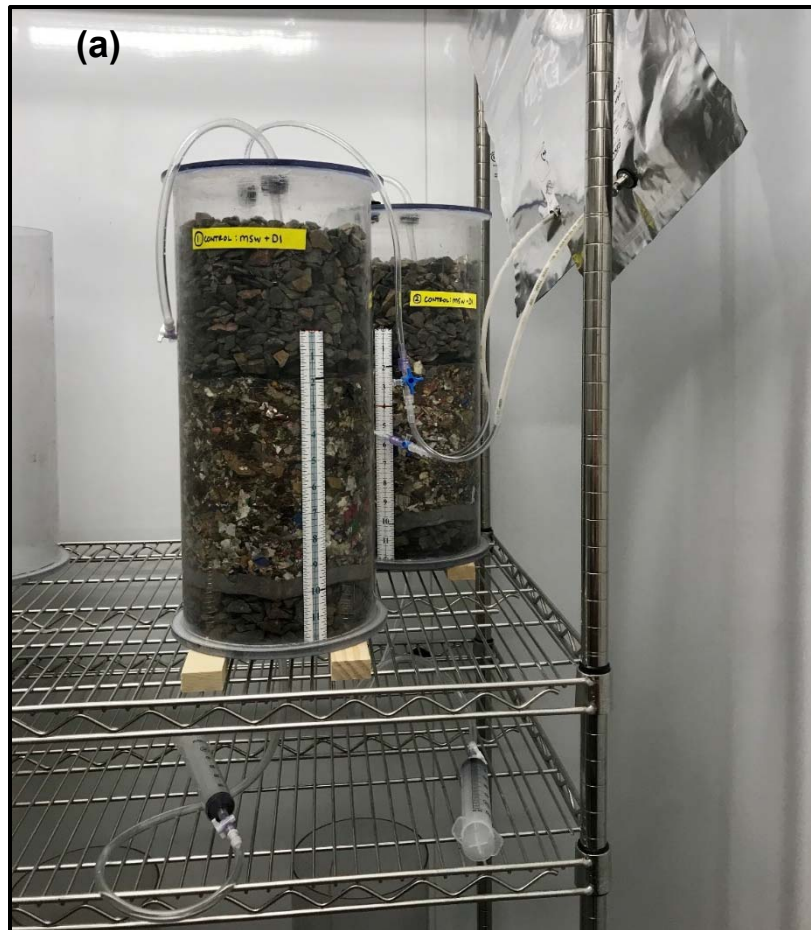


Figure C-2. (a) Final constructed control reactors and (b) temperature control room with 24 reactor experiments in operation.



Figure C-3. Weekly recirculation: (a) reactor leachate is pulled from the gravel storage layer via syringe, (b) samples are collected and stored in vials, and (c) leachate volume is measured via syringe, collected in a beaker, and buffered before reinjection into the influent port.

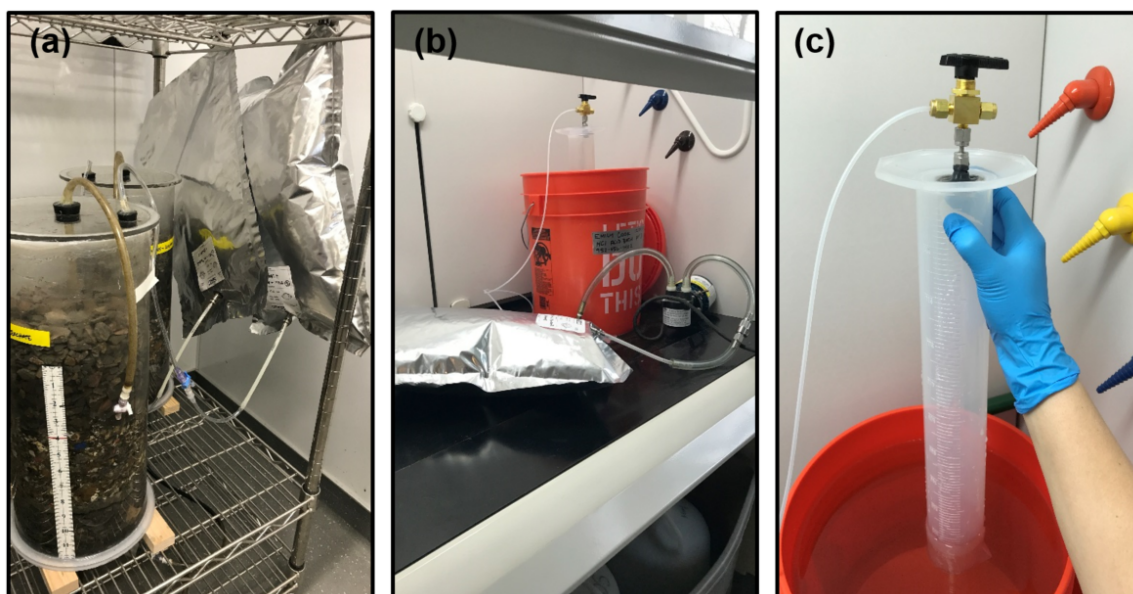


Figure C-4. Reactor gas management: (a) gas is collected in bags, (b) gas bag is connected to vacuum pump for volume measurement, and (c) gas is measured via volume displacement using an inverted 1-L graduated cylinder.

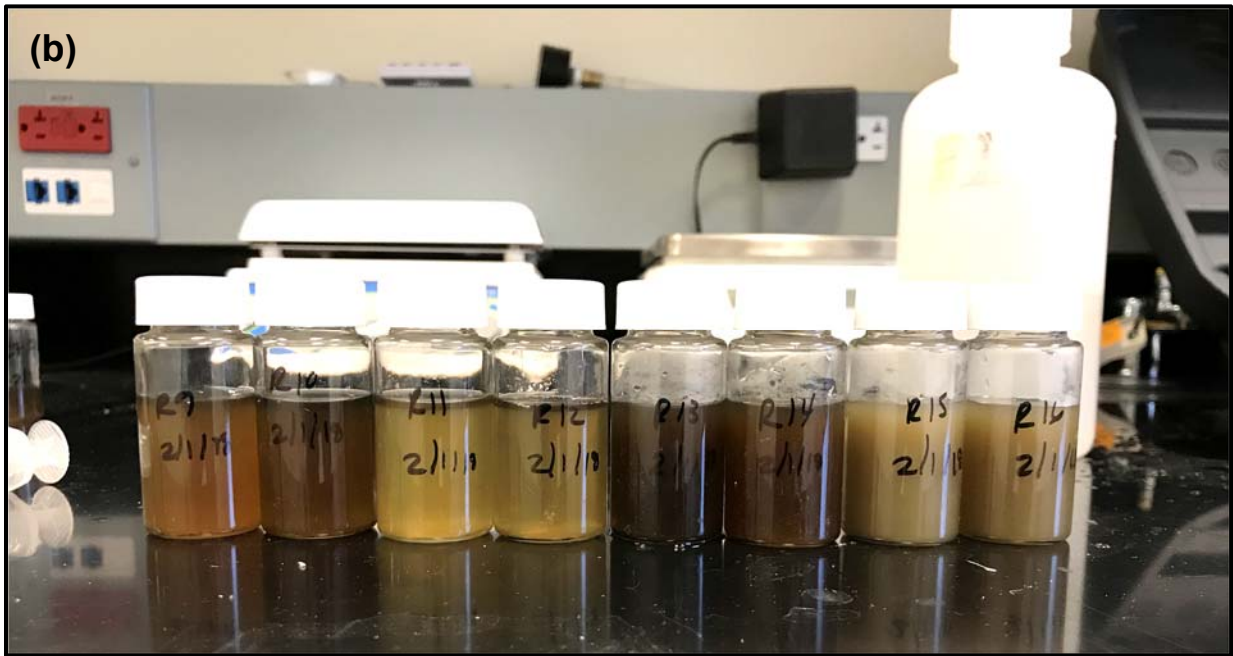


Figure C-5. Treatment of high strength manufacturing wastewater (MW-H) via one recirculation of through the waste mass: (a) initial white/high solids liquid waste prior to recirculation and (b) translucent brown MW-H leachate after first recirculation through the waste mass (“R13” and R14”, 5<sup>th</sup> and 6<sup>th</sup> from the left, respectively)



Figure C-6. Operational considerations including (a) reactor clogging due to AD sludge addition and (b) sulfate reduction, indicated by the black coloration in the GB reactors.

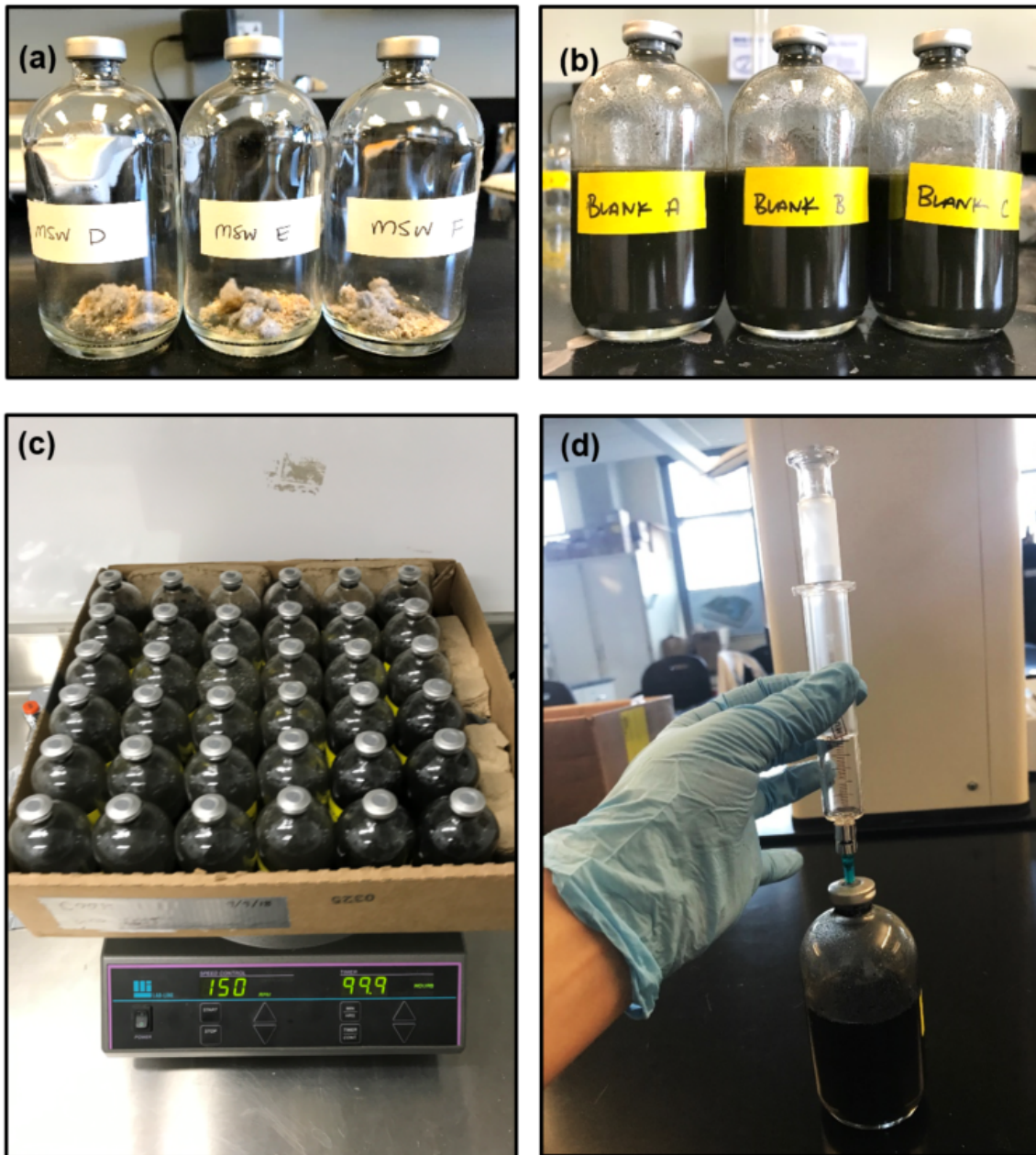
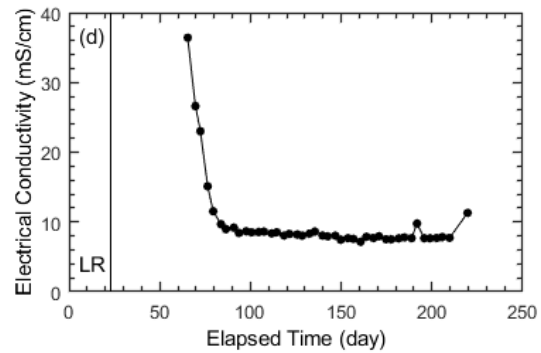
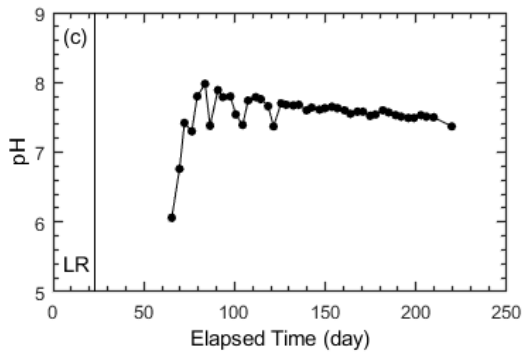
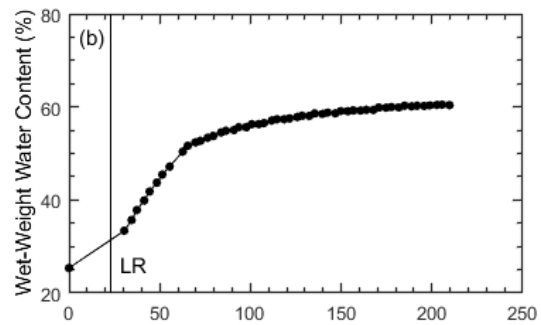
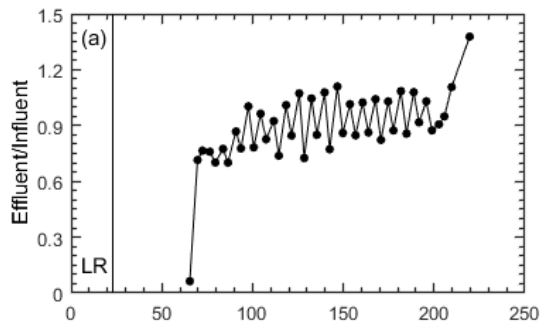


Figure C-7. Biochemical methane potential (BMP) assays: (a) solid waste sample added to assay bottle, (b) BMP control consisting of 50 mL nutrient media and 50 mL anaerobic inoculum, (c) bottles in temperature controlled room on shaker table, and (d) venting gas bottle prior to sampling using a wetted glass syringe.

## APPENDIX D – Compilation of Reactor Data for Study 2

Table D-1. Reactor information, initial conditions, and final conditions for R1.

Reactor Information		Initial Conditions	
Reactor No.	R1	Specimen thickness (mm)	202
Startup date	12/18/18	Total unit weight (kN/m <sup>3</sup> )	3.44
Experiment duration (d)	220	Wet weight water content (%)	25
Solid waste mass (g)	2400	Final Conditions	
Dose volume (L/Mg-MSW)	40	Total unit weight (kN/m <sup>3</sup> )	6.54
Dose volume (mL)	96	Water balance wet weight water content (%)	60
Dose frequency (week)	0.5	Measured wet weight water content (%)	56
Dose rate (L/Mg-MSW/month)	320	Lag-time (d)	14
Cumulative leachate (L/Mg-MSW)	2160	Decay rate (1/yr)	1.91



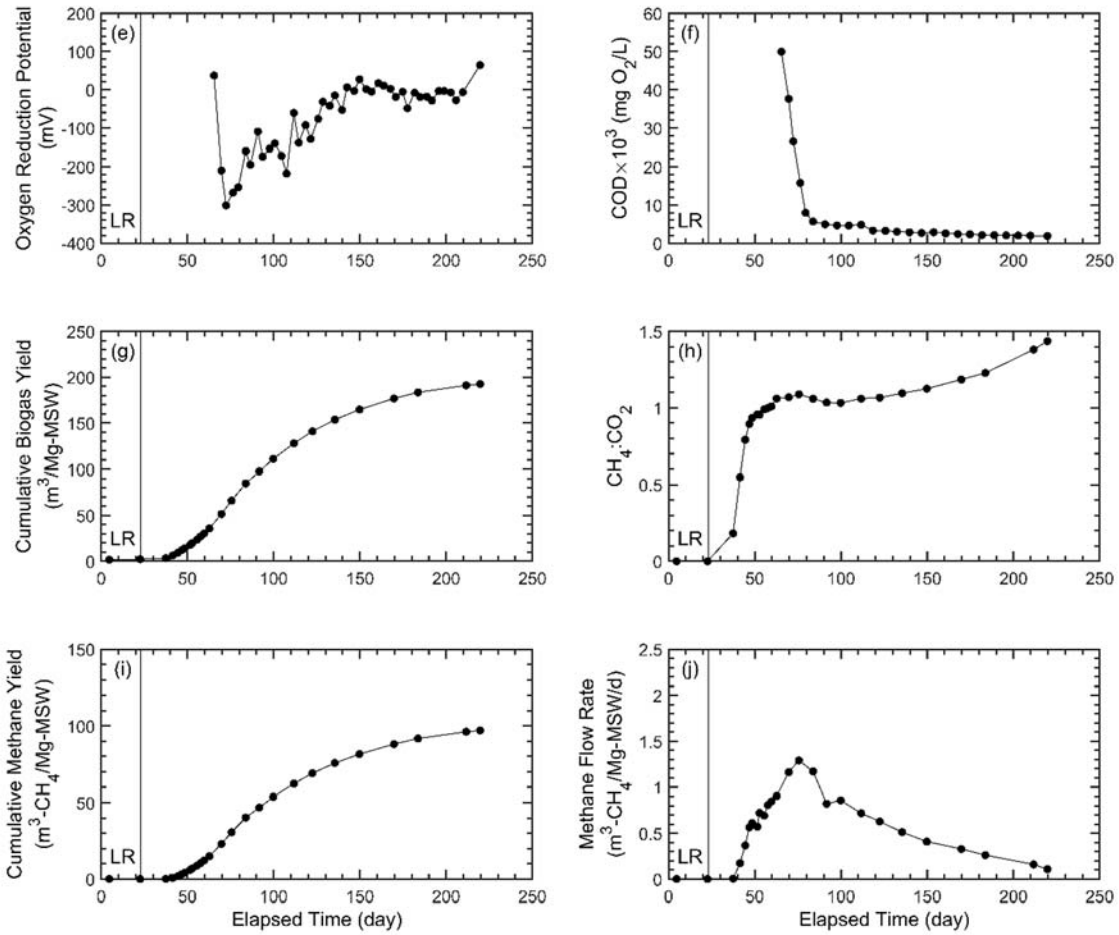
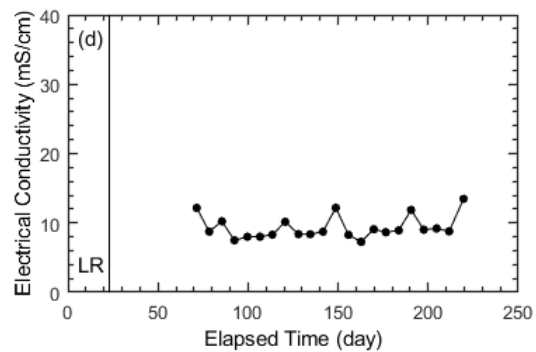
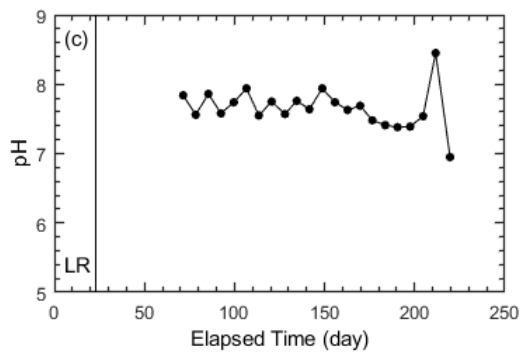
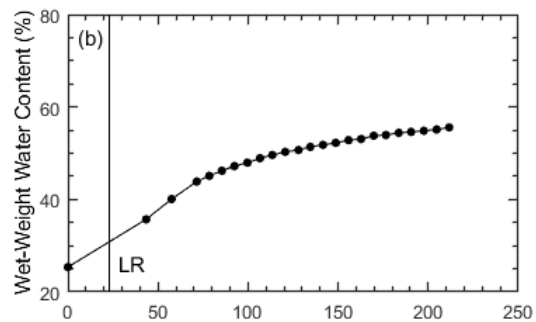
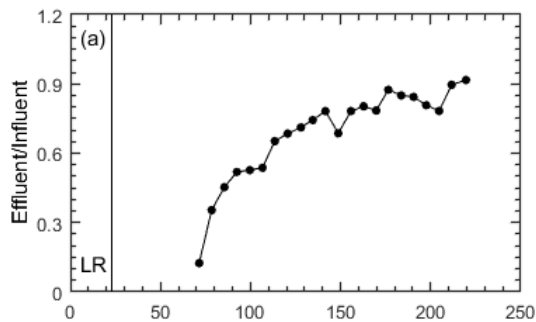


Figure D-1. Temporal trends of operational data collected for R1: (a) ratio of influent to effluent volumes; (b) wet weight water content; (c) leachate pH; (d) leachate electrical conductivity; (e) leachate oxidation reduction potential; (f) leachate chemical oxygen demand; (g) cumulative biogas yield; (h) ratio of methane to carbon dioxide; (i) cumulative methane yield; and (j) methane flow rate.

Table D-2. Reactor information, initial conditions, and final conditions for R2.

Reactor Information		Initial Conditions	
Reactor No.	R2	Specimen thickness (mm)	202
Startup date	12/18/18	Total unit weight (kN/m <sup>3</sup> )	3.44
Experiment duration (d)	220	Wet weight water content (%)	25
Solid waste mass (g)	2400	Final Conditions	
Dose volume (L/Mg-MSW)	40	Total unit weight (kN/m <sup>3</sup> )	5.74
Dose volume (mL)	96	Water balance wet weight water content (%)	56
Dose frequency (week)	1	Measured wet weight water content (%)	53
Dose rate (L/Mg-MSW/month)	160	Lag-time (d)	20
Cumulative leachate (L/Mg-MSW)	1120	Decay rate (1/yr)	1.23



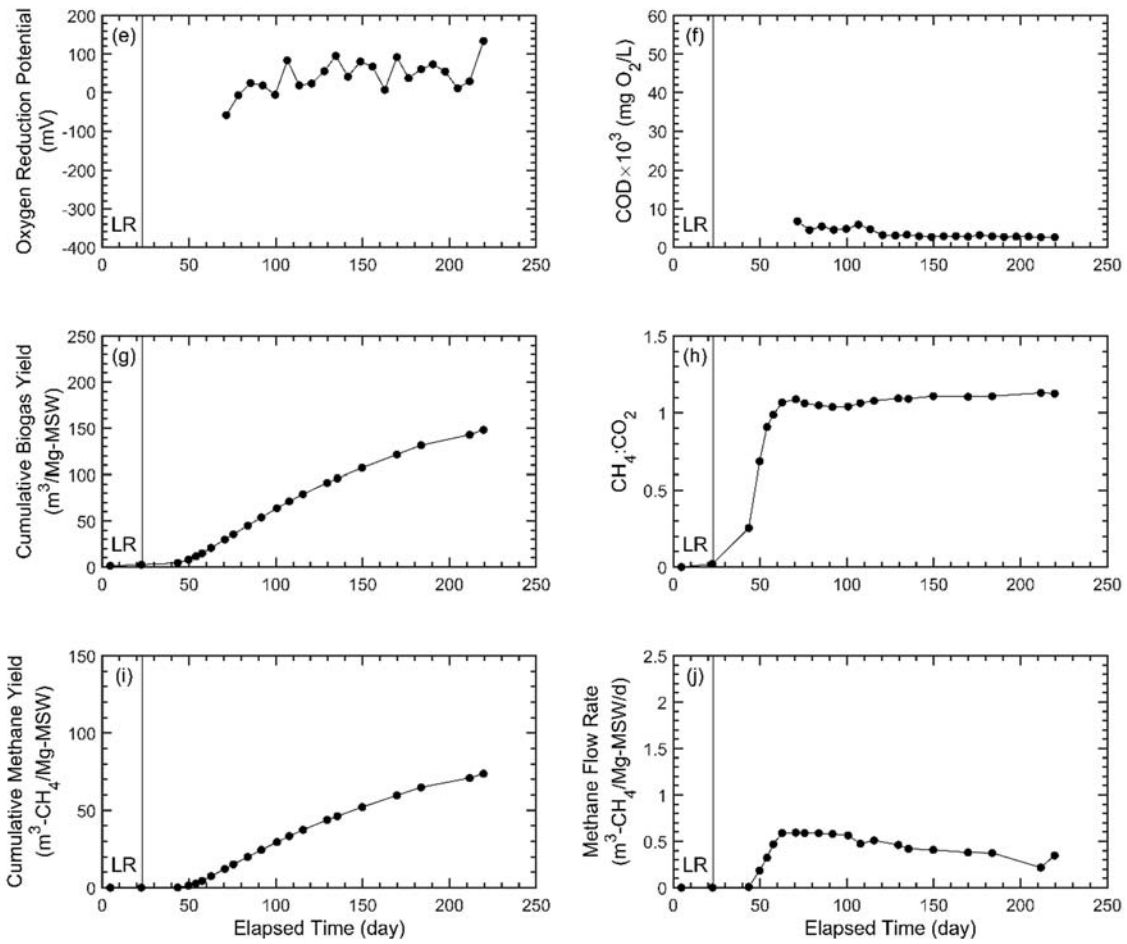
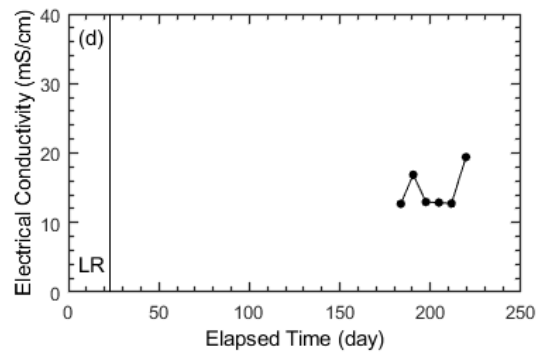
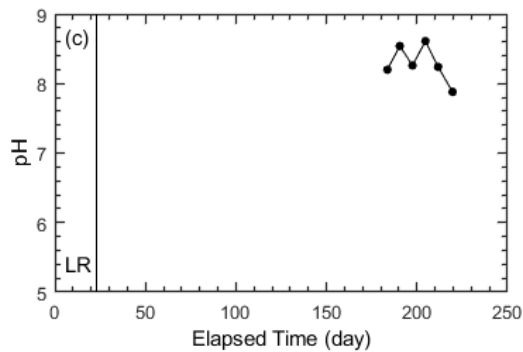
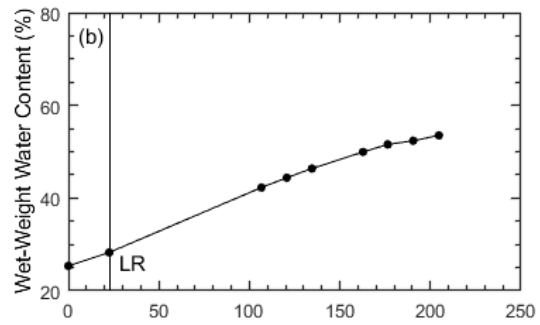
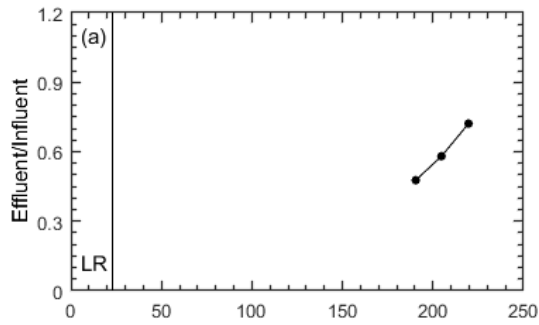


Figure D-2. Temporal trends of operational data collected for R2: (a) ratio of influent to effluent volumes; (b) wet weight water content; (c) leachate pH; (d) leachate electrical conductivity; (e) leachate oxidation reduction potential; (f) leachate chemical oxygen demand; (g) cumulative biogas yield; (h) ratio of methane to carbon dioxide; (i) cumulative methane yield; and (j) methane flow rate.

Table D-3. Reactor information, initial conditions, and final conditions for R3.

Reactor Information		Initial Conditions	
Reactor No.	R3	Specimen thickness (mm)	202
Startup date	12/18/18	Total unit weight (kN/m <sup>3</sup> )	3.46
Experiment duration (d)	220	Wet weight water content (%)	25
Solid waste mass (g)	2400	Final Conditions	
Dose volume (L/Mg-MSW)	40	Total unit weight (kN/m <sup>3</sup> )	5.87
Dose volume (mL)	96	Water balance wet weight water content (%)	54
Dose frequency (week)	2	Measured wet weight water content (%)	53
Dose rate (L/Mg-MSW/month)	80	Lag-time (d)	32
Cumulative leachate (L/Mg-MSW)	560	Decay rate (1/yr)	0.73



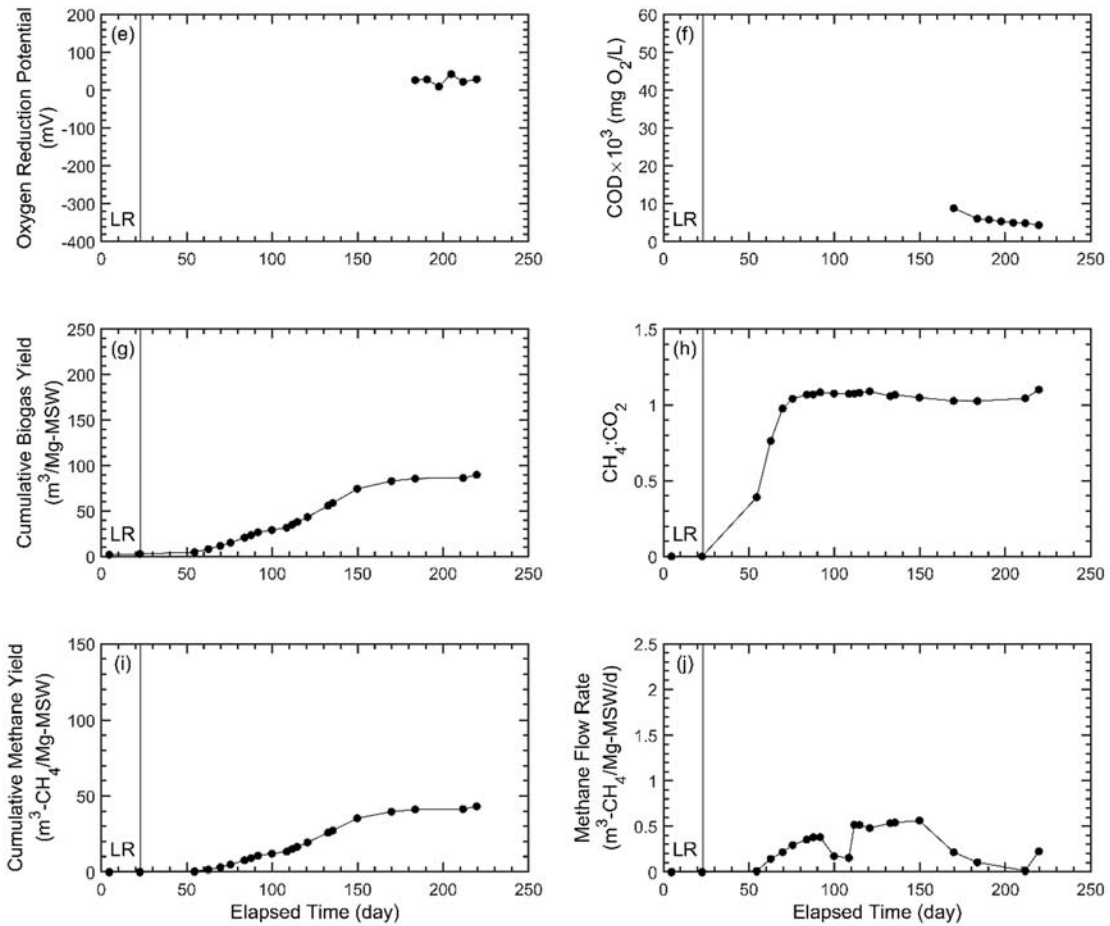


Figure D-3. Temporal trends of operational data collected for R3: (a) ratio of influent to effluent volumes; (b) wet weight water content; (c) leachate pH; (d) leachate electrical conductivity; (e) leachate oxidation reduction potential; (f) leachate chemical oxygen demand; (g) cumulative biogas yield; (h) ratio of methane to carbon dioxide; (i) cumulative methane yield; and (j) methane flow rate.

Table D-4. Reactor information, initial conditions, and final conditions for R4.

Reactor Information		Initial Conditions	
Reactor No.	R4	Specimen thickness (mm)	203
Startup date	12/18/18	Total unit weight (kN/m <sup>3</sup> )	3.41
Experiment duration (d)	220	Wet weight water content (%)	25
Solid waste mass (g)	2400	Final Conditions	
Dose volume (L/Mg-MSW)	40	Total unit weight (kN/m <sup>3</sup> )	4.62
Dose volume (mL)	96	Water balance wet weight water content (%)	42
Dose frequency (week)	4	Measured wet weight water content (%)	26
Dose rate (L/Mg-MSW/month)	40	Lag-time (d)	48
Cumulative leachate (L/Mg-MSW)	280	Decay rate (1/yr)	0.40

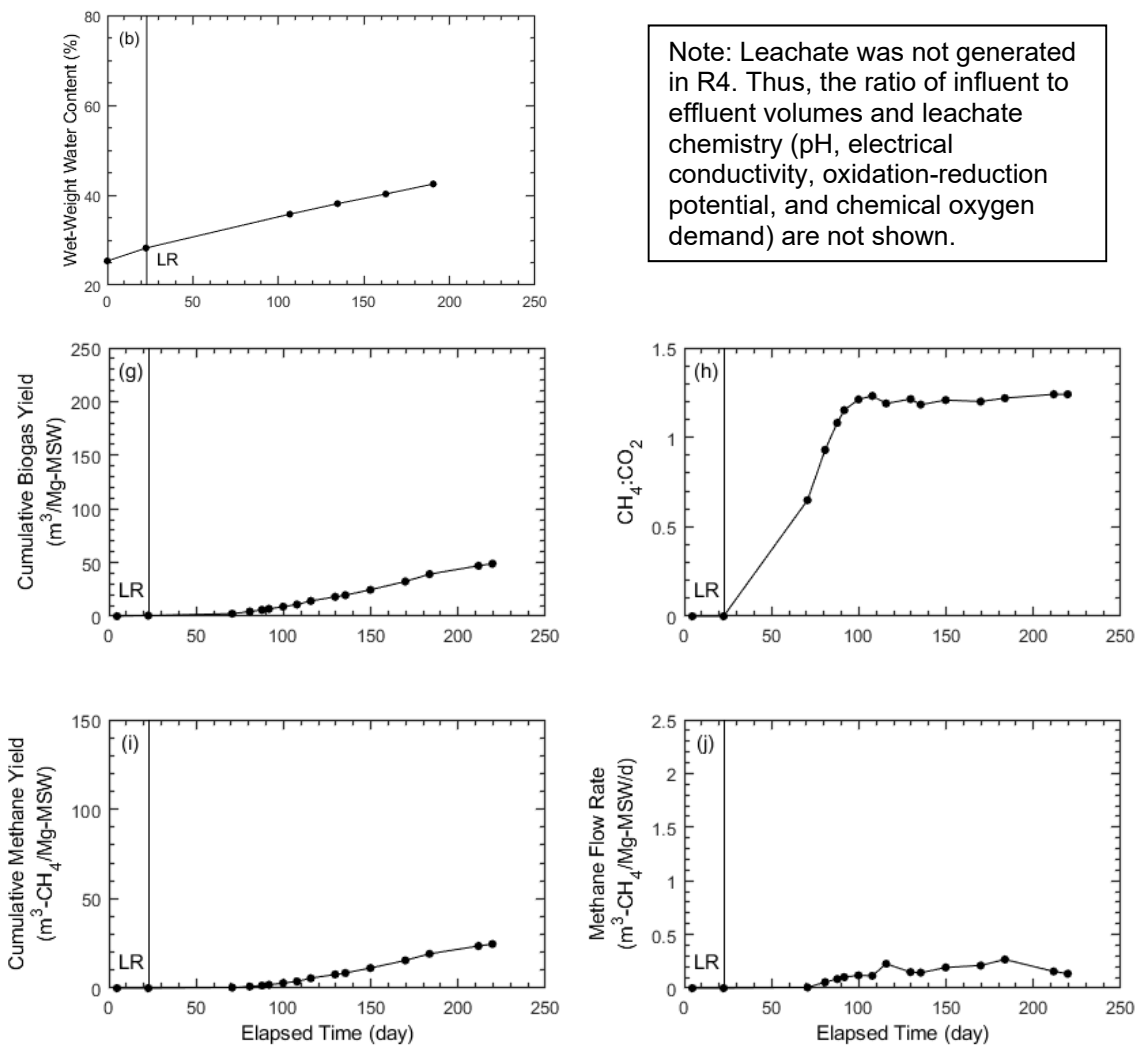
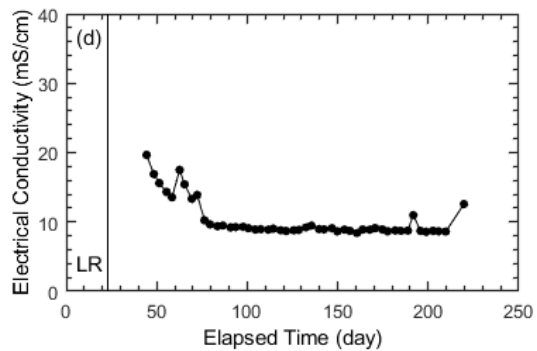
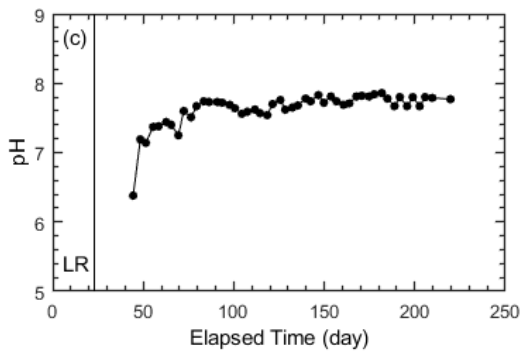
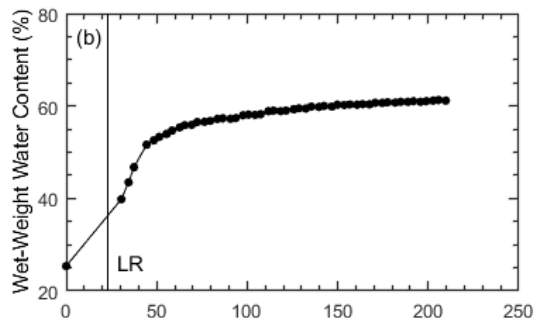
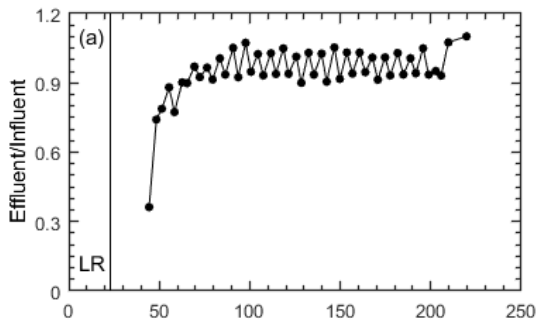


Figure D-4. Temporal trends of operational data collected for R4: (b) wet weight water content; (g) cumulative biogas yield; (h) ratio of methane to carbon dioxide; (i) cumulative methane yield; and (j) methane flow rate.

Table D-5. Reactor information, initial conditions, and final conditions for R5.

Reactor Information		Initial Conditions	
Reactor No.	R5	Specimen thickness (mm)	200
Startup date	12/18/18	Total unit weight (kN/m <sup>3</sup> )	3.46
Experiment duration (d)	220	Wet weight water content (%)	25
Solid waste mass (g)	2400	Final Conditions	
Dose volume (L/Mg-MSW)	80	Total unit weight (kN/m <sup>3</sup> )	6.4
Dose volume (mL)	192	Water balance wet weight water content (%)	61
Dose frequency (week)	0.5	Measured wet weight water content (%)	55
Dose rate (L/Mg-MSW/month)	640	Lag-time (d)	14
Cumulative leachate (L/Mg-MSW)	4320	Decay rate (1/yr)	2.12



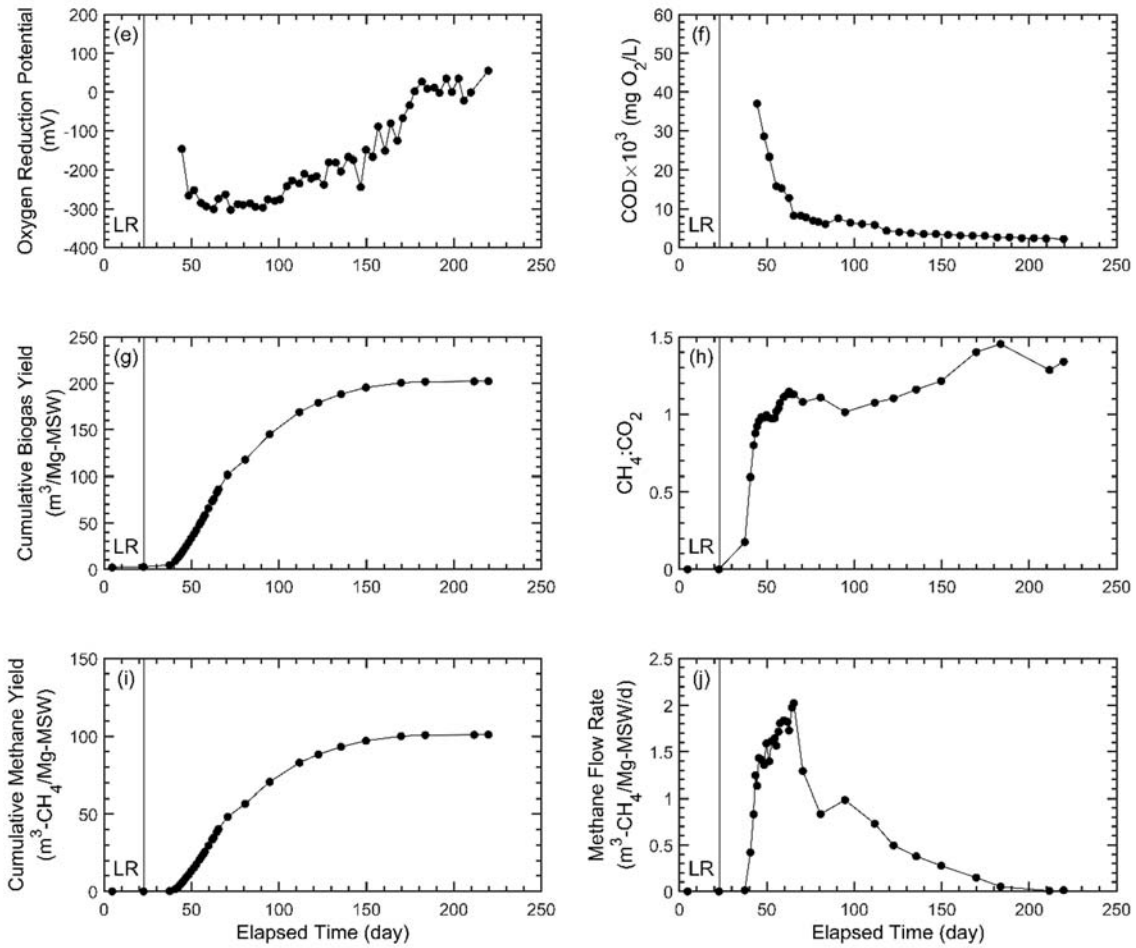
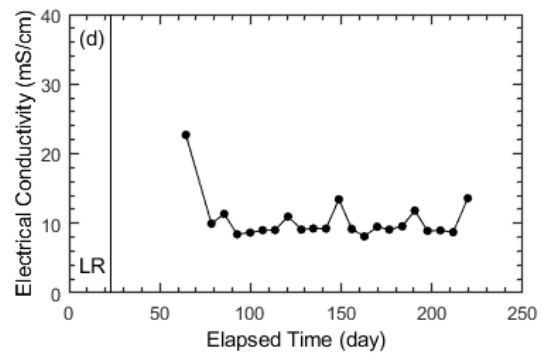
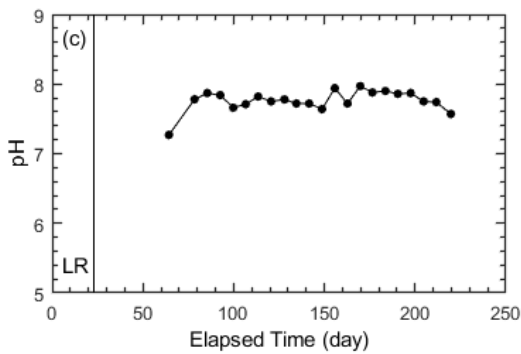
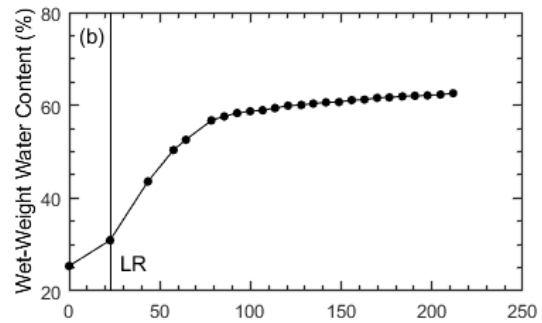
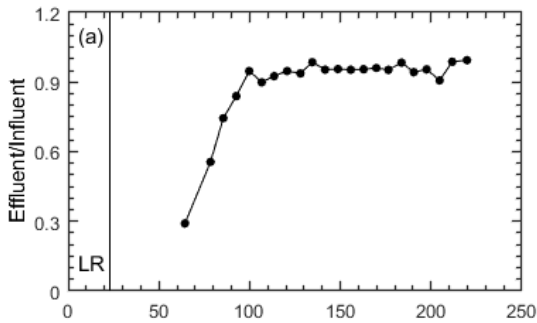


Figure D-5. Temporal trends of operational data collected for R5: (a) ratio of influent to effluent volumes; (b) wet weight water content; (c) leachate pH; (d) leachate electrical conductivity; (e) leachate oxidation reduction potential; (f) leachate chemical oxygen demand; (g) cumulative biogas yield; (h) ratio of methane to carbon dioxide; (i) cumulative methane yield; and (j) methane flow rate.

Table D-6. Reactor information, initial conditions, and final conditions for R6.

Reactor Information		Initial Conditions	
Reactor No.	R6	Specimen thickness (mm)	192
Startup date	12/18/18	Total unit weight (kN/m <sup>3</sup> )	3.61
Experiment duration (d)	220	Wet weight water content (%)	25
Solid waste mass (g)	2400	Final Conditions	
Dose volume (L/Mg-MSW)	80	Total unit weight (kN/m <sup>3</sup> )	6.83
Dose volume (mL)	192	Water balance wet weight water content (%)	63
Dose frequency (week)	1	Measured wet weight water content (%)	56
Dose rate (L/Mg-MSW/month)	320	Lag-time (d)	19
Cumulative leachate (L/Mg-MSW)	2240	Decay rate (1/yr)	1.97



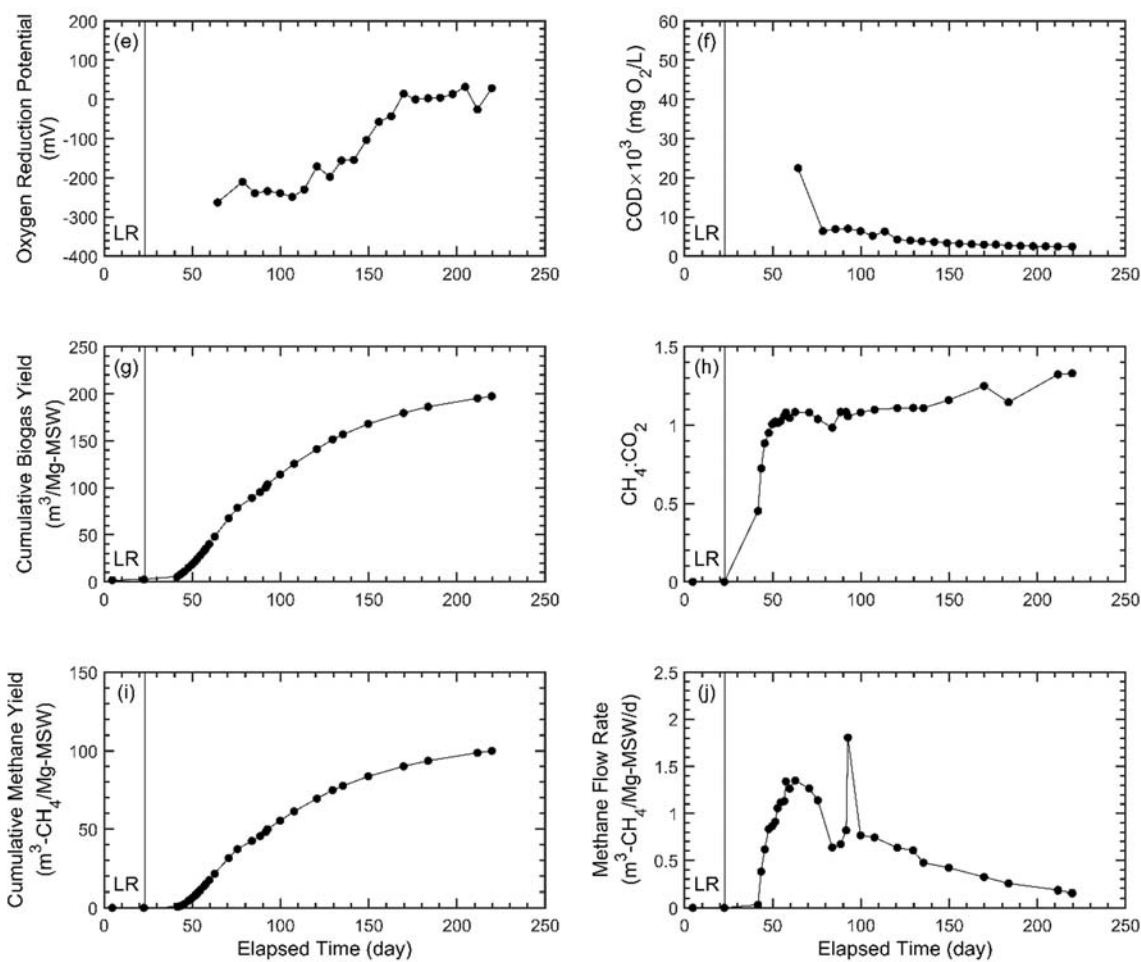
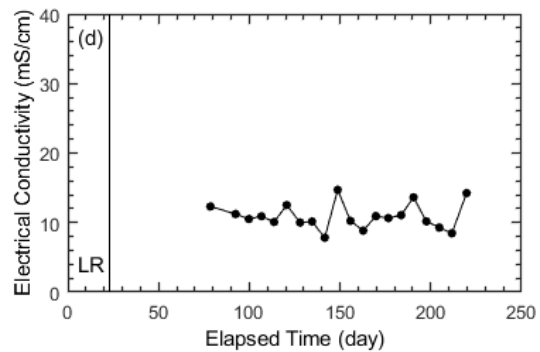
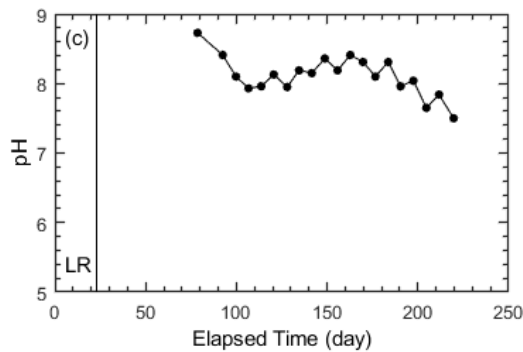
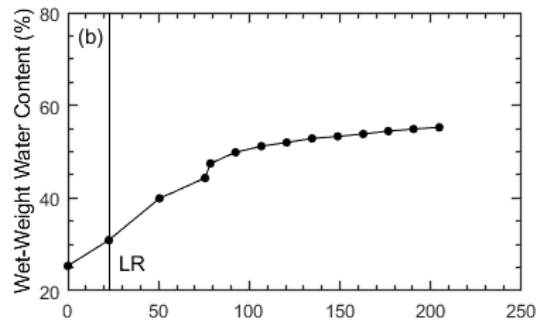
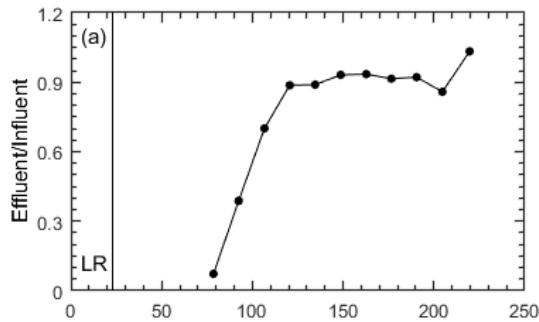


Figure D-6. Temporal trends of operational data collected for R6: (a) ratio of influent to effluent volumes; (b) wet weight water content; (c) leachate pH; (d) leachate electrical conductivity; (e) leachate oxidation reduction potential; (f) leachate chemical oxygen demand; (g) cumulative biogas yield; (h) ratio of methane to carbon dioxide; (i) cumulative methane yield; and (j) methane flow rate.

Table D-7. Reactor information, initial conditions, and final conditions for R7.

Reactor Information		Initial Conditions	
Reactor No.	R7	Specimen thickness (mm)	200
Startup date	12/18/18	Total unit weight (kN/m <sup>3</sup> )	3.46
Experiment duration (d)	220	Wet weight water content (%)	25
Solid waste mass (g)	2400	Final Conditions	
Dose volume (L/Mg-MSW)	80	Total unit weight (kN/m <sup>3</sup> )	5.72
Dose volume (mL)	192	Water balance wet weight water content (%)	55
Dose frequency (week)	2	Measured wet weight water content (%)	55
Dose rate (L/Mg-MSW/month)	160	Lag-time (d)	22
Cumulative leachate (L/Mg-MSW)	1120	Decay rate (1/yr)	1.68



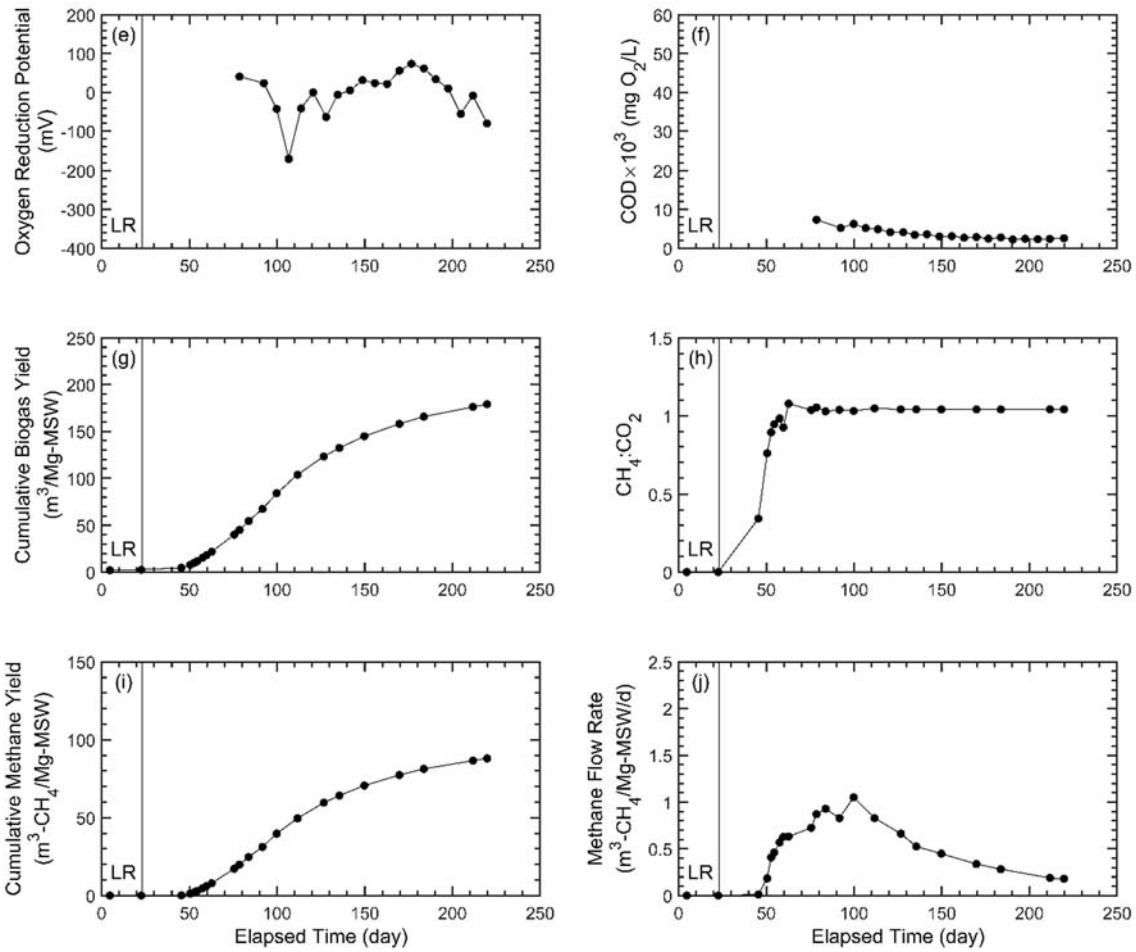
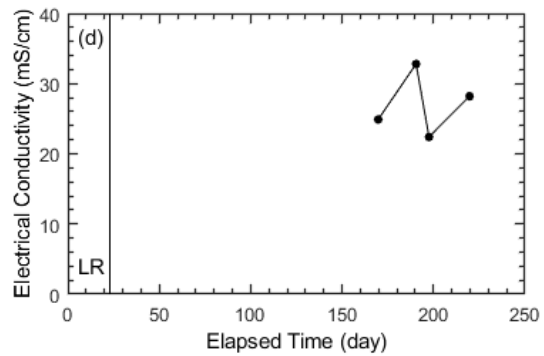
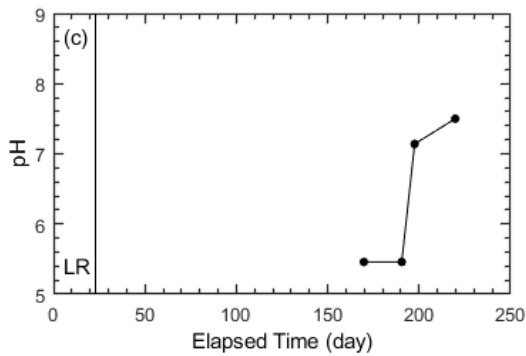
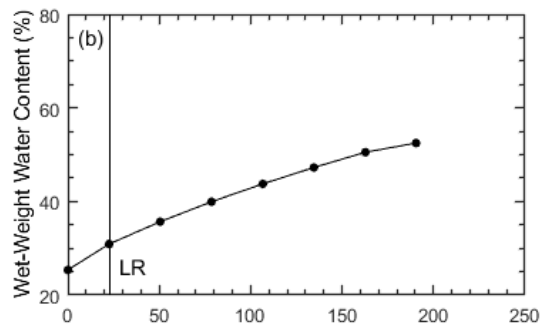
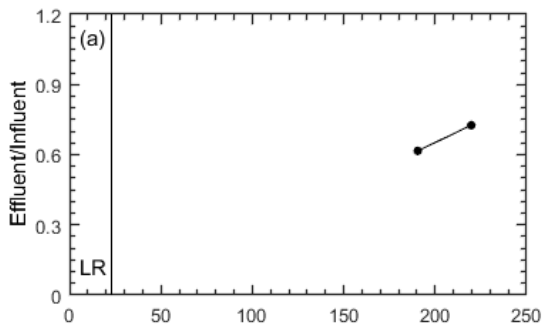


Figure D-7. Temporal trends of operational data collected for R7: (a) ratio of influent to effluent volumes; (b) wet weight water content; (c) leachate pH; (d) leachate electrical conductivity; (e) leachate oxidation reduction potential; (f) leachate chemical oxygen demand; (g) cumulative biogas yield; (h) ratio of methane to carbon dioxide; (i) cumulative methane yield; and (j) methane flow rate.

Table D-8. Reactor information, initial conditions, and final conditions for R8.

Reactor Information		Initial Conditions	
Reactor No.	R8	Specimen thickness (mm)	203
Startup date	12/18/18	Total unit weight (kN/m <sup>3</sup> )	3.41
Experiment duration (d)	220	Wet weight water content (%)	25
Solid waste mass (g)	2400	Final Conditions	
Dose volume (L/Mg-MSW)	80	Total unit weight (kN/m <sup>3</sup> )	5.49
Dose volume (mL)	192	Water balance wet weight water content (%)	52
Dose frequency (week)	4	Measured wet weight water content (%)	48
Dose rate (L/Mg-MSW/month)	80	Lag-time (d)	35
Cumulative leachate (L/Mg-MSW)	560	Decay rate (1/yr)	0.81



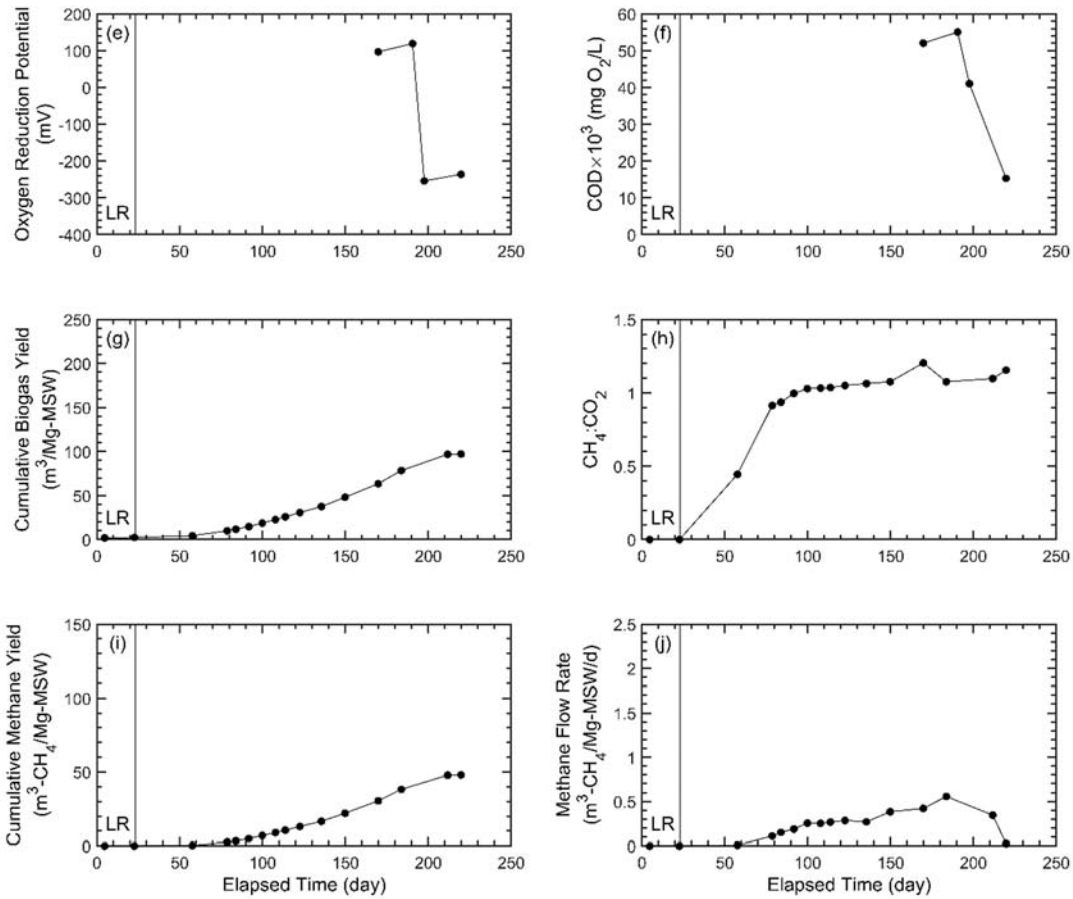
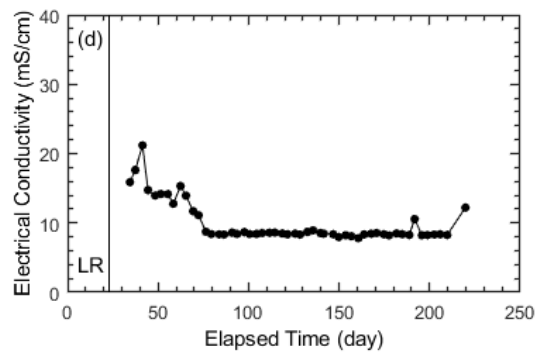
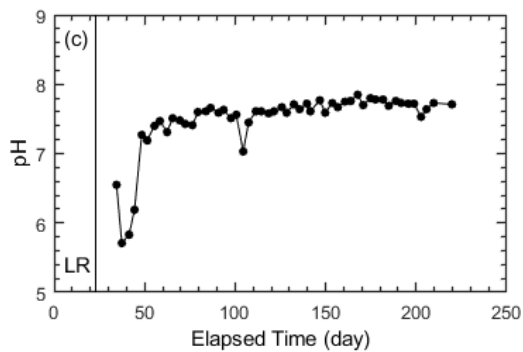
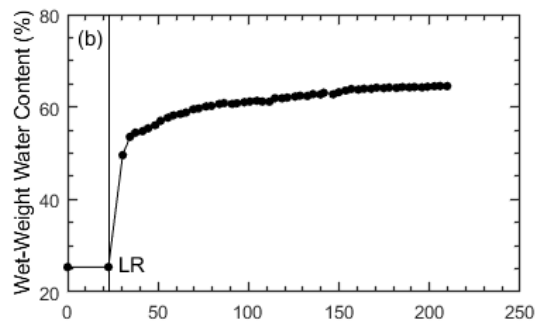
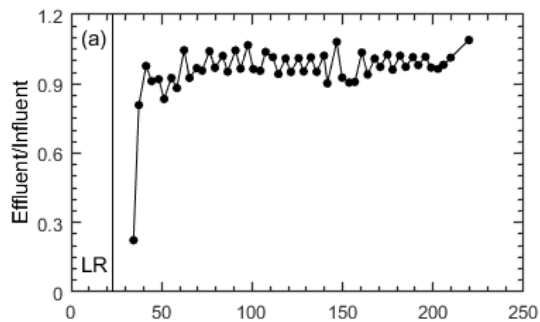


Figure D-8. Temporal trends of operational data collected for R8: (a) ratio of influent to effluent volumes; (b) wet weight water content; (c) leachate pH; (d) leachate electrical conductivity; (e) leachate oxidation reduction potential; (f) leachate chemical oxygen demand; (g) cumulative biogas yield; (h) ratio of methane to carbon dioxide; (i) cumulative methane yield; and (j) methane flow rate.

Table D-9. Reactor information, initial conditions, and final conditions for R9.

Reactor Information		Initial Conditions	
Reactor No.	R9	Specimen thickness (mm)	197
Startup date	12/18/18	Total unit weight (kN/m <sup>3</sup> )	3.52
Experiment duration (d)	220	Wet weight water content (%)	25
Solid waste mass (g)	2400	Final Conditions	
Dose volume (L/Mg-MSW)	160	Total unit weight (kN/m <sup>3</sup> )	7.21
Dose volume (mL)	384	Water balance wet weight water content (%)	64
Dose frequency (week)	0.5	Measured wet weight water content (%)	53
Dose rate (L/Mg-MSW/month)	1280	Lag-time (d)	11
Cumulative leachate (L/Mg-MSW)	8690	Decay rate (1/yr)	2.26



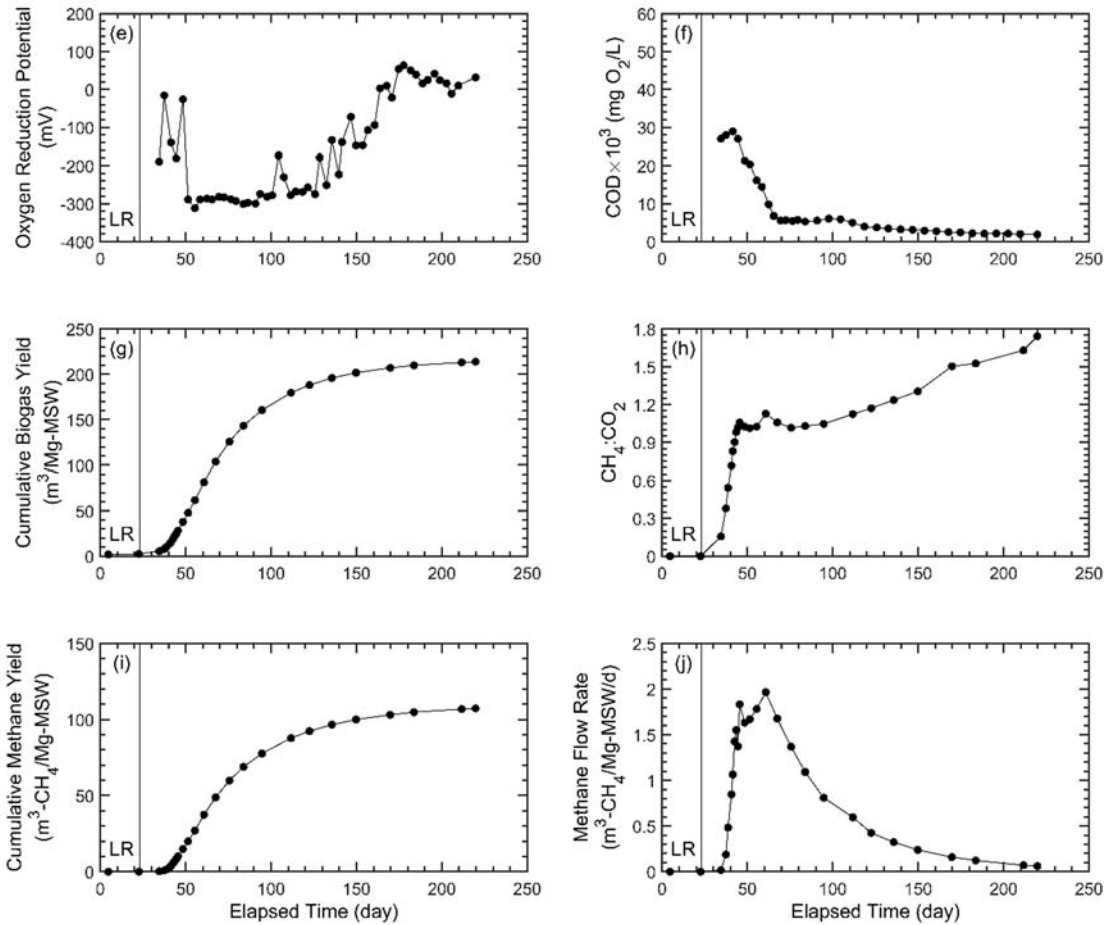
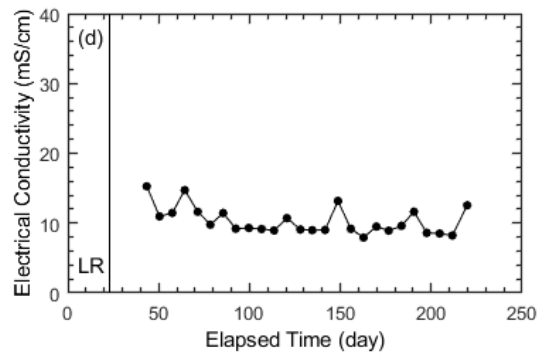
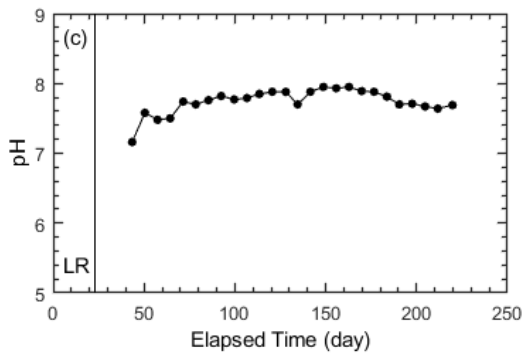
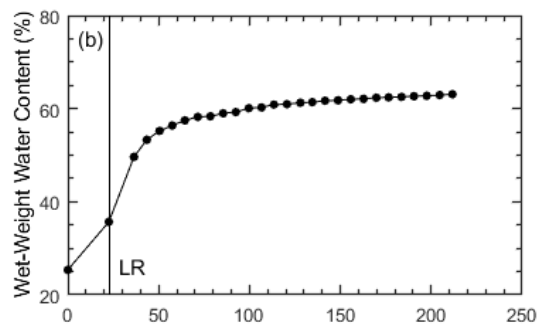
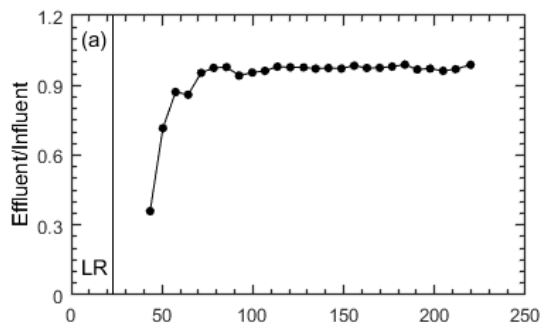


Figure D-9. Temporal trends of operational data collected for R9: (a) ratio of influent to effluent volumes; (b) wet weight water content; (c) leachate pH; (d) leachate electrical conductivity; (e) leachate oxidation reduction potential; (f) leachate chemical oxygen demand; (g) cumulative biogas yield; (h) ratio of methane to carbon dioxide; (i) cumulative methane yield; and (j) methane flow rate.

Table D-10. Reactor information, initial conditions, and final conditions for R10.

Reactor Information		Initial Conditions	
Reactor No.	R10	Specimen thickness (mm)	200
Startup date	12/18/18	Total unit weight (kN/m <sup>3</sup> )	3.46
Experiment duration (d)	220	Wet weight water content (%)	25
Solid waste mass (g)		Final Conditions	
Dose volume (L/Mg-MSW)	160	Total unit weight (kN/m <sup>3</sup> )	6.89
Dose volume (mL)	384	Water balance wet weight water content (%)	63
Dose frequency (week)	1	Measured wet weight water content (%)	56
Dose rate (L/Mg-MSW/month)	640	Lag-time (d)	13
Cumulative leachate (L/Mg-MSW)	4500	Decay rate (1/yr)	2.10



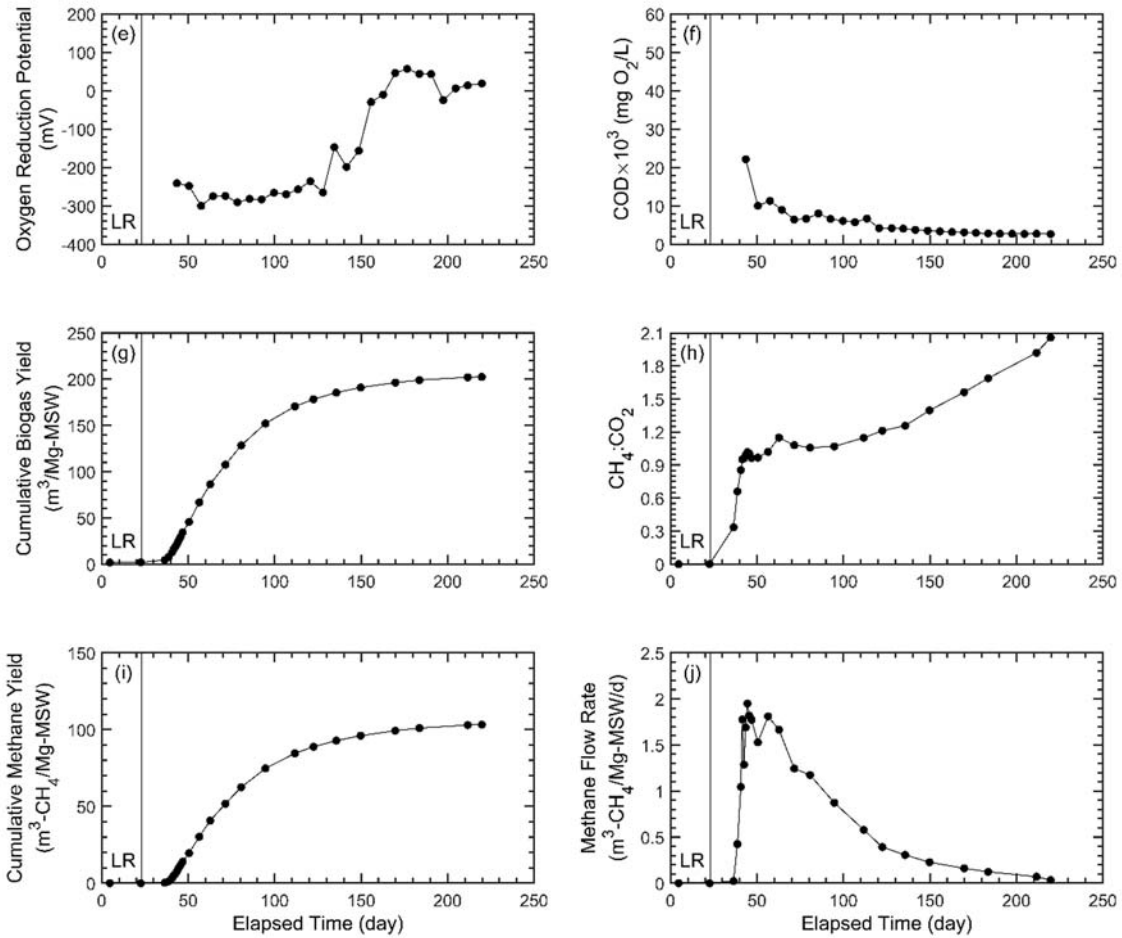
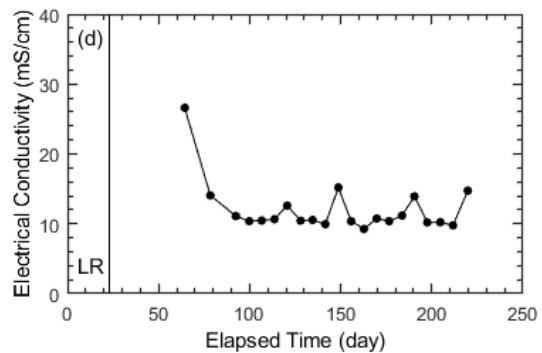
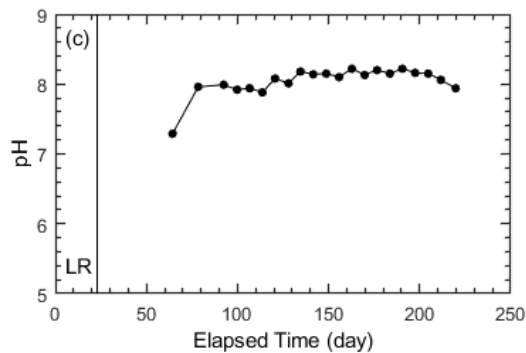
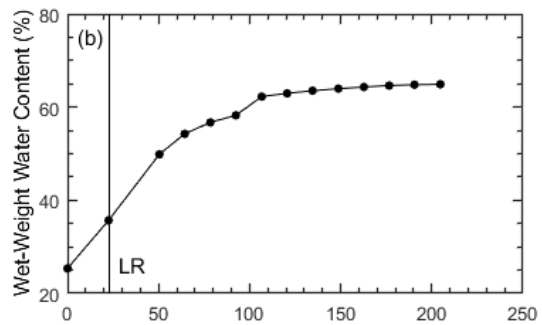
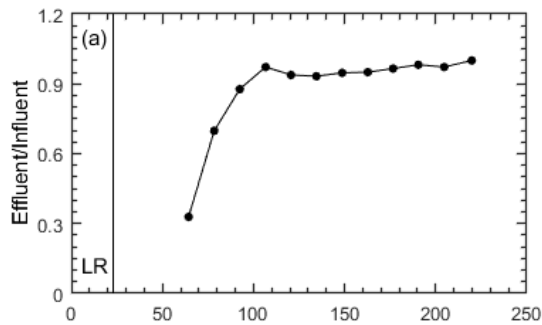


Figure D-10. Temporal trends of operational data collected for R10: (a) ratio of influent to effluent volumes; (b) wet weight water content; (c) leachate pH; (d) leachate electrical conductivity; (e) leachate oxidation reduction potential; (f) leachate chemical oxygen demand; (g) cumulative biogas yield; (h) ratio of methane to carbon dioxide; (i) cumulative methane yield; and (j) methane flow rate.

Table D-11. Reactor information, initial conditions, and final conditions for R11.

Reactor Information		Initial Conditions	
Reactor No.	R11	Specimen thickness (mm)	195
Startup date	12/18/18	Total unit weight (kN/m <sup>3</sup> )	3.55
Experiment duration (d)	220	Wet weight water content (%)	25
Solid waste mass (g)	2400	Final Conditions	
Dose volume (L/Mg-MSW)	160	Calculated total unit weight (kN/m <sup>3</sup> )	7.62
Dose volume (mL)	384	Water balance wet weight water content (%)	65
Dose frequency (week)	2	Measured wet weight water content (%)	55
Dose rate (L/Mg-MSW/month)	320	Lag-time (d)	22
Cumulative leachate (L/Mg-MSW)	2250	Decay rate (1/yr)	2.17



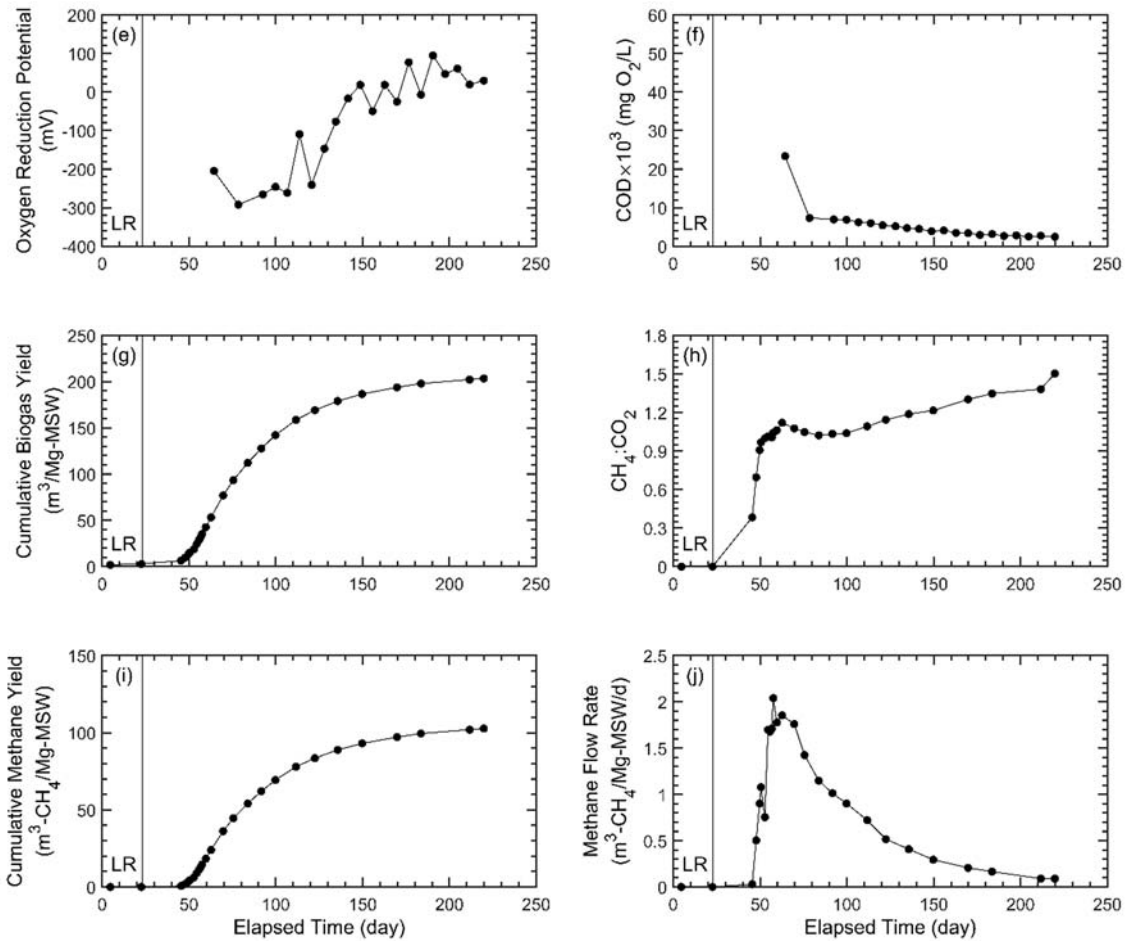
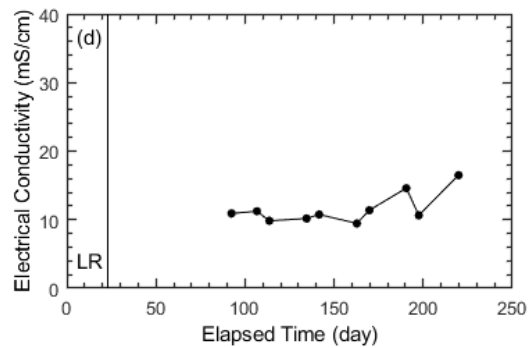
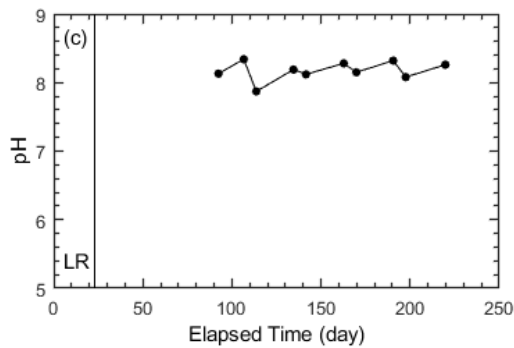
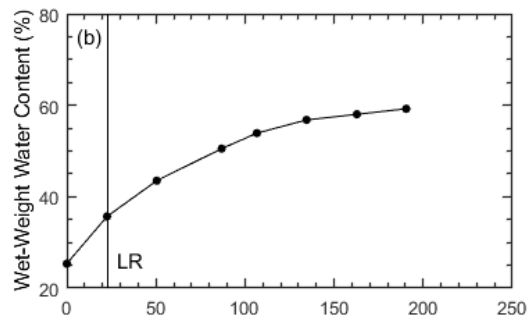
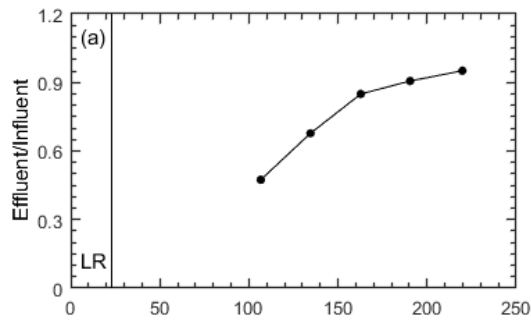


Figure D-11. Temporal trends of operational data collected for R11: (a) ratio of influent to effluent volumes; (b) wet weight water content; (c) leachate pH; (d) leachate electrical conductivity; (e) leachate oxidation reduction potential; (f) leachate chemical oxygen demand; (g) cumulative biogas yield; (h) ratio of methane to carbon dioxide; (i) cumulative methane yield; and (j) methane flow rate.

Table D-12. Reactor information, initial conditions, and final conditions for R12.

Reactor Information		Initial Conditions	
Reactor No.	R12	Specimen thickness (mm)	200
Startup date	12/18/18	Total unit weight (kN/m <sup>3</sup> )	3.46
Experiment duration (d)	220	Wet weight water content (%)	25
Solid waste mass (g)		<b>Final Conditions</b>	
Dose volume (L/Mg-MSW)	160	Total unit weight (kN/m <sup>3</sup> )	6.12
Dose volume (mL)	384	Water balance wet weight water content (%)	59
Dose frequency (week)	4	Measured wet weight water content (%)	57
Dose rate (L/Mg-MSW/month)	160	Lag-time (d)	27
Cumulative leachate (L/Mg-MSW)	1130	Decay rate (1/yr)	1.76



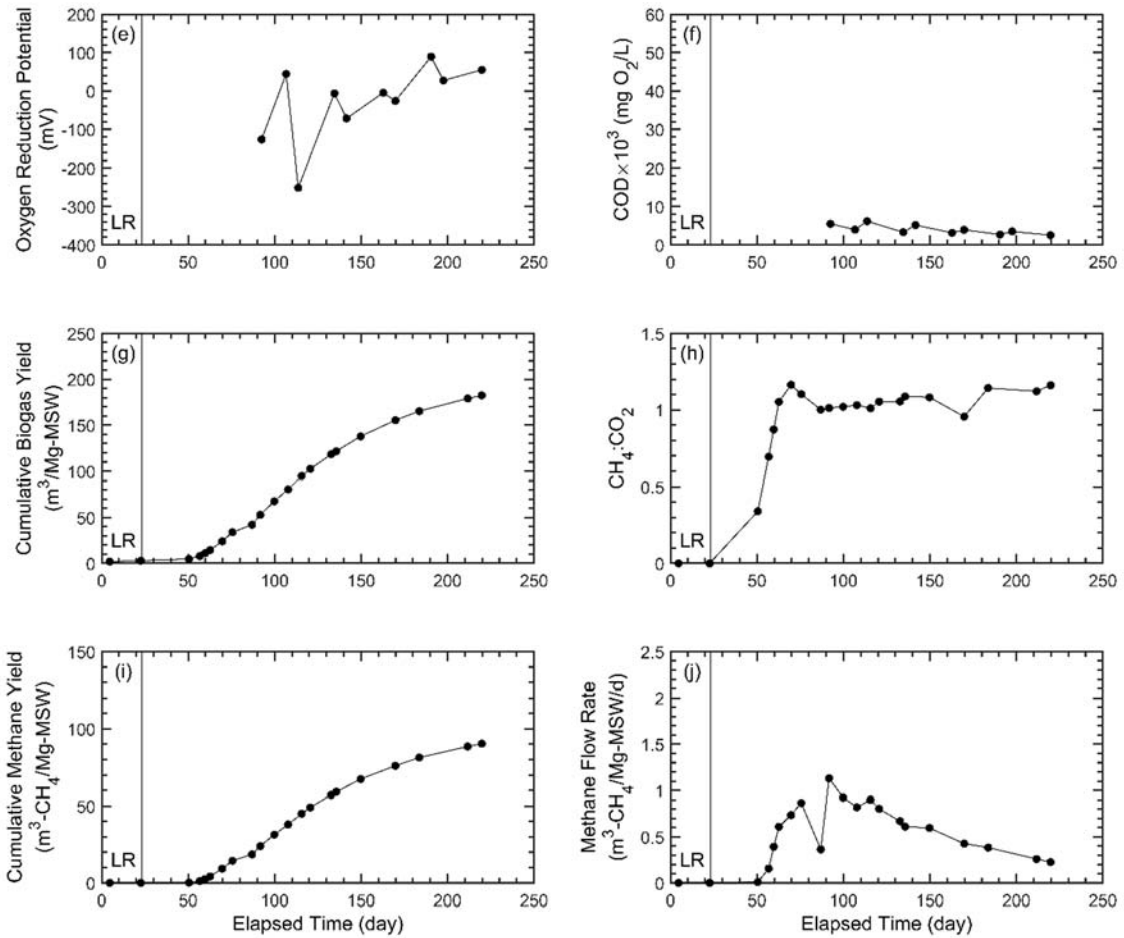
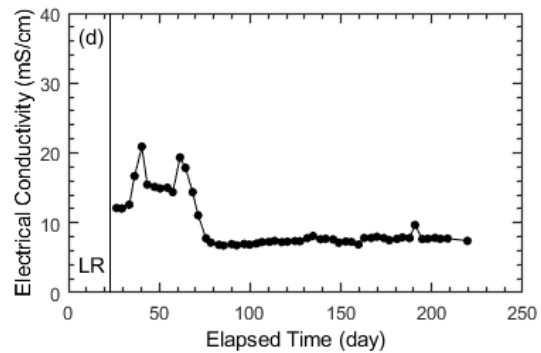
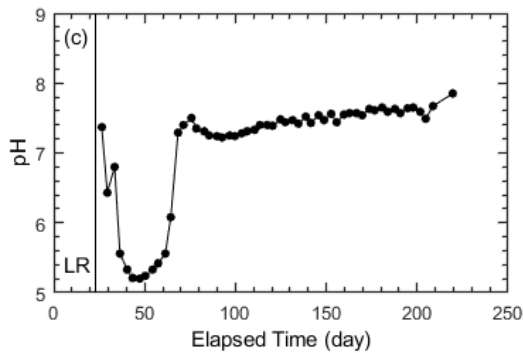
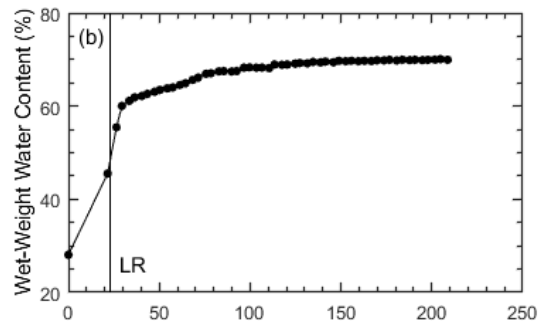
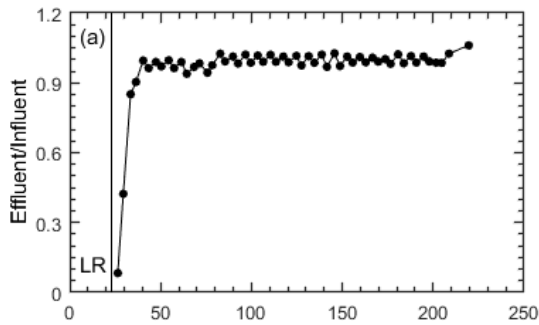


Figure D-12. Temporal trends of operational data collected for R12: (a) ratio of influent to effluent volumes; (b) wet weight water content; (c) leachate pH; (d) leachate electrical conductivity; (e) leachate oxidation reduction potential; (f) leachate chemical oxygen demand; (g) cumulative biogas yield; (h) ratio of methane to carbon dioxide; (i) cumulative methane yield; and (j) methane flow rate.

Table D-13. Reactor information, initial conditions, and final conditions for R13.

Reactor Information		Initial Conditions	
Reactor No.	R13	Specimen thickness (mm)	202
Startup date	12/18/18	Total unit weight (kN/m <sup>3</sup> )	3.44
Experiment duration (d)	220	Wet weight water content (%)	25
Solid waste mass (g)	2400	Final Conditions	
Dose volume (L/Mg-MSW)	320	Total unit weight (kN/m <sup>3</sup> )	7.05
Dose volume (mL)	768	Water balance wet weight water content (%)	70
Dose frequency (week)	0.5	Measured wet weight water content (%)	60
Dose rate (L/Mg-MSW/month)	2560	Lag-time (d)	7
Cumulative leachate (L/Mg-MSW)	17,280	Decay rate (1/yr)	2.78



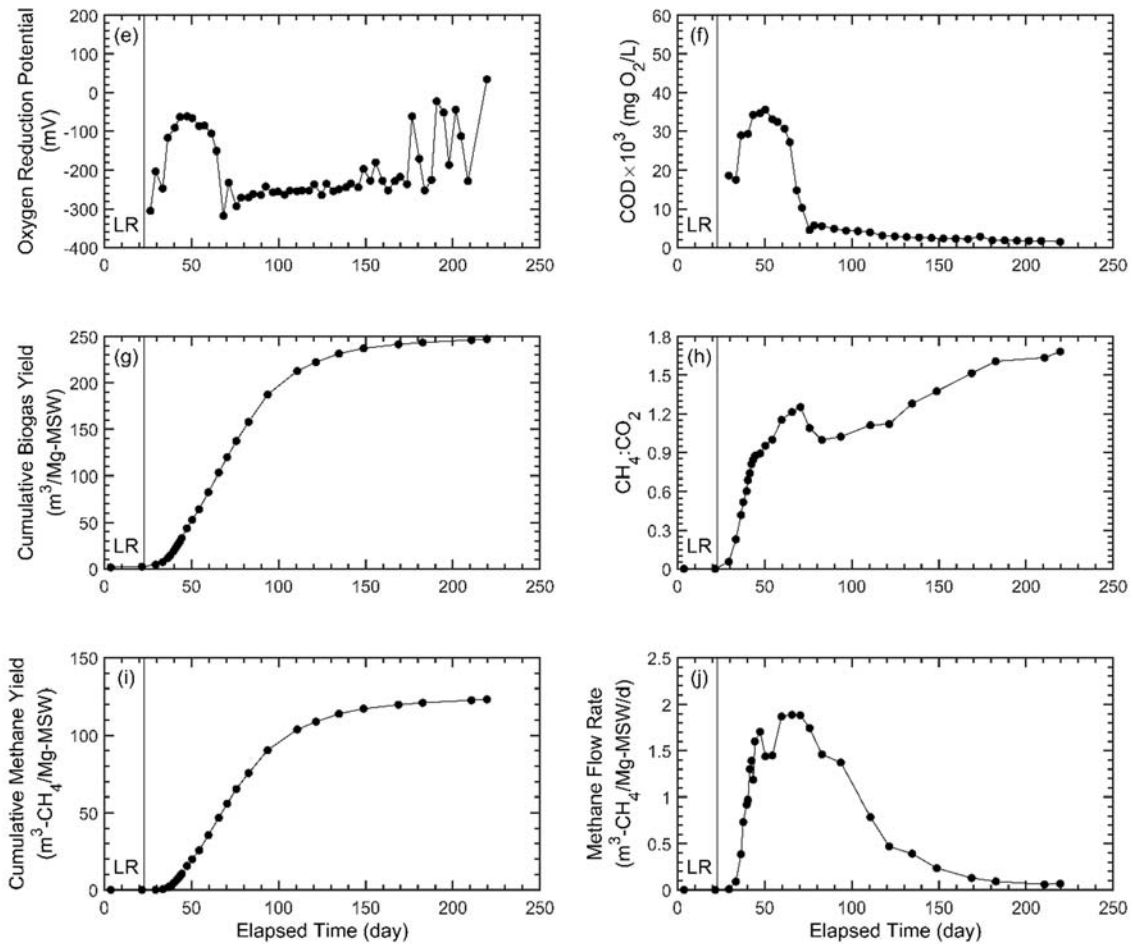
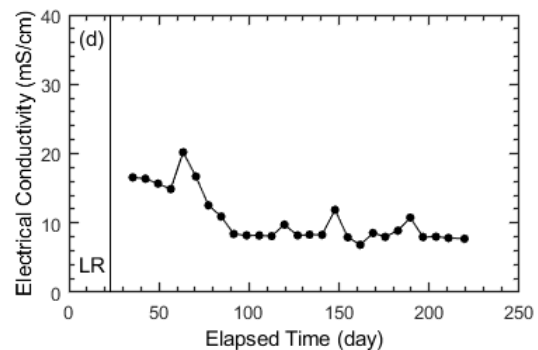
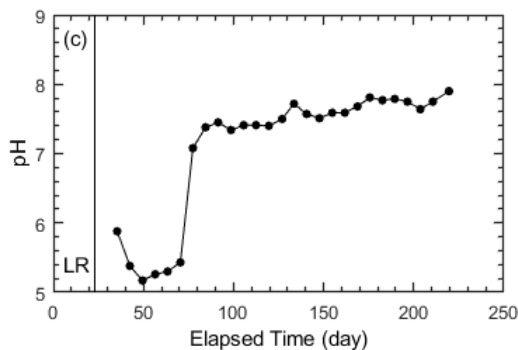
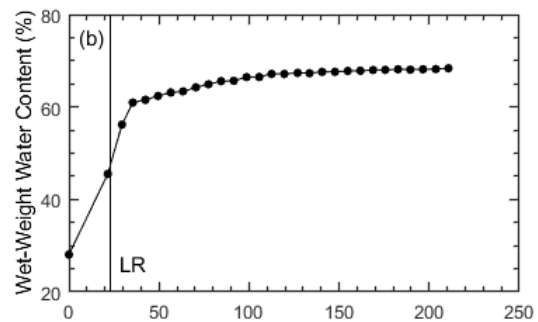
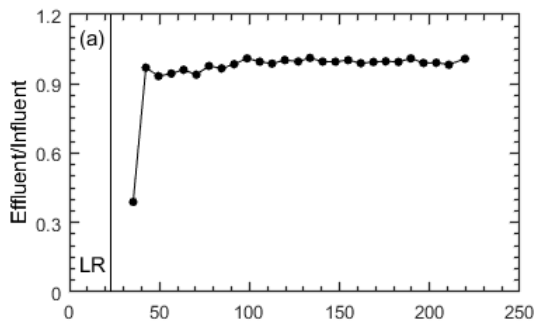


Figure D-13. Temporal trends of operational data collected for R13: (a) ratio of influent to effluent volumes; (b) wet weight water content; (c) leachate pH; (d) leachate electrical conductivity; (e) leachate oxidation reduction potential; (f) leachate chemical oxygen demand; (g) cumulative biogas yield; (h) ratio of methane to carbon dioxide; (i) cumulative methane yield; and (j) methane flow rate.

Table D-14. Reactor information, initial conditions, and final conditions for R14.

Reactor Information		Initial Conditions	
Reactor No.	R14	Specimen thickness (mm)	200
Startup date	12/18/18	Total unit weight (kN/m <sup>3</sup> )	3.46
Experiment duration (d)	220	Wet weight water content (%)	28
Solid waste mass (g)		<b>Final Conditions</b>	
Dose volume (L/Mg-MSW)	320	Total unit weight (kN/m <sup>3</sup> )	7.68
Dose volume (mL)	768	Water balance wet weight water content (%)	68
Dose frequency (week)	1	Measured wet weight water content (%)	57
Dose rate (L/Mg-MSW/month)	1280	Lag-time (d)	7
Cumulative leachate (L/Mg-MSW)	8960	Decay rate (1/yr)	1.91



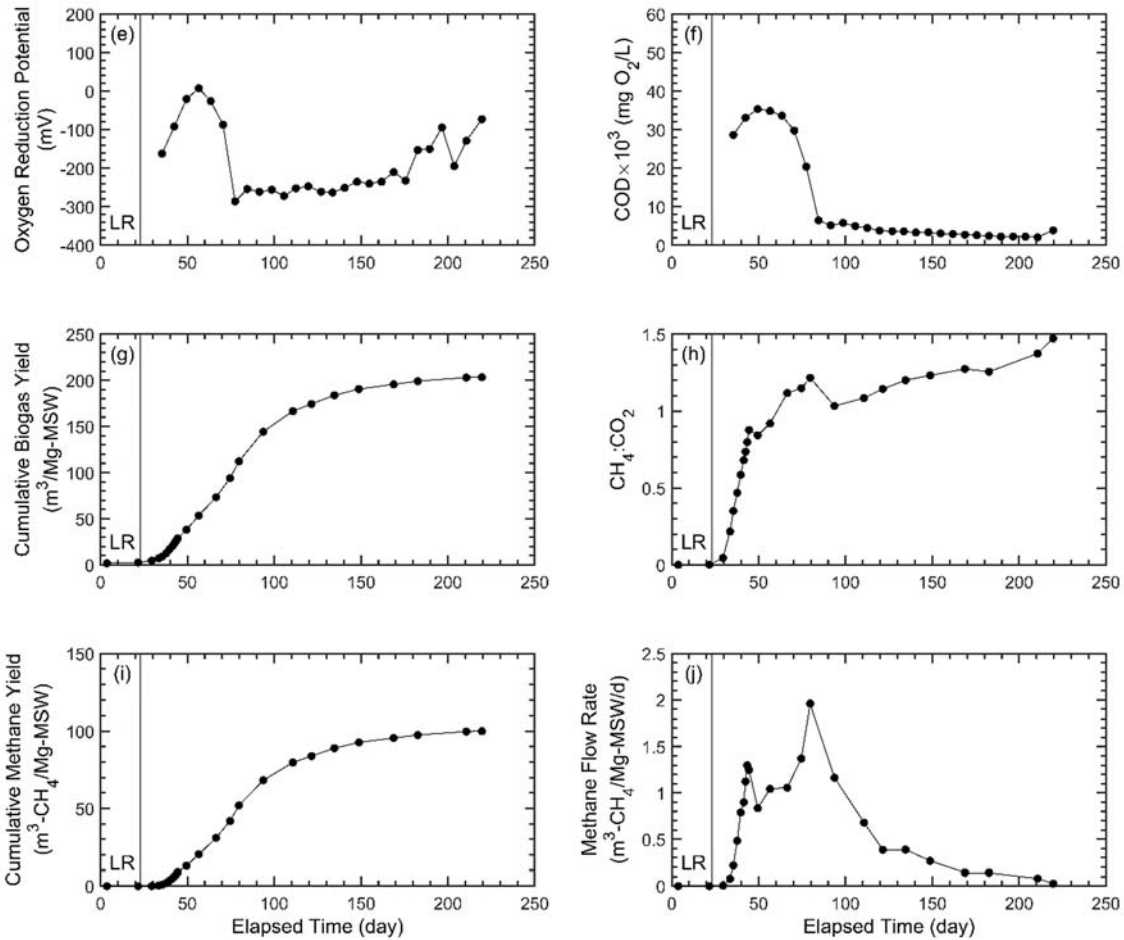
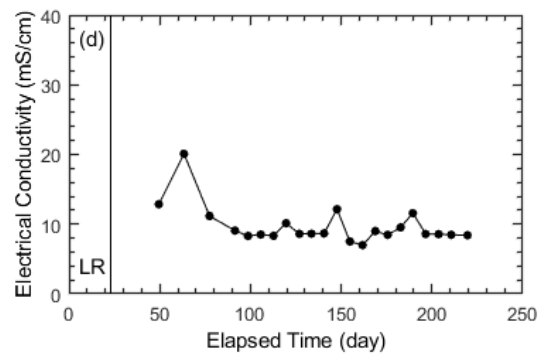
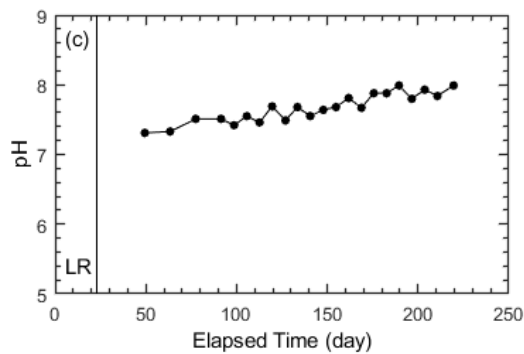
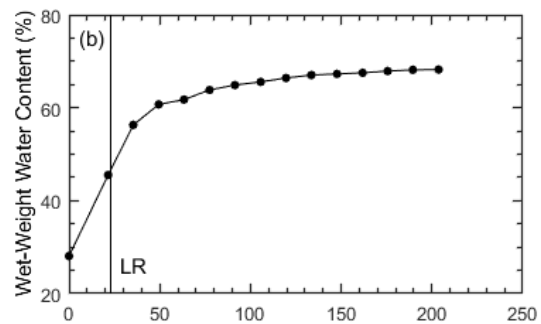
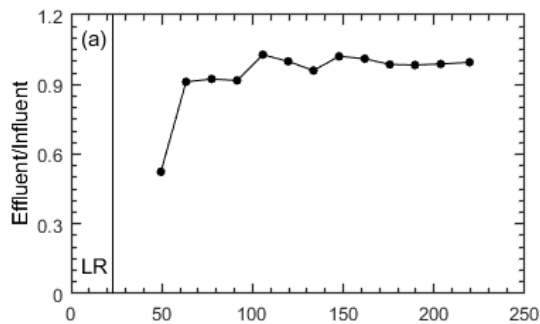


Figure D-14. Temporal trends of operational data collected for R14: (a) ratio of influent to effluent volumes; (b) wet weight water content; (c) leachate pH; (d) leachate electrical conductivity; (e) leachate oxidation reduction potential; (f) leachate chemical oxygen demand; (g) cumulative biogas yield; (h) ratio of methane to carbon dioxide; (i) cumulative methane yield; and (j) methane flow rate.

Table D-15. Reactor information, initial conditions, and final conditions for R15.

Reactor Information		Initial Conditions	
Reactor No.	R15	Specimen thickness (mm)	202
Startup date	12/18/18	Total unit weight (kN/m <sup>3</sup> )	3.44
Experiment duration (d)	220	Wet weight water content (%)	28
Solid waste mass (g)		<b>Final Conditions</b>	
Dose volume (L/Mg-MSW)	320	Total unit weight (kN/m <sup>3</sup> )	7.25
Dose volume (mL)	768	Water balance wet weight water content (%)	68
Dose frequency (week)	2	Measured wet weight water content (%)	60
Dose rate (L/Mg-MSW/month)	640	Lag-time (d)	7
Cumulative leachate (L/Mg-MSW)	4480	Decay rate (1/yr)	2.80



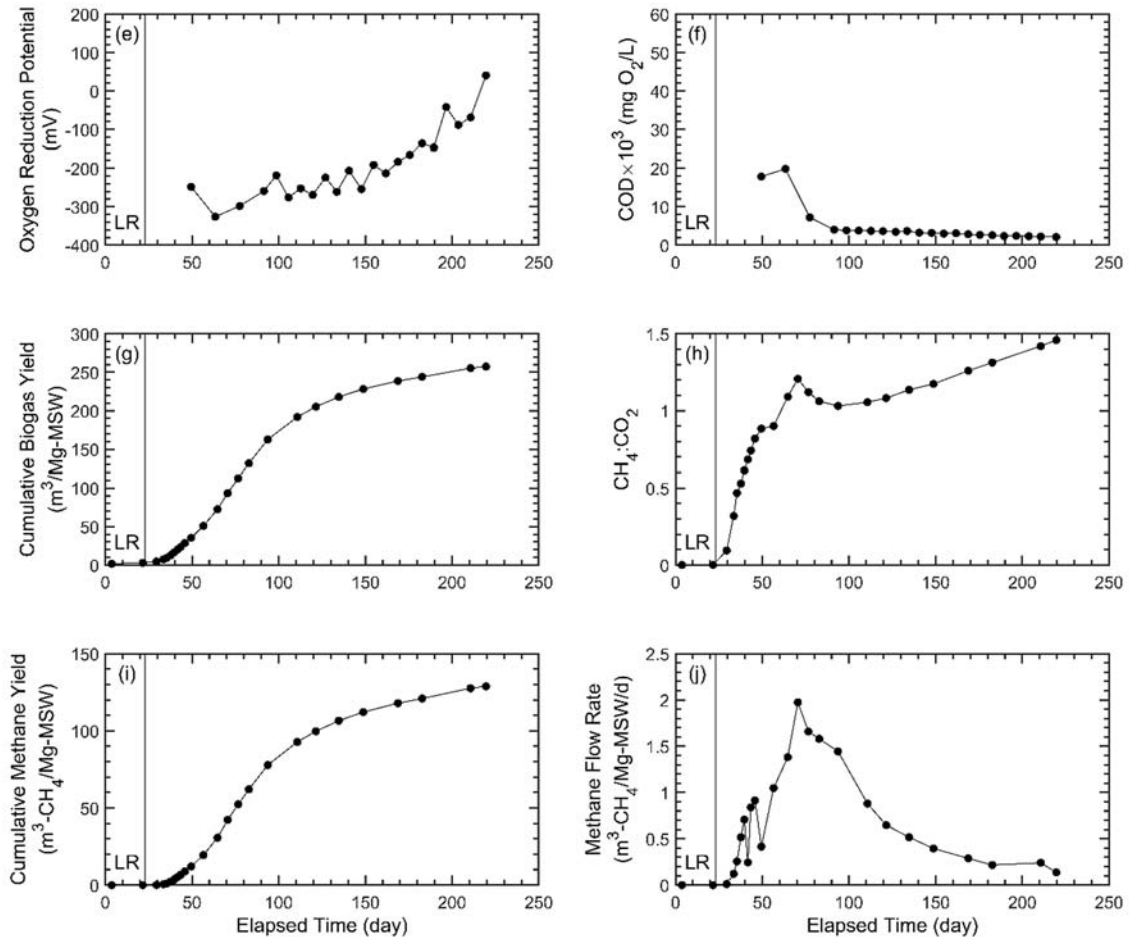
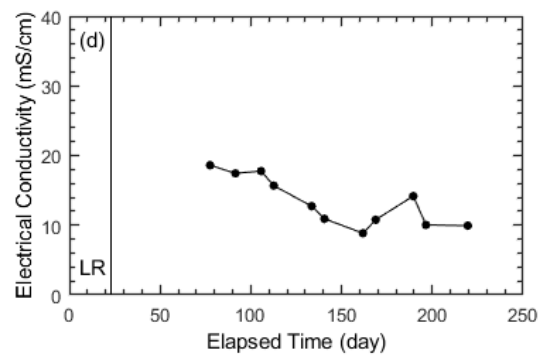
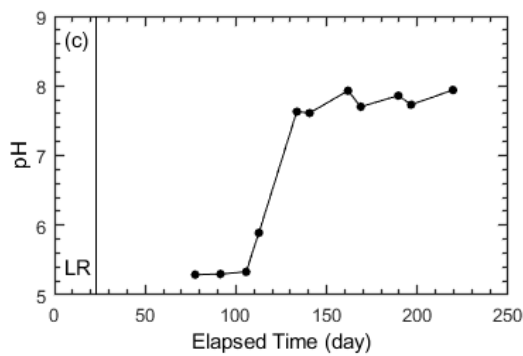
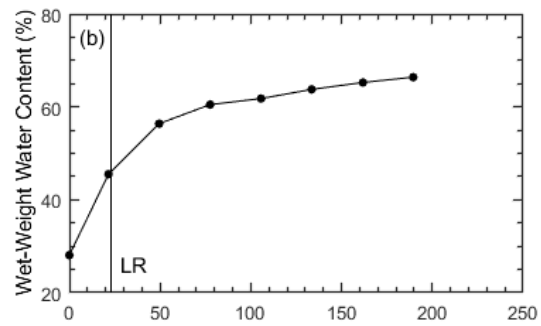
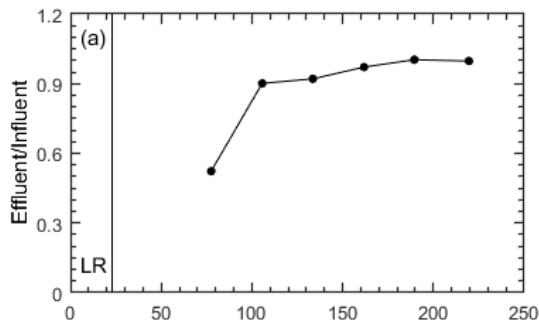


Figure D-15. Temporal trends of operational data collected for R15: (a) ratio of influent to effluent volumes; (b) wet weight water content; (c) leachate pH; (d) leachate electrical conductivity; (e) leachate oxidation reduction potential; (f) leachate chemical oxygen demand; (g) cumulative biogas yield; (h) ratio of methane to carbon dioxide; (i) cumulative methane yield; and (j) methane flow rate.

Table D-16. Reactor information, initial conditions, and final conditions for R16.

Reactor Information		Initial Conditions	
Reactor No.	R16	Specimen thickness (mm)	195
Startup date	12/18/18	Total unit weight (kN/m <sup>3</sup> )	3.55
Experiment duration (d)	220	Wet weight water content (%)	28
Solid waste mass (g)	2400	Final Conditions	
Dose volume (L/Mg-MSW)	320	Total unit weight (kN/m <sup>3</sup> )	7.18
Dose volume (mL)	768	Water balance wet weight water content (%)	66
Dose frequency (week)	4	Measured wet weight water content (%)	58
Dose rate (L/Mg-MSW/month)	320	Lag-time (d)	7
Cumulative leachate (L/Mg-MSW)	2240	Decay rate (1/yr)	1.93



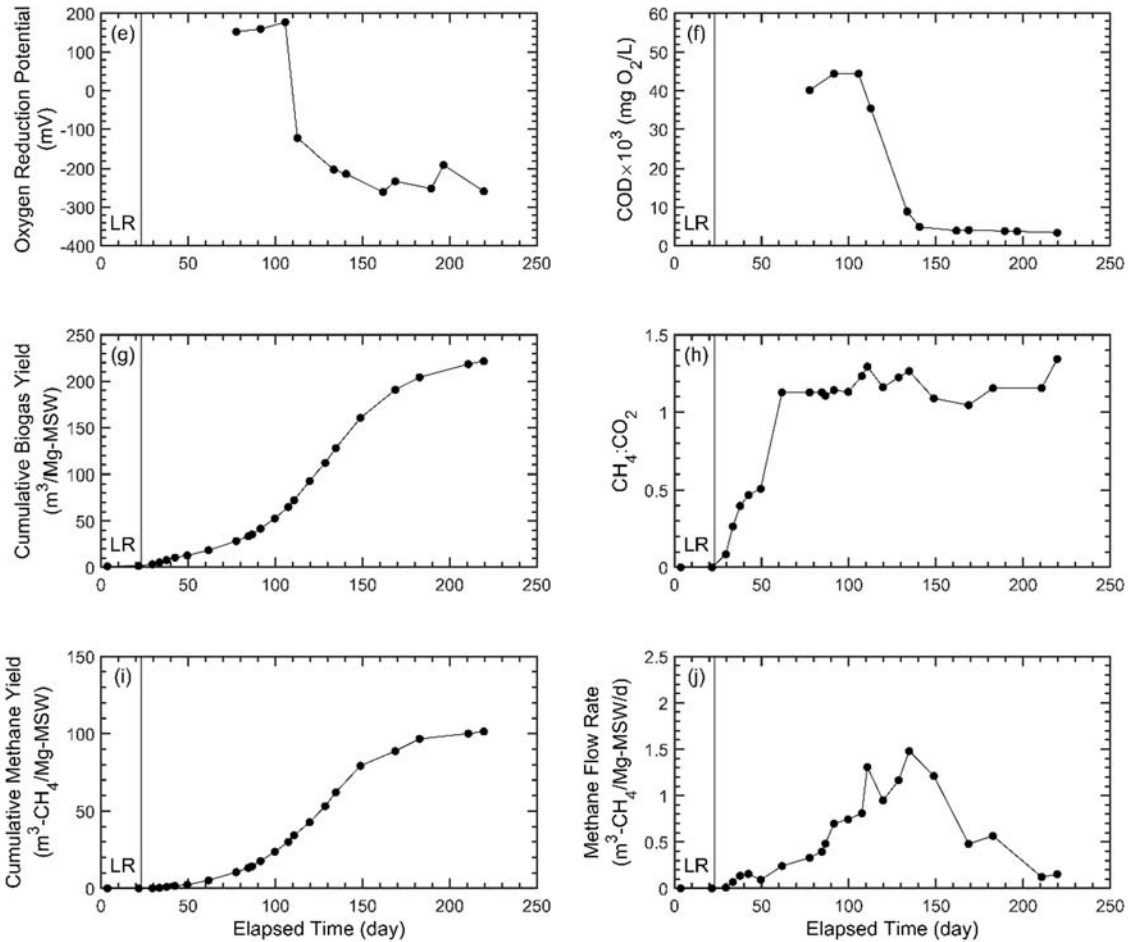


Figure D-16. Temporal trends of operational data collected for R16: (a) ratio of influent to effluent volumes; (b) wet weight water content; (c) leachate pH; (d) leachate electrical conductivity; (e) leachate oxidation reduction potential; (f) leachate chemical oxygen demand; (g) cumulative biogas yield; (h) ratio of methane to carbon dioxide; (i) cumulative methane yield; and (j) methane flow rate.

## APPENDIX E – Photographs from Reactor Setup and Operation for Research Study 2

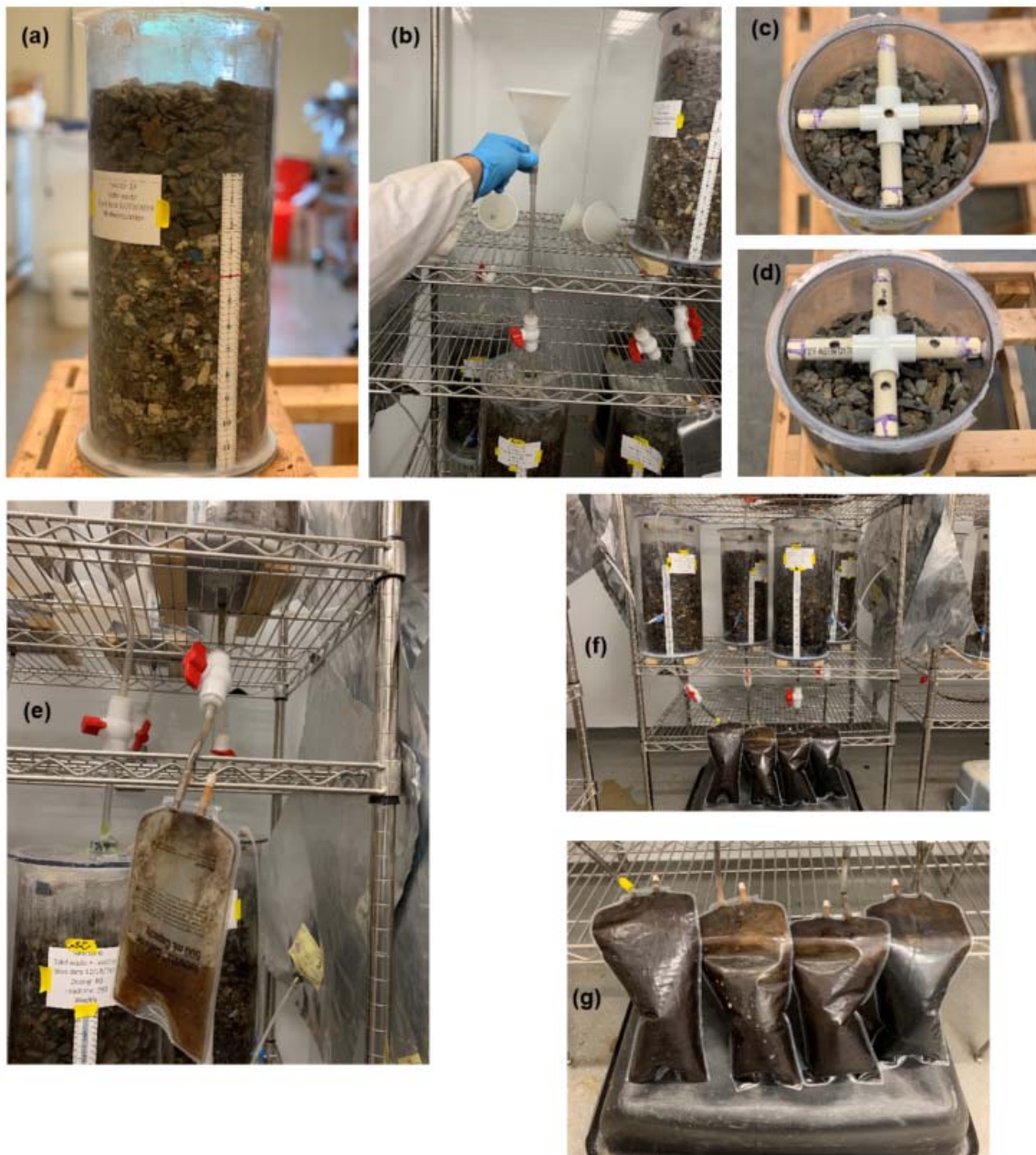


Fig. E-1. Reactor leachate injection, distribution, and collection system: (a) constructed reactor before sealing and operation with a top and bottom layer of gravel; (b) funnel for adding liquid / leachate; (c) top view of perforated PVC pipe for leachate distribution; (d) bottom view of perforated PVC pipes for leachate distribution; (e) leachate collection system; (f and g) leachate collection bag for reactors with dosing rate of 320 L/Mg-MSW.



Fig. E-2. Reactor gas management: (a) biogas collection system; (b) biogas measurement apparatus that included a 10-L inverted graduated cylinder, vacuum pump, and acidified water with  $\text{pH} \approx 3$ ; (c) filled gasbags acclimating to laboratory temperature; and (d) injecting biogas sample into GC machine.

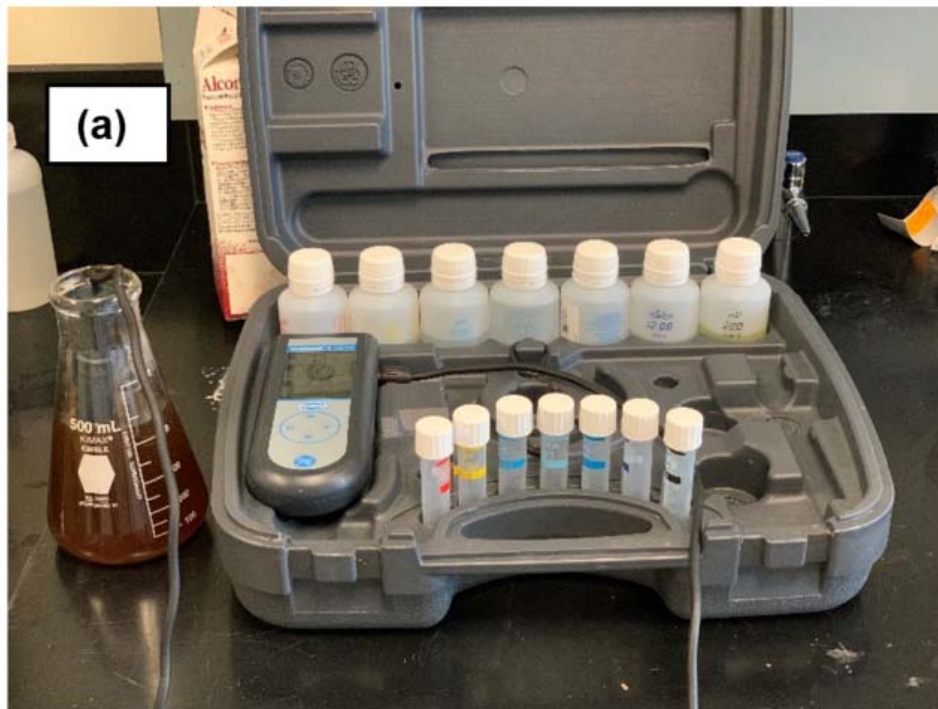


Fig. E-3. (a) Measuring leachate chemistry (pH, electrical conductivity, and oxygen reduction potential) via probe and (b) effluent leachate samples.

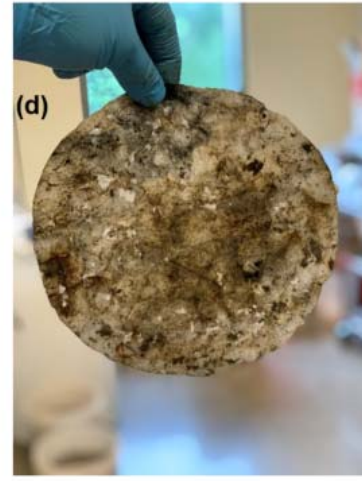


Fig. E-4. Reactor after termination: (a) decomposed MSW (top layer); (b) bottom layer of gravel which was uniformly wet; and (c and d) top and bottom layer of geotextile that were used for leachate distribution and collection.



Fig. E-5. Reactors during operation in the temperature control room.